University of Alberta

Examination of the Role and Regulation of the Tyrosine Kinase Pyk2 in Cytotoxic T Lymphocytes

by

Tara Lynn Lysechko

A thesis submitted to the Faculty of Graduate Studies and Research
in partial fulfillment of the requirements for the degree of

Doctor of Philosophy
in
Immunology

Department of Medical Microbiology and Immunology

Edmonton, Alberta
Spring 2007

Library and
Archives Canada

Published Heritage
Branch

395 Wellington Street
Ottawa ON K1A 0N4
Canada

Bibliothèque et
Archives Canada

Direction du
Patrimoine de l'édition

395, rue Wellington
Ottawa ON K1A 0N4
Canada

Your file Votre référence
ISBN: 978-0-494-29706-3
Our file Notre référence
ISBN: 978-0-494-29706-3

NOTICE:
The author has granted a non-exclusive license allowing Library and Archives Canada to reproduce, publish, archive, preserve, conserve, communicate to the public by telecommunication or on the Internet, loan, distribute and sell theses worldwide, for commercial or non-commercial purposes, in microform, paper, electronic and/or any other formats.

The author retains copyright ownership and moral rights in this thesis. Neither the thesis nor substantial extracts from it may be printed or otherwise reproduced without the author's permission.

AVIS:
L'auteur a accordé une licence non exclusive permettant à la Bibliothèque et Archives Canada de reproduire, publier, archiver, sauvegarder, conserver, transmettre au public par télécommunication ou par l'Internet, prêter, distribuer et vendre des thèses partout dans le monde, à des fins commerciales ou autres, sur support microforme, papier, électronique et/ou autres formats.

L'auteur conserve la propriété du droit d'auteur et des droits moraux qui protège cette thèse. Ni la thèse ni des extraits substantiels de celle-ci ne doivent être imprimés ou autrement reproduits sans son autorisation.

In compliance with the Canadian Privacy Act some supporting forms may have been removed from this thesis.

While these forms may be included in the document page count, their removal does not represent any loss of content from the thesis.

Conformément à la loi canadienne sur la protection de la vie privée, quelques formulaires secondaires ont été enlevés de cette thèse.

Bien que ces formulaires aient inclus dans la pagination, il n'y aura aucun contenu manquant.

Canada

ABSTRACT

Cytotoxic T lymphocytes (CTL) are immune effector cells that play a critical role in eliminating virally infected or transformed cells. CTL become activated to kill their targets by antigen-specific triggering of the T cell receptor (TCR) which induces a signalling cascade that initiates the cytotoxic response. One protein that becomes tyrosine phosphorylated and activated upon stimulation of the TCR is the tyrosine kinase Pyk2. Little is known about the regulation and role of this protein during CTL activation.

Examination of the localization of Pyk2 in CTL demonstrated that some Pyk2 is found at the CTL/target cell interface suggesting it might interact with proteins assembled around the TCR/CD3 complex. Indeed it was found that Pyk2 was recruited to this complex. The phosphorylation of Pyk2 is regulated by Ca^{2+} in many cell types but this regulation is controversial in T cells. In CTL, Pyk2 was inducibly phosphorylated in response to stimulation with intracellular Ca^{2+} mobilizers and was partially dependent upon Src family kinases. TCR-stimulated Pyk2 phosphorylation partially required Ca^{2+} under specific conditions. To date, no structural information exists for Pyk2. This study presents biochemical evidence that a conformational change occurs within the focal adhesion targeting (FAT) domain of Pyk2. Two populations of Pyk2 were identified in CTL based on their ability to associate with paxillin, which binds the FAT domain of Pyk2. The results are consistent with a model that has been proposed for the related tyrosine kinase FAK. The results suggest that Pyk2 displays a compact FAT domain when bound to paxillin and an unfolded FAT domain that favours phosphorylation of Y881 when not bound to paxillin. Studies aimed at examining the function of Pyk2 in

CTL by overexpression of Pyk2 truncation mutants revealed that expression of these mutants appeared to lower the threshold for activation as more cells were observed to spread and degranulate upon immobilized anti-CD3 stimulation. The use of Pyk2 siRNA hinted at possible roles for Pyk2 in signal amplification upon TCR stimulation and in de-adhesion of CTL from target cells. Together, these findings further define the regulation and role of Pyk2 in CTL function.

ACKNOWLEDGEMENTS

I would like to thank my supervisor, Dr. Hanne Ostergaard, for all her support and guidance over the years. I also acknowledge the support I received from family and friends, especially my husband Russell Higginson. I would like to thank my supervisory committee members Dr. Deborah Burshtyn and Dr. Luis Schang for their input into the project. Thanks to Dr. Kevin Kane for constructive criticism during lab meetings and for reviewing manuscripts and Gerry Barron for her assistance with the presentation of confocal microscopy images. Many of the past and present members of Dr. Ostergaard's laboratory have provided help with various assays used in this work. Barbara Simon prepared many of the stock reagents and media used during this project. Financial support for the project was provided by The National Cancer Institute of Canada and the Alberta Heritage Foundation for Medical Research.

TABLE OF CONTENTS

CHAPTER 1: Introduction

The adaptive immune system........1

T cell development........3

T cell differentiation in the periphery........4

Cytotoxic T cells........5

Signalling through the TCR/CD3 complex........6

The immunological synapse, lipid rafts and TCR microclusters........11

Integrins are involved in cell-matrix and cell-cell adhesions........12

FAK and Pyk2: the two members of the focal adhesion tyrosine kinase family........14

The regulation of tyrosine kinase activity by phosphorylation........16

Proteins that interact with the N-terminal region of FAK and Pyk2........18

Proteins that interact with the C-terminal region of FAK and Pyk2........19

Splice variants of FAK and Pyk2........22

Pyk2 activation in T cells........24

The regulation of Pyk2 activity in T cells........25

Localization of Pyk2 in T cells and NK cells........27

Pyk2 function........28

Differences between FAK and Pyk2........32

Study objectives........34

CHAPTER 2: Materials and Methods

Cells........35

Antibodies........36

Reagents........37

Cloning murine Pyk2-H........38

Antibody immobilization..........39

Cell stimulation with cross-linked and immobilized anti-CD3..........39

Stimulation with calcium mobilizing agents..........40

Recovery of complexes associated with immobilized antibody..........41

Immunoprecipitation..........41

Western blotting and Coomassie Blue staining..........42

Lck in vitro kinase assays..........43

Pyk2 in vitro kinase assays..........44

Cell surface biotinylation and stimulation with cross-linked anti-CD3..........44

Fibronectin immobilization and stimulation with ionomycin in 96 well plates..........45

Degranulation assay..........46

Nucleofection of cloned CTL with plasmid or siRNA..........46

Conjugate formation, spreading on immobilized anti-CD3 and confocal staining..........47

CD107a cell surface expression upon stimulation with immobilized anti-CD3 and target cells..........49

Disruption of conjugates between cloned CTL nucleofected with Pyk2 siRNA and EL4 target cells..........51

Stimulation of nucleofected clone 11 on immobilized anti-CD3 in 96 well plates..........51

GST fusion protein pulldowns..........52

Quantification of the amount of phospho-protein relative to unphosphorylated protein..........52

Statistical analysis..........53

Reproducibility of results..........53

CHAPTER 3: Differential Src family kinase activity requirements for CD3ε / CD3ζ phosphorylation and Pyk2 / ZAP-70 recruitment to the TCR/CD3 complex

A. Introduction..........54

B. Results

Stimulation of CTL clones with immobilized anti-CD3 results in specific recruitment of a number of tyrosine phosphorylated proteins to the TCR/CD3 complex..........56

CD3ζ, but not CD3ε, is tyrosine phosphorylated in the presence of the SFK inhibitor PP2..........61

CD3ζ is phosphorylated after TCR/CD3 stimulation in Lck-deficient Jurkat T cells..........68

Pyk2 and Itk are recruited to the TCR/CD3 complex in a SFK-independent manner..........70

C. Disscussion..........72

CHAPTER 4: Regulation of Pyk2 phosphorylation by increases in intracellular calcium concentration

A. Introduction..........79

B. Results

Treatment of CTL clones with reagents that increase intracellular calcium levels induce Pyk2 phosphorylation..........84

Stimulation of CTL clones through the TCR in the presence of the intracellular calcium chelator BAPTA partially inhibits the induction of Pyk2phosphorylation..........89

TCR stimulation-induced Pyk2 phosphorylation is inhibited in the presence of cytochalasin E when cells are activated with immobilized, but not cross-linked, anti-CD3..........91

Stimulation of CTL clones through the TCR in the presence of the extracellular calcium chelator EGTA does not inhibit Pyk2 phosphorylation..........93

Stimulation of ConA blasts with ionomycin or thapsigargin induces Pyk2 phosphorylation..........95

Calcineurin and CaMKII are not involved in inducing Pyk2 phosphorylation in response to an increase in intracellular calcium levels..........95

Pyk2 phosphorylation is not induced by increases in intracellular calcium in all cell types..........99

Stimulation of CTL clones with ionomycin alone or fibronectin alone induces Pyk2 phosphorylation while stimulation with both induces an additive increase in phosphorylation........102

C. Discussion........105

CHAPTER 5: Two distinct populations of Pyk2 exist in CTL clones based on their differential ability to bind to paxillin

A. Introduction........112

B. Results

There are two distinct populations of Pyk2 in unstimulated CTL clones; one that is associated with paxillin and one that is not........118

Phosphorylation of Pyk2 is one factor involved in the differential recognition of Pyk2 by the F298 and F245 antibodies........120

Pyk2 capable of associating with paxillin is less phosphorylated than Pyk2 that does not associate with paxillin........123

There is no difference in catalytic activity between paxillin-associated and non-associated Pyk2........127

Pyk2 that associates with paxillin localizes to the MTOC in unstimulated cells........129

Upon target cell stimulation, Pyk2 that associates with paxillin at the MTOC translocates with the MTOC to the CTL/target cell interface........131

F245-immunoreactive Pyk2 associates with surface biotinylated proteins in unstimulated CTL clones........133

C. Discussion........136

CHAPTER 6: Examination of the function of Pyk2 in CTL

A. Introduction........143

B. Results

Expression of the N-terminal and C-terminal Pyk2 constructs........149

Localization of the N-terminal and C-terminal Pyk2 fusion proteins........154

The effect of overexpression of NT Pyk2 and CT Pyk2 on MTOC reorientation........157

The effect of overexpression of NT Pyk2 and CT Pyk2 on cell surface translocation of CD107a (Lamp-1)........159

The effect of knockdown of Pyk2 expression on cell surface expression of CD107a on CTL clones........166

The effect of overexpression of NT Pyk2 and CT Pyk2 on cell spreading on immobilized anti-CD3........172

The effect of Pyk2 knockdown and overexpression of NT Pyk2 and CT Pyk2 on signalling after stimulation through the TCR........175

Assessing Pyk2 interacting proteins with GST-truncated Pyk2 fusion proteins........179

C. Discussion........183

CHAPTER 7: General discussion

A. Summary of results........196

B. Points of special interest

Common themes in the induction of Pyk2 phosphorylation........202

Pyk2 as a signal amplifier?........203

Recruitment of Pyk2 to the TCR/CD3 complex........204

A role for Pyk2 in MTOC polarization?........205

The potential involvement of Pyk2 in de-adhesion of CTL from target cells........209

C. Future directions........213

CHAPTER 8: Bibliography........216

APPENDIX

A.1 *CTL clones AB.1 and Clone 11 express low levels of Fyn*........242

A.2 *The protein complexes that form around the TCR/CD3 chains are not pre-formed*........242

A.3 *Two populations of Pyk2 exist in NIH-3T3 fibroblasts based on their differential ability to associate with paxillin*........245

A.4 *Phosphorylated Pyk2 is recruited to the CTL/target cell interface*........247

A.5 *Nck and ZAP-70 are present in a Pyk2 immunoprecipitation*........249

LIST OF TABLES

TABLE 6-1. Overexpression of NT Pyk2 and CT Pyk2 has no significant effect on MTOC reorientation 160

TABLE 6-2. Comparison of the percentages of GFP$^+$ CD107a$^+$ cells between clones expressing EGFP, EGFP-NT Pyk2 and EGFP-CT Pyk2 162

TABLE 6-3. Comparison of the percentages of CD107a$^+$ cells between clones nucleofected with Pyk2 siRNA or vehicle 169

TABLE 6-4. The absolute numbers and percentages of spreading nucleofected CTL clones 174

LIST OF FIGURES

FIGURE 1-1. CTL recognition of an appropriate target cell and lysis of the target by release of lytic granules........ 7

FIGURE 1-2. Major T cell signalling pathways........8

FIGURE 1-3. The structure, splice variants and major binding partners of FAK and Pyk2......17

FIGURE 3-1. Several tyrosine phosphorylated proteins are recruited to the TCR/CD3 complex upon stimulation of CTL clones with immobilized anti-CD3........57

FIGURE 3-2. Specific complexes form in association with CD3 after stimulation of CTL clones with plate-bound anti-CD3........59

FIGURE 3-3. Effect of the SFK inhibitor, PP2, on CTL functional responses, Lck activity, and tyrosine phosphorylation after TCR stimulation........62

FIGURE 3-4. CD3ζ, but not CD3ε, is phosphorylated and recruits ZAP-70 after anti-CD3 stimulation in the presence of the SFK inhibitor PP2........64

FIGURE 3-5. CD3ζ is phosphorylated in the presence of the SFK inhibitor, PP2, after stimulation of Con A blasts........67

FIGURE 3-6. CD3ζ phosphorylation and ZAP-70 recruitment occur after CD3 stimulation of JCaM1.6 cells........69

FIGURE 3-7. Pyk2 and Itk are recruited to the TCR/CD3 complex independent of SFK activity........71

FIGURE 4-1. Calcium signalling in T cells........81

FIGURE 4-2. Stimulation of CTL clones with the calcium ionophore ionomycin induces Pyk2 phosphorylation........85

FIGURE 4-3. Pyk2 phosphorylation is induced when $[Ca^{2+}]_i$ is increased with thapsigargin........88

FIGURE 4-4. Pyk2 phosphorylation induced upon cross-linked TCR stimulation is partially inhibited in the presence of the intracellular Ca^{2+} chelator BAPTA........90

FIGURE 4-5. Inhibiting actin polymerization with cytochalasin E has no effect on the induction of Pyk2 phosphorylation upon stimulation with cross-linked anti-CD3........92

FIGURE 4-6. Chelation of extracellular Ca^{2+} with EGTA does not inhibit the increase in Pyk2 phosphorylation induced upon TCR stimulation........94

FIGURE 4-7. Stimulation of Con A blasts with Ca^{2+} mobilizers induces Pyk2 phosphorylation....96

FIGURE 4-8. Pyk2 phosphorylation induced by ionomycin is calcineurin- and CaMKII-independent, but is partially SFK-dependent....98

FIGURE 4-9. Upon stimulation of CTL clones with ionomycin, no unique proteins interacting with Pyk2 could be detected when compared to control-treated cells....100

FIGURE 4-10. A significant increase in Pyk2 phosphorylation is not seen in all types of cells stimulated with ionomycin....101

FIGURE 4-11. A cumulative increase in Pyk2 phosphorylation is seen when CTL clones are simultaneously stimulated with fibronectin and ionomycin....104

FIGURE 5-1. Model for the interaction of the FAK FAT domain with the LD motifs of paxillin....115

FIGURE 5-2. A substantial amount of paxillin is only associated with F245-captured Pyk2....119

FIGURE 5-3. The F245 antibody preferentially recognizes Pyk2 that has reduced phosphorylation....122

FIGURE 5-4. The recognition sites for the F298 and F245 antisera....124

FIGURE 5-5. Pyk2 immunoreactive with the F298 antibody is more heavily phosphorylated on Y881....126

FIGURE 5-6. Pyk2 recovered with the F298 or F245 antiserum is catalytically active....128

FIGURE 5-7. Pyk2 that is capable of associating with paxillin co-localizes with paxillin at the MTOC....130

FIGURE 5-8. The localization of Pyk2 in CTL/target cell conjugates....132

FIGURE 5-9. F245-immunoreactive Pyk2 associates with surface biotinylated proteins in unstimulated cells....134

FIGURE 6-1. The sequences of Pyk2 used to make fusion proteins....150

FIGURE 6-2. Amplification of Pyk2 sequences from cDNA....151

FIGURE 6-3. Transfection efficiency achieved using Amaxa nucleofection on CTL clones..152

FIGURE 6-4. The extent of overexpression of the NT Pyk2 and CT Pyk2 constructs....153

FIGURE 6-5. The localization of EGFP and the EGFP-NT Pyk2 and –CT Pyk2 fusion proteins in CTL clones....155

FIGURE 6-6. A closer examination of the localization of the EGFP-NT Pyk2 fusion protein........156

FIGURE 6-7. A closer examination of the localization of the EGFP-CT Pyk2 fusion protein........158

FIGURE 6-8. CD107a (Lamp-1) cell surface expression upon degranulation in response to immobilized anti-CD3 stimulation........163

FIGURE 6-9. A representative example of the extent of knockdown of Pyk2 protein........167

FIGURE 6-10. CTL clones nucleofected with Pyk2 siRNA may adhere to their targets better than clones nucleofected with vehicle........171

FIGURE 6-11. Examination of the morphology of nucleofected CTL clones spreading on immobilized anti-CD3........173

FIGURE 6-12. The effect of knockdown of Pyk2 on the induction of general tyrosine phosphorylation in response to stimulation with immobilized anti-CD3........176

FIGURE 6-13. The effect of overexpression of the NT Pyk2 and CT Pyk2 fusion proteins on the induction of general tyrosine phosphorylation in response to stimulation with immobilized anti-CD3........178

FIGURE 6-14. Expression of the truncated Pyk2 GST fusion proteins........180

FIGURE 7-1. Model for the induction of Pyk2 phosphorylation upon stimulation of CTL clones with ionomycin or thapsigargin........198

FIGURE 7-2. Model for a conformational change within the FAT domain of Pyk2........200

FIGURE 7-3. Model for the potential involvement of Pyk2 in MTOC reorientation upon TCR stimulation........207

APPENDIX-1 CTL clones express very little Fyn compared to Jurkat T cells........243

APPENDIX-2 Recruited complexes are not pre-formed........244

APPENDIX-3 Two populations of Pyk2 exist NIH-3T3 fibroblasts based on their differential ability to associate with paxillin........246

APPENDIX-4 Phosphorylated Pyk2 is concentrated at the CTL/target cell interface........248

APPENDIX-5 Nck and ZAP-70 are present in a Pyk2 immunoprecipitation........250

LIST OF ABBREVIATIONS

aa	Amino acid
Ab	Antibody
ADAP	Adaptor adhesion and degranulation promoting adaptor protein
APC	Antigen presenting cell
ARF	ADP-ribosylation factor
ASAP1	Arf-GAP containing SH3, ankyrin repeats, and PH domain
ATP	Adenosine 5'-triphosphate
BAPTA-AM	[bis-(o-aminophenoxy)ethane-N,N,N',N'-tetra-acetic acid Tetrakis (acetoxymethyl ester)]
BCR	B cell receptor
BLT	Nα-benzylcarbonil-L-lysine thiobenzyl ester
BSA	Bovine serum albumin
CADTK	Calcium dependent tyrosine kinase
CAKβ	Cell adhesion kinase β
CaMK	Ca^{2+}/calmodulin-dependent protein kinase
CIAP	Calf intestinal alkaline phosphatase
ConA	Concanavalin A
CRAC	Ca^{2+}-release-activated Ca^{2+} channel
CRNK	CADTK or CAKβ-related non-kinase
Cska-ζ	Cytoskeleton-associated zeta
CTL	Cytotoxic T lymphocyte
DAG	Diacylglycerol
dCS	Defined bovine calf serum
DMEM	Dulbecco's Modified Eagle's Medium
DMSO	Dimethyl sulphoxide
D-PBS	Dulbecco's phosphate buffered saline
DTNB	5,5'-dithio-bis(2-nitrobenzoic acid)
ECL	Enhanced chemiluminescence
ECM	Extracellular matrix
EDTA	Ethylenediaminetetraacetic acid
EGF	Epidermal growth factor
EGFP	Enhanced green fluorescent protein
EGTA	Ethylene glycol tetra acetic acid
ER	Endoplasmic reticulum
ERK	Extracellular regulated kinase
ETK	Epithelial and endothelial kinase

FACS	Fluorescence-activated cell sorting
FAK	Focal adhesion kinase
FasL	Fas ligand
FAT	Focal adhesion targeting
FCS	Fetal calf serum
FERM	4.1 ezrin radixin moesin
FN	Fibronectin
FRNK	FAK-related non-kinase
Fyn	Fibroblast Src/Yes novel gene
GADS	Grb2-related adaptor protein
GAP	GTPase-activating protein
GDP	Guanosine 5'-diphosphate
GFP	Green fluorescent protein
Graf	GTPase regulator associated with FAK
Grb2	Growth factor receptor-bound protein-2
GST	Glutathione-S-transferase
GTP	Guanine 5'-triphosphate
Hic-5	Hydrogen peroxide inducible clone-5
HP	Hydrophobic patch
HRP	Horseradish peroxidase
ICAM-1	Intercellular adhesion molecule 1
Ig	Immunoglobulin
IMM	Immobilized antibody
IP	Immunoprecipitation
IP_3	Inositol-1,4,5-trisphosphate
IP_3R	Inositol-1,4,5-trisphosphate receptor
IS	Immunological synapse
ITAM	Immunoreceptor tyrosine-based activation motif
ITK	Interleukin-2 tyrosine kinase
JAK	Janus kinase
Lamp-1	Lysosome-associated membrane protein 1
LAT	Linker for activation of T cells
Lck	Lymphocyte-specific cytoplasmic protein-tyrosine kinase
LD	Leucine-rich motif
LFA-1	Lymphocyte function-associated antigen 1
mAb	Monoclonal antibody
MBP	Myelin basic protein
MHC	Major histocompatibility complex
MIP1-α, β	Macrophage inflammatory protein 1-α, β
MTOC	Microtubule organizing center

NFAT	Nuclear factor of activated T cells
NIR	Pyk2 N-terminal domain-interacting receptors
NK	Natural killer
NMR	Nuclear magnetic resonance
NP-40	Nonidet P-40
NRS	Normal rabbit serum
$p130^{CAS}$	v-CRK-associated tyrosine kinase substrate
PAK	p21-associated kinase
Pap	Pyk2 C-terminus-associated protein
PCL-γ	Phospholipase C-γ
PDGF	Platelet-derived growth factor
PE	Phycoerythrin
PI3K	Phosphoinositide 3-kinase
PIP_2	Phosphatidylinositol-4,5-bisphosphate
PKC	Protein kinase C
PP2	4-Amino-5-(4-chlorophenyl)-7-(*t*-butyl)pyrazolo[3,4-d]pyrimidine
PP3	4-Amino-7-phenylpyrazol[3,4-d]pyrimidine
PRNK	Pyk2-related non-kinase
PSGAP	PH and SH3 domain contining rhoGAP protein
PTK	Protein tyrosine kinase
PVDF	Polyvinylidene difluoride
Pyk2	Proline rich tyrosine kinase 2
Pyk2-H	Proline rich tyrosine kinase 2 - hematopoietic
RAFTK	Related adhesion focal tyrosine kinase
RANTES	Regulated upon activation normal T expressed and secreted
RIPA	Radioimmunoprecipitation assay
RPMI	Roswell Park Memorial Institute
RT-PCR	Reverse transcription – polymerase chain reaction
SDF-1α	Stromal-derived factor 1α
SDS-PAGE	Sodium dodecyl sulphate polyacrylamide gel electrophoresis
SERCA	Sarco-endoplasmic reticulum Ca^{2+}-ATPases
SFK	Src family kinase
SH2	Src homology 2
SH3	Src homology 3
siRNA	Short interfering ribonucleic acid
SLP-76	SH2 domain-containing leukocyte protein-76
SMAC	Supramolecular activation cluster
SMC	Smooth muscle cells
SOC	Store-operated channel
TCR	T cell receptor
TNF-α	Tumor necrosis factor-α

WASP	Wiskott-Aldrich syndrome protein
XL	Cross-linked antibody
ZAP-70	Zeta-associated protein-70

CHAPTER 1: Introduction

The adaptive immune system

The immune response is a highly specific defensive reaction of the body to invasion by substances or organisms that are recognized as foreign or non-self. The reaction to foreign material, or antigen, occurs in two waves; the innate immune response is triggered first and then the adaptive response is initiated. Innate mechanisms are not specifically altered by prior exposure to the same antigen while adaptive immunity creates a long-lasting defense that is specific to that antigen.

The innate immune system is composed of cells such as monocytes, macrophages, polymorphonuclear leukocytes, dendritic, mast and natural killer cells (NK). These cells are readily available to fight a diverse range of microorganisms and they require no previous exposure to defend against pathogens. However, these cells are generally not capable of totally eliminating these organisms. The adaptive immune response therefore exists to provide a more versatile defense system. However, the adaptive response takes 4-7 days to develop, thus the innate immune system is critical for containing an infection during this time and for providing activation signals for cells of the adaptive immune system. Together, these two systems provide effective protection against most invading organisms.

The cells that constitute the adaptive immune response are the B and T lymphocytes. B cells are responsible for antibody-mediated immunity (humoral immunity) as these cells differentiate into plasma cells that secrete antibodies upon activation. T cells are involved in cell-mediated immunity. There are two main types of T cells. The first type comprises the cytotoxic T lymphocytes (CTL) that kill cells infected with intracellular pathogens and tumour cells. The second type is composed of the T helper cells (T_H). T_H cells differentiate into T_H1, T_H2 or T_H17 cells that specialize in cytokine secretion. T_H cell differentiation is directed by the cytokines produced by pathogen-activated cells of the innate immune system. T_H1 cells enhance the clearance of intracellular pathogens. T_H2 cells mediate humoral immunity and allergic responses. T_H17 cells have been implicated in the response against extracellular bacterial pathogens. Regulatory T cells are another subset of T_H cells that mediate suppression of the immune system. A minor subset of T cells, called the γ:δ T cells, are found in the lymphoid tissue and in the epithelium. The function of these cells is still not clear.

B and T lymphocytes each express a single type of antigen receptor on the cell surface, the B cell receptor (BCR) and T cell receptor (TCR) respectively, which allows them to recognize to foreign antigens (such as molecules on the surface of microorganisms or substances such as toxins, drugs and chemicals). These cells are able to mount a specific immune response to most foreign antigens as each cell expresses a unique variant of the receptor. Therefore, the population of B and T cells in the body as a whole expresses a vast, highly diverse repertoire of receptors.

The TCR recognizes peptides derived from foreign protein bound to membrane glycoproteins called major histocompatibitiy complex (MHC) molecules. There are two types of MHC molecules. MHC class I molecules are expressed by all types of nucleated cells and present peptides derived from proteins located in the cytosol, such as proteins produced by viruses during an infection. MHC class II molecules are expressed only on the surface of professional antigen presenting cells (APC) (dendritic cells, macrophages and B cells). Dendritic cells uptake antigen at the site of an infection and transport it to the secondary lymphoid organs (spleen, lymph nodes and mucosal lymphoid tissues) where they encounter circulating T cells. MHC class II molecules present peptides from proteins in intracellular vesicles, such as those derived from microorganisms that have been phagocytosed or that persist within the vesicles of an APC. CTL are restricted to recognizing peptide in the context of MHC class I while T_H cells only recognize peptide in the context of MHC class II.

T cell development

As mentioned above, each T cell expresses a single, unique variant of the TCR. The receptor chain genes (α, β, γ and δ) are encoded in several pieces or gene segments that assemble by gene rearrangement. Each gene segment consists of multiple copies and it is the random selection of a single copy from each gene segment that allows for a large number of possible combinations and thus the great diversity of receptor repertoire. The process of TCR gene rearrangement occurs during T cell development. Progenitor T cells emigrate from the bone marrow to the thymus. These early progenitors are termed double negative (DN) cells based on their lack of expression of the co-receptors CD4 and CD8. Developing thymocytes commit to one of two lineages based on rearrangements of different TCR chain (α, β, γ or δ) gene loci and can either become γδ T cells or αβ T cells. The TCR β, γ and δ chain genes rearrange simultaneously within DN thymocytes. Although it is not completely understood how lineage commitment occurs, productive rearrangements of the γ and δ genes result in the expression of a γδ TCR. Productive rearrangement of a β chain gene allows the β chain to pair with a surrogate α chain forming a pre-TCR. The majority of developing thymocytes will commit to the αβ lineage. Once these rearrangements have occurred, the cells begin to proliferate and express both CD4 and CD8 and hence become double positive cells (DP). The α chain then attempts to rearrange, and if successful, pairs with the β chain and the cells bear a unique $\alpha\beta$TCR. DP thymocytes then undergo the processes of positive and negative selection. During positive selection, the cells that can recognize self major histocompatibility complex (MHC) receive a survival signal while those that cannot die by apoptosis (a form of cell suicide). During negative selection, thymocytes that express a TCR that binds too strongly to self peptide are removed from the repertoire (die by apoptosis) as they could, if left to mature, initiate autoimmune reactions. Only a small percentage of thymocytes survive these screening processes and mature further to become single positive (SP) cells that express either CD4 or CD8. These cells eventually emigrate from the thymus into the periphery. SP cells that express CD4 express a TCR that is restricted to MHC class II molecules (T_H) and SP cells that express CD8 express a TCR that is restricted to MHC class I molecules (CTL).

T cell differentiation in the periphery

Once in the periphery, T cells recirculate between the blood and the secondary lymphoid tissues. These T cells are called “naïve” as they have not yet encountered antigen. When a naïve T cell encounters and recognizes antigen presented by an APC in the secondary lymphoid tissues, it stops circulating and begins to proliferate. This process, known as clonal expansion, increases the number of rare antigen-specific T cells. These clones then differentiate into either CTL or T_H effector cells. These processes take approximately 3-5 days and account for the delay in the activation of the adaptive immune response. Effector cells then migrate to the site of infection where they will perform their effector function. Once foreign antigen has been removed from the body, most effector cells will die by apoptosis. However, some cells persist as memory cells. The number of memory T cells is approximately 100 to 1000 fold larger than the initial frequency of the responding antigen-specific T cells. These cells will become activated more quickly than naïve cells upon reinfection with the same pathogen.

Cytotoxic T cells

Effector $CD8^+$ T cells, or CTL, use two different effector mechanisms to kill their targets (cells presenting the appropriate foreign peptide in the context of MHC class I). The first is the upregulation of cell surface expression of FasL (Fas ligand) and the second is secretion of lytic granules containing perforin and granzymes (such as granzyme B) (Wong and Pamer 2003). FasL binds to and cross-links its ligand Fas (a member of the tumour necrosis factor death receptor family) expressed on target cells. This activates a cascade of cellular proteases called caspases which leads to apoptosis of the target cell (Groscurth and Filgueira 1998). Lytic granules contain a number of effector molecules including perforin and granzyme B. Perforin is a pore-forming protein that may create holes in the target cell membrane and granzyme B is a serine proteinase that, once inside the cytosol of a target cell, induces apoptosis by caspase-dependent and -independent mechanisms. Recent evidence suggests that these two effector molecules work together to induce apoptosis in that granzyme B is taken up by target cells via receptor-mediated endocytosis and perforin may then be involved in the release of granzyme B from endosomes (reviewed in (Barry and Bleackley 2002).

There are many steps leading up to the release of lytic granules (degranulation) and lysis of target cells (Figure 1-1). The initial interaction between a CTL and a potential target cell is mediated by adhesion molecules and integrins such as LFA-1 (leukocyte function-associated antigen-1). If the target cell expresses the appropriate peptide/MHC complex (pMHC), then the TCR is triggered. Signalling through the TCR causes a conformational change in LFA-1 thereby increasing its affinity for ligand on the surface of the target (Dustin and Springer 1989). This results in tighter adhesion to the target cell. During this time, extensive cytoskeletal rearrangements occur within the CTL. These rearrangements polarize the CTL to facilitate the focused delivery of effector molecules to the area of contact with the target cell. Reorganization of the actin cytoskeleton occurs along the contact site as the CTL maximizes its interaction with the target cell. The microtubule-organizing center (MTOC), the structure from which the microtubules emanate, reorients (along with the Golgi apparatus) to an area just underneath the contact site (Kupfer and Dennert 1984). Lytic granules then move along the microtubules and a fraction of the granules are released directionally towards the contact site (Trambas and Griffiths 2003). Upon delivery of this "lethal hit", the CTL releases from the dying target cell and then searches for another potential target.

Signalling through the TCR/CD3 complex

Upon recognition of pMHC complexes, a signal is received through the TCR and is transmitted inside the T cell (Figure 1-2). The TCR α and β chains (which bind directly to pMHC) are non-covalently associated with CD3 γ, δ, ε and ζ chains which contain signalling motifs within their cytoplasmic domains. Each αβ TCR associates

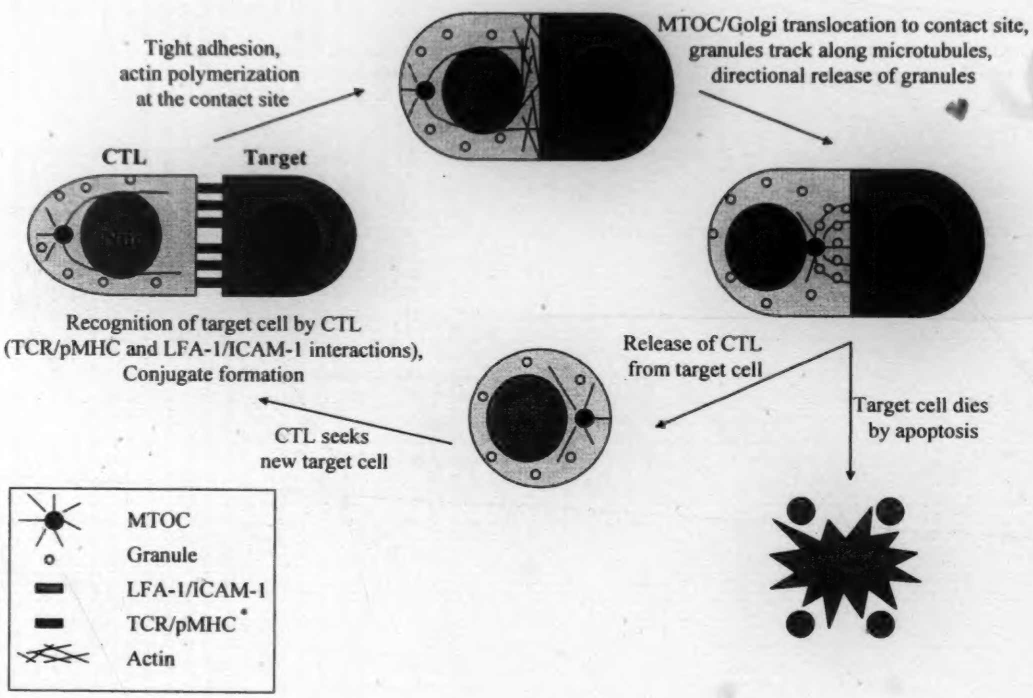

Tight adhesion,
actin polymerization
at the contact site
MTOC/Golgi translocation to contact site,
granules track along microtubules,
directional release of granules
CTL
Target
Recognition of target cell by CTL
(TCR/pMHC and LFA-1/ICAM-1 interactions),
Conjugate formation
Release of CTL
from target cell
Target cell dies
by apoptosis
CTL seeks
new target cell
MTOC
Granule
LFA-1/ICAM-1
TCR/pMHC*
Actin

FIGURE 1-1. CTL recognition of an appropriate target cell and lysis of the target by release of lytic granules.

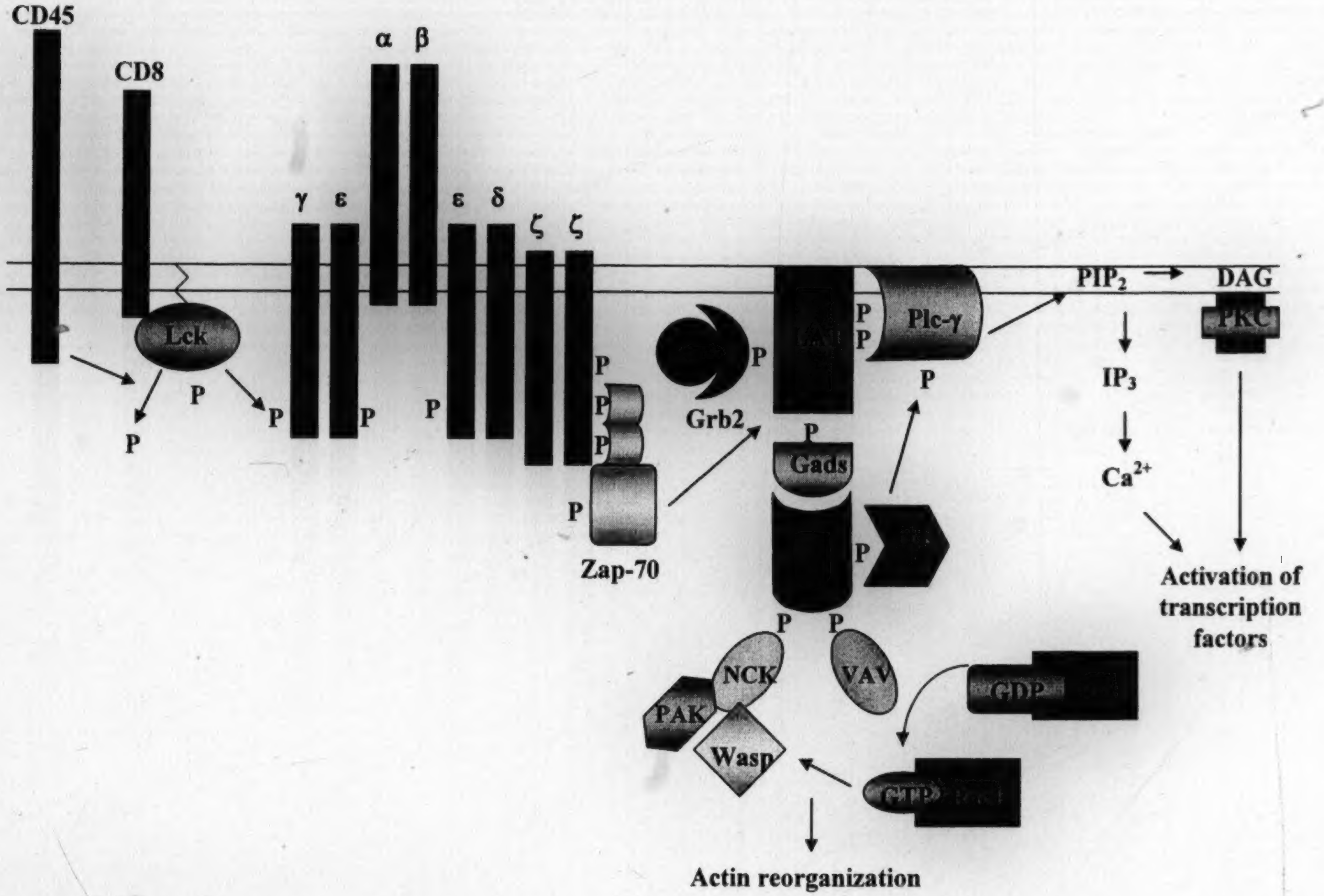
CD45
CD8
Lck
P
P
P
γ
ε
P
α
β
ε
δ
P
ζ
ζ
P
P
P
P
Zap-70
Grb2
P
P
P
Gads
P
Plc-γ
P
P
P
P
NCK
PAK
Wasp
VAV
GDP
GTP
Actin reorganization
PIP2
DAG
PKC
IP3
Ca2+
Activation of transcription factors

FIGURE 1-2. Major T cell signalling pathways.

with one δε and γε heterodimer and one ζζ homodimer (Kuhns et al. 2006). The signalling motifs within the CD3 chains are called ITAMs (immunoreceptor tyrosine-based activation motifs) and the γ, δ and ε chains each contain one ITAM while the ζ chain contains three ITAMs. Upon TCR stimulation, a tyrosine phosphorylation cascade is induced by protein tyrosine kinases (PTK). It is generally accepted that the Src family kinases (SFK) Lck (lymphocyte-specific cytoplasmic protein-tyrosine kinase) and Fyn (fibroblast src/yes novel gene) initiate the cascade. Lck associates with the cytoplasmic domains of the co-receptors CD4 and CD8 (Turner et al. 1990) and Fyn is thought to be directly associated, at low stoichiometry, with the TCR/CD3 complex (Samelson et al. 1990; Sarosi et al. 1992). These kinases become activated by constitutive dephosphorylation of the negative regulatory site by the transmembrane tyrosine phosphatase CD45 (Ostergaard et al. 1989; Hurley et al. 1993) and inducible phosphorylation of the autophosphorylation site. Upon TCR stimulation, these kinases are brought into close proximity by clustering of TCR/CD3 complexes and by binding of the co-receptors to MHC molecules which allows for trans-autophosphorylation. Active Lck, and to a lesser extent Fyn, phosphorylates the tyrosine residues located within the ITAMs of the CD3 chains (Iwashima et al. 1994; Weiss and Littman 1994; van Oers et al. 1996). Phosphorylation of CD3ζ allows for the recruitment and phosphorylation of the Syk family PTK ZAP-70 (zeta-associated protein-70) (Chan et al. 1992; Iwashima et al. 1994). Active ZAP-70 phosphorylates the integral membrane adaptor protein LAT (linker for activation of T cells) (Zhang et al. 1998). Phosphorylated LAT recruits a number of cytosolic adaptor proteins including Grb2 (growth factor receptor-bound protein-2) (Zhang et al. 1998), GADS (Grb2-related adaptor protein) (Liu et al. 1999) and

SLP-76 (SH2 domain-containing leukocyte protein-76) through the interaction of GADS (Liu et al. 1999). SLP-76 binds additional proteins and consequently a large complex of proteins is assembled around LAT/SLP-76. Two proteins that are recruited to the LAT/SLP-76 complex are PLC-γ (phospholipase C-γ) and the Tec family kinase ITK (interleukin-2 tyrosine kinase) (Zhang et al. 1998; Su et al. 1999). ITK phosphorylates PLC-γ thereby fully activating PLC-γ to catalyze the breakdown of the membrane lipid PIP_2 (phosphatidylinositol-4,5-bisphosphate) into DAG (diacylglycerol) and IP_3 (inositol-1,4,5-trisphosphate) (Schaeffer et al. 1999). DAG binds to serine/threonine protein kinase C (PKC) enzymes. The binding of IP_3 to its receptor in the membrane of the endoplasmic reticulum (ER) results in the release of Ca^{2+} from intracellular stores (Imboden and Stobo 1985) and initiation of the Ca^{2+} signalling cascade. The downstream effects of the activation of PKCs and Ca^{2+} signalling include the activation of transcription factors involved in IL-2 gene transcription and other genes important for cell proliferation.

Proteins involved in facilitating the reorganization of the actin cytoskeleton are also recruited to the TCR/CD3 signalling complex. The adaptor protein Nck facilitates the binding of WASP (Wiskott-Aldrich syndrome protein) to the LAT/SLP-76 complex (Barda-Saad et al. 2005). WASP is an adaptor protein that directly binds to actin and the Arp2/3 complex that comprises the molecular machinery for the initiation of actin polymerization (Marchand et al. 2001). VAV is also recruited to the LAT/SLP-76 complex (Wu et al. 1996) and acts as a guanine nucleotide exchange factor for the small GTPase family proteins Rac1 and CDC42 (Tybulewicz 2005). These small GTPases are regulators of the actin cytoskeleton. Thus, signalling initiated by TCR engagement activates a number of pathways in the T cell that collaborate to facilitate gene transcription and cytoskeletal rearrangements. In CTL, these pathways facilitate degranulation and killing upon recognition of a target cell.

The immunological synapse, lipid rafts and TCR microclusters

During the productive interaction between a T cell and an APC or target cell, significant reorganization of engaged receptors occurs at the contact site, which has been named the "immunological synapse" (IS) (Grakoui et al. 1999). These rearrangements are hypothesized to facilitate and sustain signalling through the TCR. Eventually, a stable "bull's-eye" structure is formed at the IS in which there is a central zone (called the central supramolecular activation cluster or cSMAC) that contains TCR/CD3 complexes and associated signalling molecules surrounded by a peripheral zone (the peripheral SMAC or pSMAC) that contains large adhesion molecules such as LFA-1 and their associated proteins (Monks et al. 1998). Beyond the pSMAC is the dSMAC (distal SMAC) which is rich in CD45 molecules (Freiberg et al. 2002). This formation is thought to aggregate signalling molecules and segregate CD45 phosphatases to prevent dephosphorylation of active SFK. Although it has been shown that this structure, or some variation of this structure, forms between many types of T cells and target cells, the precise mechanism by which it is formed and its function are under debate.

It is clear that TCR signalling occurs before the "bull's-eye" structure is formed (Freiberg et al. 2002; Lee et al. 2002). It has been hypothesized that aggregation of lipid rafts, plasma membrane microdomains enriched in sphingolipids and cholesterol along with certain signalling molecules such as Lck and LAT, is involved in mediating SMAC formation (Marwali et al. 2004). It has also been suggested that the actin cytoskeleton is involved due to the substantial actin polymerization that occurs at the contact site (reviewed in (Dustin and Cooper 2000). More recently, the concept of microclusters involving protein-protein interactions between TCRs, kinases and adaptor molecules as the initiators of signalling at the immunological synapse has been proposed (Campi et al. 2005; Yokosuka et al. 2005). Studies performed on T cells contacting artificial lipid bilayers containing pMHC and ICAM-1 (intercellular adhesion molecule 1; the ligand for LFA-1) have demonstrated that microclusters of TCRs that associate with important signalling molecules and adaptors such as Lck, ZAP-70, LAT and SLP-76 form within seconds of contact with the lipid bilayer (Campi et al. 2005; Yokosuka et al. 2005). These microclusters formed at the periphery of the contact site and then migrated towards the center (Campi et al. 2005; Yokosuka et al. 2005). Interestingly, the microclusters signalled as they migrated and disassembled as they reached the center of the contact site, implying that the cSMAC was an accumulation of partially disassembled microclusters (Campi et al. 2005; Yokosuka et al. 2005). However, the mechanism of formation and movement of microclusters has yet to be determined. Therefore, the precise mechanism by which signalling is initiated at an immunological synapse remains elusive, although themes such as protein clustering and exclusion are likely to be involved.

Integrins are involved in cell-matrix and cell-cell adhesions

Integrins are cell surface receptors that exist as heterodimers consisting of an α-subunit and a β-subunit. These receptors mediate the adhesion of cells to the extracellular matrix (ECM) or to other cells by linking the signals received from outside of the cell to the actin cytoskeleton on the inside of the cell. Integrin receptors display no intrinsic kinase activity and thus rely on protein complex formation with adaptor and signalling proteins to transmit the signal received from binding to a ligand or ECM component. Integrin subfamilies are typically identified by three β subunits (β1, β2 and β3). β1 and β3 integrins bind to components of the ECM such as fibronectin. LFA-1 is a β2 integrin which binds to ICAM-1 and plays an important role in adhesion of T cells to their targets and to endothelial cells during lymphocyte recirculation (Kinashi 2005).

Adhesion of cells to the ECM through integrins results in cell spreading and migration and is an important process during development, wound healing and inflammation. Following integrin ligation, integrins form small clusters which become associated with a number of proteins including cytoskeletal adaptor proteins, GTPases, kinases, phosphatases and proteases (Wozniak et al. 2004). These signalling complexes are called focal complexes and are formed at the periphery of spreading or migrating cells. Signalling initiated at focal complexes activates the small GTPases Rac1 and CDC42 which induce actin polymerization and the formation of actin filaments which allows for protrusion of the leading edge (Pollard and Borisy 2003). Some focal complexes transform into focal adhesions which are more stable structures that provide robust anchors to the ECM that can withstand pulling of the cell body in the direction of migration (Zaidel-Bar et al. 2003). Focal adhesions are located at the periphery of the cell and more centrally than focal complexes and are associated with the ends of stress fibres (bundles of actin filaments) (Wozniak et al. 2004). These two types of matrix adhesions are generally formed in adherent cells and differ in their protein composition (Zaidel-Bar et al. 2003). Proteins that are associated with these adhesions include, but are not limited to, talin, paxillin, vinculin, α-actinin, p130^{CAS} (v-CRK-associated tyrosine kinase substrate), FAK (focal adhesion kinase) and SFK (Zamir and Geiger 2001). These structures are continuously assembled and disassembled during migration in order to promote forward movement.

Leukocytes are highly motile cells and do not form focal complexes, focal adhesions or stress fibres (Samstag et al. 2003). Monocytes/macrophages, immature dendritic cells and osteoclasts instead form complexes called podosomes (Samstag et al. 2003; Marzia et al. 2006). Podosomes contain many of the same proteins as focal complexes and adhesions, however, they are much more dynamic (Marzia et al. 2006). T cells also form protein complexes around the cytoplasmic faces of clustered integrins at the leading edge of migrating cells. Such complexes are also formed during conjugation with an APC or target cell.

FAK and Pyk2: the two members of the focal adhesion tyrosine kinase family

Focal adhesion kinase (FAK) is a 125 kDa non-receptor tyrosine kinase that was originally cloned by Schaller and colleagues in 1992 as a substrate of the Rous sarcoma virus-encoded oncogene pp60$^{v\text{-}src}$ (Schaller et al. 1992). It was also independently cloned by Hanks and colleagues while attempting to identify new protein tyrosine kinases (Hanks et al. 1992). Based on its localization to focal adhesions in chicken embryo cells and increase in tyrosine phosphorylation upon integrin cross-linking, this new tyrosine kinase was designated as a focal adhesion kinase (Schaller et al. 1992). FAK is expressed in most tissues and cell types in mammalian species and homologues have been found in zebrafish (Henry et al. 2001), *Drosophila* (Dfak56) (Fox et al. 1999; Fujimoto et al. 1999; Palmer et al. 1999) and *C. albicans* (CaFak) (Santoni et al. 2002).

The second member of the focal adhesion kinase family, proline-rich tyrosine kinase 2 (Pyk2), was cloned in 1995 by Lev and colleagues as a Grb2-interacting protein (Lev et al. 1995). This 116 kDa protein was also cloned independently by four other groups and called cell adhesion kinase β (CAKβ) (Sasaki et al. 1995), related adhesion focal tyrosine kinase (RAFTK) (Avraham et al. 1995), calcium-dependent protein-tyrosine kinase (CADTK) (Yu et al. 1996) and FAK2 (Herzog et al. 1996). The expression of Pyk2 is more restricted than that of FAK in that it is primarily expressed in cells of the central nervous system and of hematopoietic lineage (Avraham et al. 2000). However, Pyk2 expression has been detected in other cell types (Yu et al. 1996; Brinson et al. 1998; Tang et al. 2002). Interestingly, even though Pyk2 is structurally related to FAK, it is generally not considered to be localized to focal adhesions. Instead, its subcellular localization has been described as diffused throughout the cytoplasm in chicken embryo fibroblasts (Schaller and Sasaki 1997), rat aortic smooth muscle cells (Zheng et al. 1998) and unstimulated monocytes (Williams and Ridley 2000; Watson et al. 2001) or perinuclear in macrophages (Duong and Rodan 2000) and in FAK$^{+/+}$ and FAK$^{-/-}$ mouse embryo fibroblasts (Sieg et al. 1998). It has also been found to co-localize with adhesive structures such as membrane ruffles and podosomes in spreading and motile monocytes and macrophages (Duong and Rodan 2000; Williams and Ridley 2000; Watson et al. 2001) and the sealing zone of osteoclasts (Lakkakorpi et al. 1999). Pyk2 has also been shown to co-localize with the microtubule cytoskeleton, at the MTOC, in both T cells and NK cells (Rodriguez-Fernandez et al. 1999; Sancho et al. 2000; Rodriguez-Fernandez et al. 2002).

FAK and Pyk2 exhibit approximately 45% amino acid identity and 65% similarity (Avraham et al. 1995; Sasaki et al. 1995; Herzog et al. 1996; Yu et al. 1996) and the proteins also share similar domain structure. Both proteins contain a centrally located kinase domain flanked by large N- and C-terminal regions (Avraham et al. 2000) (Figure 1-3). These two proteins differ from most other non-receptor tyrosine kinases in that they do not contain SH2 (Src homology 2) or SH3 (Src homology 3) domains. However, FAK and Pyk2 contain two proline-rich regions within the C-terminus that can interact with SH3 domain-containing proteins. Pyk2 also has a number of tyrosine residues which, upon phosphorylation, bind to SH2 domain-containing proteins (Avraham et al. 2000).

The regulation of tyrosine kinase activity by phosphorylation

There are four tyrosine residues that are conserved at analogous positions within FAK and Pyk2 (Figure 1-3). Tyrosine 397/402 (FAK/Pyk2 respectively) is located at the 3' end of the N-terminal domain and serves as the autophosphorylation site (Schaller et al. 1994; Park et al. 2004). Once this site becomes phosphorylated, the SFK SH2 domain can bind to FAK/Pyk2 (Cobb et al. 1994; Avraham et al. 2000). Two tyrosine residues (Y576/Y577 and Y579/Y580 of FAK and Pyk2 respectively) located within the activation loop of the catalytic domain function to enhance catalytic activity upon phosphorylation (Calalb et al. 1995; Park et al. 2004). The fourth tyrosine residue, Y925 in FAK and Y881 in Pyk2, has been implicated in recruiting the adaptor protein Grb2

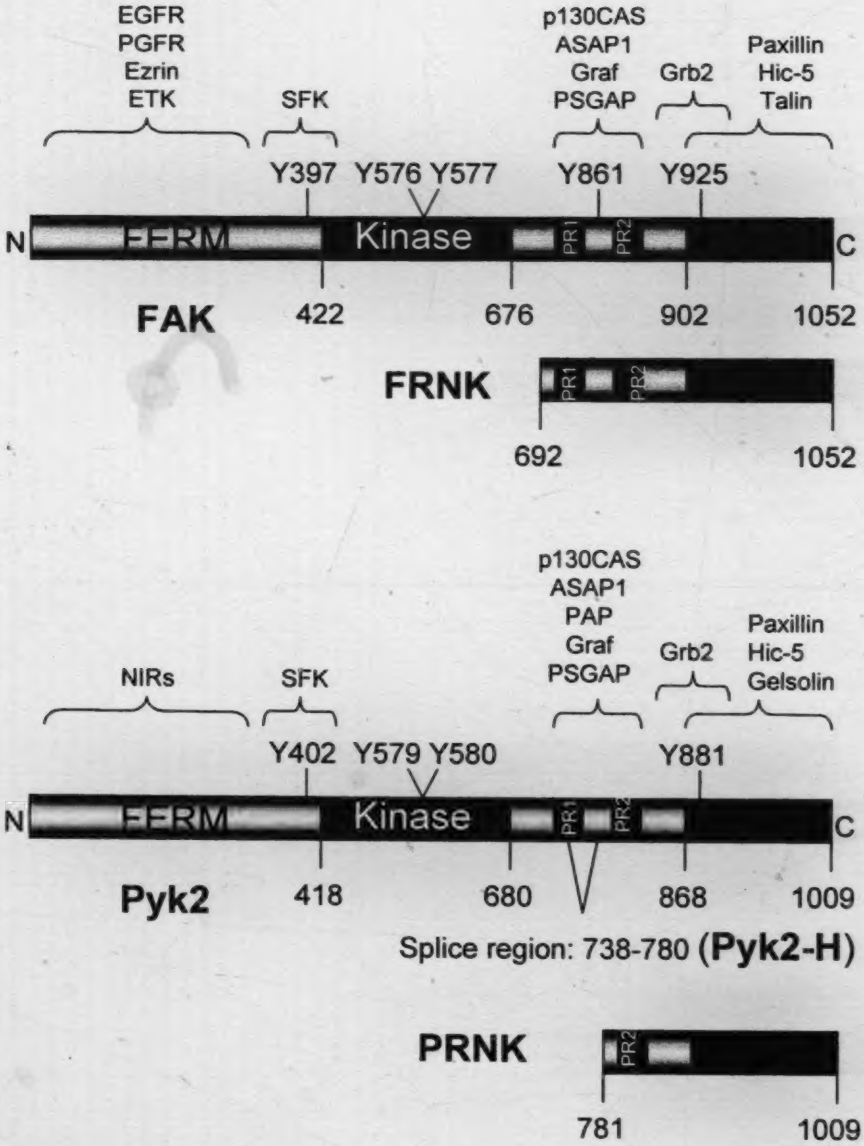
EGFR
PGFR
Ezrin
ETK
SFK
p130CAS
ASAP1
Graf
PSGAP
Grb2
Paxillin
Hic-5
Talin
Y397
Y576 Y577
Y861
Y925
N
FERM
Kinase
PR1
PR2
C
FAK
422
676
902
1052
FRNK
PR1
PR2
692
1052
p130CAS
ASAP1
PAP
Graf
PSGAP
NIRs
SFK
Grb2
Paxillin
Hic-5
Gelsolin
Y402
Y579 Y580
Y881
N
FERM
Kinase
PR1
PR2
C
Pyk2
418
680
868
1009
Splice region: 738-780 (Pyk2-H)
PRNK
PR2
781
1009

FIGURE 1-3. The structure, splice variants and major binding partners of FAK and Pyk2.

upon phosphorylation (Schlaepfer et al. 1994; Lev et al. 1995). The current model for activation of these two kinases is that upon stimulation, these proteins become autophosphorylated as a result of trans-autophosphorylation which allows for the recruitment of SFK. SFK phosphorylate additional tyrosine residues within the proteins thus enhancing catalytic activity and providing new docking sites for SH2 domain-containing proteins (Toutant et al. 2002; Park et al. 2004).

Proteins that interact with the N-terminal region of FAK and Pyk2

The N-terminal regions of FAK and Pyk2 have homology with FERM (4.1/Ezrin Radixin Moesin) domains (Figure 1-3). These domains are typically involved in binding to the cytoplasmic tail of transmembrane proteins and are found in proteins that act as cross-linkers between the plasma membrane and the actin cytoskeleton (Girault et al. 1999). The FERM domains of FAK and Pyk2 exhibit an approximate 14% mean identity with classical members of FERM domain-containing proteins (ezrin, radixin and moesin) and have therefore been deemed divergent FERM domains (Girault et al. 1999). Recently, it has been shown that these domains can also be involved in intramolecular interactions or homophilic interactions. For instance, the FERM domains of ezrin, radixin and moesin bind intramolecularly to a site in the C-terminus (Bretscher et al. 2002). This conformation suppresses the actin filament and membrane-binding activities of these proteins (Bretscher et al. 2002). A direct interaction has been shown to occur between the divergent FERM domain and kinase domain of Janus kinase (JAK) (Zhou et al. 2001). Interestingly, a similar intramolecular interaction (or homophilic interaction) has been demonstrated for FAK that appears to negatively regulate kinase activity

(Toutant et al. 2002; Cooper et al. 2003; Dunty et al. 2004). Although there has been speculation that the N-terminus of FAK binds to the cytoplasmic domain of integrins (and thus might be responsible for targeting the molecule to focal adhesions), there is no experimental evidence to support this notion. However, the N-terminus of FAK has been implicated in binding to the cytoplasmic domains of the EGF (epidermal growth factor) and PDGF (platelet-derived growth factor) receptors (Sieg et al. 2000). It has also been shown to interact with ezrin and the TEC-family kinase ETK (epithelial and endothelial kinase) (Chen et al. 2001; Poullet et al. 2001). To date, the function of the divergent FERM domain in Pyk2 has not been elucidated. The N-terminus of Pyk2 has been shown to bind to NIR (Pyk2 N-terminal domain-interacting receptors) proteins which are membrane-associated and localize to the ER and Golgi membranes (Lev et al. 1999; Lev 2004). Nir proteins display phosphotidylinositol transfer activity and have been implicated in lipid signalling, trafficking and metabolism as well as regulation of cytoskeletal elements (Lev et al. 1999; Lev 2004). The significance of this interaction is currently unknown.

Proteins that interact with the C-terminal region of FAK and Pyk2

As mentioned above, the C-termini of FAK and Pyk2 contain two proline-rich regions (Figure 1-3). The SH3 domain-containing proteins that have been demonstrated to interact with these proline-rich regions seem to fall into two categories. The first category comprises docking proteins that are found within focal adhesions such as p130^{CAS} (Polte and Hanks 1995; Harte et al. 1996; Astier et al. 1997; Ohba et al. 1998).

The second category is comprised of proteins which act as GTPase-activating proteins (GAP) towards members of the Ras superfamily of small GTP-binding proteins.

Small GTPases exist in two conformations: an active GTP-bound conformation and an inactive GDP-bound conformation (Hall 2005). The exchange of GDP for GTP is catalyzed by guanine nucleotide-exchange factors (GEFs) and the intrinsic GTPase activity of the small GTPase is stimulated by GAP proteins (Hall 2005). ASAP1 (Arf-GAP containing SH3, ankyrin repeats, and PH domain 1) binds to the second proline-rich region of FAK (Liu et al. 2002). ASAP1 displays GTPase-activity towards the Arf (ADP-ribosylation factor) family of small GTP-binding proteins which are normally implicated in endocytosis and vesicle trafficking, but have also been implicated in cytoskeletal remodelling (Norman et al. 1998). Overexpressed ASAP1 localized to focal adhesions and inhibited cell spreading and localization of FAK and paxillin to focal adhesions (Liu et al. 2002). ASAP1 has also been shown to interact with both proline-rich regions of Pyk2 (Kruljac-Letunic et al. 2003). Pyk2, but not FAK, was shown to tyrosine phosphorylate ASAP1 thus inhibiting GAP activity (Kruljac-Letunic et al. 2003; Kruljac-Letunic and Blaukat 2005). Pyk2 also interacts with another ARF-GAP (presumably through its proline-rich region) called Pap (Pyk2 C-terminus-associated protein) that displays 68% identity with ASAP1 (Andreev et al. 1999). Pyk2 (but not FAK) was also shown to phosphorylate Pap (Andreev et al. 1999). The functional significance of the interaction between Pyk2 and these ARF-GAP proteins remains to be determined. Another GAP that interacts with both FAK and Pyk2 is the Rho-GAP Graf (GTPase regulator associated with FAK) (Hildebrand et al. 1996; Ohba et al. 1998). The significance of these interactions was not elucidated. However, they may be important for remodelling the actin cytoskeleton as Rho family small GTP-binding proteins are regulators of the actin cytoskeleton. The RhoA/CDC42-GAP PSGAP (PH and SH3 domain containing rhoGAP protein), that has a structure that resembles that of Graf, also interacts with the proline-rich region of FAK and Pyk2 (Ren et al. 2001). Pyk2, but not FAK, phosphorylates PSGAP and thus abolishes the negative effect of PSGAP on GTP-CDC42 (Ren et al. 2001). Overexpression of PSGAP caused alterations in cell morphology in fibroblasts and disrupted focal adhesions (Ren et al. 2001). These results also implicate Pyk2 in the regulation of cytoskeletal organization.

The extreme C-termini of both FAK and Pyk2 contain a focal adhesion targeting (FAT) domain (Figure 1-3). This domain has been shown to be solely responsible for targeting FAK to focal adhesions (Hildebrand et al. 1993). Interestingly, the FAT domain of Pyk2, when overexpressed, targets to focal adhesions (Schaller and Sasaki 1997; Xiong et al. 1998). In contrast, overexpressed full length Pyk2 does not (Schaller and Sasaki 1997; Xiong et al. 1998). This suggests that the FAT domain of Pyk2 is indeed functional, but this domain may be somehow masked when the full length protein is expressed. Alternatively, the N-terminus of the protein may direct Pyk2 localization within the cell. The FAT domains of FAK and Pyk2 are responsible for binding to the cytoskeletal adaptor protein paxillin and the closely related adaptor protein Hic-5 (hydrogen peroxide inducible clone-5) (Hildebrand et al. 1995; Fujita et al. 1998; Matsuya et al. 1998; Xiong et al. 1998). The FAT domain of FAK also binds to the focal adhesion protein talin (Chen et al. 1995; Zheng et al. 1998). The actin-binding protein gelsolin has been shown to associate with the FAT domain of Pyk2 (Wang et al. 2003).

Splice variants of FAK and Pyk2

FAK and Pyk2 undergo alternative splicing. Most of the isoforms identified for FAK are preferentially expressed in neurons. They contain a three amino acid insertion in the C-terminus with or without additional amino acid insertions clustering around the autophosphorylation site, Y397 (Burgaya and Girault 1996; Burgaya et al. 1997). The function of these alternatively spliced isoforms is not known, but it has been suggested that amino acid insertions around Y397 enhance the rate of autophosphorylation by adding more length to the protein thus facilitating intramolecular phosphorylation of Y397 by the kinase domain (Toutant et al. 2002). Another isoform of FAK, named FAK-related non-kinase (FRNK), was originally cloned from chicken embryo fibroblasts (Schaller et al. 1993). FRNK consists of only the C-terminal portion of the protein and thus displays no kinase activity (Schaller et al. 1993) (Figure 1-3). FRNK encodes a protein of approximately 40 kDa, and like FAK, was found to target to focal adhesions (Schaller et al. 1993). Interestingly, expression of FRNK has been shown to be driven by an alternative promoter contained within an intron occurring 3' to the kinase domain and 5' to the C-terminal domain (Nolan et al. 1999). This isoform appears to have limited expression (Nolan et al. 1999) and is now thought to be primarily expressed in smooth muscle cells (SMC) (Taylor et al. 2001). It is speculated that the 5' coding region of FRNK contains SMC-specific promoter regions and this accounts for such selective expression (Taylor et al. 2001). FRNK is thought to act as a dominant negative towards full length FAK by sequestering FAK-interacting proteins. Some reported negative effects of overexpression of FRNK include reduced endogenous FAK phosphorylation (Richardson and Parsons 1996; Taylor et al. 2001), reduced tyrosine phosphorylation of

FAK substrates such as paxillin, p130CAS and tensin (Richardson and Parsons 1996; Richardson et al. 1997; Taylor et al. 2001) and decreased cell spreading and motility (Gilmore and Romer 1996; Richardson et al. 1997; Taylor et al. 2001).

Only two splice variants of Pyk2 (in addition to full length Pyk2) have been described (Figure 1-3). The first has been designated Pyk2-H or Pyk2s and is found primarily in hematopoietic cells (Dikic and Schlessinger 1998; Li et al. 1998; Xiong et al. 1998). Pyk2-H is missing exon 23 which encodes the 42 amino acids that encompass the second half of the first proline-rich region and some intervening sequence between the two proline-rich regions (Dikic and Schlessinger 1998; Li et al. 1998; Xiong et al. 1998). It is thought that this isoform is generated by alternative splicing as potential splice donor and acceptor splice sites are found in the sequence surrounding the spliced region (Li et al. 1998). It is not known why certain cells express only full length Pyk2 or Pyk2-H whereas others express both isoforms. It has been found that the C-termini of Pyk2 and Pyk2-H can associate with different tyrosine phosphorylated proteins (Dikic and Schlessinger 1998). Indeed, the binding of SH3 domain-containing proteins via the first proline-rich region may be compromised in the Pyk2-H isoform. The second isoform of Pyk2 is called Pyk2-related non-kinase (PRNK) and, like FRNK, constitutes the C-terminal portion of the protein (Xiong et al. 1998). PRNK encodes a 238 amino acid protein of approximately 29 kDa and encompasses the second proline-rich region and the FAT domain (Xiong et al. 1998). To date, this splice variant has only been demonstrated at the message level and was found to be expressed to the greatest extent in the brain and spleen (Xiong et al. 1998). Although it has not been demonstrated to naturally occur at the protein level, PRNK has been overexpressed in adherent cells and was found to target to focal adhesions unlike its full length counterpart (Schaller and Sasaki 1997; Xiong et al. 1998). PRNK may function as an endogenous dominant-negative inhibitor, as does FRNK. Indeed it has been shown that overexpression of PRNK in monocytes inhibited adhesion-induced phosphorylation of Pyk2, cell spreading and cell motility (Watson et al. 2001).

Pyk2 activation in T cells

Pyk2 has been shown to become activated in response to numerous extracellular signals including, but not limited to, integrin engagement, antigen receptor stimulation, activation of G-protein-coupled receptors (including chemokine receptors) and cytokine binding (reviewed in (Avraham et al. 2000). As this thesis involves the study of Pyk2 in T cells, this section will describe stimuli that activate Pyk2 in T cells. FAK activation has mainly been studied in response to integrin engagement of the ECM and will not be discussed in detail here. For the purposes of this thesis, it is important to note that FAK can also become phosphorylated in response to integrin engagement and TCR stimulation in T cells (Maguire et al. 1995; Berg and Ostergaard 1997; Ma et al. 1997).

Pyk2 becomes phosphorylated and activated upon stimulation of T cells with antibodies that bind the TCR/CD3 complex (Berg and Ostergaard 1997; Ganju et al. 1997; Qian et al. 1997). Although co-stimulation does not seem be necessary for the induction of Pyk2 phosphorylation, CD28 co-stimulation can enhance anti-CD3-induced Pyk2 phosphorylation (van Seventer et al. 1998; Katagiri et al. 2000). Similar to FAK, Pyk2 has been shown to become phosphorylated in response to stimulation through β_1 (van Seventer et al. 1998), β_2 (Rodriguez-Fernandez et al. 1999) and β_3 integrins (Ma et al. 1997). Integrin engagement can also provide a co-stimulatory signal to sub-stimulatory TCR stimulation (van Seventer et al. 1998). Other adhesion molecules that induce Pyk2 phosphorylation include CD44 (Li et al. 2001) and CD2 (Sunder-Plassmann and Reinherz 1998; Fukai et al. 2000). Pyk2 also becomes activated in T cells upon cytokine and chemokine binding to their receptors. Specifically, it becomes activated in response to IL-2, in a JAK-dependent manner (Miyazaki et al. 1998), and the chemokines MIP-1β (macrophage inflammatory protein 1β), RANTES (regulated upon activation normal T expressed and secreted) and SDF-1α (stromal-derived factor 1α) (Davis et al. 1997; Dikic and Schlessinger 1998; Ganju et al. 2000).

The regulation of Pyk2 activity in T cells

As mentioned earlier, SFK play a role in the activation of Pyk2. Autophosphorylated Y402 serves as a docking site for SFK which then bind and phosphorylate other tyrosine residues within Pyk2 (Park et al. 2004). The SFK implicated in binding to Pyk2 in T cells are Lck and Fyn (Berg and Ostergaard 1997; Ganju et al. 1997; Qian et al. 1997). Qian and colleagues examined the phosphorylation of Pyk2 in response to TCR stimulation in wild type, Lck- or Fyn-deficient thymocytes and lymph node T cells (Qian et al. 1997). They found that Pyk2 appeared to be a preferred substrate of Fyn, although both SFK could bind to Pyk2 (Qian et al. 1997).

Ca^{2+} is another second messenger that regulates Pyk2 phosphorylation and activation. Pyk2 was first described as a Ca^{2+}-dependent tyrosine kinase since its phosphorylation was dependent upon an increase in intracellular Ca^{2+} ($[Ca^{2+}]_i$) (Lev et al. 1995; Yu et al. 1996). Although the regulation of Pyk2 phosphorylation by Ca^{2+} has been well documented in many cell types, whether this occurs in T cells remains a matter of debate. Two groups have found that Pyk2 phosphorylation and activation could not be induced by an increase in $[Ca^{2+}]_i$ alone, as treatment of T cells with calcium ionophores did not induce Pyk2 phosphorylation or kinase activity (Qian et al. 1997; Rodriguez-Fernandez et al. 2002). Stimulation through the TCR causes an influx of extracellular Ca^{2+} and a consequent rise in $[Ca^{2+}]_i$. While one group found that chelating extracellular Ca^{2+} with EGTA (ethylene glycol tetra acetic acid) had no effect on TCR-induced Pyk2 phosphorylation (Qian et al. 1997), two other groups found that this resulted in a partial reduction in Pyk2 phosphorylation (Ganju et al. 1997; Tsuchida et al. 1999). Therefore, a more thorough investigation is necessary to clarify these results. Interestingly, the sequence of Pyk2 has not been predicted to contain a Ca^{2+} binding domain which suggests that it may be indirectly regulated by Ca^{2+}. The mechanism by which Ca^{2+} can mediate Pyk2 phosphorylation is currently unknown.

Pyk2 phosphorylation and activation also appear to be regulated by the actin cytoskeleton. One group found that stimulation of phytohemagglutinin-activated lymphoblasts through the integrin LFA-1 in the presence of cytochalasin D (which disrupts the actin cytoskeleton) or colchicine (which disrupts the microtubule cytoskeleton) inhibited Pyk2 kinase activity (Rodriguez-Fernandez et al. 1999). Another group found that stimulation of Jurkat T cells with cross-linked anti-CD3 in the presence of cytochalasin D caused a reduction in Pyk2 phosphorylation (Ganju et al. 1997). Results from our laboratory have shown that Pyk2 phosphorylation is induced by CD3 cross-linking (Berg and Ostergaard 1997). However, this method of stimulation does not require an active cytoskeleton (Berg et al. 1998). Therefore, the contribution of the actin cytoskeleton to the regulation of Pyk2 activation is unclear.

Many kinases undergo autoinhibition. One such mechanism has been described for FAK whereby an intramolecular interaction between the N-terminus and the kinase domain results in inhibition of FAK activity (Toutant et al. 2002; Cooper et al. 2003; Dunty et al. 2004). Although such a mechanism is conceivable for Pyk2, there is no experimental evidence to support the existence of such an autoinhibitory interaction.

Localization of Pyk2 in T cells and NK cells

The localization of Pyk2 in T cells and NK cells has been studied in response to both the recognition of target cells and integrin stimulation. In unconjugated Jurkat T cells, Pyk2 was found to form a cluster in the cytoplasm (Sancho et al. 2002). Upon stimulation of Jurkat T cells with either anti-CD3-coated beads or superantigen-pulsed target cells, Pyk2 was translocated to the interface between the T cell and target cell/bead (Sancho et al. 2002). Although the precise manner in which Pyk2 was recruited to the contact site was not elucidated, Lck activity and a phosphorylated ITAM were required (Sancho et al. 2002). Translocation to the interface was also observed in IL-2-activated NK cells interacting with target cells (Sancho et al. 2000). In this case, Pyk2 was also found in a cluster in the cytoplasm that co-localized with the MTOC (Sancho 2000). Upon conjugate formation, both the MTOC and Pyk2 translocated to the contact site (Sancho et al. 2000). It is likely that the cluster observed in Jurkat T cells was also co-localized with the MTOC, although this was not specifically addressed (Sancho et al. 2002). Co-localization of Pyk2 and the MTOC was also detected in IL-2-activated NK cells adhered to fibronectin (Sancho et al. 2000) and human T lymphoblasts stimulated through LFA-1 (Rodriguez-Fernandez et al. 1999; Rodriguez-Fernandez et al. 2002). Pyk2 was found to be concentrated in large aggregates at the adhesion site (plane closest to the surface of the slide) of cloned CTL adhered to immobilized fibronectin, as were tyrosine phosphorylated proteins (Doucey et al. 2003). Thus, in T cells and NK cells, Pyk2 appears to concentrate at the MTOC and in the adhesion zones that occur between an effector cell and its target and a T cell adhered to immobilized fibronectin.

Pyk2 function

Pyk2 knockout mice have been created and are viable and fertile (Okigaki et al. 2003). Compared to wild type littermates, these mice did not display any anatomical abnormalities, even in tissues in which Pyk2 is highly expressed (brain, spleen and thymus) (Okigaki et al. 2003). There was also no difference in the distribution of different lymphoid populations (macrophages, monocytes, NK cells, T cells or B cells) within the thymus, spleen, lymph nodes, bone marrow and peritoneal cavity (Okigaki et al. 2003). Although no defect with respect to T cells was noted, defects in both marginal zone B cells (B cells that reside at the red pulp/white pulp junction of the spleen) (Guinamard et al. 2000) and macrophages (Okigaki et al. 2003) were observed.

In Pyk2-deficient mice, marginal zone B cells are absent and the failure to form this compartment of the spleen was found to be due to an intrinsic B cell defect (Guinamard et al. 2000). The authors speculate that the absence of these cells occurs as a result of an impairment in motility and responsiveness to chemokines as other B cell populations in these mice displayed reduced motility and migration towards chemokine gradients (Guinamard et al. 2000).

Although no abnormality in the number and distribution of macrophages was noted in Pyk2-deficient mice, Okigaki and colleagues still examined the morphology and migration of macrophages isolated from these mice (Okigaki et al. 2003). Macrophage migration in response to a stimulus occurs in five identifiable steps: 1) the leading edge is extended towards the extracellular stimulus, 2) the leading edge adheres to the substrate, 3) the cytoplasm moves into the leading edge, 4) the lagging edge detaches from the substratum and 5) membrane receptors from the lagging edge recycle to the leading edge (Okigaki et al. 2003). Macrophages isolated from wild type mice expressed both FAK and Pyk2 and there was no increased expression of FAK in Pyk2-deficient macrophages (Okigaki et al. 2003). Pyk2-deficient macrophages displayed impaired migration in response to the chemokine SDF-1α {Okigaki, 2003 #176}. They were slower to form a leading edge than their wild type counterparts, failed to detach the lagging edge from the substratum and had a reduced ability to move the cell body into the leading edge (Okigaki et al. 2003). These cells also displayed an increase in the size of lamellipodia formed and in the number of cells spreading in response to MIP-1α (Okigaki et al. 2003). F-actin accumulated at multiple sites in the cell periphery of Pyk2-deficient macrophages exposed to MIP-1α, consistent with the extension of multiple lamellipodia and failure to orient properly towards a chemokine gradient (Okigaki et al. 2003). *In vivo*, Pyk2$^{-/-}$ macrophages migrated inefficiently during an acute inflammatory response (Okigaki et al. 2003). Pyk2-deficient macrophages also did not exhibit chemokine-induced Ca^{2+} release (Okigaki et al. 2003). Upon adhesion of Pyk2$^{-/-}$ macrophages to fibronectin, these cells displayed reduced activation of the small GTPase Rho and activation of PI3K (phosphoinositide 3-kinase) (Okigaki et al. 2003). Thus, the phenotypes of the Pyk2-deficient marginal zone B cells and macrophages suggest that Pyk2 plays an important role in the response to chemokines and cell polarization events.

Overexpression studies performed in hematopoietic and neuronal cells provide further insight into the role of Pyk2 in various cell processes. Watson and colleagues observed that transfection of freshly isolated monocytes, which do not express detectable FAK, with a GST (glutathione-S-transferase) fusion of the C-terminus of Pyk2 resulted in a defect in spreading and motility (Watson et al. 2001). Transduction of neutrophils with a Tat peptide fused to the C-terminus of Pyk2 inhibited the phosphorylation of endogenous Pyk2 and reduced chemokine-induced cell spreading (Han et al. 2003). Expression of PRNK blocked neurite outgrowth promoted by stimulation of neuronal PC12 cells with growth factors and integrins (Ivankovic-Dikic et al. 2000). Studies performed in NK cells have suggested that Pyk2 may be involved in cell polarization and lysis of target cells as overexpression of a kinase-inactive version of Pyk2 caused a defect in MTOC reorientation (Sancho et al. 2000) and inefficient lysis of target cells (Gismondi et al. 2000; Sancho et al. 2000). Overexpression of kinase-inactive Pyk2 also inhibited NK cell transendothelial migration in response to chemokines by reducing the activation of the small GTPase Rac (Gismondi et al. 2003). In this study, Pyk2 was implicated as an integration point between chemokine receptor and integrin stimulation (Gismondi et al. 2003). Very few overexpression studies have been performed in T cells. Overexpression of an autophosphorylation mutant of Pyk2-H (Y402F) in Jurkat T cells inhibited the phosphorylation and activation of endogenous Pyk2 in response to co-stimulation with anti-CD3 and anti-CD28 (Katagiri et al. 2000). In these cells, IL-2 production was reduced by a factor of two (Katagiri et al. 2000). Transfection of Jurkat T cells with PRNK inhibited integrin trans-regulation (Rose et al. 2003). Integrin trans-regulation occurs when the signals generated by engagement of one integrin affect the function of a second integrin. Together, these overexpression studies also point to a role for Pyk2 in the regulation of the cytoskeleton and cell polarization events.

A function for Pyk2 in linking integrin activation to cell migration and adhesion was highlighted in studies performed on B cells (McLeod et al. 2004; Durand et al. 2006). In this respect, it has been proposed that Pyk2 is a downstream target of Rap GTPase signalling (McLeod et al. 2004; Durand et al. 2006). The Rap GTPases are members of the Ras superfamily which have recently been implicated in inside-out signalling to integrins. Inside-out signalling occurs when signals from the cytoplasm, generated by external stimuli, result in changes in integrin activity. These signals can regulate the affinity and/or avidity modulation of these adhesive proteins (Kinashi and Katagiri 2004). Affinity and avidity modulation of integrins serves to increase the adhesiveness of cells to integrin ligands, which is central to lymphocyte trafficking and antigen recognition (Kinashi and Katagiri 2004). In lymphocytes, inside-out signaling is triggered in response to intracellular signals generated by antigen receptor and chemokine receptor ligation. Rap GTPases have also been implicated in cell polarization of lymphocytes (Shimonaka et al. 2003). In B cells, Rap is involved in integrin-dependent adhesion, cell spreading, actin polymerization (McLeod et al. 2004) and cell migration in response to a chemokine gradient (McLeod et al. 2004; Durand et al. 2006). Blocking Rap activation in B cells plated on collagen/fibronectin ECM and stimulated with chemokines, inhibited chemokine-induced Pyk2 phosphorylation (McLeod et al. 2004; Durand et al. 2006). Thus it was suggested that chemokine-induced Rap activation increases integrin adhesiveness which allows for outside-in integrin signalling that results in the induction of Pyk2 phosphorylation (Durand et al. 2006). In this way, Pyk2 may serve to link Rap activation to integrin-mediated signalling events that modulate cell migration in response to chemokine gradients (Durand et al. 2006).

Differences between FAK and Pyk2

Although FAK and Pyk2 display a high degree of sequence similarity and phosphorylate and bind to a common subset of proteins, there is evidence that these two proteins are not totally redundant. For instance, each protein is capable of binding to unique proteins via their N- and C-terminal domains (as discussed in the sections above). There are also differences in the regulation of FAK and Pyk2, in that only Pyk2 appears to be regulated by Ca^{2+} (Lev et al. 1995; Yu et al. 1996). One striking difference between these two proteins is illustrated when the localization of the two proteins are compared in adherent cells. While FAK targets to focal adhesions, Pyk2 is found diffused throughout the cytoplasm (Schaller and Sasaki 1997; Xiong et al. 1998). However, despite the differences with respect to binding partners and cellular localization, both FAK and Pyk2 have been implicated in facilitating similar biological outcomes such as cell spreading and migration (Ilic et al. 1995; Duong and Rodan 2000; Watson et al. 2001).

More evidence that FAK and Pyk2 are not totally redundant stems from studies performed on cells isolated from FAK and Pyk2 knockout mice. $FAK^{-/-}$ mice are embryonic lethal (Ilic et al. 1995), which suggests that Pyk2 cannot compensate for the loss of FAK function during gastrulation. FAK-deficient mice displayed the same overall phenotype as fibronectin-deficient mice (Ilic et al. 1995). Therefore, the response to binding to fibronectin was studied in embryonic fibroblasts isolated from FAK$^{-/-}$ mice (Ilic et al. 1995). FAK-deficient embryonic fibroblasts adhered to fibronectin but exhibited a rounded morphology and had an increased number of focal adhesions (Ilic et al. 1995). These cells also did not display a polarized migratory shape and had decreased migration rates compared to FAK-expressing embryonic fibroblasts (Ilic et al. 1995). A later study demonstrated that even though Pyk2 expression and SFK kinase activity were increased in these cells, compared to FAK-expressing cells, migration on fibronectin could not be recapitulated to nearly the same extent as re-introducing FAK into FAK-deficient cells (Sieg et al. 1998). Similarly, it was shown that FAK was expressed by Pyk2-deficient macrophages, and FAK expression was not able to compensate for the inability of these cells to properly polarize and migrate in response to a chemokine gradient (Okigaki et al. 2003). Although compensation was not observed in cells from FAK- or Pyk2-deficient mice, similar phenotypes were observed in cells lacking either FAK or Pyk2. For example, cells deficient in either protein exhibited an inability to polarize properly, and displayed increased adherence and reduced mobility (Ilic et al. 1995; Sieg et al. 1998; Okigaki et al. 2003). This suggests that although the two kinases may not become activated or be regulated in similar manners, they may function to effect similar biological outcomes. Differential expression of the two kinases by different cell types also suggests that the cell type in question plays an important part in which kinase is likely to play a more dominant role in effecting such biological outcomes.

Study objectives

The goal of the present study was to further examine the role and regulation of Pyk2 in T cells. The specific questions that were addressed include:

1) Is Pyk2 recruited to the TCR/CD3 complex?
2) Is Pyk2 phosphorylation and activation regulated by protein folding or intramolecular interactions?
3) Is Pyk2 phosphorylation regulated by an increase in intracellular Ca^{2+} in CTL?
4) What is the function of Pyk2 during CTL activation?

By determining a role for this protein in CTL, I will learn more about how these cells become activated to perform their cytolytic function to eliminate cells infected with pathogens and tumour cells.

CHAPTER 2: Materials and Methods

Cells

The murine CD8$^+$ CTL clone AB.1 and clone 11 (H-2^d anti H-2^b) have been described previously (Blakely et al. 1987; Kane et al. 1989). The clones were stimulated weekly with irradiated allogeneic C57BL/6 splenocytes and recombinant IL-2 and were used for experiments 4–6 days after stimulation. Clones were maintained in RPMI supplemented with 10% fetal calf serum (FCS), L-glutamine, penicillin/streptomycin, non-essential amino acids, sodium pyruvate and β-mercaptoethanol. Con A (Concanavalin A) blasts were generated by culturing C57BL/6 splenocytes with 2 μg/ml Con A for 48 hours. WEHI-231 cells were kindly provided by Dr. M. R. Gold (University of British Columbia, Vancouver, BC). Con A blasts and WEHI-231 were cultured in RPMI supplemented with 10% FCS, L-glutamine, sodium pyruvate and β-mercaptoethanol. EL4, human Jurkat T cells and the Lck-deficient variant JCaM1.6 were obtained from American Type Culture Collection. Jurkat T cells and JCaM1.6 were maintained in RPMI supplemented with 8% and 10% FCS respectively. NIH-3T3 cells were obtained from Dr. J. C. Stone (University of Alberta, Edmonton, AB) and were maintained in DMEM supplemented with 10% FCS. RNK-LY49P and L1210$^{Kb/Dd}$ were a gift from Dr. K. P. Kane (University of Alberta, Edmonton, AB). RNK-LY49P cells were cultured in RPMI with 10% FCS, L-glutamine, penicillin/streptomycin and β-mercaptoethanol. B3Z cells were a generous gift from Dr. N. Shastri (University of California, Berkley, CA). B3Z, EL4 and L1210$^{Kb/Dd}$ were cultured in DMEM with 8% defined bovine calf serum (dCS).

Antibodies

The source and purification of antibodies from hybridomas producing 145-2C11 (anti-CD3ε), H57–597 (anti-TCRβ), I3/2.3 (anti-CD45, pan-specific), MB23G2 (anti-CD45RB), MB4B4 (anti-CD45RB), M1/42.3.9.8 (anti-MHC class I), OKT3 (anti-CD3ε), and PY72.10.5 (anti-phosphotyrosine) have been described previously (Ostergaard et al. 1998). The hybridoma producing H146-968A was obtained from Dr. M. C. Miceli (University of California, Los Angeles, CA) (Rozdzial et al. 1994). Polyclonal anti-Lck (C437) used for Lck immunoprecipitations was generated in our laboratory using a bovine serum albumin (BSA)-coupled peptide based on amino acids (aa) 476–509 of Lck. Polyclonal anti-GST (F307) was generated in our laboratory by injecting GST (glutathione-S-transferase) protein into rabbits. The polyclonal anti-Pyk2 antibodies F298 and F245 were generated in our laboratory by injecting New Zealand White rabbits with a peptide corresponding to aa 2-12 (F298) or aa 720-826 fused to GST (F245) and have been described previously (Berg and Ostergaard 1997). Anti-ERK2, anti-Lck, anti-Pyk2/CAKβ, anti-Nck, anti-paxillin, anti-ZAP70 and anti-rat Ig-PE (phycoerythrin) were purchased from BD Biosciences (Mississauga, ON). Anti-CD3ε (M-20), anti-CD3ζ (6B10.2), anti-CD107a (LAMP-1), anti-Nck1/2 (C-19), anti-αPAK (N-20), anti-Pyk2 (C-19 and N-19), and anti-goat IgG-HRP (horseradish peroxidise) were purchased from Santa Cruz Biotechnology (Santa Cruz, CA). The Pyk2 phospho-specific antibodies pY^{402}, pY^{579}, pY^{580} and pY^{881} were purchased from Biosource International (Camarillo, CA). Anti-phospho-Pyk2 Y^{881} was also purchased from Sigma (St. Louis, MO) as was anti-actin. Anti-phospho-Pyk2 Y^{402} (mouse monoclonal) was purchased from Upstate Cell Signaling Solutions (Charlottesville, VA). Anti-phospho-p44/42 MAPK (anti-phospho-ERK) was purchased from Cell Signaling Technology (Beverly, MA). Anti-α-tubulin (mouse monoclonal), anti-GFP (rabbit polyclonal), anti-GFP (mouse monoclonal), anti-mouse-Alexa Fluor 488, anti-rabbit-Alexa Fluor 488 anti-rabbit-Alexa Fluor 594 and anti-goat-Alexa Fluor 555 were purchased from Molecular Probes (Eugene, OR). Anti-α-tubulin (rabbit polyclonal) was purchased from Abcam Inc (Cambridge, MA). Anti-hamster IgG-HRP, goat anti-hamster IgG, anti-mouse IgG-HRP, anti-mouse-rhodamine, anti-rabbit-FITC and streptavidin-DTAF were purchased from Jackson ImmunoResearch Laboratories (West Grove, PA).

Reagents

Protein A-HRP and EZ-Link Sulpho-NHS-Biotin were purchased from Pierce (Rockford, IL). Protein A Sepharose and Glutathione Sepharose 4B were purchased from Amersham Biosciences (Piscataway, NJ). Calf intestinal alkaline phosphatase (CIAP) was purchased from Invitrogen (Carlsbad, CA). Ionomycin, BAPTA-AM, KN-62, the SFK inhibitor, PP2, and the inactive analog, PP3, were purchased from Calbiochem (San Diego, CA). Myelin basic protein (MBP), cytochalasin E, colchicine, propyl gallate and thapsigargin were purchased from Sigma (St. Louis, MI). CellTracker Orange CMRA was purchased from Molecular Probes (Eugene, OR). Human cellular fibronectin was purchased from Upstate Biotechnology (Lake Placid, NY). FK506 and cyclosporin A were a kind gift from Dr. S. L. Schreiber (Howard Hughes Medical Institute, Boston, MA). Pyk2 siRNA (short interfering ribonucleic acid) oligomers were designed, chemically synthesized and annealed by Dharmacon Research Inc. (Lafayette, CO). The oligonucleotide sequence for murine Pyk2 was 5' GAA CAU GGC UGA UCU CAU

AUU 3' (sense strand). ERK2 (MAPK1) oligos were provided with the RNAi Human/Mouse Control Kit distributed by Qiagen (Mississauga, ON).

Cloning murine Pyk2-H

RNA was extracted from AB.1 cells using Trizol reagent (Invitrogen, Carlsbad, CA). First strand cDNA was synthesized using SuperScript II reverse transcriptase (Invitrogen, Carlsbad, CA) and Oligo (dT) primers. Amplification of full length Pyk2 (FL Pyk2 – aa 1 - 1009), the N-terminus of Pyk2 (NT Pyk2 – aa 1-421) and the C-terminus of Pyk2 (CT Pyk2 – aa 678 – 1009) was performed from first strand cDNA (aa numbering based on the sequence of full length Pyk2). The primers for FL Pyk2 were 5' CAT AGG AAT TCG CAG TCT GAG AGG ATG TCC 3' (forward) and 5' CAG GTT CGT CGA CGA AGA TGC AGG CAG GTG G 3' (reverse) which introduced an EcoR I and Sal I site respectively into the ends of the amplified sequence. The forward primer for NT Pyk2 was the same forward primer used for FL Pyk2 and the reverse primer was 5' CTT CGG AGT CGA CGG CAA CAC CGT ACT GTG G 3' which inserted a Sal I site on the end of the sequence. The forward primer for CT Pyk2 was 5' CCA GTG AAT TCC AGC CTC AGT GAC ATT TAT C 3' which inserted an EcoR I site on the end of the sequence and the reverse primer was the same primer used for FL Pyk2. PCR products were purified using the Qiaquick PCR purification kit (Qiagen, Mississauga, ON). PCR products and vectors (pBluescript SK (+/-), pEGFP-C1, pDsRed-Monomer-C1 and pGEX-4T-3) were then digested with EcoR I and Sal I for 4 hours at 37°C. Digests were run on 0.75% TAE gels with 1 mM guanosine. Bands were excised and run through glass wool columns and DNA was extracted with phenol/chloroform. FL Pyk2 was ligated into pBluescript and NT Pyk2 and CT Pyk2 were ligated into pEGFP-C1, pDsRed-Monomer-C1 and pGEX-4T-3.

Antibody immobilization

For immobilizing antibodies on plastic, 60 mm, non-tissue culture-treated plates were incubated with 10 μg/ml 145-2C11 or other monoclonal antibody overnight at 4°C. The plates were washed twice with Dulbecco's phosphate buffered saline (D-PBS) containing calcium and magnesium, blocked with 2% BSA/PBS for 30-60 minutes at 37°C, and then washed three times with D-PBS before use.

Cell stimulation with cross-linked and immobilized anti-CD3

Cloned CTL were harvested and washed three times with D-PBS (Life Technologies). For cross-linked anti-CD3 stimulation, cells were resuspended at 1 X 10^7 cells/ml D-PBS or RPMI 1640 and chilled on ice. 1 X 10^7 cells were incubated with 10 μg/ml 145-2C11 for 15 minutes on ice. After 15 minutes, the cells were pelleted and resuspended in D-PBS or RPMI 1640 (with drug or carrier control if applicable) and 5 μg/ml goat anti-hamster was added to cross-link the 145-2C11 antibody. Cells were incubated at 37°C for an appropriate time, after which the cells were pelleted, resuspended in 1% NP-40 lysis buffer (1% Nonidet P-40, 10 mM Tris (pH 7.5), 150 mM NaCl, and 1 mM sodium vanadate) and lysed on ice for 20 minutes. Post-nuclear lysates were then used for immunoprecipitation. A sample of post-nuclear lysate containing 4 X 10^5 cell equivalents was saved for further analysis.

For immobilized anti-CD3 stimulation, clones were resuspended at 1 X 10^7 cells/500 µl D-PBS or RPMI and chilled on ice. 1 X 10^7 cells were added to BSA- or 145-2C11-coated dishes (as described in *Antibody immobilization*) and incubated at 37°C for an appropriate time. Cells were lysed in the dishes for 20 minutes by addition of 1.5% NP-40 lysis buffer. Lysates were removed from the dishes. Post-nuclear lysates were then used for immunoprecipitation. A sample of post-nuclear lysate containing 2.7 X 10^5 cell equivalents was saved for further analysis.

Where indicated, clones were pretreated with PP2, PP3, BAPTA-AM, cytochalasin E or 4 mM EGTA/8 mM $MgCl_2$ for 15 minutes on ice before anti-CD3 stimulation.

Stimulation with calcium mobilizing agents

Cells were harvested and washed three times with D-PBS. Cells were resuspended at 1 X 10^7 cells/ml D-PBS and chilled on ice. Either ionomycin, thapsigargin or DMSO (dimethyl sulphoxide) (carrier control) was added to 1 X 10^7 cells and the cells were incubated at 37°C for 10 minutes. After 10 minutes, the cells were pelleted and lysed in 1% NP-40 lysis buffer for 20 minutes on ice. Post-nuclear lysates were then ready to use for immunoprecipitation.

Where indicated, cells were pretreated with 4 mM EGTA/8 mM $MgCl_2$, FK506, cyclosporin A, KN-62 or 10 µM PP2/PP3 for 15 minutes on ice. A sample of post-nuclear lysate containing 4 X 10^5 cell equivalents was saved for further analysis.

Recovery of complexes associated with immobilized antibody

Cells were stimulated with immobilized anti-CD3 with or without PP2/PP3 as described above (*Cell stimulation with anti-CD3*). After removal of the cell lysates, BSA- or 145-2C11-coated dishes were vigorously washed three times with 1% NP-40 lysis buffer to ensure that all cellular debris was removed. The immobilized antibodies and associated proteins were eluted from the dish by adding 80 μl of 1X Laemmli reducing sample buffer and heating the plates to 55°C. The entire sample of eluted protein was loaded into a single lane of an SDS-PAGE (sodium dodecyl sulphate polyacrylamide gel electrophoresis) gel. When used, PP2 was not added to the lysis buffer used to wash plates, because we have found that its inclusion in the washes does not impact the quality or quantity of phospho-proteins recruited to the TCR/CD3 complex.

Immunoprecipitation

Post-nuclear cell lysates containing 1 X 10^7 cell equivalents were incubated with anti-Pyk2 antisera (F298 or F245), anti-phosphotyrosine (PY72) or anti-Lck antisera (C437) for 15 minutes on ice. Protein A Sepharose was then added (30 μl of a 50% slurry) and samples were rotated at 4°C for approximately 2 hours (Pyk2 and Lck) or overnight (phosphotyrosine). Beads were pelleted and washed three times with either 1% NP-40 lysis buffer or radioimmunoprecipitation assay (RIPA) buffer. Beads were resuspended in 80 μl of 1X Laemmli reducing sample buffer and boiled for 3 minutes. Samples were then loaded onto SDS-PAGE gels.

For sequential Pyk2 immunoprecipitations, post-nuclear lysates were immunoprecipitated with the first Pyk2 antisera (either F298 or F245) overnight at 4°C at which time, the beads were pelleted and the lysate was transferred to a new tube. Beads from the first immunoprecipitation were washed three times with RIPA buffer, resuspended in 1X Laemmli reducing sample buffer and boiled for 3 minutes. The lysate was next immunoprecipitated with the second Pyk2 antisera (either F298 or F245) overnight at 4°C. Beads were washed and resuspended as described above.

For alkaline phosphatase treatment of Pyk2 immunoprecipitates, 2 hour Pyk2 immunoprecipitates were washed three times with 1% NP-40 lysis buffer and then subjected to treatment with CIAP or CIAP dilution buffer as a carrier control (100 μl reaction volume). Beads were resuspended in 70 μl of sterile water. 10 μl of 10X buffer was added along with 20 μl of CIAP (20 Units) or dilution buffer. Reactions proceeded at 37°C for 3 hours with occasional agitation. After 3 hours, beads were pelleted, washed twice with 1% NP-40 lysis buffer, resuspended in 1X Laemmli reducing sample buffer and boiled.

Western blotting and Coomassie Blue staining

Samples were loaded onto SDS-PAGE gels that were run at 7 mA overnight. The gels were then either transferred to polyvinylidene difluoride (PVDF) membranes or stained with Coomassie Blue. Immunoblotting was performed using the appropriate primary and HRP-coupled secondary antibody and was visualized by enhanced chemiluminescence (ECL) (PerkinElmer Life Science Products, Boston, MA). When multiple immunoblots were performed on the same membrane, the membrane was stripped (in buffer containing β-mercaptoethanol, SDS and Tris-HCl (pH 6.7) at 56°C) in between each blot. Anti-phosphotyrosine blots were always executed first and loading controls were usually completed last.

Lck in vitro kinase assays

AB.1 cells were washed three times with D-PBS, and 1 X 10^7 cells were resuspended in RPMI 1640. Cells were pretreated with DMSO carrier control, a titration of PP2, or 20 μM PP3 for 15 minutes on ice. Cells were lysed with 1% NP-40 lysis buffer with or without PP2/PP3. Lck or normal rabbit serum (NRS) immunoprecipitations were performed on post-nuclear lysates. Immunoprecipitates were washed twice with RIPA buffer with or without PP2/PP3 and once with HEPES kinase buffer (10 mM HEPES (pH 7.1) and 10 mM $MnCl_2$) with or without PP2/PP3. Kinase reactions contained Lck or NRS immunoprecipitates, 5 μg of MBP substrate, 1 mM ATP, and either PP2 or PP3 in 50 μl. Kinase reactions proceeded for 30 minutes at 32°C, at which time the beads containing immunoprecipitates were pelleted (6,000 RPM for 1 minute at 4°C), and 40 μl of the supernatant containing the substrate was transferred to a new tube. Substrate-containing supernatant was loaded onto a 15% SDS-PAGE gel. Proteins were transferred, and the membrane was probed with anti-phosphotyrosine. A portion of the sample was stained with Coomassie Blue to detect MBP protein loading. Lck immunoprecipitates were run on an 8.5% gel and transferred, and the membrane was blotted for Lck as a loading control.

Pyk2 in vitro kinase assays

AB.1 cells were stimulated with cross-linked anti-CD3 (or secondary antibody only as an unstimulated control) for 10 minutes as described in *Cell stimulation with anti-CD3*. Cells were lysed and duplicate Pyk2 immunoprecipitations were performed for 3 hours with either F298 or F245 antisera as mentioned above (*Immunoprecipitation*). One set of immunoprecipitations was used to determine the level of phosphorylation due to anti-CD3 stimulation and was washed three times with RIPA buffer, resuspended in 1X Laemmli reducing sample buffer and boiled. The other set of immunoprecipitations was subjected to an *in vitro* kinase assay. These samples were washed twice with RIPA buffer and once with HEPES kinase buffer. Beads were resuspended in kinase buffer and 1 mM ATP was added (total reaction volume = 50 μl). Kinase reactions proceeded for 30 minutes at 32°C at which time beads were pelleted and resuspended in 1X Laemmli reducing sample buffer and boiled. All samples were run on a 7.5% SDS-PAGE gel and transferred to a membrane. The membrane was immunoblotted for phosphotyrosine and Pyk2 (F298).

Cell surface biotinylation and stimulation with cross-linked anti-CD3

AB.1 cells were harvested and washed three times with D-PBS. Cells were resuspended at 5 X 10^7 cells/ml D-PBS and 1 ml of cells was aliquoted into a 1.5 ml Eppendorf tube. To 1 ml of cells, 50 μl of a freshly prepared 4.4 mg/ml biotin solution (in D-PBS) was added and the cells were incubated at room temperature for 10 minutes. Cells were then washed twice with 1 ml of 5 mM glycine/PBS in the Eppendorf tube and then the cells were transferred to a 15 ml conical tube and washed twice with 5 ml D-

PBS. Samples were resuspended in 5 ml RPMI and chilled on ice before anti-CD3 stimulation. For cross-linked anti-CD3 stimulation, 10 µg/ml 145-2C11 was added to the appropriate tubes and the tubes were incubated on ice for 15 minutes. The cells were pelleted and resuspended in 2.5 ml RPMI. To cross-link the anti-CD3, 5 µg/ml rabbit-α-hamster was added and cells were incubated at 37°C for 10 minutes. For unstimulated cells, only the secondary antibody was added.

Fibronectin immobilization and stimulation with ionomycin in 96 well plates

The appropriate number of wells of a 96 well Nunc Maxisorp immuno-plate were coated with 10 µg/ml of human cellular fibronectin overnight at 4°C. Before use, the wells were washed twice with D-PBS, blocked for 30 minutes with 2% BSA/PBS at 37°C and then washed three times with D-PBS. AB.1 cells were harvested, washed three times in D-PBS, resuspended at 1 X 10^5 cells per 40 µl D-PBS and chilled on ice. DMSO (carrier control) or 0.5 µM ionomycin was added to the clones and 1 X 10^5 cells were added to individual wells. The 96 well plate was then incubated at 37°C, and samples were removed at 10, 20, 40 and 60 minutes by adding 40 µl of 2X Laemmli reducing sample buffer, transferring the contents of the well to a tube and boiling for 3 minutes. Samples were loaded onto a 7.5% SDS-PAGE gel, transferred and blotted for phosphotyrosine and Pyk2 (F298).

Degranulation assay

The degranulation assay has been described in detail previously (Berg and Ostergaard 1995). Briefly, 2 X 10^5 AB.1 cells (pre-treated with a titration of PP2 or PP3 for 10 minutes on ice) were stimulated on BSA- or 145-2C11-coated wells of a 96 well plate for 4 hours at 37°C. After 4 hours of incubation, 25 μl of culture supernatant was removed from each well and mixed with 150 μl of substrate (Nα-benzylcarbonil-L-lysine thiobenzyl ester (BLT) and 5,5'-dithio-bis(2-nitrobenzoic acid) (DTNB)). The reaction was allowed to proceed for 10 – 20 minutes at room temperature at which time the absorbance at 405 nm was measured. The experiment was performed in triplicate and the average absorbance for each sample (background subtracted) was calculated and plotted with standard deviation.

Nucleofection of cloned CTL with plasmid or siRNA

CTL clones were nucleofected with pEGFP-C1-NTPyk2 and pEGFP-C1-CTPyk2 following the manufacturer's protocol (Mouse T Cell Nucleofector Kit, Amaxa Biosciences, Gaithersburg, MD). AB.1 or clone 11 were harvested 4 days after stimulation with allogeneic stimulator cells and pelleted. The clones were resuspended at 1 X 10^6 cells/ml D-PBS and then 1 ml aliquots of cells were centrifuged for 10 minutes, 90 x *g* at room temperature. Cells were resuspended in 100 μl of Mouse T Cell Nucleofector solution. Before nucleofection, 4 μg of plasmid was added to the cells. Cells were nucleofected using the X-01 program and then transferred to a well of a 12 well dish filled with 1 ml of pre-warmed media (Mouse T Cell Nucleofector Medium supplemented with Component A and B, 2 mM L-glutamine, 10% clone FCS, 53 nM β-mercaptoethanol and 10 μl recombinant IL-2). Cells were used for experiments and assayed for expression of GFP by flow cytometry 24 hours post-nucleofection.

For nucleofection with Pyk2 siRNA, clones were nucleofected with 3 μg siRNA and were harvested 48 hours post-nucleofection. Knock down was assessed by running a lysate (1 X 10^5 cell equivalents) on an SDS-PAGE gel and comparing expression of Pyk2 to the expression of actin (as assessed by immunoblotting).

Conjugate formation, spreading on immobilized anti-CD3 and confocal staining

For conjugate formation and subsequent confocal staining, CTL clones AB.1 or clone 11 were harvested and washed three times with D-PBS. Clones were resuspended at 6 X 10^6 cells/ml D-PBS and chilled on ice. Allogeneic target cells, L1210$^{Kb/Dd}$, were also washed three times with D-PBS, resuspended at 3 X 10^6 cells/ml D-PBS and chilled on ice. 100 μl of clones (6 X 10^5 cells) were mixed with 100 μl of target cells (3 X 10^5 cells) or 100 μl of D-PBS (for unstimulated samples) in 2 ml Eppendorf tubes on ice (E:T of 2:1). Tubes were centrifuged for 1 minute, 800 RPM (Eppendorf Microfuge 5415R) at 4°C. Tubes were then incubated in a 37°C water bath for 2-3 minutes (clone 11) or 5-6 minutes (AB.1) to allow for conjugate formation. After the incubation, conjugates were briefly vortexed to select for tight conjugates. The cells were then applied (using a wide bore pipet tip) to dry poly-L-lysine-coated coverslips and allowed to adhere for 7 minutes (clone 11) or 10 minutes (AB.1) at room temperature. The coverslips were then washed once with 1% FCS/PBS. The cells were fixed with 4% paraformaldehyde for 10 minutes at room temperature, and then the coverslips were washed twice with 1% FCS/PBS. The cells were permeabilized with 0.2% NP-40/PBS for 5 minutes at room temperature and the coverslips were subsequently washed three times with 1% FCS/PBS. Coverslips were incubated with each primary and flourochrome-conjugated secondary antibody diluted in 1% FCS/PBS for 45-60 minutes at room temperature in a dark chamber. The coverslips were washed three times with D-PBS for 5 minutes after each antibody incubation. Coverslips were mounted on glass slides using propyl gallate. Cells were visualized using a Zeiss LSM 510 confocal microscope with a x40 oil-immersion objective (N.A. 1.3).

Where indicated, cloned CTL were pretreated with 5 mM colchicine on ice for 15 minutes. Colchicine was washed out immediately prior to conjugation formation.

For visualizing cell spreading on immobilized anti-CD3, coverslips coated overnight at 4°C with 10 μg/ml 145-2C11 (anti-CD3) were utilized. Nucleofected clone 11 were harvested and washed three times with PBS. Cells were resuspended at approximately 5 X 10^5 cells per 200 μl of PBS and were chilled on ice. 200 μl of cells were added to anti-CD3 coated coverslips (blocked with 1% FCS/PBS) and the cells were allowed to adhere for 20 minutes at 37°C. The coverslips were then washed once with 1% FCS/PBS and then cells were fixed, permeabilized and immunostained as above. Cell spreading was determined using the differential interference contrast image and cells were scored as spread if they displayed a flattened morphology with visible lamellipodia formation around the cell body. Non-spread CTL appear round and refractory and are easily scored as not spread.

CD107a cell surface expression upon stimulation with immobilized anti-CD3 and target cells

For stimulation on immobilized anti-CD3, nucleofected clone 11 were harvested and washed three times with D-PBS. During the washes, 24 well plates coated overnight at 4°C with either 10 μg/ml (maximum stimulation) or 0.5 μg/ml (sub-stimulatory) 145-2C11 were washed twice with D-PBS and then blocked with 2% BSA/PBS for 30-60 minutes. The plates were then washed three times with D-PBS before use. One nucleofected sample contained approximately 5×10^5 cells and was resuspended in 250 μl D-PBS and added to a BSA-blocked well. The plate was incubated at 37°C for 30 minutes, at which time 750 μl of cold D-PBS was added to the wells and the plate was rocked for 10 minutes at 4°C. Cells were removed from the wells and transferred to FACS tubes. Cells were stained with anti-CD107a (Lamp-1) diluted in 1% FCS/PBS for 30 minutes on ice and then washed twice with D-PBS. Cells were then incubated with anti-rat Ig-PE for 30 minutes on ice (in 1% FCS/PBS) and then washed three times with D-PBS. Cells were immediately subjected to flow cytometry (FACScan, Becton Dickson, San Jose, CA) and the data was analyzed using CellQuest (version 3.3) software. Cells were gated for GFP expression and surface expression of CD107a was determined. The ratio of the percentage of GFP^+ $CD107a^+$ cells of clones nucleofected with either NTPyk2 or CTPyk2 relative to those nucleofected with empty vector was calculated as follows: clones nucleofected with Pyk2 construct (stimulated with anti-CD3 – unstimulated) / clones nucleofected with empty vector (stimulated with anti-CD3 – unstimulated).

For stimulation with target cells, nucleofected clone 11 and target cells (either L1210 or L1210$^{Kb/Dd}$) were washed three times with D-PBS. Target cells were resuspended at 3 X 10^5 cells/100 μl 4% FCS/RPMI and clones were resuspended to approximately 3 X 10^5 cells/100 μl of 4% FCS/RPMI. The cells were chilled on ice and 100 μl of clones and 100 μl of targets (E:T of 1:1) were added to FACS tubes on ice. Cells were encouraged to conjugate by centrifuging tubes at 700 RPM for 3 minutes at 4°C (Beckman GS-15R centrifuge, S4180 rotor). Tubes were then incubated in a 37°C water bath for 15 minutes, upon which time the tubes were vortexed and ice-cold 5mM EDTA/PBS was added to separate conjugates. Cells were pelleted, resuspended in 5mM EDTA/PBS and incubated at room temperature for 10 minutes. Cells were pelleted, resuspended in 4% FCS/5mM EDTA/PBS and stained with anti-CD107a as above. All washes and antibody incubations were performed in the presence of 5 mM EDTA. Cells were then subjected to flow cytometry. Cells were gated for GFP expression and surface CD107a expression was determined. The ratio of the percentage of GFP$^+$ CD107a$^+$ cells of clones nucleofected with either NTPyk2 or CTPyk2 relative to those nucleofected with empty vector was calculated as follows: clones nucleofected with Pyk2 construct (stimulated with L1210$^{Kb/Dd}$ – unstimulated (L1210)) / clones nucleofected with empty vector (stimulated with L1210$^{Kb/Dd}$ – unstimulated (L1210).

Disruption of conjugates between cloned CTL nucleofected with Pyk2 siRNA and EL4 target cells

Nucleofected clone 11 were harvested and washed three times with D-PBS. EL4 target cells were harvested and stained with CellTracker Orange CMRA. Clone 11 were resuspended at approximately 5 X 10^5 cells/100 µl of 4% dCS/RPMI and EL4 were resuspended at 1.25 X 10^5 cells/100 µl 4% dCS/RPMI. 100 µl of nucleofected clones and 125 µl of targets (E:T of 4:1) were mixed together in FACS tubes on ice. Tubes were centrifuged at 700 RPM for 3 minutes at 4°C (Beckman GS-15R centrifuge, S4180 rotor) to encourage conjugation and then incubated at 37°C for 1 hour. After 1 hour, reserved clone 11 and EL4 (kept on ice while conjugate assay proceeded) were mixed together on ice and were used as the 0' time point (unstimulated cells). All tubes were centrifuged and the cells were washed once with 5mM EDTA/PBS. Cells were resuspended in 5mM EDTA/PBS and incubated at room temperature for 10 minutes to separate conjugates. After 10 minutes, the cells were pelleted and fixed in 2% formaldehyde/5mM EDTA/PBS for 20 minutes at room temperature.

Stimulation of nucleofected clone 11 on immobilized anti-CD3 in 96 well plates

The appropriate number of wells of a 96 well flexible, flat-bottomed, non-tissue culture-treated plate were coated with 10 µg/ml of 145-2C11 (anti-CD3) overnight at 4°C. Before use, the wells were washed twice with D-PBS, blocked for 30 minutes with 2% BSA/PBS at 37°C and then washed three times with D-PBS. Nucleofected clone 11 were harvested, washed three times in D-PBS, resuspended at approximately 1 X 10^5

cells per 40 μl D-PBS and chilled on ice. 40 μl of cells were added to each well and the 96 well plate was incubated at 37°C. Samples were removed from the plate at 2, 10, 30 and 60 minutes by adding 40 μl of 2X Laemmli reducing sample buffer, transferring the contents of the well to a tube and boiling for 3 minutes. Samples were loaded onto an 8.5% SDS-PAGE gel.

GST fusion protein pulldowns

GST fusion proteins were expressed and purified with Glutathione Sepharose 4B according to the manufacturer (Amersham Biosciences, Piscataway, NJ). Beads were added to unstimulated or stimulated (immobilized anti-CD3) AB.1 post-nuclear lysates (1 X 10^7 cell equivalents) and rotated overnight at 4°C. Beads were washed three times with 1% NP-40 lysis buffer, resuspended in 80 μL 1X Laemmli reducing sample buffer and boiled for 3 minutes. Samples were run on 10 or 12% SDS-PAGE gels.

Quantification of the amount of phospho-protein relative to unphosphorylated protein

Immunoblots were scanned using an Agfa Duoscan T1200 and analyzed using Odyssey (volume 1.2) software. For each band, the integrated intensity of pixels (pixel intensity) was determined for the phosphorylated band (on a phosphotyrosine blot) and the unphosphorylated band (Pyk2 blot). Background was subtracted from each value and the ratio of phosphorylated protein/unphosphorylated protein was calculated and plotted on a bar graph.

Statistical analysis

Results from three experiments were averaged and the means were compared using a Student's two-tailed t test.

Reproducibility of results

Unless otherwise stated, experiments were repeated at least three times and representative data are shown.

CHAPTER 3: Differential Src family kinase activity requirements for CD3ε / CD3ζ phosphorylation and Pyk2 / ZAP-70 recruitment to the TCR/CD3 complex

Most of the data presented in this chapter is reproduced, with permission, from:

Tara L. Lysechko and Hanne L. Ostergaard

The Journal of Immunology, 2005, 174:7807-7814.

Copyright 2005. The American Association of Immunologists, Inc.

A. Introduction

Phosphorylation of CD3ζ is one of the earliest detectable events that occur after TCR stimulation of T cells (Baniyash et al. 1988). Ample evidence suggests that the SFK, Lck and, to a lesser extent, Fyn, phosphorylate the ITAMs of CD3ζ (Iwashima et al. 1994; Weiss and Littman 1994; van Oers et al. 1996). ZAP-70 is recruited to CD3ζ, binding to dually phosphorylated ITAMs, via its tandem SH2 domains (Chan et al. 1992; Wange et al. 1993; Iwashima et al. 1994; Hatada et al. 1995). Once recruited, ZAP-70 is phosphorylated by Lck or Fyn, which renders it catalytically active (Chan et al. 1992; Iwashima et al. 1994; Chan et al. 1995; Wange et al. 1995; van Oers et al. 1996), leading to phosphorylation of downstream substrates, including the adaptor protein, linker for activation of T cells (Zhang et al. 1998). Tyrosine phosphorylation of linker for activation of T cells, in turn, allows for the recruitment of a number of proteins to the signalling complex (Zhang et al. 1998).

I have developed a biochemical method to capture and analyze proteins found complexed with the TCR after TCR stimulation. In this approach, an immobilized stimulatory antibody (Ab) is used to both stimulate T cells and, after cell lysis, capture protein complexes regardless of how they are associated with the complex. This immobilized Ab capture approach is similar to the solid phase immunoisolation assay described by Tamura et al. (Tamura et al. 1984), in which Abs were immobilized to plastic to capture labeled proteins from cell lysates. This solid phase immunoisolation was shown to be highly specific, with low background binding (Tamura et al. 1984). I have adapted this technique to use anti-TCR/CD3 stimulatory Ab to capture protein complexes formed in live T cells to study TCR-proximal signalling events. This approach can also be used as a tool to identify novel proteins that are associated with such protein complexes.

Using solid phase immunoisolation, I have found that TCR-associated CD3ζ can be phosphorylated and recruits ZAP-70 in the presence of the SFK inhibitor PP2, a potent inhibitor of Lck and Fyn activity in T cells (Hanke et al. 1996). By contrast, PP2 did block both CD3ε and ZAP-70 phosphorylation and all additional downstream tyrosine phosphorylation events. These data suggest that there is a differential SFK requirement for CD3ζ and CD3ε/ZAP-70 phosphorylation. Furthermore, I observed CD3ζ phosphorylation and ZAP-70 recruitment in Lck-deficient Jurkat cells. My results indicate that during TCR stimulation, the PP2-inhibitable SFK, Lck and Fyn, are not uniquely capable of mediating CD3ζ phosphorylation, resulting in ZAP-70 recruitment. However, Lck and/or another SFK are absolutely required for CD3ε and ZAP-70 phosphorylation and recruitment of additional proteins to the CD3 complex, suggesting that the levels of active SFK needed for phosphorylation of the various CD3 subunits differ substantially.

B. Results

Stimulation of CTL clones with immobilized anti-CD3 results in specific recruitment of a number of tyrosine phosphorylated proteins to TCR/CD3 complex

I have established a biochemical approach to evaluate proteins recruited to the TCR complex by capturing the TCR complex and associated proteins after cell stimulation with immobilized monoclonal antibody (mAb). Proteins that remain bound to the plate are recovered after cell lysis and removal of cellular debris. I demonstrate that numerous tyrosine-phosphorylated proteins are enriched after stimulation of the CTL clone AB.1 and recovery of the proteins bound to the plate (Figure 3-1a). A number of tyrosine-phosphorylated proteins that cannot be detected in the cell lysate prepared from stimulated cells are enriched after capturing the complexes on the plate. As expected, the SFK Lck and Syk family kinase ZAP-70 was found complexed with CD3ε (Figure 3-1a). I was unable to detect Fyn in the CD3ε complexes; however, these CTL clones express very low levels of Fyn (Appendix Figure 1). The SH2/SH3 adapter Nck was also found in the CD3ε complexes (Figure 3-1a).

I have performed a number of experiments to validate this approach. To determine whether this method results in the recovery of preformed complexes or whether I am indeed detecting inducible recruitment, I prepared lysates of unstimulated CTL clones, added the lysates to the plate, recovered CD3ε, and analyzed associated proteins. There is no specific recruitment of tyrosine-phosphorylated proteins or of Lck, Nck, or ZAP-70 from lysates of unstimulated cells (Figure 3-1b), confirming that I am observing TCR-induced complex formation. Also of note, the recovery of associated

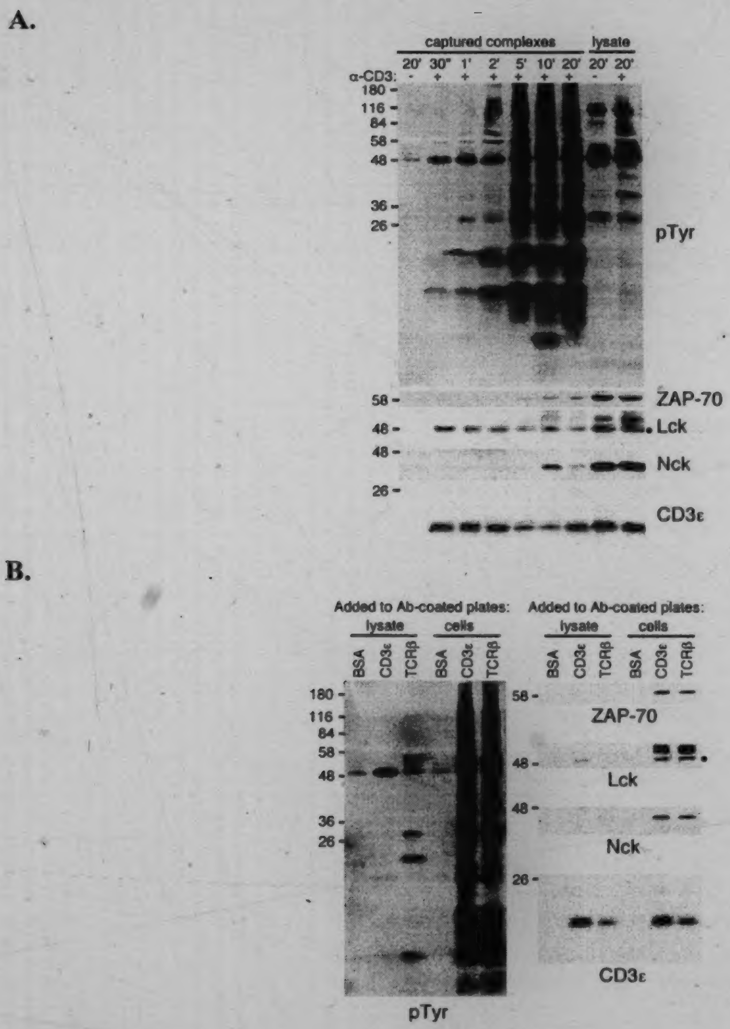

A.
captured complexes
lysate
20' 30" 1' 2' 5' 10' 20' 20' 20'
α-CD3: - + + + + + + - +
180
116
84
58
48
36
26
pTyr
58
ZAP-70
48
Lck
48
Nck
26
CD3ε
B.
Added to Ab-coated plates:
lysate
cells
BSA CD3ε TCRβ BSA CD3ε TCRβ
180
116
84
58
48
36
26
pTyr
Added to Ab-coated plates:
lysate
cells
BSA CD3ε TCRβ BSA CD3ε TCRβ
58
ZAP-70
48
Lck
48
Nck
26
CD3ε

FIGURE 3-1. Several tyrosine phosphorylated proteins are recruited to the TCR/CD3 complex upon stimulation of CTL clones with immobilized anti-CD3. a) AB.1 CTL clones were stimulated with plate-bound anti-CD3 (145-2C11) for the indicated time or were left unstimulated by plating on BSA as a control (-). Cells were then lysed in the plates, the lysate was removed, and a sample was saved for analysis (indicated as lysate). The proteins associated with the immobilized mAb were recovered as described in *Materials and Methods*. Samples were run on SDS-PAGE gels, transferred to membranes, and probed with the indicated mAb. The dot in the Lck panels designates the Ig H chain. b) AB.1 cells were exposed to BSA or immobilized anti-CD3ε or anti-TCRβ (indicated as cells) as in (a), or lysates from unstimulated AB.1 cells were added to plates pre-coated with anti-CD3ε or anti-TCRβ, and complexes from the lysate that bound to the plate were recovered and analyzed (indicated as lysate).

proteins is essentially identical after stimulation with either anti-CD3ε or anti-TCRβ (Figure 3-1b).

Because cells spread on the anti-CD3 and become tightly adhered to the mAb, it could be argued that many of these proteins are nonspecifically recovered, perhaps as a result of trapping large membrane fragments or cellular debris. To control for this possibility, I plated cells on immobilized anti-CD45, which results in dramatic cell spreading (Arendt et al. 1995), and analyzed captured protein for the presence of CD45 or CD3ε. CD3ε is only captured when cells are plated on anti-CD3ε, and CD45 is only captured when cells are plated on anti-CD45 (Figure 3-2a). These results clearly demonstrate that there is specificity to the protein capture, and proteins do not nonspecifically adhere to, or become trapped on, the plates. As an additional control, I plated cells on anti-class I MHC to compare class I MHC-captured proteins with those captured with anti-CD3ε and anti-TCRβ. The Coomassie Blue-stained gel in figure 3-2b demonstrates that different proteins are recruited to complexes captured with anti-class I MHC, anti-CD45 and anti-CD3ε/anti-TCRβ. Very few tyrosine-phosphorylated proteins were recovered with immobilized anti-class I MHC (Figures 3-2c, d) compared with anti-CD3ε and TCRβ. As well, no ZAP-70 (Figure 3-2d), Lck, or Nck (Figure 3-2c) complexed with class I MHC in these cells.

Because I wanted to use this procedure for the isolation of intracellular proteins that associate with the TCR complex, I needed to demonstrate that intracellular proteins do not nonspecifically associate with the complex. I examined two kinases that become activated upon TCR stimulation, but have not been shown to associate with the TCR complex: ERK2 and αPAK. Immunoblots with anti-ERK2 and anti-αPAK demonstrate

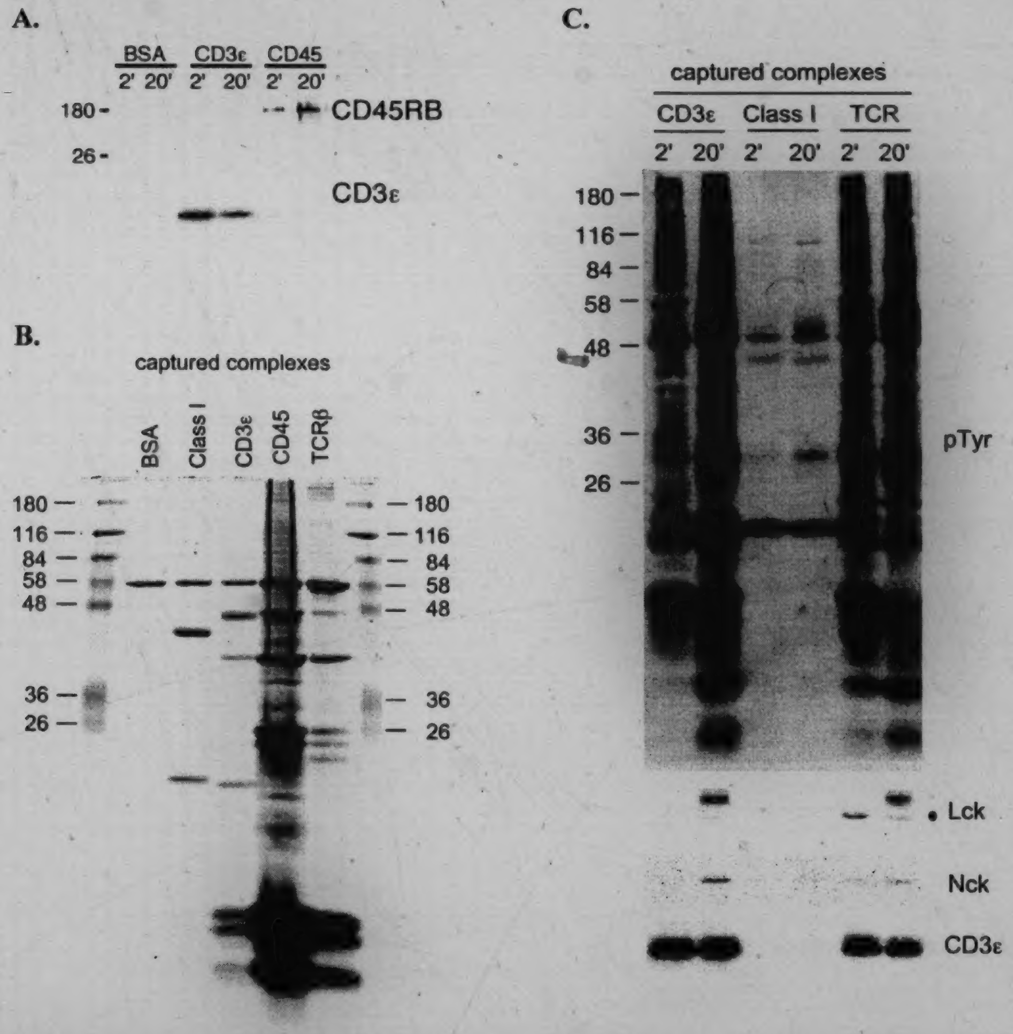
A.
BSA
CD3ε
CD45
2' 20' 2' 20' 2' 20'
180
26
CD45RB
CD3ε
B.
captured complexes
BSA
Class I
CD3ε
CD45
TCRβ
180
116
84
58
48
36
26
C.
captured complexes
CD3ε
Class I
TCR
2' 20' 2' 20' 2' 20'
180
116
84
58
48
36
26
pTyr
• Lck
Nck
CD3ε

FIGURE 3-2. Specific complexes form in association with CD3 after stimulation of CTL clones with plate-bound anti-CD3. a) Cells were plated on immobilized anti-CD3 or anti-CD45 for the indicated time, and complexes were recovered as described in Figure 3-1a. Samples were probed with anti-CD3ε or anti-CD45RB. b) Cells were plated on immobilized anti-class I MHC, anti-CD3ε, anti-CD45 or anti-TCRβ for 20 min. Cells were lysed and complexes were recovered. Samples were run on a SDS-PAGE gel and the gel was subsequently stained with Coomassie Blue. c) Cells were stimulated on immobilized anti-class I MHC, anti-CD3ε, or anti-TCRβ for 2 or 20 min and complexes were recovered as described in Figure 1a. Samples were probed with anti-phosphotyrosine, anti-CD3ε, anti-Lck or anti-Nck. The dot designates the Ig H chain. d) CTL clones were stimulated as in (c) for 20 min, and complexes were recovered. A sample of the lysate containing the unbound proteins, which was removed from the plate, is also shown. Immunoblots for phosphotyrosine, ERK2, αPAK, and ZAP-70 are shown. d) Next page.

D.

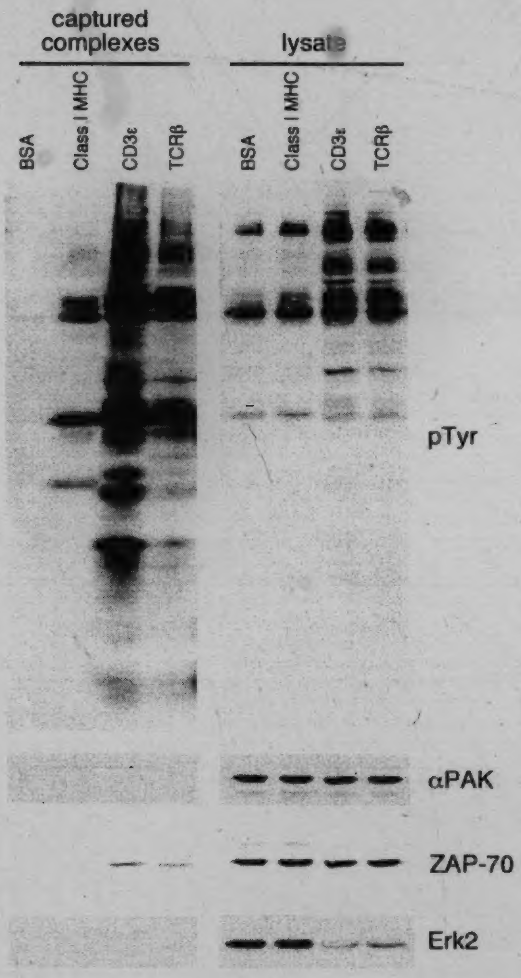
captured complexes
lysate
BSA
Class I MHC
CD3ε
TCRβ
BSA
Class I MHC
CD3ε
TCRβ
pTyr
αPAK
ZAP-70
Erk2

that these proteins are not recovered with anti-CD3ε and TCRβ complexes after stimulation, even though both proteins are clearly present in the lysate (Figure 3-2d). These results demonstrate that there is specificity to the recruitment of proteins.

CD3ζ, but not CD3ε, is tyrosine phosphorylated in the presence of the SFK inhibitor PP2

The phosphorylation cascade induced by T cell activation is generally accepted to be initiated by SFK (Pitcher et al. 2003). To confirm in my system that the bulk of the tyrosine-phosphorylated proteins that are recruited to the TCR/CD3 complex during immobilized mAb stimulation are dependent on the activation of SFK, I examined the effect of inhibiting SFK activity with PP2, a potent and selective inhibitor of SFK, particularly Lck and Fyn (Hanke et al. 1996; Zhu et al. 1999). I first assessed the effect of PP2 on a CTL functional response, specifically degranulation. At concentrations of 5–20 μM, PP2 completely inhibited TCR-triggered degranulation, whereas the inactive analog, PP3, had no impact on degranulation (Figure 3-3a). To ensure that these concentrations of PP2 effectively inhibited SFK activity, I examined the ability of Lck to phosphorylate a protein substrate (MBP) on tyrosine in the presence of PP2 or PP3. I was unable to examine Fyn activity because its expression was barely detectable in these cells (Appendix Figure 1). Lck was immunoprecipitated from unstimulated AB.1 cells in the presence of PP2 or PP3 with an anti-C-terminal Ab, which results in maximal Lck activity (H. Ostergaard unpublished observation), probably by binding in such a way that the Lck is in an open and active conformation. The Lck immunoprecipitates were then used in *in vitro* kinase reactions with MBP as a substrate in the presence of PP2 or PP3.

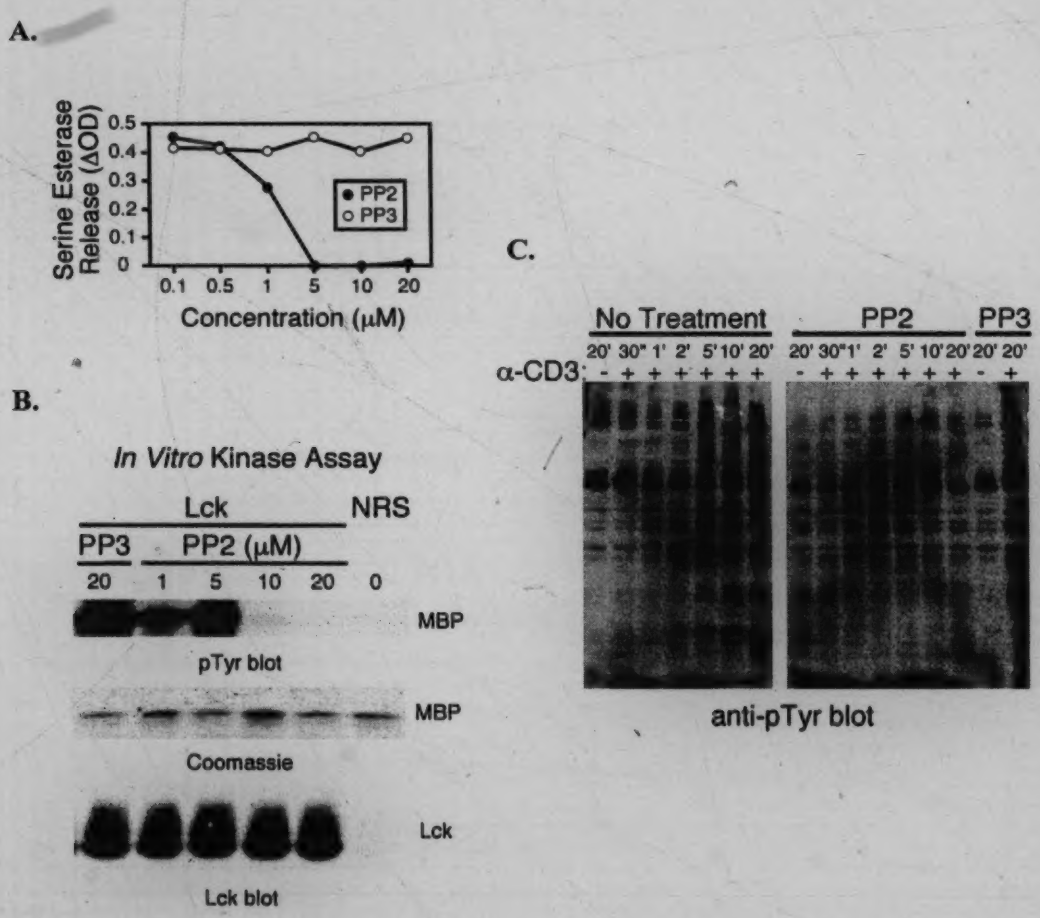

FIGURE 3-3. Effect of the SFK inhibitor, PP2, on CTL functional responses, Lck kinase activity, and tyrosine phosphorylation after TCR stimulation. a) Serine esterase release (degranulation) was measured from AB.1 in response to 10 μg/ml immobilized anti-CD3 in the presence of different concentrations of PP2 and its inert analog, PP3. b) Kinase activity of Lck immunoprecipitated from control and PP2-treated cells was assessed by an *in vitro* kinase assay using MBP as a substrate. AB.1 cellss were pretreated with PP2 or PP3 and lysed. Lck immunoprecipitations were performed, mixed with the MBP substrate and reaction mix, and incubated for 30 min. The Lck-bound beads were subjected to centrifugation, and a sample of the MBP-containing supernatant was removed. A phosphotyrosine blot (*top panel*) shows the degree of MBP phosphorylation, and a Coomassie stain (*middle panel*) is an indication of the amount of MBP in the assay. An Lck blot of the immunoprecipitate is shown in the *bottom panel*. An NRS immunoprecipitate was included as a control for background phosphorylation of MBP. c) Anti-phosphotyrosine blot of postnuclear cell lysates from AB.1 stimulated with immobilized anti-CD3ε in the absence or the presence 10 μM PP2 or PP3.

After the reaction, Lck immunoprecipitates were recovered by centrifugation, and the supernatant containing MBP was used to analyze the phosphorylation status of MBP. In the presence of PP3, Lck is active and phosphorylates MBP on tyrosine residues (Figure 3-3b). However, with concentrations of PP2 ranging from 10 to 20 μM, MBP was not phosphorylated, indicating that Lck kinase activity was effectively inhibited in this assay system. An NRS (normal rabbit serum) control immunoprecipitate was used in an identical kinase reaction to detect any kinase activity that may be nonspecifically associated with protein A-coated beads. A Coomassie stain of a gel containing a fraction of the substrate supernatants showed that equal amounts of MBP were present in each sample. The Lck proteins bound to the protein A-coated beads were also loaded onto gels and probed with anti-Lck to demonstrate that similar amounts of Lck were present in the kinase assays. I also examined the effect of SFK inhibition on general tyrosine phosphorylation and recruitment of proteins to the TCR/CD3 complex after stimulation with immobilized anti-CD3. It is clear that 10 μM PP2 is sufficient to abolish nearly all detectable anti-CD3-induced tyrosine phosphorylation in the lysate (Figure 3-3c).

The impact of SFK inhibition on the recruitment of tyrosine-phosphorylated proteins after CD3 stimulation was next assessed. As shown in Figure 3-1, a number of tyrosine-phosphorylated proteins were captured with the plate-bound Ab in the absence of any inhibitor (Figure 3-4a). With the inactive analog PP3, a similar profile of tyrosine-phosphorylated proteins was recruited to the TCR/CD3 complex (Figure 3-4a). In the presence of PP2, this recruitment was almost totally abolished, except, surprisingly, for CD3ζ, which remained phosphorylated (Figure 3-4a). After stimulation, with or without the inert analog PP3, a substantial fraction of phosphorylated CD3ζ appeared as a 19-kDa

A.

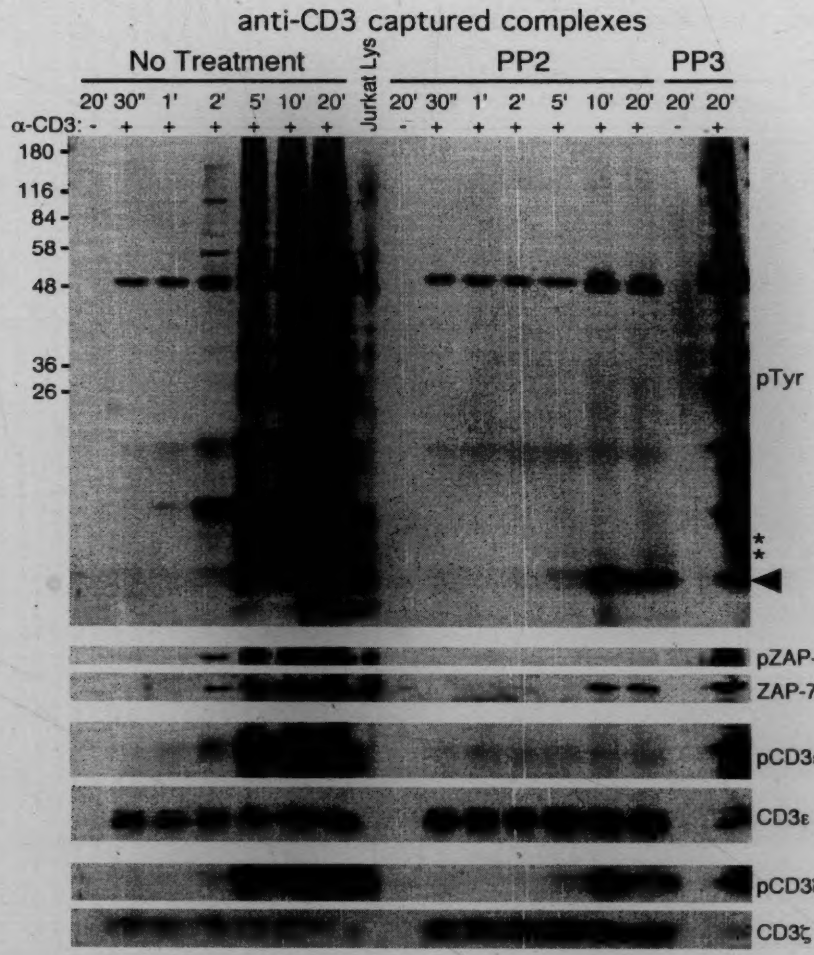
anti-CD3 captured complexes
No Treatment
Jurkat Lys
PP2
PP3
20' 30" 1' 2' 5' 10' 20'
20' 30" 1' 2' 5' 10' 20' 20' 20'
α-CD3: - + + + + + + - + + + + + + - +
180
116
84
58
48
36
26
pTyr
*
*
pZAP-70
ZAP-70
pCD3ε
CD3ε
pCD3ζ
CD3ζ

FIGURE 3-4. CD3ζ, but not CD3ε, is phosphorylated and recruits ZAP-70 after anti-CD3 stimulation in the presence of the SFK inhibitor PP2. Immunoblots are shown of complexes captured with plate-bound anti-CD3 after stimulation of AB.1 with immobilized anti-CD3 as described in Figure 3-1a in the absence or the presence of 10 μM PP2 or PP3. Tyrosine phosphorylation of CD3ε, CD3ζ, and ZAP-70 was detected by immunoblotting for phosphotyrosine. Phosphorylation of these proteins was inferred by co-localization upon reprobing for CD3ε, CD3ζ and ZAP-70. Blots were stripped and reprobed for CD3ε, CD3ζ, and ZAP-70. The arrowhead indicates the position of the 19-kDa form, and the asterisks indicate the positions of the 21- and 23-kDa forms of CD3ζ. b) A darker exposure of a representative phosphotyrosine blot of an experiment similar to that described in (a). The arrowhead shows the position of the 19-kDa form of CD3ζ. The p21 and p23 forms of CD3ζ are indicated by asterisks (* and ** respectively). b) Next page.

B.

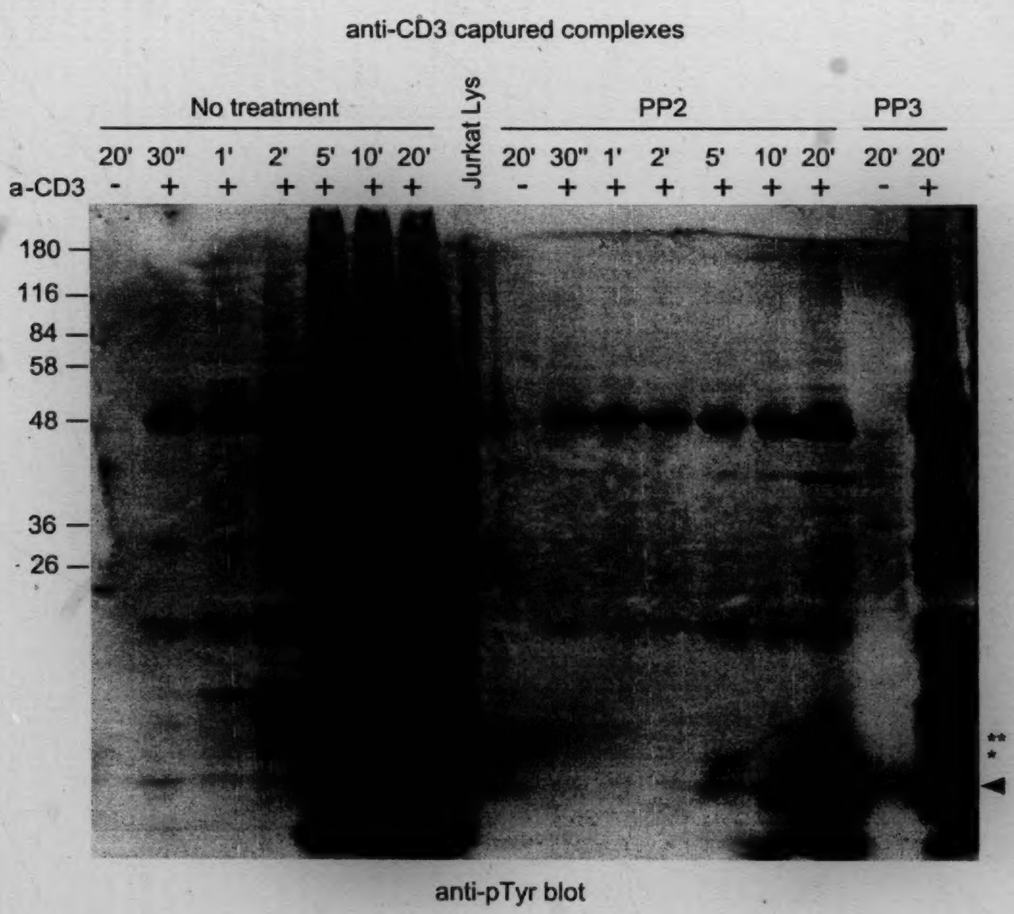
anti-CD3 captured complexes
No treatment
Jurkat Lys
PP2
PP3
20' 30" 1' 2' 5' 10' 20'
20' 30" 1' 2' 5' 10' 20'
20' 20'
a-CD3
- + + + + + +
- + + + + + +
- +
180
116
84
58
48
36
26
**
*
anti-pTyr blot

form, which was previously described (Moran and Miceli 1998), in addition to the 21- and 23-kDa forms of CD3ζ (Figure 3-4a). In the presence of PP2 I detected primarily the 19-kDa and low levels of the 21-kDa form, but never the 23-kDa form, of CD3ζ (Figure 3-4a, b). These results suggest that CD3ζ is subject to tyrosine phosphorylation in the absence of detectable Lck activity.

The detection of CD3ζ phosphorylation in the presence of the SFK inhibitor PP2 was surprising and was investigated further. As an additional indirect confirmation of CD3ζ phosphorylation, I determined whether ZAP-70 was recruited to the complex in the presence of PP2. Interestingly, ZAP-70 recruitment could easily be detected in the captured complexes isolated from cells treated with PP2 (Figure 3-4a). The reduced recruitment in the presence of PP2 could stem from the inability of cells to strongly adhere to the immobilized mAb in the presence of PP2, thereby not allowing for optimal association of the cells with the immobilized mAb. Although ZAP-70 was clearly recruited to the complex, it was not phosphorylated in the presence of PP2 (Figure 3-4a), thus confirming that SFK activity was indeed effectively inhibited. Furthermore, unlike CD3ζ, CD3ε was not phosphorylated in the presence of PP2 (Figure 3-4a). Similar results were seen in Con A (Concanavalin A) blasts prepared from C57BL/6 spleen cells (Figure 3-5). I clearly detected CD3ζ phosphorylation in the captured CD3ε complexes in the presence of PP2. ZAP-70 recruitment was reduced in these cells, but was still detectable (Figure 3-5). Thus, there is a differential requirement for either SFK family members or levels of active SFK in the phosphorylation of CD3 components, because CD3ζ can be phosphorylated in the presence of PP2, whereas CD3ε phosphorylation is completely abolished by this SFK inhibitor.

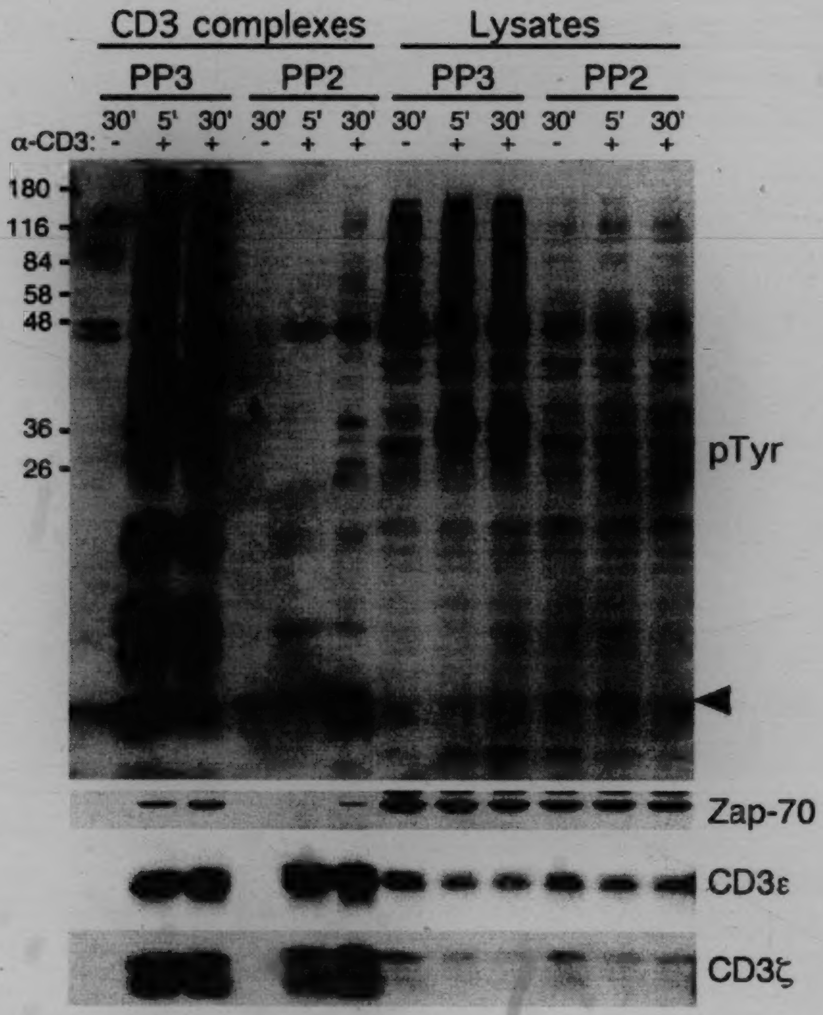
CD3 complexes
Lysates
PP3
PP2
PP3
PP2
30' 5' 30' 30' 5' 30' 30' 5' 30' 30' 5' 30'
α-CD3: - + + - + + - + + - + +
180
116
84
58
48
36
26
pTyr
Zap-70
CD3ε
CD3ζ

FIGURE 3-5. CD3ζ is phosphorylated in the presence of the SFK inhibitor, PP2, after stimulation of Con A blasts. Spleen cells from C57BL6/J mice were stimulated to proliferate with Con A. These Con A blasts were stimulated with plate-bound anti-CD3 for the indicated time in the presence of 10 μM PP2 or PP3. Complexes captured with the plate-bound anti-CD3ε were recovered and probed with the indicated Ab. A sample of the postnuclear lysate is also shown. The arrowhead indicates the position of CD3ζ.

CD3ζ is phosphorylated after TCR/CD3 stimulation in Lck-deficient Jurkat T cells

To further explore the apparent Lck-independent phosphorylation of CD3ζ, I examined whether CD3ζ is phosphorylated in JCaM1.6, Jurkat cells deficient in Lck expression (Straus and Weiss 1992). I used different anti-CD3ε concentrations to stimulate Jurkat and JCaM1.6 cells and found, as previously documented (Straus and Weiss 1992), that induction of tyrosine phosphorylation in the lysates of JCaM1.6 cells stimulated with anti-CD3 is severely compromised (Figure 3-6a). I then examined recruitment of tyrosine-phosphorylated proteins to the TCR/CD3 complex by capturing complexes with the stimulatory anti-CD3 on plastic. Surprisingly, I found that there are a number of tyrosine-phosphorylated proteins that are recruited to the complex in JCaM1.6 cells, although the degree of protein recruitment was significantly lower than that in wild-type Jurkat cells (Figure 3-6b). Similar to what was found for the CTL clones treated with PP2, phosphorylated CD3ζ (Figure 3-6b) and ZAP-70 recruitment (Figure 3-6c) could be detected in CD3ε complexes obtained from JCaM1.6 cells, confirming that CD3ζ is indeed phosphorylated in the absence of Lck (Figure 3-6c). There are lower levels of ZAP-70 recruited in these cells; however, I found that there were also substantially lower levels of expression (Figure 3-6d) and recovery of CD3ζ (Figure 3-6c) in these cells compared with Jurkat cells. These results indicate that CD3ζ is phosphorylated in the absence of Lck in JCaM1.6 cells. Combined with the results obtained using the SFK inhibitor with the CTL clones, CD3ζ appeared to be phosphorylated in an Lck-independent, and possibly a Fyn-independent, manner.

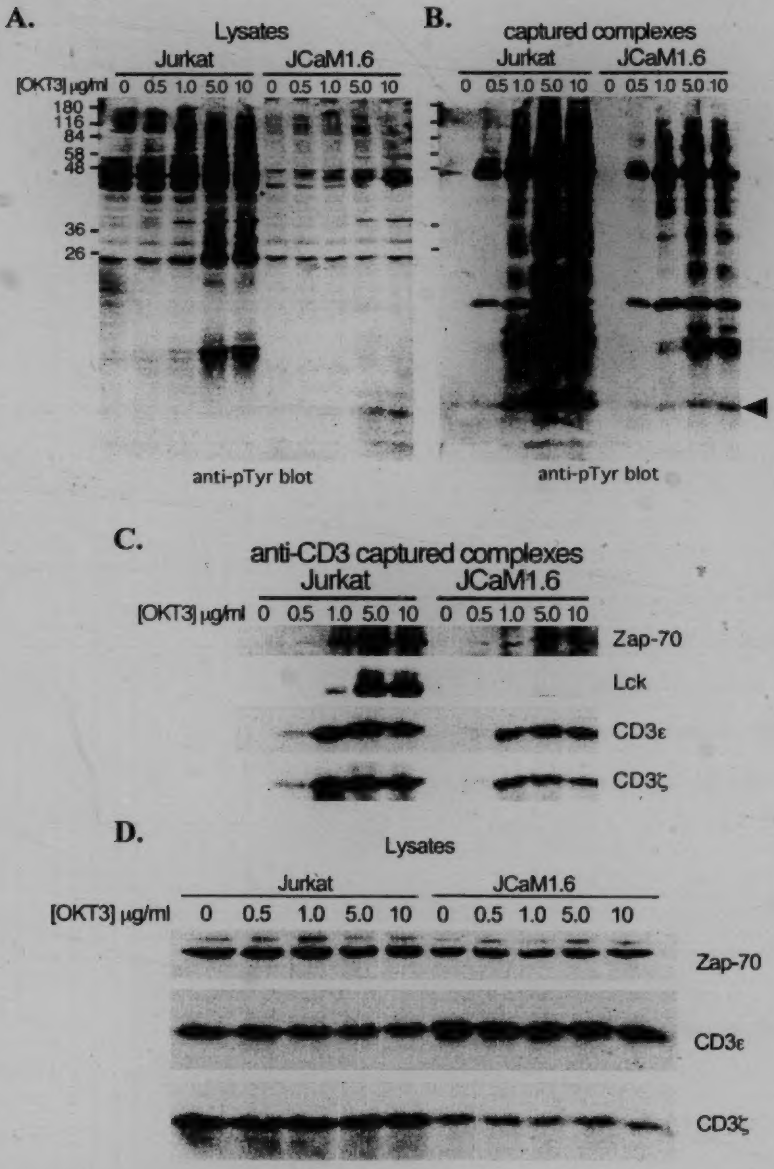
A.
Lysates
Jurkat
JCaM1.6
[OKT3] µg/ml 0 0.5 1.0 5.0 10 0 0.5 1.0 5.0 10
180
116
84
58
48
36
26
anti-pTyr blot
B.
captured complexes
Jurkat
JCaM1.6
0 0.5 1.0 5.0 10 0 0.5 1.0 5.0 10
anti-pTyr blot
C.
anti-CD3 captured complexes
Jurkat
JCaM1.6
[OKT3] µg/ml 0 0.5 1.0 5.0 10 0 0.5 1.0 5.0 10
Zap-70
Lck
CD3ε
CD3ζ
D.
Lysates
Jurkat
JCaM1.6
[OKT3] µg/ml 0 0.5 1.0 5.0 10 0 0.5 1.0 5.0 10
Zap-70
CD3ε
CD3ζ

FIGURE 3-6. CD3ζ phosphorylation and ZAP-70 recruitment occur after CD3 stimulation of JCaM1.6 cells. a) Jurkat and JCaM1.6 cells were stimulated with the indicated concentration of plate-bound anti-CD3 (OKT3) for 10 min, after which a sample of the cell lysate was removed from the plate, subjected to SDS-PAGE, and probed with anti-phosphotyrosine. b) Complexes remaining on the mAb-coated plates after removal of lysate from (a) were recovered as described in Figure 3-1a, run on a gel, and probed with anti-phosphotyrosine. c) Membrane from (b) was probed with Abs to CD3ε, CD3ζ, ZAP-70, and Lck. The arrowhead indicates the position of CD3ζ. d) Membrane from (a) was reprobed with anti-ZAP-70, CD3ε and CD3ζ.

Pyk2 and Itk are recruited to the TCR/CD3 complex in a SFK-independent manner

In an effort to identify proteins that may be capable of phosphorylating CD3ζ in an Lck-independent manner, I immunoblotted anti-CD3ε-captured complexes (in the presence of increasing concentrations of PP2) for tyrosine kinases that are known to be recruited to the T cell/APC interface or have been shown to be involved in membrane proximal signalling events. I chose to examine recruitment of the tyrosine kinases Pyk2 and Itk. Under conditions in which Lck activity is not effectively inhibited (<10 μM PP2, Figure 3-3b), both proteins were recruited to the TCR/CD3 complex (Figure 3-7). Interestingly, when concentrations of PP2 that effectively inhibit Lck activity were used (10 or 20 μM), Pyk2 and Itk were still recruited to the TCR/CD3 complex (Figure 3-7). However, the amount of Itk present with 10 or 20 μM PP2 was substantially reduced compared to non-inhibiting concentrations of PP2 (Figure 3-7). These results demonstrate that some tyrosine kinases are indeed recruited to the TCR/CD3 complex in an Lck-independent manner, however, whether these kinases are responsible for phosphorylating CD3ζ under these conditions remains to be determined.

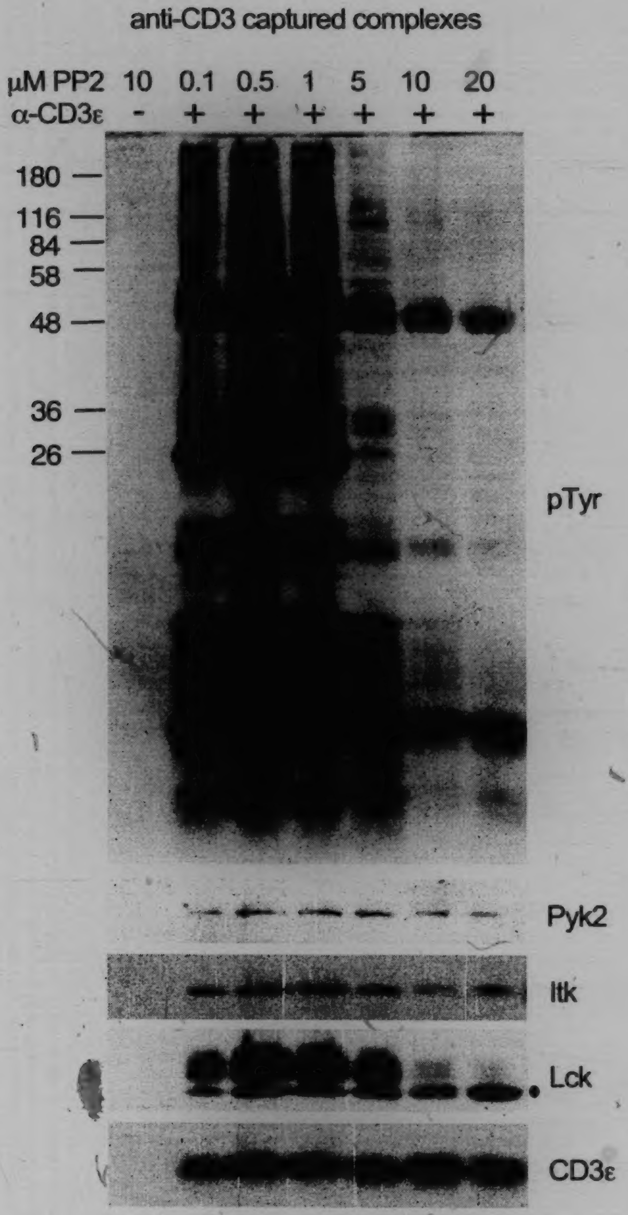
anti-CD3 captured complexes
μM PP2 10 0.1 0.5 1 5 10 20
α-CD3ε - + + + + + +
180
116
84
58
48
36
26
pTyr
Pyk2
Itk
Lck
CD3ε

FIGURE 3-7. Pyk2 and Itk are recruited to the TCR/CD3 complex independent of SFK activity. AB.1 CTL clones were stimulated on immobilized anti-CD3 for 20 min in the presence of increasing concentrations of PP2. Complexes were recovered as described in Figure 3-1a. Immunoblots for phosphotyrosine, CD3ε, Lck, Itk and Pyk2 were performed. The dot designates the Ig H chain.

C. Discussion

In this study I document a novel approach to analyze proteins associated with the TCR complex after T cell activation. This method differs from that described by Harder and Kuhn (Harder and Kuhn 2000), in which TCR-associated membrane fragments are isolated from homogenates. I use detergent to disrupt the cells and to remove proteins that are nonspecifically bound to the complexes captured on the plates. This approach will probably preserve interactions that would presumably be disrupted during standard immunoprecipitation procedures.

I found that the process of stimulating CTL on immobilized Ab and then capturing complexes significantly enriches for engaged TCR signalling complexes as the cells spread on the immobilized Ab. Stimulation with immobilized Ab also more closely mimics stimulation by APC or target cells than does stimulation with soluble cross-linked Ab. For example, immobilized Ab stimulation generates more sustained signalling, provides a polarized stimulus, and leads to degranulation of CTL (Berg et al. 1998), as is observed with target cells. Unlike stimulation with APC, in which engaged molecules can move freely within membranes, immobilized Ab provides a fixed plane of stimulatory Ab that does not allow for rearrangement of engaged TCR/CD3 complexes or formation of a mature immunological synapse/supramolecular activation cluster (Monks et al. 1998; Grakoui et al. 1999). However, in light of the recent findings demonstrating that tyrosine kinase signalling occurs before a mature synapse forms (Freiberg et al. 2002; Lee et al. 2002), this method of stimulation still enables us to study the very early events in T cell activation, such as initial phosphorylation events and recruitment of proteins to the TCR/CD3 complex.

I have used a number of controls to demonstrate the specificity of the proteins recruited to the TCR/CD3 complex with my novel assay. I show that virtually no proteins bind to BSA-coated plates and that very few proteins (other than the protein to which the Ab is specific) within an unstimulated lysate will bind to immobilized anti-CD3ε or anti-TCRβ (Figure 3-1b). I have also performed experiments in which stimulated lysates were plated onto immobilized anti-CD3ε and found, as with an unstimulated lysate, that there are very few proteins that can bind the immobilized Ab (Appendix Figure 2). These results clearly demonstrate that intact cells must be stimulated to induce complex formation around the TCR/CD3 complex. As well, I have shown that proteins do not nonspecifically adhere to or become trapped on the plates as the cells spread on the immobilized stimulatory Ab (Figure 3-2a). Control experiments performed with immobilized anti-class I MHC demonstrate that a different and less complex set of proteins is recruited to the immobilized Ab (Figure 3-2b, c, d). In addition to detecting proteins known to associate with the TCR/CD3 complex, I was unable to detect proteins that would not be expected to associate with the TCR/CD3 complex (Figure 3-2d). I therefore conclude that my method of immunoisolation is highly specific and the proteins recruited are physiologically relevant.

My most surprising finding is that CD3ζ can become phosphorylated in the absence of detectable Lck activity. I found that both CD3ζ phosphorylation and ZAP-70 recruitment can occur in normal T cells after treatment with the SFK inhibitor, PP2, even though phosphorylation of CD3ε and ZAP-70 is completely inhibited under these conditions (Figures 3-4a and 3-5). I could also detect CD3ζ phosphorylation and ZAP-70 recruitment in JCaM1.6, a Lck-deficient variant of Jurkat cells (Figure 3-6). JCaM1.6

cells still express Fyn, albeit at low levels (Denny et al. 2000); therefore, I cannot rule out a role for Fyn in the phosphorylation of CD3ζ in these cells. However, the results from the CTL clones and Con A blasts treated with PP2 suggest that neither SFK is responsible for this phosphorylation. Therefore, my results suggest that another kinase(s), in addition to Lck or Fyn, is capable of phosphorylating CD3ζ. It is possible that the kinase responsible for CD3ζ phosphorylation is a SFK that is not inhibited by PP2. This is nonetheless interesting, because this would imply that this other SFK, or perhaps reduced levels of SFK activity, could function to phosphorylate CD3ζ, but is not able to compensate for the lack of Lck activity with respect to the phosphorylation of CD3ε or ZAP-70. This study seems to contradict other studies that concluded that Lck is required for CD3ζ phosphorylation; however, this approach has not been used previously, and I may be significantly enriching for TCR signalling complexes, thus improving the ability to recover and detect phosphorylated CD3ζ.

What is the nature of the CD3ζ phosphorylation that is detected using this approach? It has been shown previously that in 30–40% of the cell surface-expressed TCR/CD3 complexes CD3ζ can associate with the cytoskeleton through the interaction of CD3ζ with monomeric actin (Caplan et al. 1995; Rozdzial et al. 1995; Caplan and Baniyash 1996). This pool of CD3ζ that can interact with the cytoskeleton is detergent insoluble and has been designated cytoskeleton-associated ζ (cska-ζ). Cska-ζ differs from detergent-soluble CD3ζ in that it is phosphorylated in resting and activated T cells, and phosphorylation does not change the mobility of cska-ζ during electrophoresis (Caplan and Baniyash 1996). With the method used in this study to recover the TCR-associated complexes, all proteins bound to the immobilized Ab are collected; therefore, it is conceivable that I may be capturing some insoluble cytoskeletal components. The predominant species of phosphorylated CD3ζ that I recover from cells stimulated in the presence of PP2 migrates at 19 kDa. This 19-kDa phosphorylated species has also been observed in a study examining the cytoskeletal recruitment of CD3ζ (Moran and Miceli 1998). I can detect a minor, less phosphorylated form of CD3ζ that seems to migrate just below the p19 species and appears to have a low level of constitutive phosphorylation that may correspond to cska-ζ. I cannot exclude the possibility that p19 is, in fact, cska-ζ; nevertheless, two pieces of evidence argue against the likelihood of this species being cska-ζ. First, the amount of cska-ζ is increased after T cell activation (Rozdzial et al. 1995; Caplan and Baniyash 1996), and I do not detect an increase in the amount of complex-associated, 19-kDa ζ protein after activation. Second, as mentioned previously, cska-ζ is basally phosphorylated (Caplan and Baniyash 1996), whereas the 19-kDa CD3ζ phosphorylation that I am detecting is clearly inducible, with little or no pre-existing phosphorylation in unstimulated cells. Furthermore, I can detect ZAP-70 with captured protein complexes, which is presumably associated with phosphorylated CD3ζ, and it has not yet been determined whether ZAP-70 is capable of interacting with phosphorylated cska-ζ. Interestingly, Caplan et al. (Caplan et al. 2001) found that cska-ζ can be phosphorylated by a kinase other than Lck *in vivo*, because treatment of cells with PP1, an SFK inhibitor, had no effect on cska-ζ phosphorylation. However, the authors were unable to identify which kinase(s) was responsible.

There are two major phosphorylated intermediates of soluble CD3ζ that form upon T cell activation, which migrate at 21 and 23 kDa. It has been shown that the 21-kDa (p21) intermediate is constitutively phosphorylated in thymocytes and peripheral T cells, and it associates with nonphosphorylated ZAP-70 as a result of *in situ* TCR interactions with peptide/MHC complexes (van Oers et al. 1993; van Oers et al. 1994). van Oers et al. (van Oers et al. 2000) have elegantly demonstrated that p21 is tyrosine phosphorylated on the two membrane-distal ITAMs. ZAP-70 can associate with p21; however, this associated ZAP-70 does not become phosphorylated (Isakov et al. 1995; van Oers et al. 2000). After activation through the TCR, p21 becomes phosphorylated at the most membrane-proximal ITAM, giving rise to p23, and the associated ZAP-70 becomes phosphorylated (van Oers et al. 2000). I did not detect basally phosphorylated CD3ζ or ZAP-70 association with the recovered complexes before TCR stimulation. The major phosphorylated form of CD3ζ that I detected after TCR stimulation in both the presence and the absence of PP2 inhibition was ~19 kDa (Figure 3-4a, b). I hypothesize that I may be capturing and detecting an earlier tyrosine-phosphorylated intermediate than p21. Indeed, it has been shown that the sites of CD3ζ phosphorylation affect the migration of CD3ζ during electrophoresis (van Oers et al. 2000). In the absence of PP2, I can detect both the p21 and p23 species, and in the presence of PP2, upon longer exposures, a band migrating at ~21 kDa can clearly be detected; however, no p23 seems to be present in any of my experiments (Figure 3-4b), suggesting that I am not fully phosphorylating CD3ζ in the presence of PP2.

I do not yet know which PTK is phosphorylating the CD3ζ in the presence of the SFK inhibitor; however, this approach lends itself to proteomic analysis to identify potential kinases that are recruited to the complex. I have found Itk and Pyk2 in the TCR complexes in the presence of PP2 (Figure 3-7). Whether these PTK or yet to be identified PTK are responsible for mediating the early CD3ζ phosphorylation remains to be determined.

There are a number of possible reasons why non-SFK might phosphorylate CD3ζ. It is not clear how Lck is recruited to the TCR complex, particularly under conditions where co-receptor engagement does not occur. Another kinase(s) might phosphorylate CD3ζ to prime the complex to allow for rapid initiation of the response once enough Lck accumulates at the complex after TCR stimulation, perhaps via binding of its SH2 domain to the phosphorylated CD3ζ. It has been shown previously that the SH2 domain of Lck can interact with phosphorylated CD3ζ (August and Dupont 1996; Straus et al. 1996) and that a functional SH2 domain of Lck is required for the earliest signalling responses (Straus et al. 1996).

Another explanation for why CD3ζ might undergo Lck-independent phosphorylation is based on the differential signalling model proposed by Pitcher and van Oers (Pitcher and van Oers 2003). In this model, the γ-, δ-, and ε-chains of the TCR/CD3 complex perform distinct functions from the CD3 ζ-chain. CD3γ, -δ, and -ε are responsible for mediating activation events (signalling, proliferation, and effector functions), whereas CD3ζ may mediate distinct signalling pathways and TCR expression and recycling. This model is based on observations that CD3ζ can interact with distinct proteins that do not bind to the other invariant chains through ITAM and non-ITAM sequences (Pitcher and van Oers 2003). That I found that CD3ζ can be phosphorylated by another PTK(s) supports the hypothesis that TCRζ could be involved in a distinct signalling pathway.

In this study I provide evidence that CD3ζ can be phosphorylated and recruit ZAP-70 in the presence of an SFK inhibitor and in the absence of detectable Lck activity. In contrast, the SFK inhibitor completely blocked CD3ε and ZAP-70 recruitment, implying that there is a differential SFK requirement for CD3ε and CD3ζ phosphorylation. My results suggest that Lck and possibly Fyn, because it is also effectively inhibited by PP2, may not be essential for CD3ζ phosphorylation and that perhaps another SFK or another PTK may be able to phosphorylate CD3ζ, but not CD3ε. Alternatively, if SFK are still required for CD3ζ phosphorylation, the levels and/or types of active SFK differ substantially from those required for CD3ε phosphorylation. Taken together, my data suggest that current models of membrane-proximal, TCR-mediated signalling events may be incomplete, and that additional studies are required to understand the apparent differential phosphorylation requirements for CD3ε and CD3ζ.

CHAPTER 4: Regulation of Pyk2 phosphorylation by increases in intracellular calcium concentration

A. Introduction

T cell receptor engagement results in the activation of a number of signalling pathways within the cell including Ca^{2+}-sensitive pathways that are activated in response to the elevation of intracellular free Ca^{2+}. These Ca^{2+} signals can be separated into short-term, rapid responses (occurring over seconds to minutes) that are involved in modulating T cell motility and polarity and long-term responses (occurring over minutes to hours) requiring activation of transcription (Lewis 2001; Randriamampita and Trautmann 2004; Gallo et al. 2006). In terms of rapid Ca^{2+} responses, an increase in $[Ca^{2+}]_i$ can modulate T cell motility by inducing a stop signal for migrating T cells. Upon recognition of an APC, a T cell switches from a motile state to an immobile state (Donnadieu et al. 1994; Negulescu et al. 1996). This switch is necessary to maximize contact with the APC and to generate sustained signals within the T cell. Within approximately 30 seconds of an interaction of a T cell with an APC, a rise in $[Ca^{2+}]_i$ occurs and shortly thereafter the T cell stops crawling and rounds up (Donnadieu et al. 1994; Negulescu et al. 1996). Ca^{2+} seems to be sufficient to induce the stop signal as calcium mobilizing agents alone can induce this behaviour (Donnadieu et al. 1994; Negulescu et al. 1996). Ca^{2+} can also modulate cell polarity events as both MTOC reorientation and exocytosis of cytolytic granules have been shown to be dependent on the presence of extracellular Ca^{2+} (Kupfer et al. 1985; Ostergaard et al. 1987; Takayama and Sitkovsky 1987; Esser et al. 1996; Lowin-Kropf et al. 1998; Kuhn and Poenie 2002), although Ca^{2+} may not be required for MTOC reorientation in all types of T cells (Ostergaard and Clark 1987). Long term calcium-mediated responses require the activation of transcription factors such as nuclear factor of activated T cells (NFAT) (involved in the induction of cytokine genes) and serve to regulate activation and proliferation of T cells (Timmerman et al. 1996).

Much work has been performed to identify the key players in calcium signalling pathways (Figure 4-1). TCR triggering, through the activation of kinases and recruitment of adaptor molecules, leads to the phosphorylation and activation of PLC-γ (Lewis 2001). PLC-γ cleaves PIP_2 in the membrane to generate DAG, which is involved in the activation of PKC, and IP_3 (Gallo et al. 2006). IP_3 binds to its receptor in the ER membrane (IP_3R) causing the release of Ca^{2+} from ER stores into the cytoplasm (Imboden and Stobo 1985). Emptying of the intracellular stores triggers an influx of extracellular Ca^{2+} across the plasma membrane (Putney 1990). This process is called capacitative Ca^{2+} entry and it results in a biphasic elevation of $[Ca^{2+}]_i$ in which the first phase comprises the release of Ca^{2+} from the stores and the second phase constitutes the influx of Ca^{2+} from the extracellular space (Putney 1990; Lewis 2001). In T cells (and lymphocytes in general), the amount of Ca^{2+} found in intracellular stores is quite low when compared to other non-excitable cells (Randriamampita and Trautmann 2004). Therefore, the initial Ca^{2+} release from stores contributes very little to the overall increase in $[Ca^{2+}]_i$, with the majority arising from the influx of extracellular Ca^{2+} (Lewis 2001). The Ca^{2+} channels responsible for the influx of Ca^{2+} from the extracellular space are store-operated channels (SOC). The type of SOC found in T cells is called the Ca^{2+} release-activated Ca^{2+} channel (CRAC) and is distinguished from other SOCs by its high Ca^{2+} selectivity (Hoth and Penner 1992; Lewis 2001). Interestingly, the mechanism by

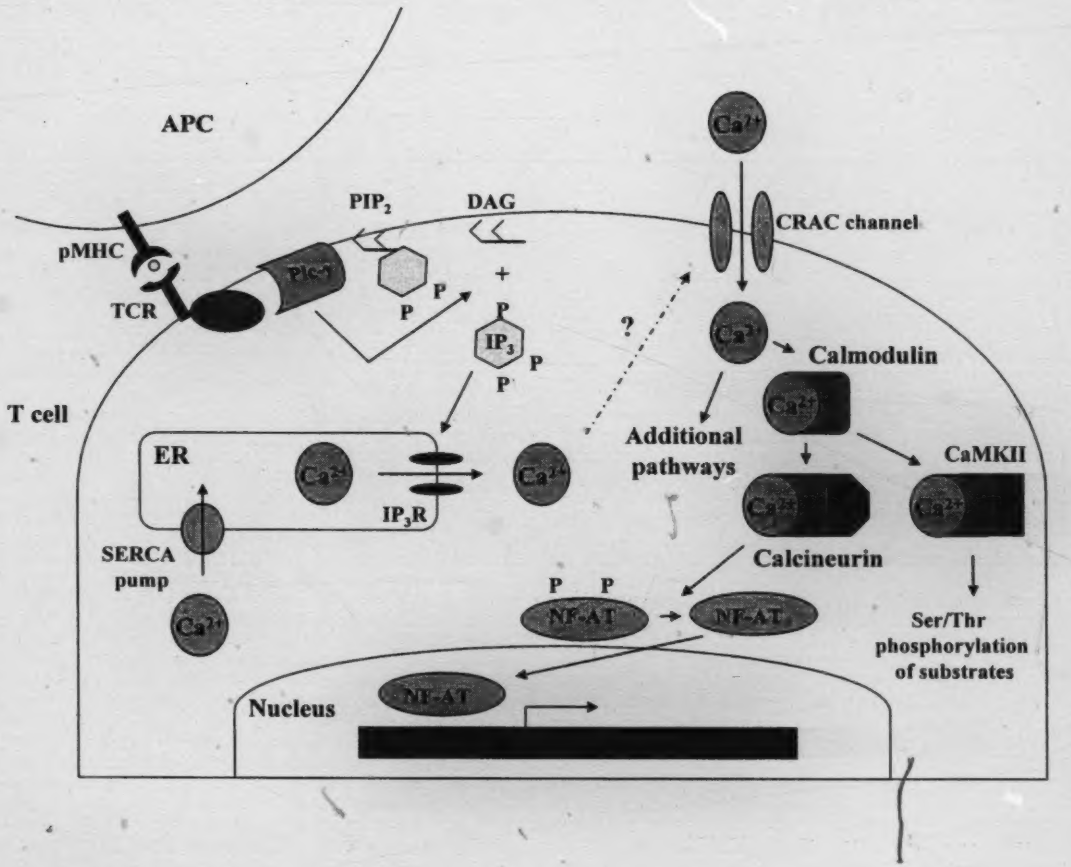
APC
pMHC
TCR
Plc-γ
PIP$_2$
P
P
DAG
+
P
IP$_3$
P
P
T cell
ER
Ca^{2+}
IP$_3$R
Ca^{2+}
SERCA
pump
Ca^{2+}
?
Ca^{2+}
CRAC channel
Ca^{2+}
Calmodulin
Ca^{2+}
Additional
pathways
CaMKII
Ca^{2+}
Ca^{2+}
Calcineurin
P P
NF-AT
NF-AT
Ser/Thr
phosphorylation
of substrates
Nucleus
NF-AT

FIGURE 4-1. Calcium signalling in T cells. TK = tyrosine kinases.

which capacitative Ca^{2+} entry occurs as well as the molecular identity of the CRAC channel remains elusive.

Once Ca^{2+} has accumulated in the cytosol, free Ca^{2+} ions bind to calmodulin. Calmodulin binds four Ca^{2+} ions and this interaction changes its conformation which ultimately promotes its interaction with various protein kinases and phosphatases (Hook and Means 2001). One family of serine/threonine kinases with which Ca^{2+}/calmodulin interacts are the multifunctional Ca^{2+}/calmodulin-dependent protein kinases (CaMK) I, II, and IV. Ca^{2+}/calmodulin can also interact with calcineurin, a serine/threonine phosphatase. Calcineurin is responsible for dephosphorylating cytosolic NFAT which unmasks a nuclear localization sequence and promotes nuclear translocation of NFAT which is necessary for it to induce transcription (Shaw et al. 1995; Luo et al. 1996).

The regulation of Pyk2 phosphorylation by an increase in $[Ca^{2+}]_i$ has been shown in many cell types such as neurons (Lev et al. 1995), epithelial cells (Yu et al. 1996), megakaryocytes (Hiregowdara et al. 1997), platelets (Raja et al. 1997) and cardiomyocytes (Hirotani et al. 2004). However, the responsiveness of Pyk2 to a rise in $[Ca^{2+}]_i$ in T cells is somewhat controversial. One group found no Ca^{2+} dependence on the phosphorylation of Pyk2 as treatment of Jurkat T cells and murine thymocytes with ionomycin (a calcium ionophore) could not induce Pyk2 phosphorylation (Qian et al. 1997). Furthermore, stimulation of these cells with cross-linked anti-CD3 in the presence of EGTA (an extracellular calcium chelator) had no effect on Pyk2 phosphorylation induced by TCR stimulation (Qian et al. 1997). Consistent with these results, another group reported that stimulation of human T lymphoblasts with either A23187 (a calcium ionophore) or thapsigargin (an inhibitor of sarco-endoplasmic reticulum Ca^{2+}-ATPases or

SERCA pumps in the ER that pump calcium into the ER) could not increase Pyk2 kinase activity (Rodriguez-Fernandez et al. 2002). In contrast, two other studies found that treatment of Jurkat T cells with EGTA, or stimulating the cells in Ca^{2+}-free media, partially reduced TCR-induced Pyk2 phosphorylation (Ganju et al. 1997; Tsuchida et al. 1999). In an attempt to resolve these discrepancies, I treated CTL clones with reagents that either increase $[Ca^{2+}]_i$ levels directly or agents that chelate calcium to determine whether there is an effect of increasing $[Ca^{2+}]_i$ on Pyk2 phosphorylation in T cells.

B. Results

Treatment of CTL clones with reagents that increase intracellular calcium levels induce Pyk2 phosphorylation

In order to perform a more thorough examination of the effect of a rise in $[Ca^{2+}]_i$ on Pyk2 phosphorylation in T cells, I treated CTL clones with reagents that directly cause an increase in $[Ca^{2+}]_i$ levels. Ionomycin is a calcium ionophore that transports Ca^{2+} across the ER membrane and into the cytosol which in turn activates store-operated CRAC channels and causes an influx of Ca^{2+} from the extracellular space (Mason and Grinstein 1993). To determine whether Pyk2 could be inducibly phosphorylated after ionomycin treatment, I subjected AB.1 cells to different concentrations of ionomycin (0.1 – 2 μM), lysed the cells and then performed Pyk2 immunoprecipitations on the cell lysates. Phosphotyrosine immunoblotting of the Pyk2 immunoprecipitations revealed that Pyk2 becomes phosphorylated after treatment with ionomycin (Figure 4-2a). Interestingly, lower concentrations of ionomycin (less than or equal to 1 μM) caused the greatest induction of phosphorylation. This was also evident in post-nuclear lysates (Figure 4-2b). Figure 4-2b demonstrates that Pyk2 is one of the major proteins that become inducibly tyrosine phosphorylated after ionomycin treatment. Immunoblotting Pyk2 immunoprecipitations performed after stimulation of AB.1 cells with the same range of ionomycin concentrations revealed that Pyk2 becomes phosphorylated on all the known phosphorylatable tyrosine residues upon stimulation of cells with ionomycin (Figure 4-2c). These antisera recognize Pyk2 in a stimulated cell lysate, however it is important to note that they also cross-react with other proteins within the cell lysate. Stimulation of CTL clones with ionomycin in the presence of EGTA to

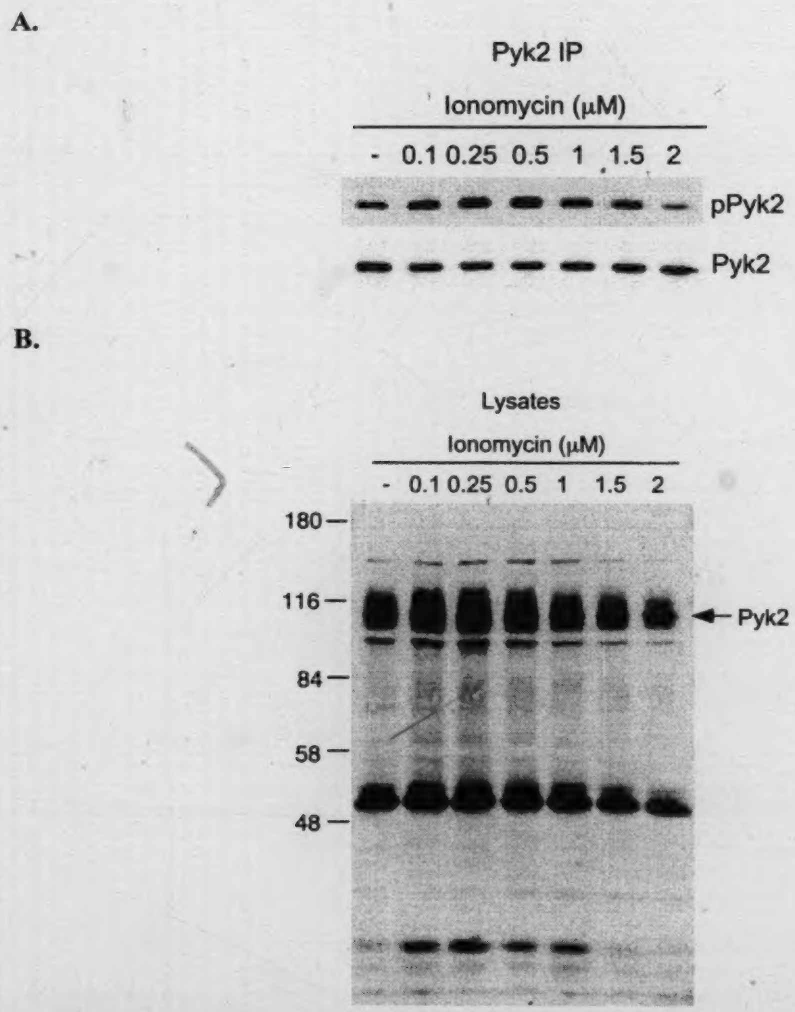

FIGURE 4-2. Stimulation of CTL clones with the calcium ionophore ionomycin induces Pyk2 phosphorylation. a) AB.1 CTL clones were stimulated with the indicated concentration of ionomycin for 10 minutes or DMSO as a carrier control. The cells were lysed and Pyk2 was immunoprecipitated from post-nuclear lysates. The IPs were run on an SDS-PAGE gel, transferred to a membrane and probed for phosphotyrosine. The membrane was then stripped and reprobed for Pyk2 (F298) as a loading control. b) A sample of the post-nuclear lysates from (a) were run on an SDS-PAGE gel, transferred to a membrane and immunoblotted with anti-phosphotyrosine. c) AB.1 were stimulated with a titration of ionomycin as in (a). The membrane was immunoblotted (in the following order) with anti- phosphotyrosine, Pyk2 phospho-specific antisera to Y580, Y881, Y579 and Y402 and anti-Pyk2 (F245). The Pyk2 phospho-specific antisera recognize Pyk2 in a cell lysate as well (not shown). d) Clones were stimulated with a titration of ionomycin with or without pre-incubation with 4 mM EGTA/8 mM $MgCl_2$ to chelate extracellular Ca^{2+}. Samples were probed with anti-phosphotyrosine and anti-Pyk2 (F245). c, d) Next page.

C.

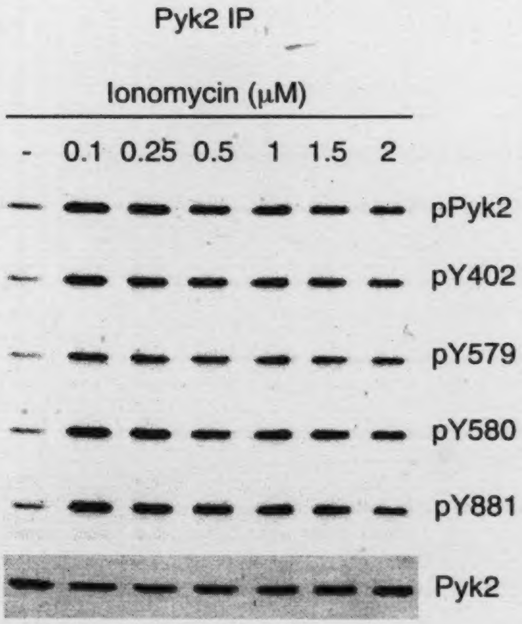
Pyk2 IP
Ionomycin (μM)
- 0.1 0.25 0.5 1 1.5 2
pPyk2
pY402
pY579
pY580
pY881
Pyk2

D.

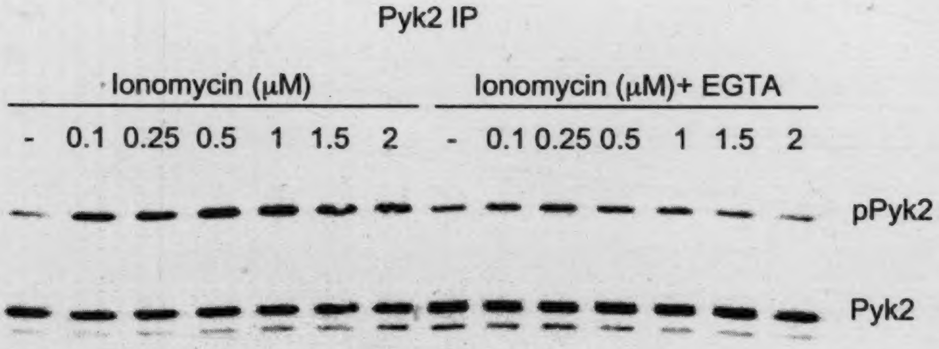
Pyk2 IP
Ionomycin (μM)
Ionomycin (μM)+ EGTA
- 0.1 0.25 0.5 1 1.5 2
- 0.1 0.25 0.5 1 1.5 2
pPyk2
Pyk2

chelate extracellular Ca^{2+} reduced, but did not completely abrogate, tyrosine phosphorylation of Pyk2 (Figure 4-2d). This suggests that the contribution to the rise in $[Ca^{2+}]_i$ due to the release of Ca^{2+} from intracellular stores is sufficient to induce low levels of Pyk2 phosphorylation, but extracellular Ca^{2+} is required for maximal phosphorylation.

I next used thapsigargin to examine the effect of increasing $[Ca^{2+}]_i$ on Pyk2 phosphorylation. Thapsigargin causes eventual emptying of Ca^{2+} from intracellular stores by inhibiting SERCA pumps in the ER that are responsible for pumping Ca^{2+} back into the ER (Mason et al. 1991). Phosphotyrosine immunoblots of Pyk2 immunoprecipitations performed on lysates of AB.1 cells treated with different concentrations of thapsigargin (0.1 – 2 μM) demonstrate that Pyk2 is inducibly phosphorylated after treatment with thapsigargin (Figure 4-3a). Pyk2 phosphorylation was induced with all concentrations used. Stimulation with thapsigargin in the presence of EGTA to chelate extracellular Ca^{2+} reduced Pyk2 phosphorylation, but a complete loss of tyrosine phosphorylation was not seen (Figure 4-3b). This result is similar to that seen with ionomycin and EGTA and again suggests that release of Ca^{2+} from intracellular stores alone is sufficient to induce low levels of Pyk2 phosphorylation. I therefore conclude that Pyk2 phosphorylation is activated in response to an increase in $[Ca^{2+}]_i$ in CTL.

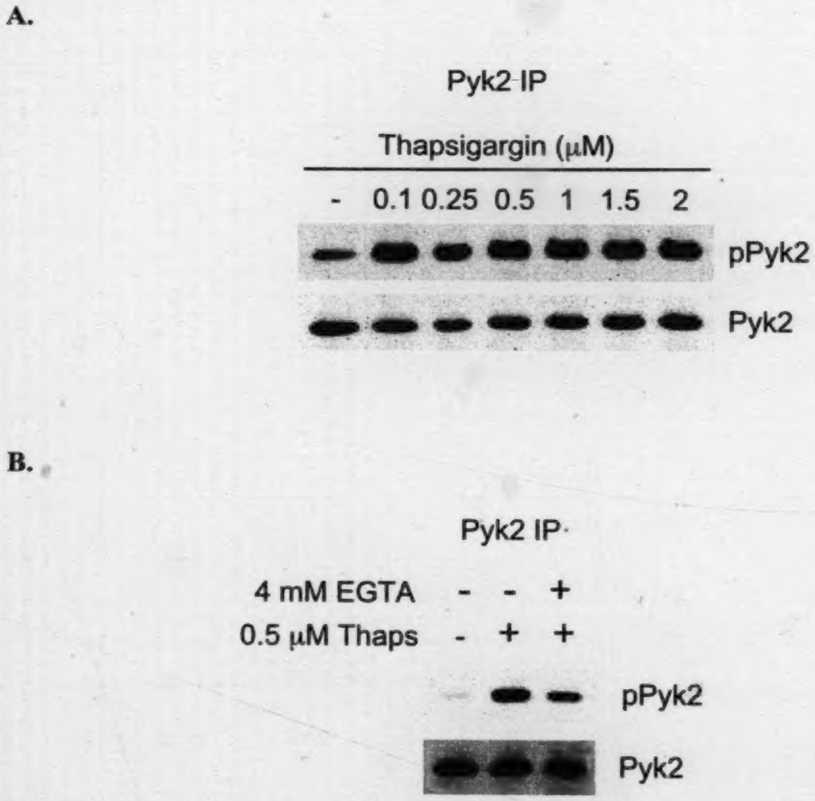
A.
Pyk2 IP
Thapsigargin (μM)
- 0.1 0.25 0.5 1 1.5 2
pPyk2
Pyk2
B.
Pyk2 IP
4 mM EGTA - - +
0.5 μM Thaps - + +
pPyk2
Pyk2

FIGURE 4-3. Pyk2 phosphorylation is induced when $[Ca^{2+}]_i$ is increased with thapsigargin. a) CTL clones were treated with a titration of thapsigargin for 10 minutes or DMSO as a carrier control. Pyk2 IPs were performed as in Figure 4-2a. Membranes were probed for phosphotyrosine and stripped and reprobed for Pyk2 (F298). b) Clones were stimulated with 0.5 μM thapsigargin for 10 minutes with or without pre-treatment with 4 mM EGTA/8 mM $MgCl_2$. Pyk2 IPs were performed and immunoblots were probed with anti-phosphotyrosine and anti-Pyk2 (F298).

Stimulation of CTL clones through the TCR in the presence of the intracellular calcium chelator BAPTA partially inhibits the induction of Pyk2 phosphorylation

As mentioned above, TCR triggering induces a rise in $[Ca^{2+}]_i$ in T cells. TCR engagement also induces phosphorylation of Pyk2 (Berg and Ostergaard 1997; Ganju et al. 1997; Qian et al. 1997; Dikic and Schlessinger 1998; Katagiri et al. 2000). To address the question of whether the rise in $[Ca^{2+}]_i$ contributes to the induction of Pyk2 phosphorylation after TCR stimulation, I subjected AB.1 CTL clones to either cross-linked or immobilized anti-CD3 stimulation in the presence of the cell-permeable intracellular Ca^{2+} chelator BAPTA-AM. The concentration of BAPTA used in these experiments was 30 μM as this concentration inhibits Ca^{2+}-dependent degranulation (based on unpublished work in the Ostergaard lab that I verified). Cross-linked anti-CD3 stimulation in the presence of 30 μM BAPTA partially inhibited the induction of Pyk2 phosphorylation (Figure 4-4a). This result implies that there is indeed a calcium-dependent component leading to Pyk2 phosphorylation after TCR triggering. Interestingly, BAPTA was unable to inhibit TCR-induced Pyk2 phosphorylation stimulated with immobilized anti-CD3 stimulation (Figure 4-4b). Note that the Pyk2 antibody used for immunoblotting in this panel is sensitive to the phosphorylation state of Pyk2 protein and will not bind as effectively to phosphorylated Pyk2. A higher concentration of BAPTA (60 μM) was also unable to cause a decrease Pyk2 phosphorylation (Figure 4-4c).

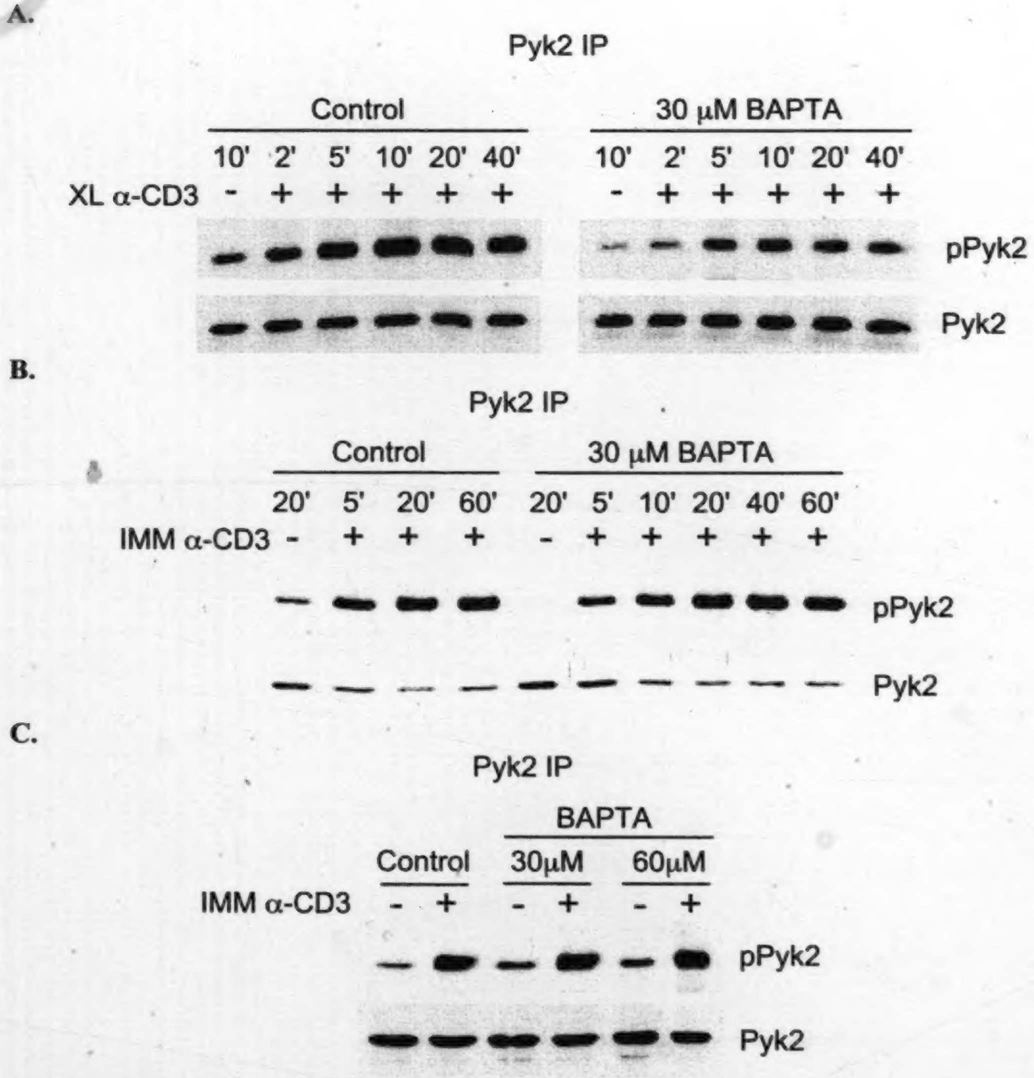
A.
Pyk2 IP
Control
30 μM BAPTA
10' 2' 5' 10' 20' 40'
10' 2' 5' 10' 20' 40'
XL α-CD3 - + + + + +
- + + + + +
pPyk2
Pyk2
B.
Pyk2 IP
Control
30 μM BAPTA
20' 5' 20' 60'
20' 5' 10' 20' 40' 60'
IMM α-CD3 - + + +
- + + + + +
pPyk2
Pyk2
C.
Pyk2 IP
BAPTA
Control
30μM
60μM
IMM α-CD3 - + - + - +
pPyk2
Pyk2

FIGURE 4-4. Pyk2 phosphorylation induced upon cross-linked TCR stimulation is partially inhibited in the presence of the intracellular Ca^{2+} chelator BAPTA. a) AB.1 cells were pre-treated with either 30 μM BAPTA or vehicle control (DMSO) for 15 minutes on ice. Clones were then stimulated with cross-linked anti-CD3 at 37°C for the indicated amount of time. Pyk2 IPs were performed as in Figure 4-2a. IPs were immunoblotted for phosphotyrosine and Pyk2 (F298) as a loading control. b) AB.1 were pre-treated as in (a) and then stimulated on immobilized anti-CD3 for the indicated time. Pyk2 IPs were performed on post-nuclear lysates and samples were probed with anti-phosphotyrosine and anti-Pyk2 (F245). c) Clones were pre-treated with either DMSO, 30 μM or 60 μM BAPTA and then stimulated for 20 minutes on immobilized anti-CD3. Pyk2 IPs were probed for phosphotyrosine and Pyk2 (F245).

TCR stimulation-induced Pyk2 phosphoylation is inhibited in the presence of cytochalasin E when cells are activated with immobilized, but not cross-linked, anti-CD3

It has previously been reported that the actin cytoskeleton plays a role in the induction of Pyk2 phosphorylation (Ganju et al. 1997; Rodriguez-Fernandez et al. 1999). Previous work in our lab has shown that an intact cytoskeleton is required for stimulation with immobilized anti-CD3 antibody but not for cross-linked antibody stimulation (Berg et al. 1998). Therefore, it is possible that the discordance noted above between the ability of BAPTA to reduce Pyk2 phosphorylation induced by cross-linked anti-CD3 and not immobilized anti-CD3 may be due to the differential contribution of the actin cytoskeleton to the two methods of stimulation. To test this theory, I stimulated CTL clones with either cross-linked or immobilized antibody in the presence of 10 μM cytochalasin E, a reagent that prevents actin polymerization and results in actin depolymerization. The induction of Pyk2 phosphorylation after immobilized anti-CD3 stimulation was completely abrogated in the presence of cytochalasin E and even the basal level of Pyk2 phosphorylation was reduced (Figure 4-5a). It is important to note that this concentration of cytochalasin E blocks the induction of general tyrosine phosphorylation upon immobilized anti-CD3 stimulation (Berg et al. 1998), therefore it is not surprising that Pyk2 phosphorylation is inhibited. However, as the basal level of Pyk2 phosphorylation is also affected, a role for the actin cytoskeleton in the induction of Pyk2 phosphorylation is suggested. Preventing actin polymerization during cross-linked anti-CD3 stimulation had no effect on the induction of Pyk2 phosphorylation (Figure 4-5b). These results imply that although the actin cytoskeleton may play a role in the

A.

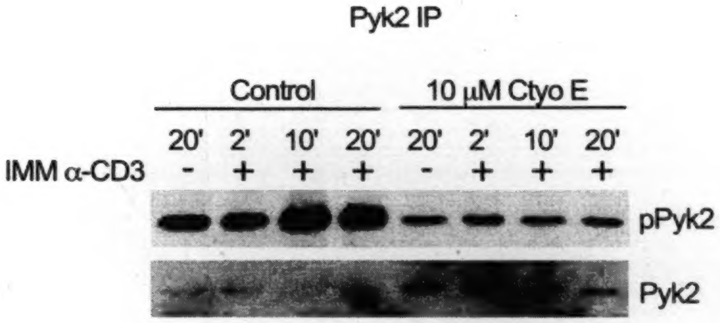
Pyk2 IP
Control
10 μM Ctyo E
20' 2' 10' 20' 20' 2' 10' 20'
IMM α-CD3 - + + + - + + +
pPyk2
Pyk2

B.

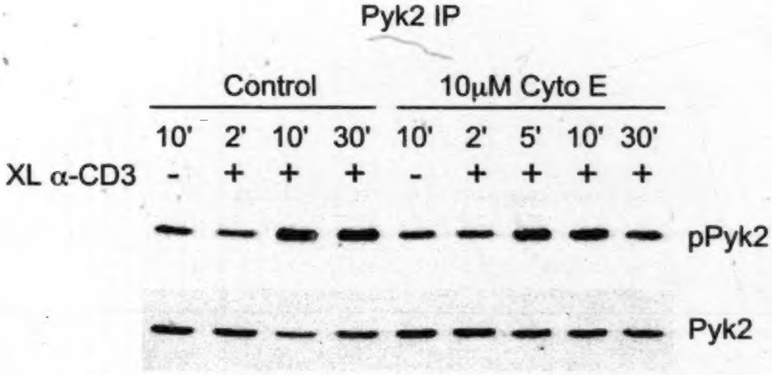
Pyk2 IP
Control
10μM Cyto E
10' 2' 10' 30' 10' 2' 5' 10' 30'
XL α-CD3 - + + + - + + + +
pPyk2
Pyk2

FIGURE 4-5. Inhibiting actin polymerization with cytochalasin E has no effect on the induction of Pyk2 phosphorylation upon stimulation with cross-linked anti-CD3. AB.1 cells were stimulated with immobilized (a) or cross-linked (b) anti-CD3 in the presence or absence of 10 μM cytochalasin E for the indicated time. Pyk2 immunoprecipitations were performed on the cell lysates. Membranes were immunoblotted with anti-phosphotyrosine and anti-Pyk2 (Pyk2 monoclonal for (a) and F245 antiserum for (b)).

induction of Pyk2 phosphorylation, it is not required. Based on the results from this section and from the BAPTA experiments, it is possible that during cross-linked anti-CD3 stimulation, a weaker signal is induced, perhaps due to a lack of induction of cytoskeletal rearrangements, and Ca^{2+} plays a significant role in the induction of Pyk2 phosphorylation. Immobilized anti-CD3 stimulation provides a much stronger stimulus in which the actin cytoskeleton is extensively rearranged. Therefore, the cytoskeleton may play a more dominant role in the induction of Pyk2 phosphorylation than does Ca^{2+} under these circumstances.

Stimulation of CTL clones through the TCR in the presence of the extracellular calcium chelator EGTA does not inhibit Pyk2 phosphorylation

To further investigate the notion that the release of Ca^{2+} from intracellular stores is involved in the induction of Pyk2 phosphorylation, I examined the effect of chelating extracellular calcium with EGTA during cross-linked TCR stimulation. Stimulation of CTL clones with cross-linked anti-CD3 in the presence of 4 mM EGTA had no adverse effect on the induction of Pyk2 phosphorylation (Figure 4-6a). Not surprisingly, immobilized anti-CD3 stimulation in the presence of EGTA also had no effect on Pyk2 phosphorylation (Figure 4-6b). Since no effect on cross-linked TCR-induced Pyk2 phosphorylation was observed when extracellular Ca^{2+} was chelated (Figure 4-6b) and a reduction in Pyk2 phosphorylation was observed when intracellular Ca^{2+} was chelated with BAPTA (Figure 4-4a), the release of Ca^{2+} from the ER stores may be sufficient to induce Pyk2 phosphorylation. I conclude that an increase in $[Ca^{2+}]_i$ can induce Pyk2

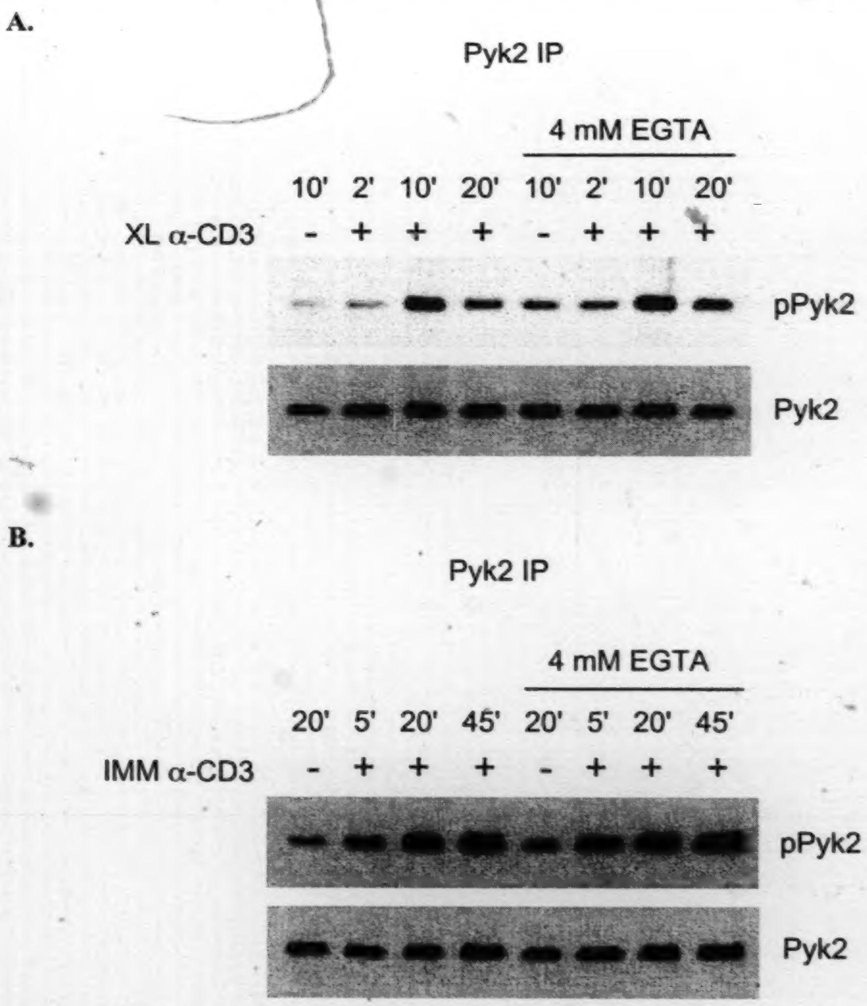
A.
Pyk2 IP
4 mM EGTA
10' 2' 10' 20' 10' 2' 10' 20'
XL α-CD3 - + + + - + + +
pPyk2
Pyk2
B.
Pyk2 IP
4 mM EGTA
20' 5' 20' 45' 20' 5' 20' 45'
IMM α-CD3 - + + + - + + +
pPyk2
Pyk2

FIGURE 4-6. Chelation of extracellular Ca^{2+} with EGTA does not inhibit the increase in Pyk2 phosphorylation induced upon TCR stimulation. a) CTL clones, pre-incubated in the presence or absence of 4 mM EGTA/8 mM $MgCl_2$, were stimulated with cross-linked anti-CD3 for the amount of time specified. Cells were lysed and Pyk2 IPs were performed as in Figure 4-2a. Phosphotyrosine and Pyk2 (F298) immunoblots are shown. b) Clones pre-treated with or without 4 mM EGTA/8 mM $MgCl_2$ were stimulated with immobilized anti-CD3 for the indicated time. Pyk2 IPs were probed for phosphotyrosine and Pyk2 (F298).

phosphorylation and that there is a calcium-sensitive component to the induction of Pyk2 phosphorylation during cross-linked TCR stimulation.

Stimulation of ConA blasts with ionomycin or thapsigargin induces Pyk2 phosphorylation

To test whether Pyk2 isolated from *ex-vivo* T cells was also sensitive to increases in $[Ca^{2+}]_i$, I generated polyclonally-activated T cells with the lectin ConA (concanavalin A) from *ex-vivo* splenocytes extracted from a C57BL/6 mouse. ConA blasts were stimulated with the same concentrations of ionomycin used above. As previously observed with the CTL clones (Figure 4-2a), Pyk2 phosphorylation was induced after treatment with ionomycin (Figure 4-7a). Similarly, lower concentrations of ionomycin were better able to induce phosphorylation (Figure 4-7a). Treatment of the blasts with 0.5 μM thapsigargin also induced Pyk2 phosphorylation (Figure 4-7b). These results suggest that in *ex-vivo* T cells, Pyk2 phosphorylation is also regulated by a rise in $[Ca^{2+}]_i$.

Calcineurin and CaMKII are not involved in inducing Pyk2 phosphorylation in response to an increase in intracellular calcium levels

I next attempted to determine how the increase in $[Ca^{2+}]_i$ transduces the signal to phosphorylate Pyk2. Pyk2 does not have a calcium binding domain and has never been shown to be directly activated by calcium/calmodulin. Therefore, Pyk2 is likely indirectly regulated by calcium. As mentioned above, two proteins that become activated upon binding of Ca^{2+}/calmodulin are calcineurin and CaMKII. To test whether these proteins are upsteam of Pyk2 phosphorylation, I pre-treated AB.1 cells with different

A.

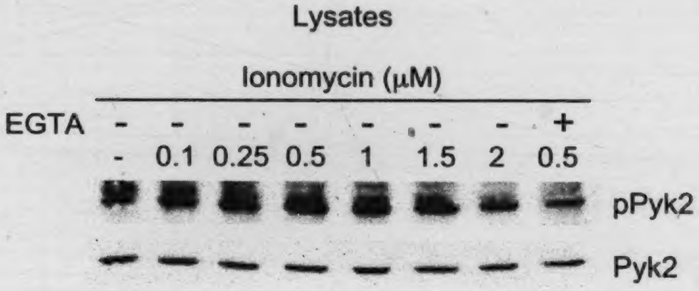
Lysates
Ionomycin (μM)
EGTA - - - - - - - +
- 0.1 0.25 0.5 1 1.5 2 0.5
pPyk2
Pyk2

B.

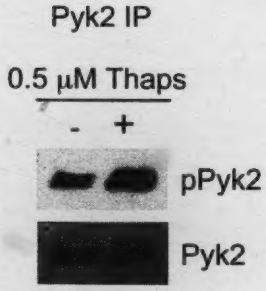
Pyk2 IP
0.5 μM Thaps
- +
pPyk2
Pyk2

FIGURE 4-7. Stimulation of Con A blasts with Ca^{2+} mobilizers induces Pyk2 phosphorylation. a) Con A blasts were stimulated in the presence or absence of 4 mM EGTA with a titration of ionomycin or DMSO carrier control. Post-nuclear lysates were immunoblotted for phosphotyrosine and Pyk2 (F298). b) Pyk2 IPs performed on lysates of Con A blasts stimulated with 0.5 μM thapsigargin or DMSO were immunoblotted for phosphotyrosine and Pyk2 (F298).

concentrations of FK506 or cyclosporin A (inhibitors of calcineurin) or KN-62 (an inhibitor of CaMKII) and then stimulated the cells with 0.5 μM ionomycin. As shown in Figure 4-8a, there was no inhibition of Pyk2 phosphorylation induced by ionomycin upon pre-treatment of the cells with FK506 or cyclosporin A. These results imply that Pyk2 phosphorylation, induced by a rise in $[Ca^{2+}]_i$, is independent of calcineurin. The results presented in figure 4-8b suggest that at high concentrations of KN-62 (75 and 100 μM), some ionomycin-induced Pyk2 phosphorylation is inhibited. The amount of DMSO (carrier for KN-62) added to the cells to yield these high concentrations of KN-62 is approximately 5 and 7% of the total reaction volume. Therefore, the reduction in Pyk2 phosphorylation may be a result of toxicity of the cells when exposed to high concentrations of DMSO. Therefore, these results should be repeated using a higher stock concentration of KN-62 to test for an inhibition of Pyk2 phosphorylation at higher concentrations of KN-62. Examination of cell viablility by Trypan Blue exclusion could be used to determine whether cytotoxicity is a problem.

SFK are known to be involved in the activation and phosphorylation of Pyk2 (Park et al. 2004). To test whether SFK may be involved in the phosphorylation of Pyk2 after treatment with ionomycin, AB.1 cells were stimulated with ionomycin in the presence of 10 μM PP2 or its inactive analog PP3. As shown in Figure 4-8c, stimulation in the presence of PP2 decreased Pyk2 phosphorylation induced by ionomycin. This suggests that SFK may be playing a role in phosphorylating Pyk2 in response to an increase in $[Ca^{2+}]_i$.

In another attempt to fit Pyk2 into a calcium signalling pathway, I tried to identify proteins that Pyk2 may interact with after ionomycin stimulation. Pyk2

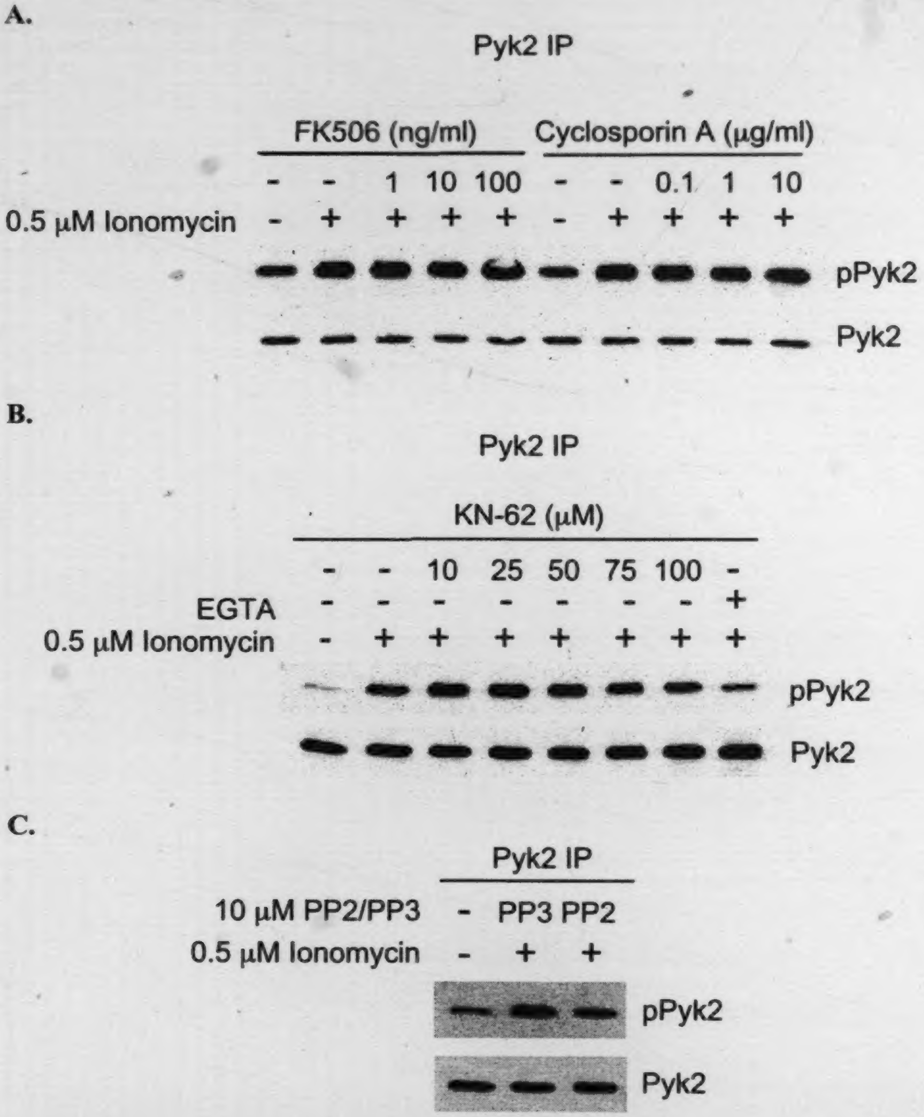
A.
Pyk2 IP
FK506 (ng/ml)
Cyclosporin A (μg/ml)
- - 1 10 100 - - 0.1 1 10
0.5 μM Ionomycin - + + + + - + + + +
pPyk2
Pyk2
B.
Pyk2 IP
KN-62 (μM)
- - 10 25 50 75 100 -
EGTA - - - - - - - +
0.5 μM Ionomycin - + + + + + + +
pPyk2
Pyk2
C.
Pyk2 IP
10 μM PP2/PP3 - PP3 PP2
0.5 μM Ionomycin - + +
pPyk2
Pyk2

FIGURE 4-8. Pyk2 phosphorylation induced by ionomycin is calcineurin- and CaMKII-independent, but is partially SFK-dependent. AB.1 cells were stimulated with 0.5 μM ionomycin or DMSO control (1.25 μl) in the presence or absence of the calcineurin inhibitors FK506 and Cyclosporin A (a) or the CaMKII inhibitor KN-62 (b) for 10 minutes with or without pre-treatment with 4 mM EGTA. Vehicle controls (-) for KN-62 = 18 μl DMSO (equivalent volume to 50 μM), FK506 = 1 μl methanol (equivalent volume in each sample), Cyclosporin A = 10 μl methanol (equivalent volume to 10 μg/ml). Pyk2 IPs were performed and were probed with phosphotyrosine and Pyk2 (F298). c) Clones were stimulated with 0.5 μM ionomycin or DMSO (1.25 μl) in the presence or absence of PP2/PP3. Vehicle control (-) for PP2/PP3 = 3 μl DMSO. Phosphotyrosine and Pyk2 (F298) immunoblots of Pyk2 IPs are shown.

immunoprecipitations were performed on CTL clone lysates from cells either left unstimulated or stimulated with ionomycin and run on an SDS-PAGE gel. The gel was subsequently stained with Coomassie Blue. Unfortunately, no obvious bands unique to ionomycin stimulation could clearly be detected (Figure 4-9). Therefore, the calcium-dependent signalling molecule(s) and pathway responsible for the induction of Pyk2 phosphorylation remain largely unidentified.

Pyk2 phosphorylation is not induced by increases in intracellular calcium in all cell types

To ascertain whether the discrepancies in the literature with respect to the regulation of Pyk2 phosphorylation by increases in $[Ca^{2+}]_i$ are partly due to the cell type used in the assay, I tested a panel of T cells and some non-T cells for a response to a rise in $[Ca^{2+}]_i$ after ionomycin stimulation. Cells that demonstrated an induction of Pyk2 phosphorylation in response to an increase in $[Ca^{2+}]_i$ include ConA blasts (primary T cells, Figure 4-7a), AB.1 CTL clones (Figure 4-2a) and B3Z cells (CTL hybridoma, Figure 4-10a). Cells which did not show significant induction of Pyk2 phosphorylation were Jurkat T cells (T leukemia, Figure 4-10b), WEHI-231 (B lymphoma, Figure 4-10c), RNK-LY49P (NK leukemia, Figure 4-10d) and NIH-3T3 (fibroblast, Figure 4-10e). It is important to point out that there is basal Pyk2 phosphorylation in most cell types, likely due to integrin engagement between the cells in suspension. The absence of basal phosphorylation in NIH-3T3 cells may reflect the fact these cells are normally adherent. When in suspension, basal Pyk2 phosphorylation may be reduced. These results suggest that not all T cells display a robust induction of Pyk2 phosphorylation in response to that

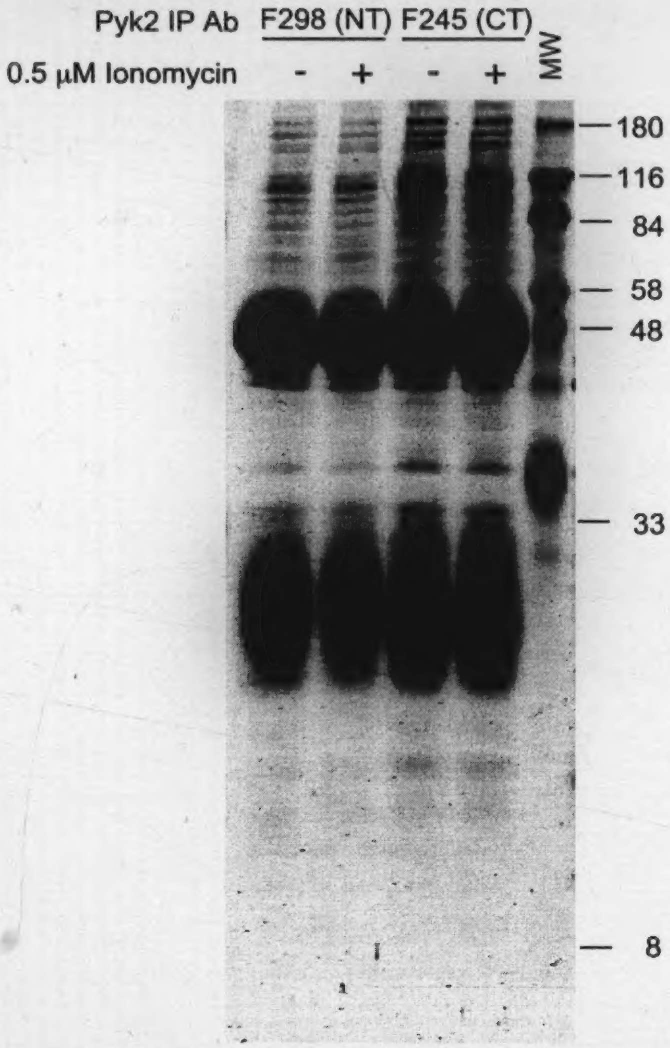
Pyk2 IP Ab
F298 (NT)
F245 (CT)
MW
0.5 μM Ionomycin
-
+
-
+
180
116
84
58
48
33
8

FIGURE 4-9. Upon stimulation of CTL clones with ionomycin, no unique proteins interacting with Pyk2 could be detected when compared to control-treated cells. AB.1 cells were stimulated with 0.5 μM ionomycin or DMSO carrier control for 10 minutes. Cells were lysed, Pyk2 immunoprecipitations were performed and run on an SDS-PAGE gel. The gel was subsequently stained with Coomassie Blue.

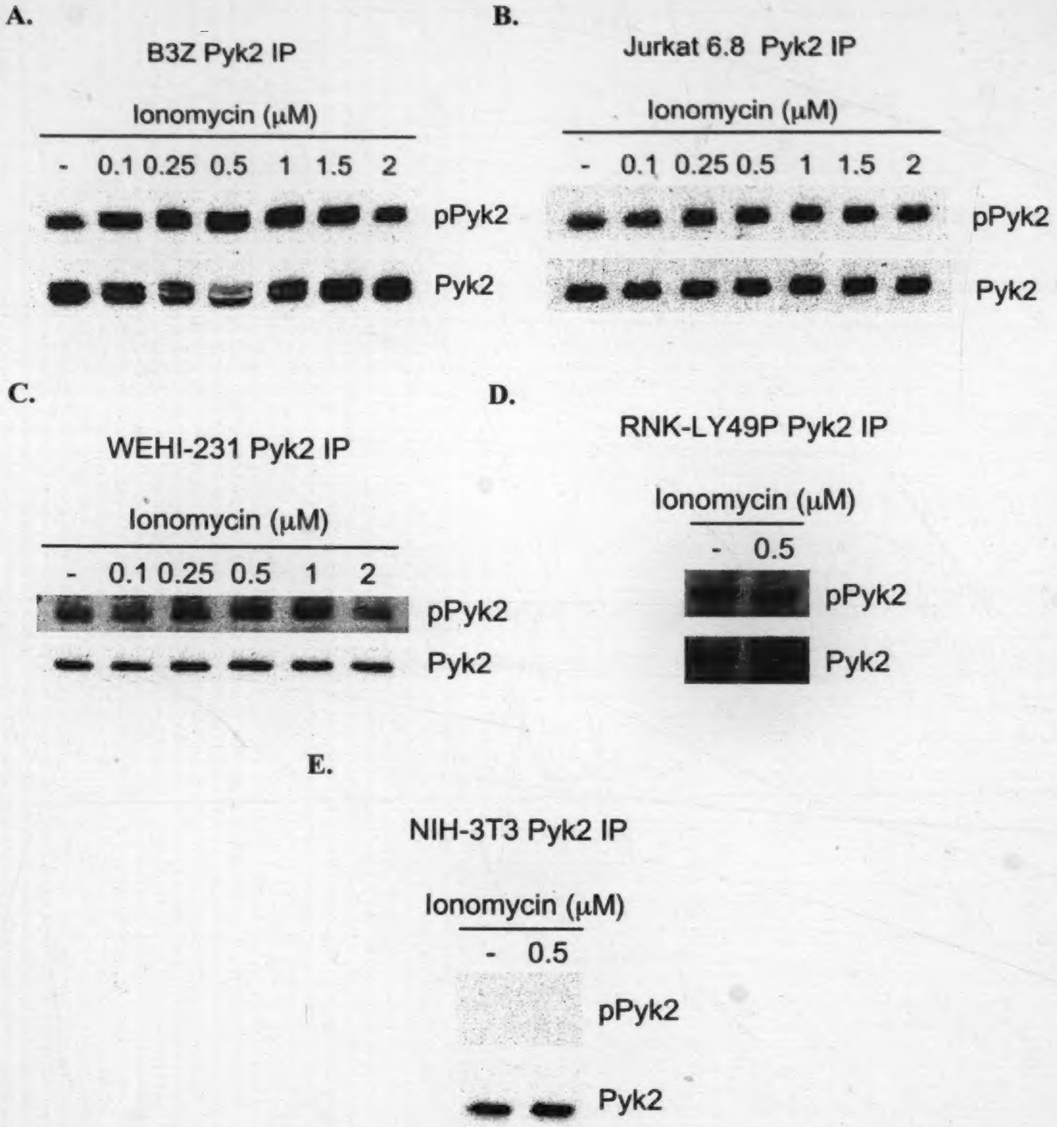
A.
B3Z Pyk2 IP
Ionomycin (μM)
- 0.1 0.25 0.5 1 1.5 2
pPyk2
Pyk2
B.
Jurkat 6.8 Pyk2 IP
Ionomycin (μM)
- 0.1 0.25 0.5 1 1.5 2
pPyk2
Pyk2
C.
WEHI-231 Pyk2 IP
Ionomycin (μM)
- 0.1 0.25 0.5 1 2
pPyk2
Pyk2
D.
RNK-LY49P Pyk2 IP
Ionomycin (μM)
- 0.5
pPyk2
Pyk2
E.
NIH-3T3 Pyk2 IP
Ionomycin (μM)
- 0.5
pPyk2
Pyk2

FIGURE 4-10. A significant increase in Pyk2 phosphorylation is not seen in all types of cells stimulated with ionomycin. B3Z (a), Jurkat 6.8 (b) and WEHI-231 (c) were stimulated with a titration of ionomycin for 10 minutes, cells were lysed and Pyk2 IPs were performed. Immunoblots were probed with phosphotyrosine and Pyk2 (F298 for Jurkat 6.8 and WEHI-231, Pyk2 monoclonal for B3Z). RNK-LY49P (d) and NIH-3T3 (e) were stimulated with 0.5 μM ionomycin or DMSO carrier control for 10 minutes. Pyk2 IPs were immunoblotted for phosphotyrosine and Pyk2 (F298 for RNK-LY49P, Pyk2 monoclonal for NIH-3T3).

stimulation with calcium ionophores alone as Jurkat T cells did not display a significant increase in Pyk2 phosphorylation. Also, whether a cell is of hematopoietic origin or not does not seem to be an indicator of whether a cell is likely to be able to respond to increases in $[Ca^{2+}]_i$ by induction of Pyk2 phosphorylation. Cell transformation does not appear to account for the differences either as both *ex-vivo* splenocytes and the B3Z CTL hybidoma, which was derived from a fusion with the BW5147 T lymphoma, underwent ionomycin-induced Pyk2 phosphorylation. Also, whether a cell is adherent or grown in suspension cannot account for the differences. Therefore, it is likely that the cell type used may indeed affect the ability to detect an increase in Pyk2 phosphorylation in response to a rise in $[Ca^{2+}]_i$. However, the reason for the differences in responses remains to be determined.

Stimulation of CTL clones with ionomycin alone or fibronectin alone induces Pyk2 phosphorylation while stimulation with both induces an additive increase in phosphorylation

As mentioned above, Ca^{2+} is involved in modulating T cell motility. When a migrating T cell encounters an APC or target cell, there is a rapid rise in $[Ca^{2+}]_i$ which causes the migrating T cell to stop and round up to maximize contact with the APC/target cell (Donnadieu et al. 1994; Negulescu et al. 1996). As Pyk2 phosphorylation is induced upon integrin engagment (involved in T cell migration) and an increase in $[Ca^{2+}]_i$, I tested the effect of inducing a “stop signal” (with ionomycin) on Pyk2 phosphorylation in cells crawling on fibronectin. AB.1 CTL clones were plated on wells coated with fibronectin or BSA as a control. Ionomycin was then added to appropriate wells and the cells were incubated at 37°C for either 10, 20, 40 or 60 minutes. Figure 4-11 demonstrates that fibronectin alone and ionomycin alone could induce Pyk2 phosphorylation, and in combination, there was an additive increase in Pyk2 phosphorylation. These results suggest that both stimuli can contribute to inducing Pyk2 phosphorylation and it is possible that both integrin engagement and Ca^{2+} flux are required for optimal Pyk2 phosphorylation. During stimulation of cells with ionomycin (in suspension), integrin stimulation may also come into play if the cells express both an integrin and its appropriate ligand. The results from this section may account for the lack of observed induction of Pyk2 phosphorylation upon ionomycin stimulation with certain cell types. In this regard, some cells may not reach a threshold of detection of Pyk2 phosphorylation with increases in $[Ca^{2+}]_i$ alone and the contribution from other stimuli, such as integrin engagement, may be required.

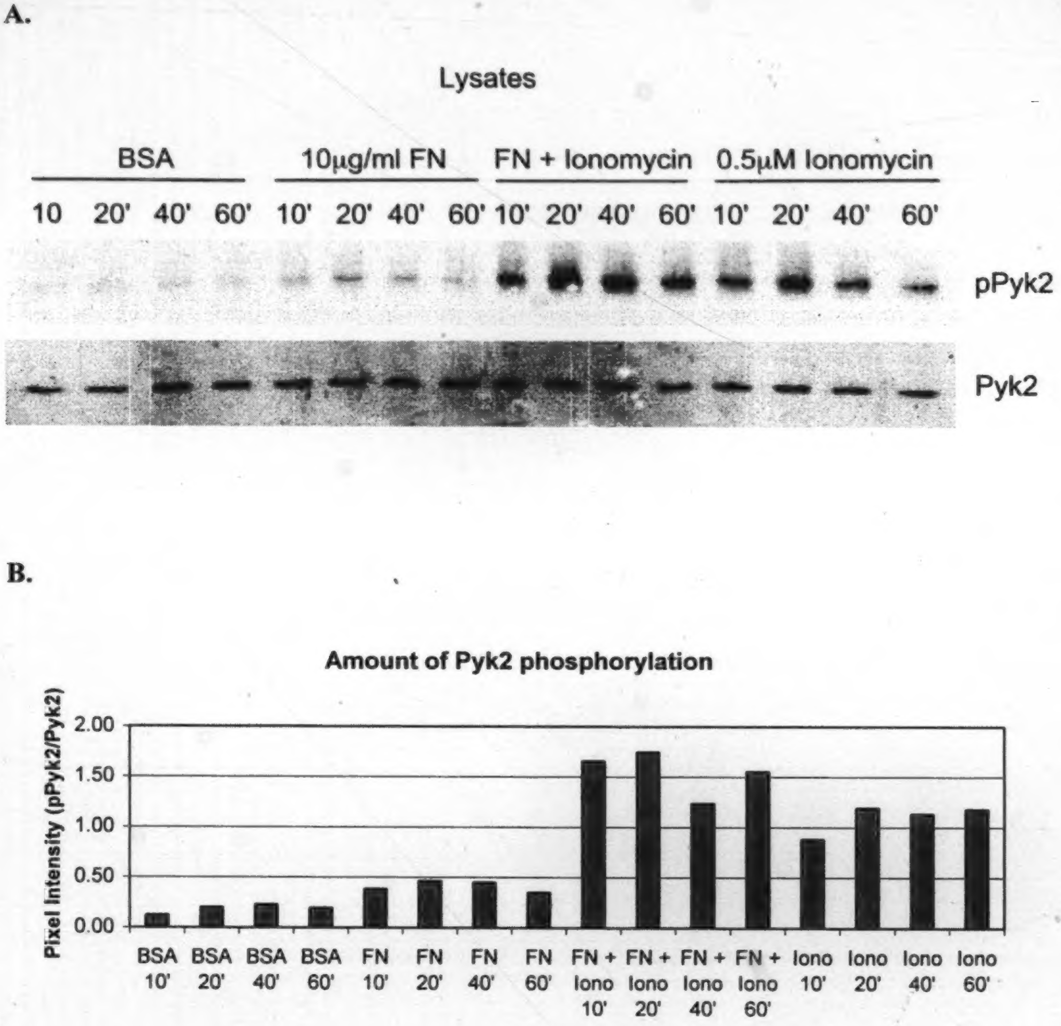

FIGURE 4-11. A cumulative increase in Pyk2 phosphorylation is seen when CTL clones are simultaneously stimulated with fibronectin and ionomycin. AB.1 cells were plated on 96 well dishes on wells coated with either BSA or 10 μg/ml fibronectin (FN). Cells were then either treated with 0.5 μM ionomycin or DMSO and incubated at 37°C for the specified time. Cells were lysed in the wells and entire samples were loaded on SDS-PAGE gels. Immunoblots for phosphotyrosine and Pyk2 (F298) were performed. Ratios of pixel intensities for each phospho-Pyk2 band to Pyk2 band were calculated for each lane as follows: integrated intensity – background (pPyk2) / integrated intensity – background (Pyk2).

C. Discussion

In this study, I examined wether Pyk2 phosphorylation was regulated by Ca^{2+} in T cells. As has been shown in many other cell types, Pyk2 was inducibly phosphorylated when $[Ca^{2+}]_i$ was increased by use of the Ca^{2+} mobilizers ionomycin and thapsigargin, in cloned CTL and *ex-vivo* T cells. Pyk2 phosphorylation induced by cross-linked anti-CD3 stimulation was decreased when intracellular Ca^{2+} was chelated with BAPTA. I further demonstrated that although normal mouse T cells exhibited Ca^{2+}-inducible Pyk2 phophorylation, not all T cell lines displayed a robust induction of Pyk2 phosphorylation in response to stimulation with a Ca^{2+} ionophore. I also implicated SFK in the regulation of Pyk2 phosphorylation upon an increase in $[Ca^{2+}]_i$.

Stimulation of both CTL clones and murine ConA blasts with a range of concentrations of ionomycin demonstrated that lower concentrations of ionomycin (less than or equal to 1 μM) caused the greatest induction of Pyk2 phosphorylation (Figures 4-1a and 4-6a). All concentrations of thapsigargin tested (0.1 – 2 μM) were able to equally induce Pyk2 phosphorylation (Figure 4-2a). Stimulation of clones with both of these Ca^{2+} mobilizing agents in the presence of EGTA reduced, but did not abrogate the phosphorylation of Pyk2 (Figures 4-1c and 4-2b). These results suggest that Pyk2 phosphorylation can be regulated by a rise in $[Ca^{2+}]_i$ in T cells and that the release of Ca^{2+} from intracellular stores is sufficient to induce low levels of Pyk2 phosphorylation.

I then asked whether a rise in $[Ca^{2+}]_i$, induced upon TCR stimulation, contributed to the phosphorylation of Pyk2 detected upon TCR triggering. To answer this question, I stimulated clones through the TCR in the presence of the intracellular Ca^{2+} chelator BAPTA. Interestingly, I found conflicting results when I compared different methods of

TCR stimulation. A partial inhibition of Pyk2 phosphorylation was detected when I stimulated the clones by cross-linking the TCR with anti-CD3 antibodies (Figure 4-4a). However, when the clones were stimulated by plating the cells on immobilized anti-CD3, no reduction in Pyk2 phosphorylation was seen (Figure 4-4b). These results clearly demonstrate that the method of stimulation plays an important role in whether or not an effect on Pyk2 phosphorylation is seen with an intracellular Ca^{2+} chelator. Our lab has previously shown that these two methods of stimulation result in very different functional outcomes (Berg et al. 1998). For instance, CTL clones will only degranulate after immobilized antibody stimulation (Berg et al. 1998). Immobilized anti-CD3 stimulation results in more sustained signalling and causes the cells to spread as would occur when a T cell interacts with an APC (Berg et al. 1998). The signals generated during immobilized antibody stimulation are therefore stronger and it is likely that multiple signals could synergize to induce Pyk2 phosphorylation (including the induction of actin polymerization during cell spreading). Immobilized anti-CD3 stimulation was still able to induce Pyk2 phosphorylation in the presence of BAPTA, to a similar extent as the control. Given, the actin cytoskeleton is active under these conditions and not during cross-linked anti-CD3 stimulation, it is likely that the actin cytoskeleton is contributing to the induction of Pyk2 phosphorylation during immobilized antibody stimulation.

I hypothesized that the type of T cell, used in an assay to asses whether Pyk2 phosphorylation can be regulated by Ca^{2+}, may be the source of some of the discrepancies in the literature. Indeed I found that not all T cells tested displayed a significant induction of Pyk2 phosphorylation after treatment with ionomycin. Interestingly, I found that Jurkat T cells, which were typically used, did not display a significant increase in Pyk2 phosphorylation (Figure 4-10b). I also could not correlate origin of the cell, cell transformation, growth properties of the cell, or the amount of Pyk2 protein expressed to whether a cell responded to an increase in $[Ca^{2+}]_i$ by phosphorylation of Pyk2. In T cells, Pyk2 phosphorylation can be induced by a number of different stimuli including integrin stimulation (Ma et al. 1997; van Seventer et al. 1998; Rodriguez-Fernandez et al. 1999; Rodriguez-Fernandez et al. 2001; Rodriguez-Fernandez et al. 2002). Stimulation through integrins may be relevant during ionomycin stimulation if the cells used express both an integrin and its ligand. Therefore, it is possible that integrin stimulation and the release of Ca^{2+} from stores could contribute in a cumulative fashion to induce Pyk2 phosphorylation during ionomycin treatment. Whether a T cell can respond to ionomycin treatment with detectable Pyk2 phosphorylation may depend on whether cumulative signals are received. Interestingly, Rodríguez-Fernández and colleagues found that ICAM-1/LFA-1 interactions were necessary for the Ca^{2+}-dependent activation of Pyk2 in human T lymphoblasts (Rodriguez-Fernandez et al. 2002). Further studies are needed to test this theory in my system as we know that our CTL clones express both LFA-1 and ICAM-1. Future experiments could include the use of LFA-1 blocking antibodies or chelation of Mg^{2+} during ionomycin treatment. Mg^{2+} is required for LFA-1 adhesion (Dransfield and Hogg 1989).

As mentioned above, there are conflicting reports in the literature as to whether Pyk2 phosphorylation is induced after a rise in $[Ca^{2+}]_i$ in T cells. Qian and colleagues found that 1 μM ionomycin was unable to induce Pyk2 phosphorylation in Jurkat T cells or murine thymocytes (Qian et al. 1997). In light of my findings, this is not surprising given that I was unable to detect a significant increase in Pyk2 phosphorylation with

Jurkat T cells. As for why no induction could be detected in thymocytes is not clear, but it is possible that the induction of Pyk2 phosphorylation may require cumulative signals to be detected in these cells. Rodríquez-Fernández and colleagues could not induce the catalytic activity (as measured by the induction of autophosphorylation) of Pyk2 isolated from human T lymphoblasts using 7 μM ionomycin (Rodriguez-Fernandez et al. 2002). It is possible that an induction of Pyk2 phosphorylation was not detected because the concentration of ionomycin used was too high as I found that lower concentrations of ionomycin (less than or equal to 1 μM) were best able to induce Pyk2 phosphorylation. This group also found that 5 μM thapsigargin was unable to induce the catalytic activity of Pyk2 (Rodriguez-Fernandez et al. 2002). It is possible that there may be differences between murine lymphoblasts and human lymphoblasts in their ability to respond to an increase in $[Ca^{2+}]_i$ by Pyk2 phosphorylation. Alternatively, there may also be a concentration issue as I did not test such a high concentration of thapsigargin. Two groups found that chelating or excluding Ca^{2+} from the extracellular space caused a partial reduction in Pyk2 phosphorylation after cross-linked TCR stimulation of Jurkat T cells (Ganju et al. 1997; Tsuchida et al. 1999). In these studies, an increase in Pyk2 phosphorylation using Ca^{2+} mobilizing agents was not tested. However, given the results obtained with EGTA or Ca^{2+}-free media, one might expect to detect an increase in Pyk2 phosphorylation. One possible explanation for this discrepancy may be that different Jurkat clones were used in these studies or that the different clones may have become divergent over time. In these Jurkat clones, the contribution from the release of Ca^{2+} from stores alone may not be sufficient to induce Pyk2 phosphorylation and Ca^{2+} influx may thus be required.

How the increase in $[Ca^{2+}]_i$ transduces the signal to phosphorylate Pyk2 remains unclear. Pyk2 does not contain an EF-hand motif nor has it been shown to bind Ca^{2+}/calmodulin. Most Ca^{2+}-regulated kinases are serine/threonine kinases, therefore it is unclear how Pyk2 becomes tyrosine phosphorylated in response to increases in $[Ca^{2+}]_i$. In some cell types it has been suggested that CaMKII may be an intermediate in the Ca^{2+}-dependent activation of Pyk2 (Ginnan and Singer 2002; Guo et al. 2004). In my study, CTL clones stimulated with ionomycin in the presence of a CaMK inhibitor displayed no inhibition of Pyk2 phosphorylation with concentrations of KN-62 ranging from 10-50 μM (Figure 4-8a). At higher concentrations (75 and 100 μM), some inhibition of Pyk2 phosphorylation was observed, however, the concentration of DMSO in these samples was very high and may have caused cytotoxicity towards the cells. Determination of a concentration of KN-62 that inhibits CaMKII activation in our CTL clones will be necessary before any firm conclusions can be drawn. I also found that inhibiting calcineurin had no effect on Pyk2 phosphorylation induced by ionomycin (Figure 4-8b). Interestingly, when I inhibited the activity of SFK, which are known to play a role in the phosphorylation of Pyk2 in response to other stimuli, I found that ionomycin-induced Pyk2 phosphorylation was decreased (Figure 4-8c). There has been another report of the inhibition of ionomycin-induced Pyk2 phosphorylation in the presence of the SFK inhibitor PP2. Ginnan and Singer found that stimulating vascular smooth muscle cells with 0.5 μM ionomycin in the presence of 10 μM PP2 decreased the phosphorylation of Pyk2 (Ginnan and Singer 2002).

It is unclear how SFK activity might be regulated by and increase in $[Ca^{2+}]_i$ induced by Ca^{2+} ionophores. It is possible that, if integrins are involved during ionomycin stimulation, SFK could be activated in response to integrin stimulation. Another explanation is that Pyk2 could be involved in the activation of SFK upon an increase in $[Ca^{2+}]_i$. SFK are repressed through intramolecular interactions involving the SH2 and SH3 domains. Formation of higher affinity interactions with these domains can disrupt the repressive intramolecular interactions, and consequently, activate the SFK (Thomas et al. 1998). FAK contains a consensus Src SH3 binding site adjacent to the autophosphorylation site (the docking site for the SH2 domain of SFK) (Thomas et al. 1998). Together, these two SFK binding motifs were found to activate Src (Thomas et al. 1998). The amino acid sequence constituting the Src SH3 binding site in FAK is similar in Pyk2, however it has not yet been demonstrated whether this site and the autophosphorylation site within Pyk2 can activate SFK. It is possible that phosphorylation of Pyk2 on Y402, upon an increase in $[Ca^{2+}]_i$, could recruit SFK which could dock, become activated and proceed to phosphorylate the remaining tyrosine residues within Pyk2. This theory is also consistent with the observation that Pyk2 tyrosine phosphorylation was not totally abrogated in the presence of PP2. Inhibition SFK does not affect phosphorylation of the autophosphorylation site.

Although I was unable to elucidate the mechanism whereby Pyk2 is phosphorylated in response to stimuli that increase $[Ca^{2+}]_i$ levels, I provided some insight as to why there are discrepancies in the literature with respect to whether Pyk2 is responsive to an increase in $[Ca^{2+}]_i$ in T cells. First, the concentration of ionomycin used in the assay may be important. Second, the method of TCR stimulation utilized when Ca^{2+} chelators are applied may play a role. Third, EGTA may not inhibit the phosphorylation of Pyk2 as the release of Ca^{2+} from intracellular stores seems to suffice to induce Pyk2 phosphorylation. Fourth, the cell type used in the assay may also have an effect as I have shown that not all cells seem to be responsive to increases in $[Ca^{2+}]_i$ via ionophore stimulation. One potential explanation for this observation is that some cells may not reach a threshold of detection of Pyk2 phosphorylation with increases in $[Ca^{2+}]_i$ alone. In these cells, simultaneous signals from other sources that can contribute to the induction of Pyk2 phosphorylation may be required to reach the threshold of detection. Alternatively, the different cell types may have differences in the subsets or ratios of signalling proteins involved in Ca^{2+} signalling in response to ionomycin. Taken together, my results show that Pyk2 can be regulated by Ca^{2+} in cloned CTL and *ex-vivo* T cells. Further studies are necessary to understand the involvement of SFK in the regulation of Pyk2 phosphorylation in response to an increase in $[Ca^{2+}]_i$.

CHAPTER 5: Two distinct populations of Pyk2 exist in CTL clones based on their differential ability to bind to paxillin

A. Introduction

FAK and Pyk2 are the two members of the focal adhesion tyrosine kinase family. They share approximately 45% amino acid identity and 65% similarity (Avraham et al. 1995; Sasaki et al. 1995; Herzog et al. 1996; Yu et al. 1996). These proteins have similar domain structure with N-terminal divergent FERM domains, centrally located kinase domains, two proline-rich regions in the C-terminus and a FAT domain within the extreme C-terminus (Ostergaard and Lysechko 2005). These proteins also have conserved tyrosine residues that, when phosphorylated, recruit SH2 domain-containing proteins (Avraham et al. 2000). Because of the similarity between the two proteins, much of the early work on determining binding partners, regulation and localization of Pyk2 was based on what was already known for FAK. While many parallels have been drawn in terms of binding partners and regulation of the two proteins, unique binding partners exist and some differences in the regulation of kinase activity have been documented. There are also significant differences in terms of localization within the cell as FAK is localized to focal adhesions and Pyk2 is diffused throughout the cytoplasm (Schaller and Sasaki 1997; Xiong et al. 1998). These differences suggest that the two proteins do not have totally redundant roles in the cell.

The regions of highest homology between FAK and Pyk2 exist within the kinase domain (~60%) (Avraham et al. 1995; Lev et al. 1995; Sasaki et al. 1995; Herzog et al. 1996) and the FAT domain (~61%) (Sasaki et al. 1995; Schaller and Sasaki 1997). High homology within the FAT domain led to speculation that Pyk2 would bind the cytoskeletal adapter protein paxillin as it had been shown that this region was responsible for FAK binding to paxillin (Turner and Miller 1994; Hildebrand et al. 1995; Tachibana et al. 1995). Indeed, earlier work demonstrated that paxillin co-immunoprecipitated with Pyk2 and that the association was constitutive (Salgia et al. 1996; Hiregowdara et al. 1997; Li and Earp 1997; Ostergaard et al. 1998). A direct interaction between the C-terminus of Pyk2 and paxillin was shown by far western blotting paxillin immunoprecipitations with fusions of the entire C-terminus of Pyk2 with GST (Hiregowdara et al. 1997) and by GST fusion protein pull downs of cell lysates with GST-C-terminus Pyk2 or GST-PRNK (comprises the C-terminus all but the first proline-rich region) (Hiregowdara et al. 1997; Schaller and Sasaki 1997; Xiong et al. 1998). The interaction was later shown to occur specifically within the FAT domain of Pyk2 as fusion proteins that were lacking part of the FAT domain failed to pull out paxillin (Xiong et al. 1998). The domains within paxillin that bind to FAK are the leucine-rich (LD) motifs (consensus sequence LDXLLXXL) LD2 and LD4, located within the N-terminus of the protein (Brown et al. 1996; Turner et al. 1999).

To date, the crystal structure of Pyk2 has not been solved and, consequently, little is known about the structure and folding of this protein. Although the intact protein has not been crystallized, the crystal structures of the FERM (Ceccarelli et al. 2006), catalytic (Nowakowski et al. 2002) and FAT domain (Arold et al. 2002; Hayashi et al. 2002) of FAK have been solved. These structures may allow us to draw parallels between the structure and folding of FAK and Pyk2.

Crystal structures and NMR (nuclear magnetic resonance) solution structures of the FAK FAT domain demonstrate that the FAT domain exists as a tightly packed four helix bundle with a hydrophobic core (Figure 5-1) (Arold et al. 2002; Hayashi et al. 2002; Liu et al. 2002). A close structural homolog of the FAT domain is the vinculin tail which also binds to paxillin in this region and targets to focal adhesions (Arold et al. 2002; Hayashi et al. 2002; Liu et al. 2002). Two hydrophobic patches were noted that formed at the interface between helicies 2 and 3 and 1 and 4 on opposite faces of the helix bundle (Hayashi et al. 2002). By use of modeling programs, it was found that peptides representing the LD motifs LD2 and LD4, in a helical conformation, fit into the hydrophobic patches very well (Hayashi et al. 2002) and this suggested that there were two sites in the FAT domain that could bind to paxillin. A crystal structure of the FAK FAT domain bound to either LD2 or LD4 confirmed the existence of the hydrophobic patches and showed that they were indeed involved in binding the LD motifs (Hoellerer et al. 2003).

An NMR solution structure of the paxillin LD2 motif bound to helicies 1 and 4 revealed that Y925 (the Grb2 binding site located within helix 1) was partially covered by the bound LD2 peptide (Liu et al. 2002). It was therefore proposed that phosphorylation of this site, and subsequent binding of Grb2, would require the release of previously bound paxillin. Indeed, there is evidence in the literature of conformational change in the FAT domain that would disrupt paxillin binding and favor Y925 phosphorylation. When attempting to crystallize the unligated FAK FAT domain, Arold and colleagues obtained two different crystal forms: one that formed a normal four helical bundle and one that contained helix-exchanged dimers in which helix 1 of one FAT domain was swapped with helix 1 of another FAT domain (Arold et al. 2002). It was suggested that the second structure represented a minor population of the FAT domains and likely resulted from a

A.

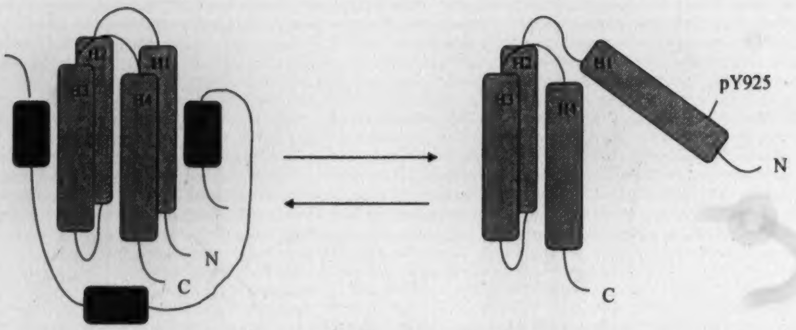

B.

```
                                             ▼ Y925          α1
mFAK      SISSPADSYNEGVKLQPQEISPPPTANLDRSNDKVYENVTGLVKAVIEMSSKIQPAPPEE 949
mPyk2     --------------------SIQPTANLDRTDDLVYHNVMTLVEAVLELKNKLGQLPPED 905
                              *  *******::* **.**  **:**:*:..*:   ***:
                                             ▲ Y881

                                 α2                                α3
mFAK      YVPMVKEVGLALRTLLATVDETIPALPASTHREIEMAQKLLNSDLGELISKMKLAQQYVM 1009
mPyk2     YVVVVKNVGLNLRKLIGSVDDLLPSLPASSRTEIEGTQKLLNKDLAELINKMKLAQQNAV 965
          ** :**:*** **.*:.:**: :*:****:: *** :*****.**.***.******* .:

                                          α4
mFAK      TSLQQEYKKQMLTAAHALAVDAKNLLDVIDQARLKMLGQTRPH- 1052
mPyk2     TSLSEDCKRQMLTASHTLAVDAKNLLDAVDQAKVVANLAHPPAE 1009
          ***.:: *:*****:*:**********.:***::       *
```

FIGURE 5-1. Model for the interaction of the FAK FAT domain with LD motifs of paxillin. a) The FAK FAT domain exists as a tightly packed four helix bundle (H1-H4) that can interact with the LD motifs of paxillin (LD2 and LD4) or exists in a conformation in which H1 separates from the bundle which favours phosphorylation of Y925 and disrupts paxillin binding. b) Comparison of the amino acid sequences of the FAT domains of mouse FAK (aa 890-1052, GenBank Accession No. M95408) and mouse Pyk2 (aa 866-1009, GenBank Accession No. Q9QVP9) using Clustal W version 1.83. The four alpha helicies that constitute the FAT domain of FAK are shown and were adapted from Hayashi et al. 2002. The triangles point to Y925 of FAK and Y881 of Pyk2 and demonstrate the overlap with helix 1.

state in which helix 1 dissociated from the bundle resulting a more open conformation of the FAT domain (Arold et al. 2002). Another group noted a difference between their NMR structure and published crystal structures of the FAK FAT domain (Prutzman et al. 2004). They found that the loop connecting helix 1 and 2 was less structured in solution and proposed that this loop served as a hinge region which could allow for conformational exchange between a "closed" helix bundle and an "open" helix bundle (Prutzman et al. 2004). A third study examined FAK FAT folding intermediates by combining hydrogen exchange data and discrete molecular dynamic simulations (Dixon et al. 2004). They described an intermediate in which helix 1 separated from the bundle and lost helical structure (Dixon et al. 2004). The findings from these studies provide support for a conformational change within helix 1 that would favor phosphorylation of Y925 and binding of Grb2 as opposed to paxillin binding. In support of this theory, a GST-helix 1 fusion protein was phosphorylated approximately 8 fold more by constitutively active Src than GST-FAT in an *in vitro* kinase assay (Prutzman et al. 2004).

Whether the FAT domain of Pyk2 interacts with paxillin LD motifs in a similar manner to FAK remains to be determined. Figure 5-1b shows a comparison of the amino acid sequences of the FAK and Pyk2 FAT domains and the location of the four alpha helices. This figure demonstrates that there are many conserved residues between the two proteins within the alpha helices. Interestingly, when examining the binding affinities of the FAK and Pyk2 FAT domains for a peptide representing the paxillin LD2 motif by isothermal titration calorimetry (ITC), Gao and colleagues found that Pyk2 FAT had very similar thermodynamic characteristics to FAK FAT when binding to LD2 at both hydrophobic patches (Gao et al. 2004). The authors concluded that their results support the notion that the FAT domains of the two proteins are structurally related and therefore may undergo similar folding and paxillin binding properties (Gao et al. 2004). In this study, I provide biochemical evidence that suggests that structural changes occur within Pyk2 to regulate its association with paxillin.

B. Results

There are two distinct populations of Pyk2 in unstimulated CTL clones; one that is associated with paxillin and one that is not

Our lab has generated two polyclonal antibodies directed against the N- and C-termini of Pyk2, named F298 and F245 respectively. F298 was produced by injection of a peptide consisting of aa 2-12 into rabbits and F245 was created by injection of aa 720-826 fused C-terminally to GST into rabbits (Berg and Ostergaard 1997). I compared the ability of these two anti-Pyk2 antisera and two other commercial polyclonal antibodies directed against the N- and C-termini of Pyk2, N-19 and C-19 respectively, to co-immunoprecipitate paxillin. AB.1 CTL clones were stimulated through the TCR with either cross-linked or immobilized anti-CD3. The cells were then lysed, and Pyk2 was immunoprecipitated from the cell lysates with each of the four antisera. Interestingly, I could only detect substantial paxillin association when Pyk2 was immunoprecipitated with our F245 antibody directed against the C-terminus of Pyk2 (Figure 5-2a). This association was constitutive as paxillin was detected in Pyk2 immunoprecipitations from unstimulated and TCR-stimulated lysates (Figure 5-2a). There appeared to be no increase in the amount of paxillin associated with Pyk2 after TCR stimulation (Figure 5-2a). Note that after stimulation with immobilized anti-CD3, paxillin undergoes phosphorylation and, consequently, displays more slowly migrating forms. That the F245-immunoreactive Pyk2 was the only Pyk2 immune complex associated with paxillin, this suggests that F245 binding may strengthen the Pyk2/paxillin interaction. Alternatively, there may be two distinct populations of Pyk2 in the clones; one that associates with paxillin and one that does not.

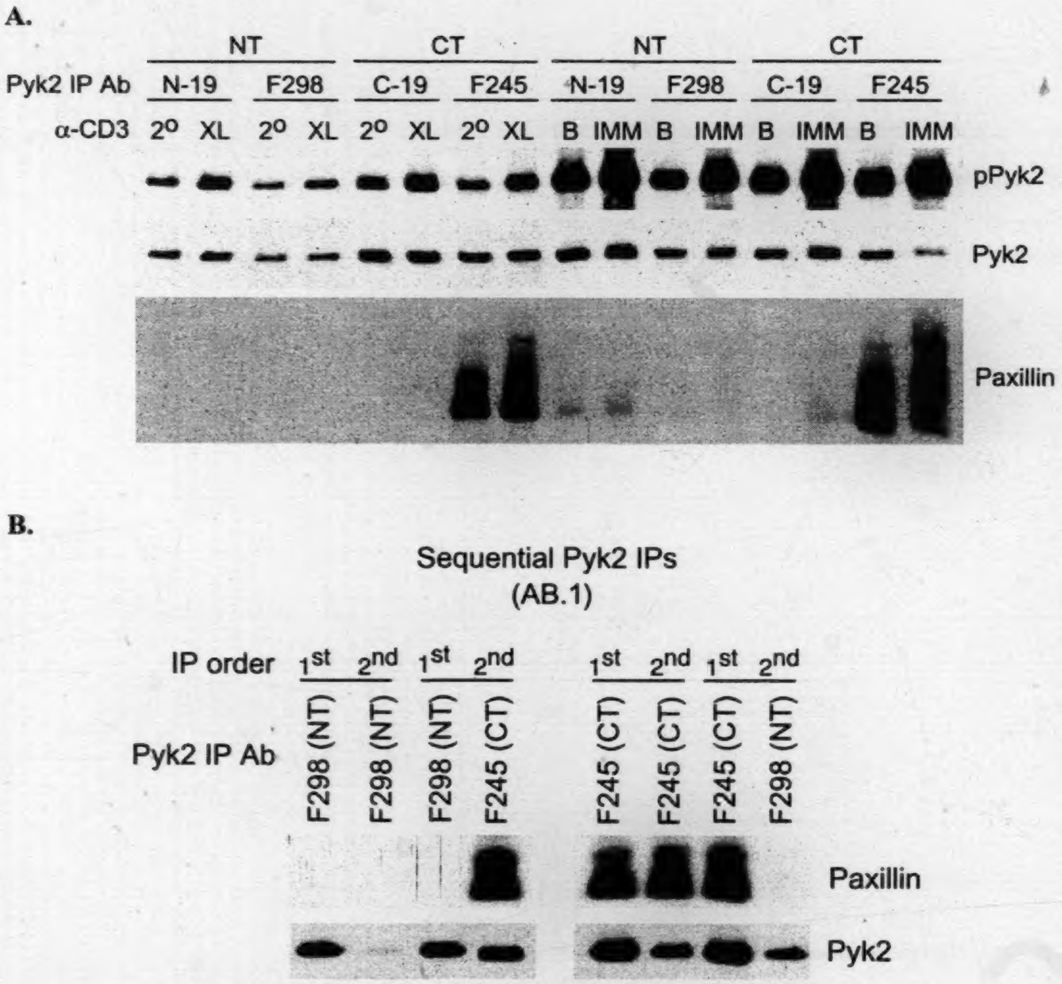
A.
NT
CT
NT
CT
Pyk2 IP Ab
N-19
F298
C-19
F245
N-19
F298
C-19
F245
α-CD3
2° XL 2° XL 2° XL 2° XL B IMM B IMM B IMM B IMM
pPyk2
Pyk2
Paxillin
B.
Sequential Pyk2 IPs
(AB.1)
IP order
1st 2nd 1st 2nd 1st 2nd 1st 2nd
Pyk2 IP Ab
F298 (NT)
F298 (NT)
F298 (NT)
F245 (CT)
F245 (CT)
F245 (CT)
F245 (CT)
F298 (NT)
Paxillin
Pyk2

FIGURE 5-2. A substantial amount of paxillin is only associated with F245-captured Pyk2. a) AB.1 CTL clones were stimulated with either cross-linked (XL) or immobilized (IMM) anti-CD3 for 10 min or 20 min respectively. Cells were lysed and Pyk2 immunoprecipitations were performed on the lysates with the anti-Pyk2 antibodies N-19, C-19, F298 and F245. Samples were run on SDS-PAGE gels, transferred to membranes and blotted for phosphotyrosine, Pyk2 (F298) and paxillin. NT and CT denote N-terminus and C-terminus respectively. B = BSA, 2° = only secondary cross-linking antibody added. b) Sequential Pyk2 immunoprecipitations were performed on unstimulated cell lysates from AB.1 CTL clones. After immunoprecipitation using the first anti-Pyk2 antibody, beads were pelleted and supernatants were transferred to new tubes. Immunoprecipitation with the second anti-Pyk2 antibody was then performed. Samples collected from the first and second immunoprecipitations were run on gels. Immunoblots for Pyk2 (Pyk2 monoclonal) and paxillin are shown.

To more closely examine whether there were two populations of Pyk2 in CTL clones, I performed sequential Pyk2 immunoprecipitations on unstimulated cell lysates with the F298 and F245 antisera. Immunoprecipitation was performed first with one antibody, then non-antibody-bound lysate was recovered and transferred to a new tube and immunoprecipitation was performed with the second anti-Pyk2 antibody. A control experiment, in which the first and second antibody used was F298, showed that most of the Pyk2 that is immunoreactive with this antibody was removed after the first immunoprecipitation (Figure 5-2b). When F245 was used as the first and second antibody, more F245-reactive Pyk2 could be recovered upon the second immunoprecipitation (Figure 5-2b). When F245 was used to pre-clear the lysate, F298 recovered more Pyk2 which was clearly not associated with paxillin (Figure 5-2b). Performing an F245 immunoprecipitation on an F298-pre-cleared lysate recovered Pyk2 that was associated with paxillin (Figure 5-2b). Similar results were found when the same experiment was performed in NIH-3T3 fibroblasts (Appendix Figure 3) demonstrating that this is not a phenomenon specific to T cells. These results suggest that there are indeed two different populations of Pyk2 in the CTL clones based on their differential ability to associate with paxillin.

Phosphorylation of Pyk2 is one factor involved in the differential recognition of Pyk2 by the F298 and F245 antibodies

Both the F298 and F245 polyclonal antibodies can be used for immunoprecipitation of Pyk2 as well as for immunoblotting Pyk2. This demonstrates that the antibodies can recognize Pyk2 in its native or denatured form and suggests that the conformation of Pyk2 is not the sole determinant of whether the antibodies can bind to Pyk2 or not. To determine whether other factors were playing a role in the differential binding of the two antibodies, I tested the ability of F298 and F245 to immunoblot Pyk2 immunoprecipitations performed with either antiserum. I performed duplicate Pyk2 immunoprecipitations with both antibodies using lysates of unstimulated CTL clones or clones stimulated with the Ca^{2+} ionophore ionomycin. One set of immunoprecipitations was then immunoblotted with F298 and the other with F245. The results show that the F298 antiserum was capable of immunoblotting Pyk2 captured with either antibody, however, the F245 antiserum was only capable of recognizing Pyk2 captured with the F245 antibody (Figure 5-3a). This observation suggested that post-translational modifications of Pyk2 may be involved in the differential binding abilities of the two antibodies. Post-translational modifications of proteins can include glycosylation, methylation, phosphorylation, ubiquitination and sumoylation, to name a few.

Pyk2 is regulated by phosphorylation. I therefore explored the possibility that phosphorylation might be one factor involved in the differential binding of the F298 and F245 polyclonal antibodies to Pyk2. Pyk2 immunoprecipitated with the F298 antibody from unstimulated CTL clones was left untreated or treated with calf intestinal alkaline phosphatase (CIAP) to remove all phosphate groups from the protein. The immunoprecipitates were then immunoblotted with the F245 antiserum. As shown in Figure 5-3b, treatment of the F298 immunoprecipitation with CIAP allowed recognition by the F245 antibody. This implies that phosphorylation is playing a role in the differential binding of the two antibodies, and further suggests that Pyk2 immunoreactive with F298 is differentially phosphorylated than Pyk2 immunoreactive with F245.

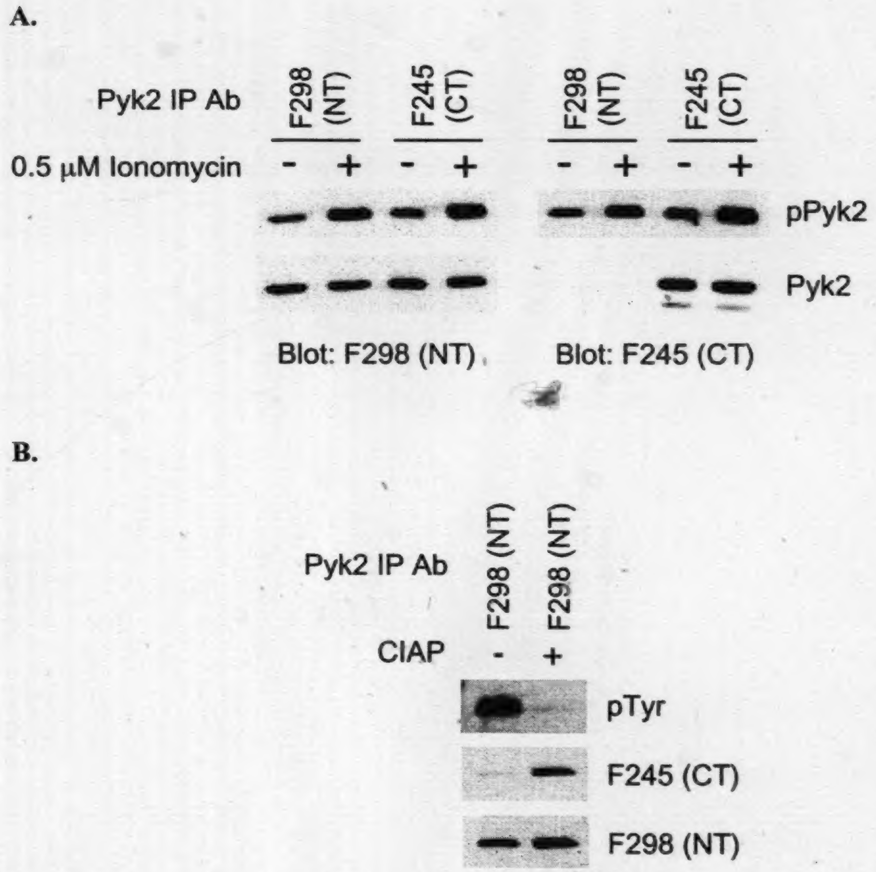
A.
Pyk2 IP Ab
F298 (NT)
F245 (CT)
F298 (NT)
F245 (CT)
0.5 μM Ionomycin
- + - + - + - +
pPyk2
Pyk2
Blot: F298 (NT)
Blot: F245 (CT)
B.
Pyk2 IP Ab
F298 (NT)
F298 (NT)
CIAP
- +
pTyr
F245 (CT)
F298 (NT)

FIGURE 5-3. The F245 antibody preferentially recognizes Pyk2 that has reduced phosphorylation. a) CTL clones were stimulated with either DMSO carrier control or 0.5 μM ionomycin for 10 min. Duplicate Pyk2 immunoprecipitations of cell lysates were carried out using the F298 and F245 antibodies. Both sets of samples were run on gels and transferred to membranes. One set of immunoprecipitations was blotted with anti-phosphotryosine and F298, the other was blotted with anti-phosphotyrosine and F245. b) Pyk2 from unstimulated cell lysates was immunoprecipitated with the F298 antibody. The immunoprecipitations were then subjected to treatment with CIAP or an equal volume of CIAP dilution buffer. Membranes were immunoblotted (in the indicated order) with anti-phosphotyrosine, F245 and F298.

Interestingly, no phosphorylation sites have as of yet been identified for the region of Pyk2 corresponding to the F245 recognition site (aa 720-826) (Figure 5-4a). As CIAP will remove phosphate groups from serine, threonine or tyrosine residues I do not yet know which type of phosphorylation is involved. Figure 5-4b shows the amino acid sequence to which the F245 antiserum was generated. As the AB.1 CTL clones express only the Pyk2-H isoform (Figure 6-2, next chapter), this leaves 64 amino acids which could contain potential phosphorylation sites. Within these 64 amino acids, there are three serine residues, one tyrosine and one threonine residue. According to the NetPhos 2.0 program, which predicts potential phosphorylation sites, Y722, S788 and S789 are candidate sites. Studies involving mass spectrometry of Pyk2 immune complexes isolated with each antibody or site-directed mutagenesis will be necessary to determine whether Pyk2 can become phosphorylated within the 64 amino acid stetch.

Pyk2 capable of associating with paxillin is less phosphorylated than Pyk2 that does not associate with paxillin

The results shown above would seem to suggest that Pyk2 that can associate with paxillin (F245-immunoreactive) is less phosphorylated than Pyk2 that does not associate with paxillin (F298-immunoreactive). Interestingly, the region implicated above (aa 720-826, in the proline-rich region) does not correspond to the paxillin binding site within Pyk2 (the FAT domain). This suggests that phosphorylation within the proline-rich region is not directly interfering with paxillin binding. As mentioned in the introduction, the FAK FAT domain is a tight helical bundle containing two hydrophobic patches (HP1, 2) that bind paxillin LD motifs (Hayashi et al. 2002). A more open conformational

A.

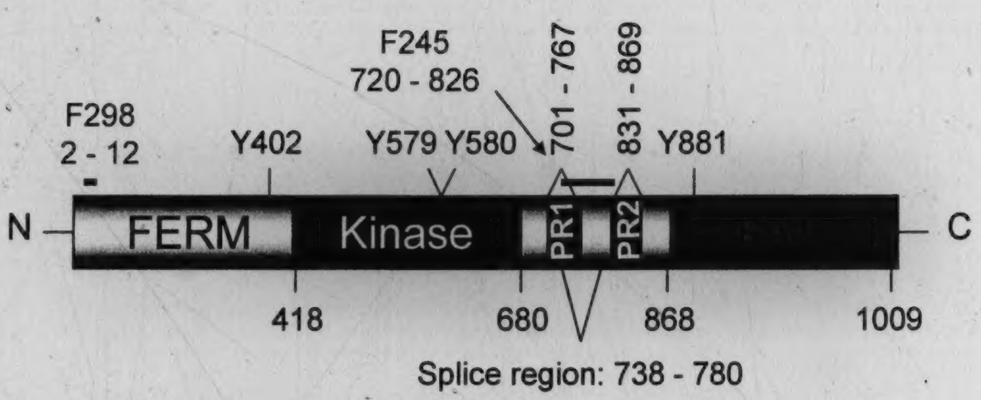

B.

```
mFAK     APPKPSRPGYPSPRSSEGFYPSPQHMVQTNHYQVS-GYPGSHGIPAMAGSIYQGQASLLD 769
mPyk2    PPPKPSRPKYRPPPQTNLLAPKLQFQVPEGLCASSPTLTSPMEYPSPVNSLHT--PPLHR 770
         .******* * .* .:: : *. *. *  .    *   ...   *: ..*::   ..*

mFAK     QTELWNHRPQEMSMWQPSVEDSAALDLRGMGQVLPPHLMEERLIRQQQEMEEDQRWLEKE 829
mPyk2    HNVFKRHSMREEDFIRPSSRE-EAQQLWEAEKIK----MKQVLERQQKQMVEDSQWLRRE 825
         :. : .*  :* .: :** .:  * :*    ::     *:: * ***::* **.:**.:*

mFAK     ERFLKPDVRLSRGSIDREDGSFQGPTGNQHIYQPVGKPDPAAPPKKPPRPGAPGHLSNLS 889
mPyk2    ERCLDPMVYMN-------DKSPLTPE------KEAGYTEFTGPPQKPPRLGAQ------- 865
         ** *.* * :.       * *   *       : .* .: :.**:**** **
```

FIGURE 5-4. The recognition sites for the F298 and F245 antisera. a) Displayed are the boundaries of the domains of Pyk2, the regions to which the F298 and F245 antibodies were generated and the splice region. b) Comparison of the amino acid sequences of the proline-rich regions of mouse FAK (aa 698-889, GenBank Accession No. M95408) and mouse Pyk2 (aa 713-865, GenBank Accession No. Q9QVP9) using Clustal W version 1.83. The highlighted region of Pyk2 denotes the sequence used to generate the F245 antibody and the underlined area within this region denotes the splice site. The amino acids displaying the dark shading show Y722, S788 and S789 which are predicted phosphorylation sites outside of the splice region based on the NetPhos 2.0 program.

structure of the FAT domain has also been proposed, which would favor phosphorylation of Y925 of FAK and directly interfere with paxillin binding at HP1 (Arold et al. 2002; Dixon et al. 2004; Prutzman et al. 2004). I therefore examined whether phosphorylation of the analogous tyrosine residue in Pyk2 (Y881) might be responsible for the lack of paxillin binding to F298-immunoreactive Pyk2. I performed Pyk2 immunoprecipitations with F298 and F245 on lysates from unstimulated AB.1 CTL clones and then immunoblotted with a phospho-specific antibody to the Y881 site. Figure 5-5a shows that Pyk2 isolated from the F298 immunoprecipitation is more phosphorylated at Y881 than that from the F245 immunoprecipitation. The paxillin immunoblot confirms that only the F245-immunoreacitve Pyk2 is capable of associating with paxillin (Figure 5-5a). Residual tyrosine phosphorylation at the Y881 site detected for Pyk2 that is associated with paxillin may represent Pyk2 that is bound to one LD motif of paxillin (as there are two potential sites of interaction). The graph presented in Figure 5-5b illustrates the average ratio of pixel intensities for pY881 in relation to Pyk2 from three independent experiments. An unpaired two sample Student's t Test was performed to compare the means for the two Pyk2 immunoprecipitations and it was found the means were statistically different to a confidence level of 90% ($p < 0.1$). The results suggest that phosphorylation at Y881 of Pyk2 may directly interfere with paxillin binding as has been proposed for FAK. Whether increased phosphorylation of Y881 was responsible for the lack of detectable paxillin association with Pyk2 captured by the N-19 and C-19 antibodies was not tested.

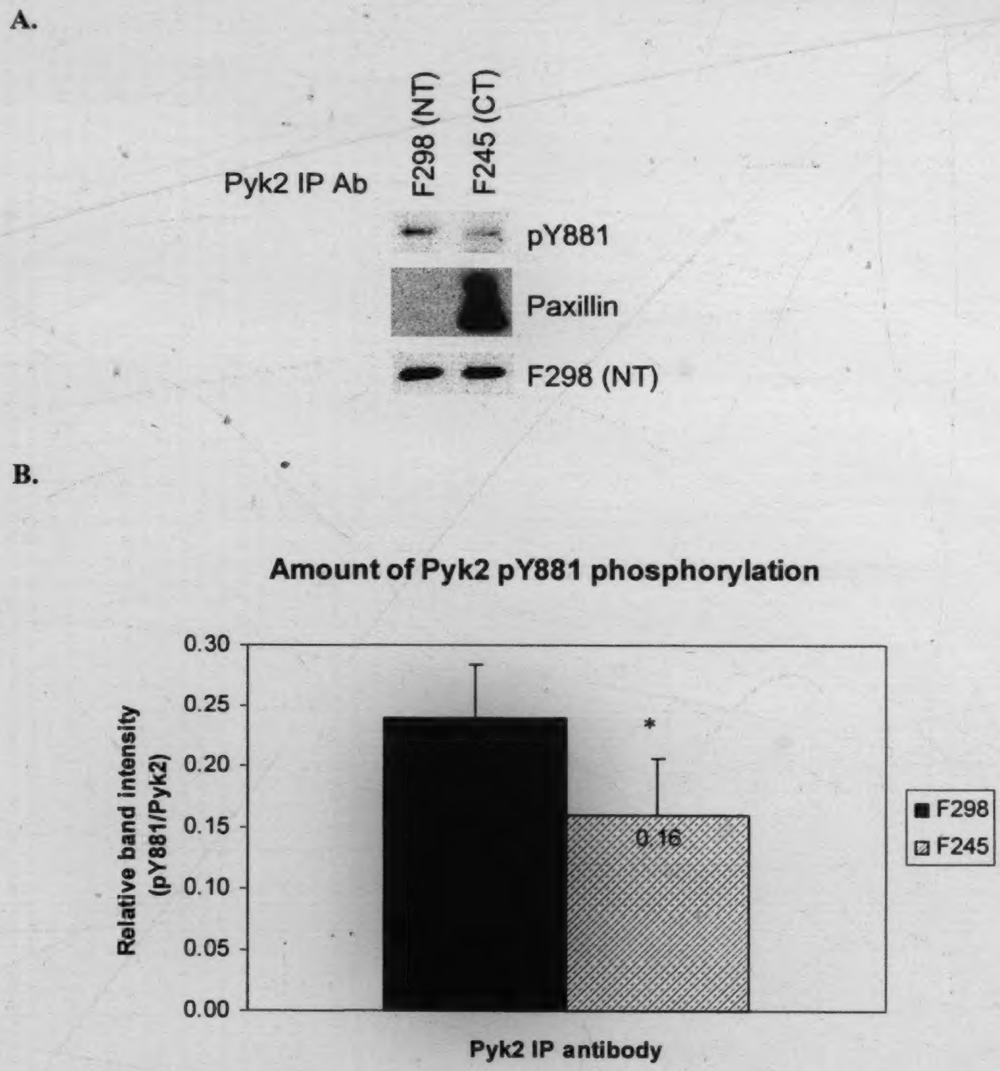

FIGURE 5-5. Pyk2 immunoreactive with the F298 antibody is more heavily phosphorylated on Y881. a) Pyk2 immunoprecipitations were performed on unstimulated CTL clone lysates with the F298 and F245 antisera. Immunoblots for phosphorylated Y881, paxillin and Pyk2 (F298) are shown. b) Ratios of pixel intensities for each phospho-Y881 band to Pyk2 band were calculated for each immunoprecipitate as follows: integrated intensity – background (pY881) / integrated intensity – background (F298). Ratios presented are averages of three independent experiments. F298 = 0.24 +/- 0.04, F245 = 0.16 +/- 0.05. The asterisk denotes a significance level of $p < 0.1$.

There is no difference in catalytic activity between paxillin-associated and non-associated Pyk2

In the previous section, I demonstrated that paxillin non-associated Pyk2 appears to be more phosphorylated at Y881. Phosphorylation at Y881 has been shown to recruit SH2-domain-containing proteins such as the signalling protein Grb2 (Blaukat et al. 1999). Therefore, one might predict that this population of Pyk2 may be involved in signal transduction, whereas Pyk2 that can interact with paxillin may be involved in forming complexes with the cytoskeleton. Indeed, paxillin has been shown to interact with both the actin (Turner 2000) and microtubule cytoskeletons (Herreros et al. 2000; Brown and Turner 2002). It is therefore possible that the two populations of Pyk2 have differences with respect to catalytic activity. To test this, I performed Pyk2 *in vitro* kinase assays with either F298 or F245 immunoprecipitations from unstimulated or TCR-stimulated cell lysates. In these assays, Pyk2 autophosphorylation was measured. The right side of Figure 5-6 shows the basal phosphorylation of Pyk2 and phosphorylation due to cross-linked TCR stimulation which are the input into the kinase assays. Once ATP was added during the kinase reactions, an increase in the autophosphorylation of Pyk2 was obserserved for both unstimulated and stimulated F298 and F245 immunoprecipitations over the input (Figure 5-6). These results demonstrate that Pyk2 immunoreactive with both antisera is catalytically activite in both unstimulated and TCR-stimulated CTL clones.

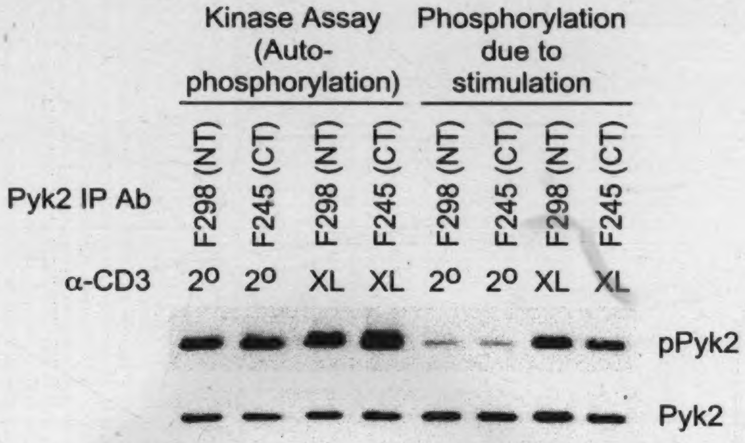
Kinase Assay (Auto-phosphorylation)
Phosphorylation due to stimulation
Pyk2 IP Ab
F298 (NT)
F245 (CT)
F298 (NT)
F245 (CT)
F298 (NT)
F245 (CT)
F298 (NT)
F245 (CT)
α-CD3
2°
2°
XL
XL
2°
2°
XL
XL
pPyk2
Pyk2

FIGURE 5-6. Pyk2 recovered with the F289 or F245 antiserum is catalytically active. AB.1 CTL clones were either left unstimulated (2°) or stimulated with cross-linked anti-CD3 (XL) for 10 min. Duplicate sets of Pyk2 immunoprecipitations were performed on cell lysates with the F298 and F245 polyclonal antibodies. One set was used to examine the extent of phosphorylation due to TCR stimulation. The other set was used in an *in vitro* kinase assay in which autophosphorylation of Pyk2 was measured. For the kinase assays, 1 mM ATP was added to Pyk2 immunoprecipitations resuspended in kinase buffer (total volume = 50 μl). Reactions proceeded for 30 minutes at 32°C. Both sets of samples were run on gels, transferred to membranes and the membranes were blotted for phosphotyrosine and Pyk2 (F298).

Pyk2 that associates with paxillin localizes to the MTOC in unstimulated cells

If the population of Pyk2 that does not associate with paxillin is involved in signal transduction and the population of Pyk2 that associates with paxillin is interacting with the cytoskeleton (through its association with paxillin), then one might expect that the localization of the two populations in the cell may differ. I examined the localization of the two populations of Pyk2 and paxillin by confocal microscopy by co-immunostaining unstimulated CTL clones with the F298 or F245 antiserum and anti-paxillin. Co-staining with F298 and anti-paxillin showed no co-localization of this population of Pyk2 with paxillin (Figure 5-7a). F298-immunoreactive Pyk2 was found to be diffused throughout the cytoplasm, consistent with previous descriptions and also appeared to be present in the nucleus (Figure 5-7a). Paxillin was also found to be diffused throughout the cytoplasm, however, there was a distinct bright spot which overlaps with the MTOC as evidenced by co-localization with α-tubulin (Figures 5-7a, 5-7b). This result supports the biochemical data showing that this antibody does not capture Pyk2 capable of associating with paxillin (Figure 5-2a). Co-staining with the F245 antibody and anti-paxillin demonstrated that this population of Pyk2 was also diffusely distributed throughout the cytoplasm and appeared to be present in the nucleus and that there was co-localization with paxillin, but only at the MTOC (Figure 5-7c). Co-staining with F245 and anti-α-tubulin also showed co-localization at the MTOC in stimulated CTL clones (Figure 5-8c). Co-localization of F245-immunoreactive Pyk2 with paxillin at the MTOC was seen in 91.7% of clones examined over four independent experiments, compared to 4.3% of clones displaying co-localization of F298-immunoreactive Pyk2 and paxillin. This result agrees with the biochemical data which showed that this antibody captures Pyk2

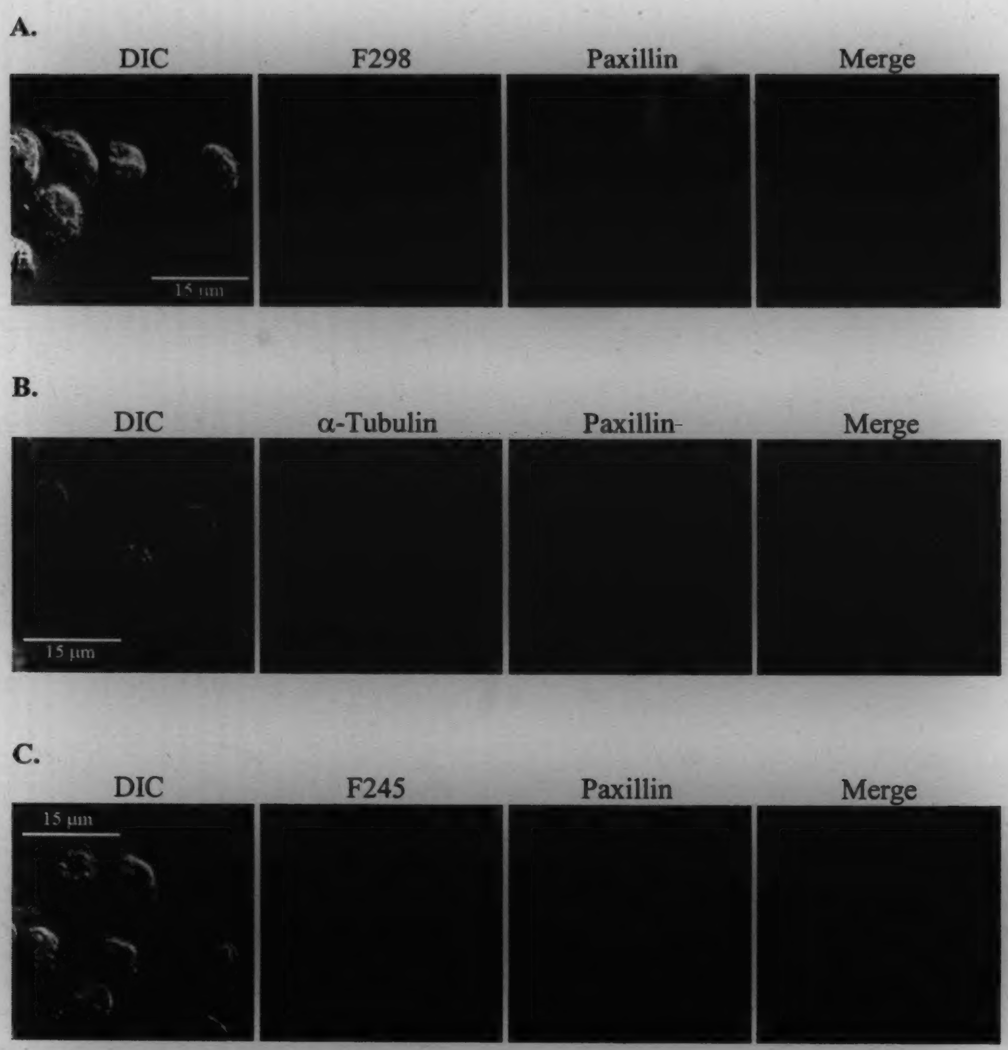
A.
DIC
F298
Paxillin
Merge
15 μm
B.
DIC
α-Tubulin
Paxillin
Merge
15 μm
C.
DIC
F245
Paxillin
Merge
15 μm

FIGURE 5-7. Pyk2 that is capable of associating with paxillin co-localizes with paxillin at the MTOC. a, b, c) Unstimulated AB.1 CTL clones were added to poly-L-lysine-coated coverslips and allowed time to adhere. The cells were then fixed and permeabilized and immunostained with the F298 polyclonal antibodies and anti-paxillin (a), anti-paxillin and anti-α-tubulin (b) or the F245 polyclonal antibodies and anti-paxillin (c). The cells were then visualized by confocal microscopy. The green flurorochrome used was Alexa 488 and the red flurorochrome was rhodamine.

associated with paxillin (Figure 5-2a) and is in accordance with a previous report that Pyk2 and paxillin co-localize with the MTOC (Sancho et al. 2000).

Upon target cell stimulation, Pyk2 that associates with paxillin at the MTOC translocates with the MTOC to the CTL/target cell interface

I next examined the localization of the two populations of Pyk2 and paxillin after stimulation of the CTL clones with allogeneic target cells. Upon recognition of target cells, most F298-immunoreactive Pyk2 remained diffused throughout the cell, while a small portion could be seen at the interface (Figure 5-8a). Under these conditions, paxillin became enriched at the CTL/target cell interface and remained associated with the translocated MTOC (Figure 5-8a). Co-staining of conjugates with F245 antiserum and anti-paxillin showed that although paxillin was translocated to the interface, the majority of the F245-immunoreactive Pyk2 did not become enriched at the interface (Figure 5-8b). However, this population of Pyk2 remained associated with paxillin at the translocated MTOC (Figures 5-8b, 5-8c). Thus, it appears as though both paxillin and F245-immunoreactive Pyk2 translocate with the MTOC to an area just below the contact site. In support of this finding, I found that in CTL clones treated with colchicine, which prevents MTOC reorientation but does not cause disruption of the MTOC, F245-immunoreactive Pyk2 and paxillin remained associated with the mis-oriented MTOC (Figure 5-8d). The localization of phosphorylated Pyk2 during conjugate formation was also examined using phospho-specific antisera that recognize the major sites of tyrosine

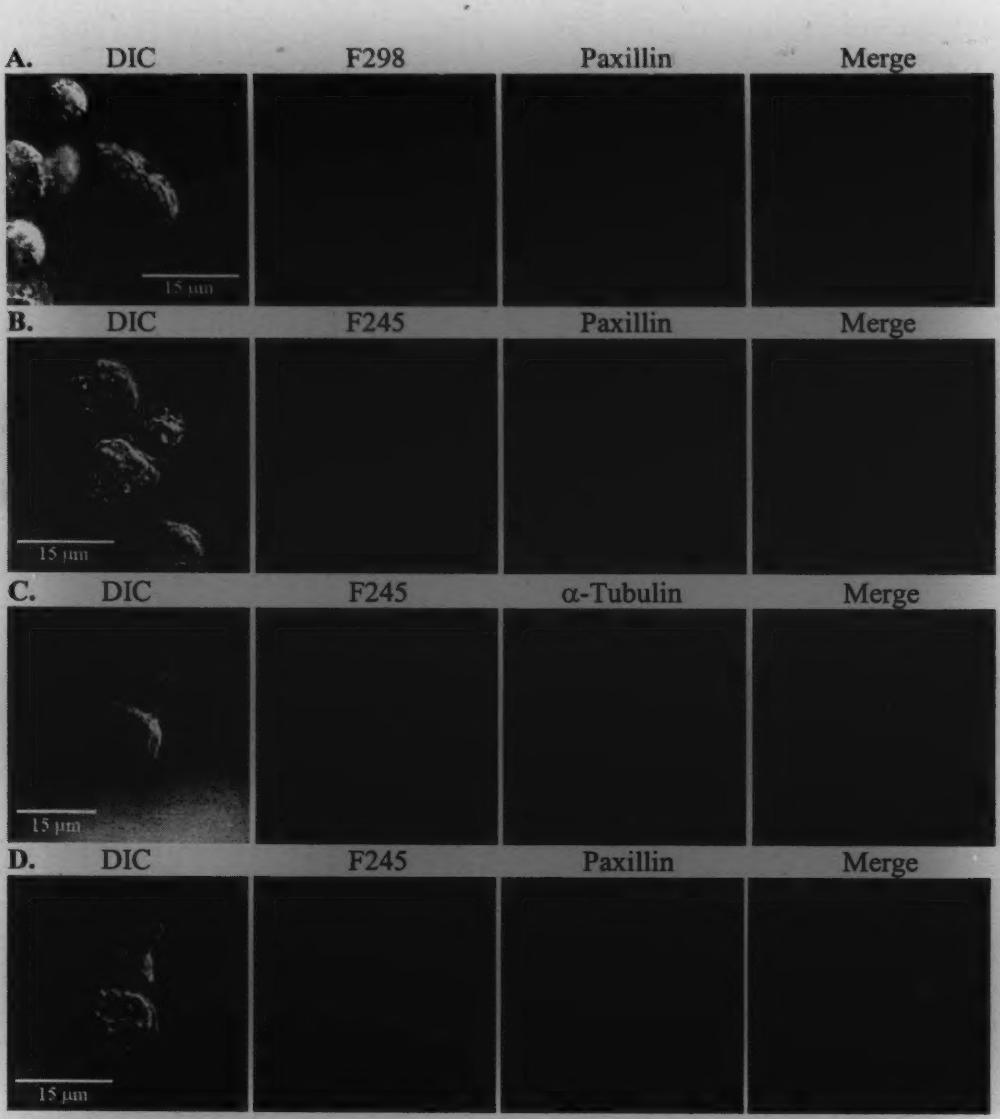
A.
DIC
F298
Paxillin
Merge
15 µm
B.
DIC
F245
Paxillin
Merge
15 µm
C.
DIC
F245
α-Tubulin
Merge
15 µm
D.
DIC
F245
Paxillin
Merge
15 µm

FIGURE 5-8. The localization of Pyk2 in CTL/target cell conjugates. a, b, c) CTL clones AB.1 or Clone 11 were stimulated with target cells transfected with an allogeneic class I MHC ($L1210^{Kb/Dd}$) for 6 or 2 min respectively. Conjugates were then allowed to adhere to poly-L-lysine-coated coverslips. Cells were then fixed and permeabilized and immunostained with F298 antiserum and anti-paxillin (a), F245 antiserum and anti-paxillin (b) or F245 antiserum and anti-α-tubulin (c). d) Clone 11 were pre-treated with 5 mM colchicine and then stimulated with $L1210^{Kb/Dd}$ for 2 min. Fixed and permeabilized conjugates were stained with the F245 polyclonal antibodies and anti-paxillin. Cells were visualized by confocal microscopy. The green flurorochrome used in (a), (b), (d) was Alexa 488 and DTAF for (c). The red flurorochrome used in (a), (b), (d) was rhodamine and texas red for (c). Note that (c) has been psuedocolored.

phosphorylation within Pyk2 (Y402, Y579, Y580 and Y881) and is shown in Appendix Figure 4. Also shown in this figure is the co-staining for Y881 and paxillin.

F245-immunoreactive Pyk2 associates with surface biotinylated proteins in unstimulated CTL clones

I have found that a small portion of both F298- and F245-immunoreactive Pyk2 is localized to the contact point between a CTL and its target (Figures 5-8a and 5-8b). At the contact point, Pyk2 could interact with proteins that are associated with the TCR/CD3 complex as I have demonstrated that Pyk2 is recruited to the TCR/CD3 complex upon stimulation with immobilized anti-CD3 (Figure 3-7). Pyk2 could also interact with proteins complexed with integrins. In order to determine whether F298- or F245-immunoreactive Pyk2 associates with membrane proteins after stimulation through the TCR, I surface biotinylated AB.1 CTL clones, stimulated the clones with cross-linked anti-CD3, lysed the cells and then immunoprecipitated Pyk2 with either F298 or F245 antiserum. In this experiment, both F298- and F245-immunoreactive Pyk2 were inducibly phosphorylated upon cross-linked anti-CD3 stimulation (Figure 5-9). Interestingly, contrary to my prediction, the streptavidin immunoblot shows that only the F245 immunoprecipitation contained surface biotinylated proteins and that this only occurred with unstimulated CTL clones (Figure 5-9). This result was unexpected as I saw no evidence for membrane localization of F245-immunoreactive Pyk2 in unstimulated cells by confocal microscopy. Based on the results from the microscopic analysis, which showed that this population of Pyk2 co-localizes with the MTOC, the surface biotinylated material in the F245 immunoprecipitation could represent

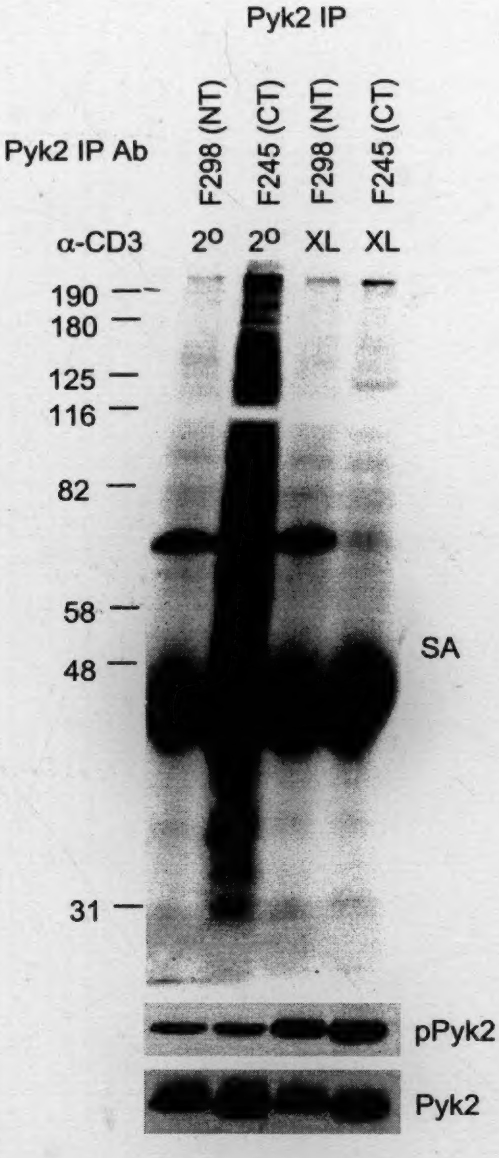
Pyk2 IP
Pyk2 IP Ab
F298 (NT)
F245 (CT)
F298 (NT)
F245 (CT)
α-CD3
2°
2°
XL
XL
190
180
125
116
82
58
48
31
SA
pPyk2
Pyk2

FIGURE 5-9. F245-immunoreactive Pyk2 associates with surface biotinylated proteins in unstimulated cells. AB.1 cells were surface biotinylated and then stimulated with cross-linked anti-CD3 for 10 minutes or left unstimulated (2°). The cells were lysed and Pyk2 immunoprecipitations were performed on the lysates using either F298 or F245 antiserum. The samples were run on a gel, transferred to a membrane and the membrane was immunoblotted with anti-phosphotyrosine (to detect phosphorylated Pyk2 – pPyk2), anti-Pyk2 (Pyk2 monoclonal) and streptavidin. The experiment was repeated twice.

endocytosed vesicles that have accumulated at the MTOC. The results from this section also show that after TCR triggering, this population of Pyk2 no longer associates with the surface biotinylated proteins (Figure 5-9). As endocytosis would not be expected to cease upon TCR stimulation, I therefore do not favour that hypothesis. A more plausible explanation is that Pyk2 could be associating with the actin cytoskeleton which is linked to membrane adhesion proteins through ERM proteins. The association of Pyk2 with the actin cytoskeleton/membrane adhesion proteins may be lost after TCR stimulation during the rearrangements of the actin cytoskeleton that occur upon stimulation. Future experiments should be aimed at determining the nature of biotinylated material. Ideally, this experiment should be performed using a more physiological stimulus in which the cytoskeleton plays a more active role such as immobilized anti-CD3 stimulation or target cell stimulation. Unfortunately, this becomes complicated as much of the surface biotinylated material that would interact with immobilized antibody could remain bound to the antibody after lysis of the cells (as shown in chapter 3) and target cell stimulation is complicated by the fact that the target cells we have used also express Pyk2.

C. Discussion

In this study, I have identified two populations of Pyk2 within CTL clones; one that is associated with paxillin and one that is not. The population of Pyk2 that is associated with paxillin is less phosphorylated at Y881 and in the proline-rich region in unstimulated cells. A portion of this population is associated with paxillin at the MTOC. Pyk2 that does not associate with paxillin is more heavily phosphorylated at Y881 and in the proline-rich region and displays no co-localization with paxillin or the MTOC in unstimulated cells. Even though differences were found in levels of phosphorylation and localization within cells, both populations of Pyk2 were catalytically active. Thus, these two populations of Pyk2 may represent two different conformations of Pyk2; one that displays a compact FAT domain that favours paxillin binding and one that that exhibits an unfolded FAT domain that is more phosphorylated and consequently loses the capacity to bind paxillin.

I tested a panel of Pyk2 polyclonal antibodies for their ability to co-immunoprecipitate paxillin. One antibody, F245 which was generated in our lab against a region corresponding to the proline-rich region of Pyk2, co-immunoprecipitated significantly more paxillin than the other antibodies tested (Figure 5-2a). The association of Pyk2 with paxillin was constitutive as it was seen in both unstimulated and TCR-stimulated CTL clones (Figure 5-2a). When an unstimulated CTL clone lysate was pre-cleared of F298-immunoreactive Pyk2, the F245 antiserum recovered Pyk2 that was associated with paxillin (Figure 5-2b). After pre-clearing with the F245 antiserum, F298-immunoreactive Pyk2 was recovered that was clearly not associated with paxillin (Figure

5-2b). These results suggest that there are two populations of Pyk2 present in CTL clones based on their differential ability to associate with paxillin.

I found a correlation between the amount of phosphorylation of Pyk2 and recognition by the F298 and F245 antibodies. When I examined the ability of the two antibodies to immunoblot denatured Pyk2 captured by either antibody, I discovered that F245 could not recognize denatured Pyk2 captured with the F298 antibody (Figure 5-3a). This led to the prediction that there may be post-translational modifications of Pyk2 involved in the differential recognition. Indeed, dephosphorylation of F298-immunoreactive Pyk2 with CIAP allowed recognition by the F245 antibody (Figure 5-3b) suggesting that phosphorylation of Pyk2 is playing a role in recognition.

The region against which the F245 antibody was generated includes the first proline-rich region, the splice region and the area between the two proline-rich regions of Pyk2 (aa 720-826) (Figures 5-4a, 5-4b). I suspect that the differential recognition of Pyk2 by the two antibodies is not due to binding to different isoforms of Pyk2 as the AB.1 CTL clones only express the Pyk2-H isoform (Figure 6-2, next chapter). Therefore, it is likely that phosphorylation of the region mentioned above is involved. The immunogen used to generate the F245 antibody was a GST fusion protein that was expressed in bacteria. It is therefore not surprising that this antibody recognized Pyk2 that is less phosphorylated as there would be no phosphorylation of a GST fusion protein isolated from bacteria. Interestingly, the early studies that demonstrated that Pyk2 could co-immunoprecipitate paxillin used antibodies against a GST fusion protein consisting of aa 681-1009 (the entire C-terminus) (Salgia et al. 1996; Hiregowdara et al. 1997) or aa 680-860 (the proline-rich regions) (Li and Earp 1997) of Pyk2. As of yet, no known phosphorylation sites have been identified within the F245 recognition site of Pyk2. Recently, new phosphorylation sites within FAK have been mapped by mass spectrometry (Grigera et al. 2005). In addition to 11 previously identified sites, this group identified 19 new sites consisting mostly of serine and threonine residues (Grigera et al. 2005). Interestingly, three clusters of phosphorylation sites were noted: one around the autophosphorylation site (Y397), one around the first proline-rich region and one around the second proline-rich region (Grigera et al. 2005). The authors speculated that these clusters might regulate FAK enzymatic activity and association with binding partners (Grigera et al. 2005). Two of the phosphorylation sites identified in the area around the autophosphorylation site are conserved residues between FAK and Pyk2. However, there is only one conserved residue found around the proline-rich regions. This may not be surprising as the area between the end of the catalytic domain and beginning of the FAT domain (includes the proline-rich regions) of FAK and Pyk2 only contains approximately 25% amino acid identity (Yu et al. 1996). This conserved site does not overlap with the F245 recognition site. As the F245 recognition site contains tyrosine, serine and threonine residues, it is possible that some of these residues may become phosphorylated and consequently interfere with F245 binding. Indeed, the NetPhos 2.0 program identified 3 potential sites for phosphorylation of Pyk2 in the region to which the F245 antiserum was generated (minus the splice region).

In accordance with the results from CIAP treatment of F298-immunoreactive Pyk2 suggesting that this population of Pyk2 is more heavily phosphorylated, I consistently observe that Pyk2 captured with this antiserum displays retarded mobility on high percentage SDS-PAGE gels compared to that captured with F245 antiserum. This shift in molecular weight could be due to increased phosphorylation, however, more detailed studies are needed to verify this theory.

I also found a correlation with the amount of phosphorylation of Pyk2 and paxillin binding. Pyk2 not associated with paxillin appeared to have increased tyrosine phosphorylation at the Y881 site (Figure 5-5). The analogous site in FAK was hypothesized to interfere with paxillin binding at the second hydrophobic patch such that the paxillin binding and tyrosine phosphorylation of Y925 were deemed mutually exclusive (Liu et al. 2002). My results suggest that phosphorylation of Y881 may interfere with paxillin binding to Pyk2. As Pyk2 that does not associate with paxillin had increased phosphorylation in the region to which the F245 antibody binds and at Y881, it is possible that the efficiency of phosphorylation of Y881 may be influenced by proximal serine/threonine/tyrosine phosphorylations in and around the proline-rich regions. It may also be influenced by the binding of SH3 domain-containing proteins to the proline-rich region such that they may serve to keep the protein in a conformation that is suitable for phosphorylation of this site.

The proposed change in conformation of the Pyk2 FAT domain, depending on paxillin binding, may allow Pyk2 to interact with a different subset of proteins, and therefore, influence its function within the cell. As both populations of Pyk2 exist in the cells, Pyk2 may be performing different functions depending on its localization. For instance, the subset of Pyk2 that interacts with the MTOC, presumably through its interaction with paxillin, may be involved in phosphorylating or recruiting cytoskeletal proteins or proteins involved in regulating the cytoskeleton. The population of Pyk2 not associated with paxillin is more tyrosine phosphorylated and may phosphorylate or recruit membrane proximal signalling molecules.

An autoinhibitory conformation has been proposed for FAK in which the N-terminus binds to the kinase domain which greatly reduces kinase activity (Cooper et al. 2003). The F298 antibody, which binds to the extreme N-terminus (aa 2-12), cannot capture Pyk2 associated with paxillin (Figure 5-2a), presumably because the antibody recognition site is inaccessible when Pyk2 is bound to paxillin. Whether this result represents a similar autoinhibitory state as that described for FAK is currently unknown. However, I found that both Pyk2 populations were catalytically active, suggesting that Pyk2 may not adopt this autoinhibitory conformation. In support of this finding, Dunty and colleagues found that the N-terminus of Pyk2 was unable to associate with co-transfected Pyk2 and found only a weak association with co-transfected FAK (Dunty et al. 2004). The N-terminus of FAK was also unable to associate with full length Pyk2 (Dunty et al. 2004). I also found that the N-terminus of Pyk2 fused to GST was unable to associate with full length Pyk2 in a CTL cell lysate (Figure 6-14b, chapter 6). Perhaps Pyk2 that is bound to paxillin undergoes folding within the N-terminus that buries the first few amino acids of the protein but does not affect catalytic activity.

Co-localization of Pyk2, paxillin and the MTOC has been previously described in NK cells (Sancho et al. 2000). I have shown that only the population of Pyk2 that associates with paxillin co-localizes with the MTOC (Figure 5-7c), suggesting that paxillin might be responsible for its localization there. However, the function that Pyk2 and paxillin might be performing at the MTOC has yet to be determined. Upon recognition of target cells, a small amount of F298- and F245-immunoreactive Pyk2 could be detected at the CTL/target cell interface (Figures 5-8a, 5-8b). Paxillin was also found to translocate to this area (Figure 5-8a, 5-8b). The role that Pyk2 and paxillin are playing at the interface remains to be determined as does the mechanism by which they are recruited.

Immunostaining for Pyk2 also suggested that there was some nuclear localization of Pyk2 in the CTL clones. Nuclear localization of Pyk2 has been reported in COS-7 cells overexpressing wild type Pyk2 and it was suggested that Pyk2 continuously shuttles between the nucleus and cytoplasm as it accumulated in the nucleus upon inhibition of nuclear export (Aoto et al. 2002). N-terminal fragments of FAK and full length FAK also accumulate in the nucleus (Kadare et al. 2003; Jones and Stewart 2004).

I have proposed a model for how these two populations of Pyk2 co-exist in CTL clones. Upon target cell binding, a CTL becomes activated and Pyk2 and paxillin, either alone or together, are recruited to the CTL/target cell interface by an unknown mechanism. Recruitment may occur via translocation with the MTOC, for the subset of Pyk2 that associates with paxillin at the MTOC. At the plasma membrane, Pyk2 is in the vicinity of SFK which can then bind and phosphorylate Pyk2 at Y881. Phosphorylation within the proline-rich regions by other kinases may facilitate efficient phosphorylation at this site. As Y881 becomes phosphorylated, any associated paxillin may be released at the second hydrophobic patch within the FAT domain. Binding of SH2 domain-containing proteins to Y881 may aid in the release of paxillin from the first hydrophobic patch and ultimately allow Pyk2 to interact with a different subset of binding partners. I do not know which population of Pyk2 is more predominant in unstimulated versus stimulated cells. This may depend on the type of stimulation the CTL receives. As Pyk2 becomes phosphorylated and activated in response to many stimuli, it is likely that Pyk2 would interact with different subsets of proteins depending on the type of stimulus and functional output required.

In this study, I have identified two populations of Pyk2 that co-exist in CTL clones based on their differential abilities to associate with paxillin. By examining these two populations of Pyk2, I have gained insight into how phosphorylation may affect the ability of Pyk2 to interact with paxillin. The results from this study also suggest that paxillin binding may influence the conformation of the Pyk2 FAT domain. Confirmation of these results awaits the derivation of the crystal structure of Pyk2 bound to paxillin and mass spectrometry of Pyk2 phosphopeptides.

CHAPTER 6: Examination of the function of Pyk2 in CTL

A. Introduction

Little is known about the function of Pyk2 in T cells. This is likely due to the fact that it is difficult to transfect T cells and thus very few overexpression studies have been performed. Two studies have been conducted in Jurkat T cells (T leukemia), as they are easier to transfect than T cell clones or primary T cells. The first study examined the role of Pyk2 in T cell activation (Katagiri et al. 2000). Overexpression of an autophosphorylation mutant of Pyk2-H (Y402F) inhibited the phosphorylation and activation of endogenous Pyk2 in response to co-stimulation with anti-CD3 and anti-CD28 (Katagiri et al. 2000). IL-2 production was also reduced by a factor of two (Katagiri et al. 2000). The second study showed that overexpression of the C-terminus of Pyk2 inhibited integrin trans-regulation (Rose et al. 2003). Integrin trans-regulation occurs when signals generated by engagement of one integrin affect the function of a second integrin. These studies provide little information with regard to the function of Pyk2 in T cells. Thus we may point to studies performed in other cell types to gain some insight.

Studies addressing the role of Pyk2 in NK cells have been performed. We may be able to draw parallels between the function of Pyk2 in these cells and CTL as both cell types demonstrate cytolytic activity towards altered-self cells. One group examined the effect of overexpression of either wild type Pyk2 (WT Pyk2) or a kinase dead version of Pyk2 (KD Pyk2) fused to EGFP (enhanced green fluorescent protein) on lysis of target cells (Sancho et al. 2000). Infection of NKL cells with recombinant vaccinia virus encoding either EGFP fusion protein caused an approximate two fold decrease in specific lysis of target cells (Sancho et al. 2000). The observed decrease in lysis was associated with a defect in MTOC reorientation (Sancho et al. 2000). Another group found that natural cytotoxicity of human polyclonal NK cells was inhibited by a factor of two upon expression of KD Pyk2, but not WT Pyk2 (Gismondi et al. 2000). These results suggest that Pyk2 plays a role in regulating the cytotoxic response in NK cells. However, since there were conflicting results between the two groups in terms of which Pyk2 constructs could cause a decrease in killing, it is not clear whether the kinase activity of Pyk2 or scaffolding potential of Pyk2 was mediating the effect.

Other studies have investigated the role of Pyk2 in cell spreading and migration. A fusion protein consisting of the entire C-terminus of Pyk2 fused to GST was electroporated into human monoctyes and was found to inhibit endogenous Pyk2 phosphorylation, adhesion-induced tyrosine phosphorylation, cell spreading and motility (Watson et al. 2001). The C-terminus of Pyk2 was also fused to a Tat peptide (Tat-CT) to facilitate uptake by neutrophils (Han et al. 2003). Transduction of Tat-CT inhibited the phosphorylation of endogenous Pyk2 and reduced TNF-α (tumour necrosis factor-α)-induced cell spreading (Han et al. 2003). In addition, studies have been performed on macrophages isolated from Pyk2$^{-/-}$ mice (Okigaki et al. 2003). Pyk2-deficient macrophages displayed impaired migration in response to an SDF-1α chemokine gradient (Okigaki et al. 2003). These macrophages were slower to form a leading edge than their wild type counterparts, failed to detach the lagging edge from the substratum and had a reduced ability to move the cell body into the leading edge (Okigaki et al. 2003). In response to MIP-1α, Pyk2$^{-/-}$ macrophages displayed an increase in the size of lamellipodia formed and the number of cells spreading (Okigaki et al. 2003). These findings suggest that deletion of Pyk2 resulted in impaired migration due the failure to orient properly towards a chemokine gradient (Okigaki et al. 2003). Collectively, the findings mentioned above implicate Pyk2 in mediating directional killing, cell migration and cell spreading, all of which require proper cell polarization towards the stimulus.

Little is also known about the function of the N- and C-termini of Pyk2. Very few proteins have been shown to interact with the N-terminus of Pyk2. Therefore, it is unclear what role the FERM domain may play. The C-terminus of Pyk2 interacts with a number of proteins that are present in focal adhesions. T cells do not form focal adhesions since they are highly motile cells. With the exception of paxillin, it is largely unknown whether these interactions occur in T cells.

Dunty and Schaller (Dunty and Schaller 2002) have investigated the functions of the N- and C-termini of Pyk2 and FAK. Although their studies were performed in adherent cells, some of the findings may be relevant to T cells. They attempted to delineate the roles of the N- and C-termini of FAK and Pyk2 by constructing chimeric Pyk2/FAK constructs (Dunty and Schaller 2002). In this study, six chimeric molecules consisting of different combinations of the FAK and Pyk2 N-terminus, kinase domain and C-terminus were transfected into chicken embryo fibroblasts. As controls, they also overexpressed full length FAK and Pyk2. Overexpression of full length Pyk2 caused sporadic cell rounding within a confluent monolayer whereas overexpression of FAK had no such effect (Dunty and Schaller 2002). The N-terminus of Pyk2 appeared to be responsible for the alterations in cell morphology, as all the chimeras containing the N-terminus of Pyk2 induced some degree of change in morphology (Dunty and Schaller 2002). The morphological changes induced with these chimeras were not associated with apoptotic death or cell cycle delay (Dunty and Schaller 2002). Interestingly, paxillin localization in these cells was altered to varying degrees in that paxillin did not always display characteristic staining at focal adhesions (Dunty and Schaller 2002). This finding suggested that changes in cytoskeletal structure had occurred (Dunty and Schaller 2002). The changes in cell shape were not due to decreased adhesion or an inability of the cells to spread, but instead appeared to be a defect in the maintenance of focal adhesions or cell shape (Dunty and Schaller 2002). These results are suggestive of a regulatory role for the Pyk2 N-terminus on the cytoskeleton or adhesive structures. The mechanism by which the N-terminus performs this function remains to be elucidated.

Another role for the N-terminus of Pyk2 was highlighted in additional studies performed by Dunty and Schaller. In chicken embryo fibroblasts, FAK targets to focal adhesions, while Pyk2 is largely cytoplasmic (Dunty and Schaller 2002). The FAT domain of FAK targets FAK to focal adhesions (Hildebrand et al. 1993). Interestingly, if overexpressed, the FAT domain of Pyk2 will localize to focal adhesions as does the C-terminal portion of Pyk2 (Schaller and Sasaki 1997; Xiong et al. 1998). All chimeras containing the C-terminus of FAK targeted to focal adhesions in fibroblasts (Dunty and Schaller 2002). In contrast, differences in the localization of the chimeras containing the C-terminus of Pyk2 were noted, depending on which N-terminus they contained. The chimera with the N- and C-terminus of Pyk2 displayed a diffuse distribution while chimeras with the N-terminus of FAK and C-terminus of Pyk2 localized to focal adhesions (Dunty and Schaller 2002). These results suggest that the C-terminus of Pyk2 is sufficient to direct focal adhesion targeting, but the N-terminus of Pyk2 may oppose this localization. The authors hypothesize that this could occur if protein folding blocks the FAT sequence or if the N-terminus is responsible for localization of the protein (Dunty and Schaller 2002).

Based on the results of the above-mentioned NK cell studies, I hypothesize that Pyk2 may play a role in polarizing a CTL towards a target cell during cytolysis. The mechanism of CTL killing involves many steps. A circulating effector CTL must first find a cell that expresses a pMHC complex that is recognized by its TCR. A migrating CTL displays a morphology that has been described as a "hand mirror" which has three distinct compartments: a leading edge followed by the main cell body including the nucleus, a narrowing transition zone called the "polarizing compartment" which contains the MTOC, and the trailing edge or uropod (Samstag et al. 2003). Upon contact with an appropriate target cell, a CTL undergoes rapid cytoskeletal rearrangements which involve both the actin and microtubule cytoskeletons. F-actin accumulates at the interface facilitating tight adhesion and stabilization of the CTL/target cell interaction. The microtubule cytoskeleton is involved in the directional movement of the lytic granules for release through the contact region. Hence, the MTOC reorients to a position near the contact site. The lytic granules track along the microtubules to the interface, resulting in the restricted delivery of the granules through the contact site. CTL undergo piecemeal degranulation and thus CTL are capable of lysing more than one target. Upon delivery of the 'lethal hit', a CTL must first detach from its target before it can find another cell expressing an appropriate pMHC.

In this study, I sought to determine the role of Pyk2 during cytolysis and the function of the N- and C-termini of Pyk2. At the beginning of my studies, I attempted to use retroviral transduction to overexpress Pyk2 constructs in our CTL clones to address these questions. However, I was unable to successfully transduce the CTL clones in this manner. I did have some success in transducing primary T cells, but the efficiency achieved was very low (approximately 10%). It was not until the end of my studies that I was able to take advantage of our recently acquired ability to transfect the CTL clones by nucleofection and start to address these important questions. I examined the effects of knockdown of Pyk2 and overexpression of the N- and C-terminal domains of Pyk2 on MTOC reorientation, degranulation and signal amplification.

B. Results

Expression of the N-terminal and C-terminal Pyk2 constructs

In order to examine the function of Pyk2 in CTL clones, two truncation mutants of murine Pyk2 were constructed and fused to EGFP (Figure 6-1). Sequences corresponding to aa residues 1-421 (the entire N-terminal domain, NT Pyk2) and aa residues 678-1009 (the entire C-terminal domain, CT Pyk2) were cloned from AB.1 CTL clones and ligated into the pEGFP-C1 vector as C-terminal fusions with EGFP. The Pyk2-H version of CT Pyk2 (missing aa 738-780) was used as I determined, by RT-PCR (reverse transcription – polymerase chain reaction), that our CTL clones only express the Pyk2-H isoform of Pyk2 (Figure 6-2), as predicted (Dikic and Schlessinger 1998; Xiong et al. 1998). I chose to use the NT Pyk2 construct to attempt to elucidate the function of the N-terminal domain of Pyk2 during T cell activation. The CT Pyk2 fusion protein was used because other groups have found that overexpression of the C-terminal domain of Pyk2 can inhibit cell spreading and migration (Watson et al. 2001; Han et al. 2003). It was also found that it can act as a dominant negative towards endogenous Pyk2 by inhibiting endogenous Pyk2 phosphorylation (Liu et al. 1999; Watson et al. 2001; Han et al. 2003).

The constructs were nucleofected into clone 11 using Amaxa nucleofection technology. I have consistently found that a transfection efficiency of 60-80% can be achieved when unfixed EGFP positive cells are visualized by flow cytometry 24 hours post-nucleofection (Figure 6-3). Transfection efficiency largely depends on the size of the construct as smaller constructs are expressed in a higher percentage of cells. The data in Figure 6-4 provides an indication of the extent of overexpression that can be achieved

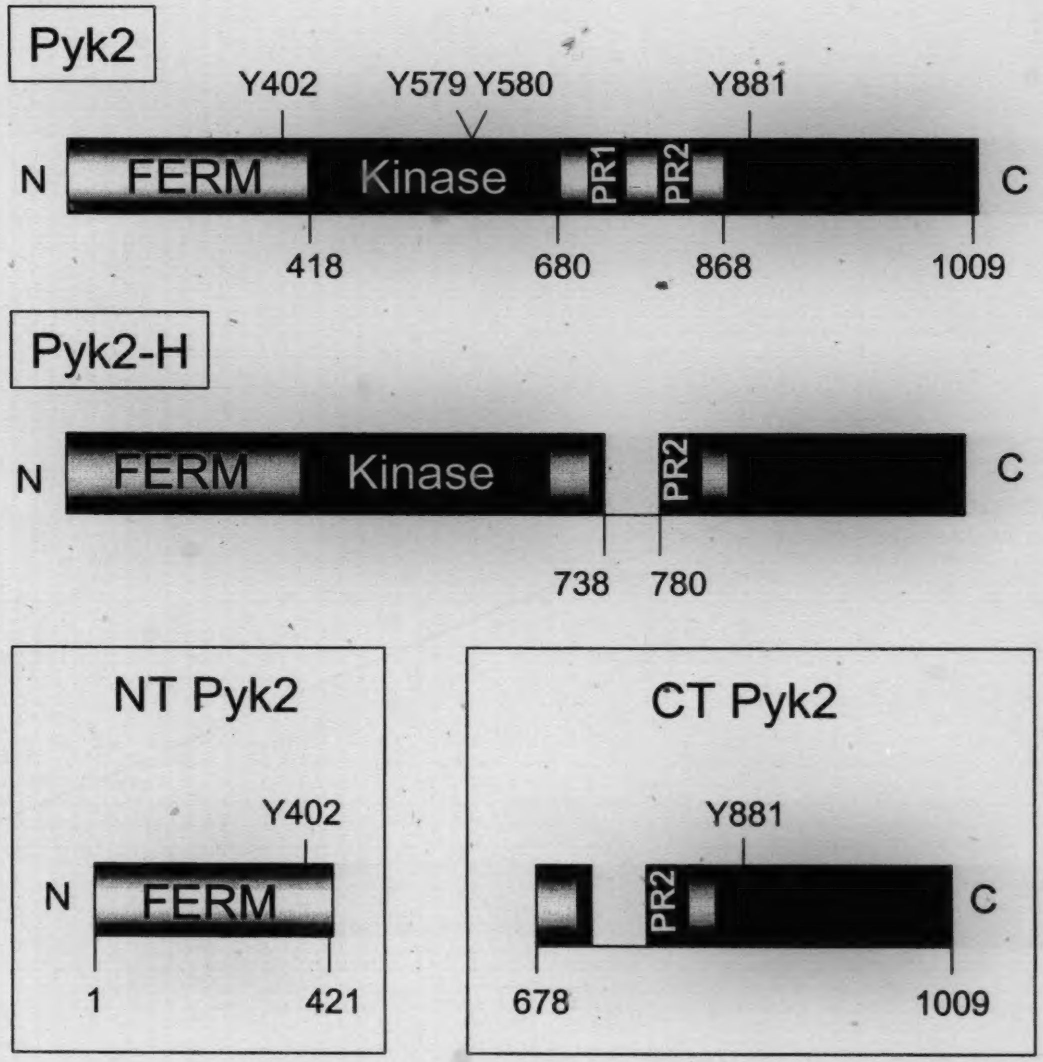
Pyk2
Y402
Y579 Y580
Y881
N
FERM
Kinase
PR1
PR2
C
418
680
868
1009
Pyk2-H
N
FERM
Kinase
PR2
C
738
780
NT Pyk2
Y402
N
FERM
1
421
CT Pyk2
Y881
PR2
C
678
1009

* Fuse constructs C-terminal to EGFP or GST

FIGURE 6-1. The sequences of Pyk2 used to make fusion proteins. Full length Pyk2, the Pyk2-H isoform, NT Pyk2 and CT Pyk2 are shown. The region missing from Pyk2-H and CT Pyk2 represents the splice region. Note that CT Pyk2 was cloned from CTL clones that express the Pyk2-H isoform. The NT Pyk2 and CT Pyk2 sequences were fused C-terminally to either EGFP (pEGFP-C1 vector) or GST (pGEX-4T-3 vector).

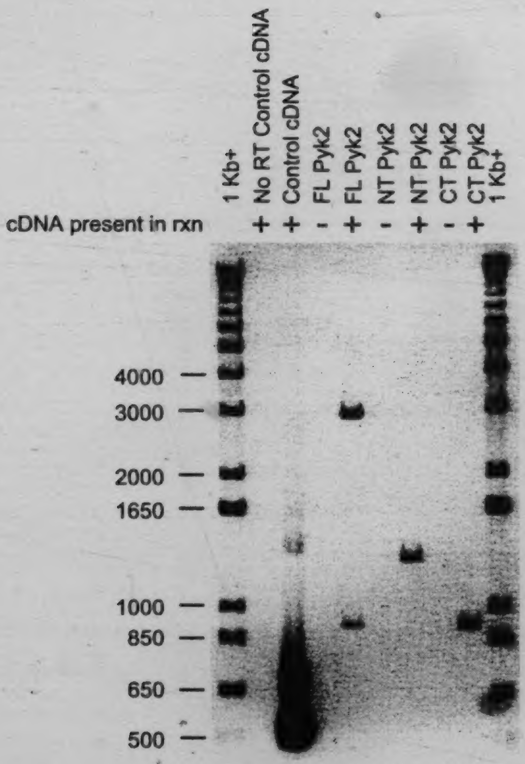
1 Kb+
No RT Control cDNA
Control cDNA
FL Pyk2
FL Pyk2
NT Pyk2
NT Pyk2
CT Pyk2
CT Pyk2
1 Kb+
cDNA present in rxn
+ + - + - + - +
4000
3000
2000
1650
1000
850
650
500

Expected band sizes:	
FL Pyk2	3076 bp
FL Pyk2-H	2950 bp
Pyk2 N-term	1276 bp
FL Pyk2 C-term	1030 bp
Pyk2-H C-term	876 bp
Control RNA	500 bp

FIGURE 6-2. Amplification of Pyk2 sequences from cDNA. RNA was isolated from AB.1 CTL clones and first strand cDNA was synthesized. PCR was performed on the cDNA using Pyk2-specific primers (listed in the Materials and Methods chapter) to amplify full length Pyk2 (FL Pyk2) or the entire N-terminal (NT Pyk2) and C-terminal (CT Pyk2) domains of Pyk2. Control cDNA and primers were provided with the first strand cDNA synthesis kit. The expected product sizes are shown in the box. Based on the observation that only one band was present in the CT Pyk2 lane and this band runs at approximately 876 bp and not 1030 bp, it appears that the AB.1 cells express only the Pyk2-H isoform. The band present between 850 bp and 1000 bp in the FL Pyk2 lane is not PRNK. Based on sequencing, it appears to be an N-terminal fragment of Pyk2.

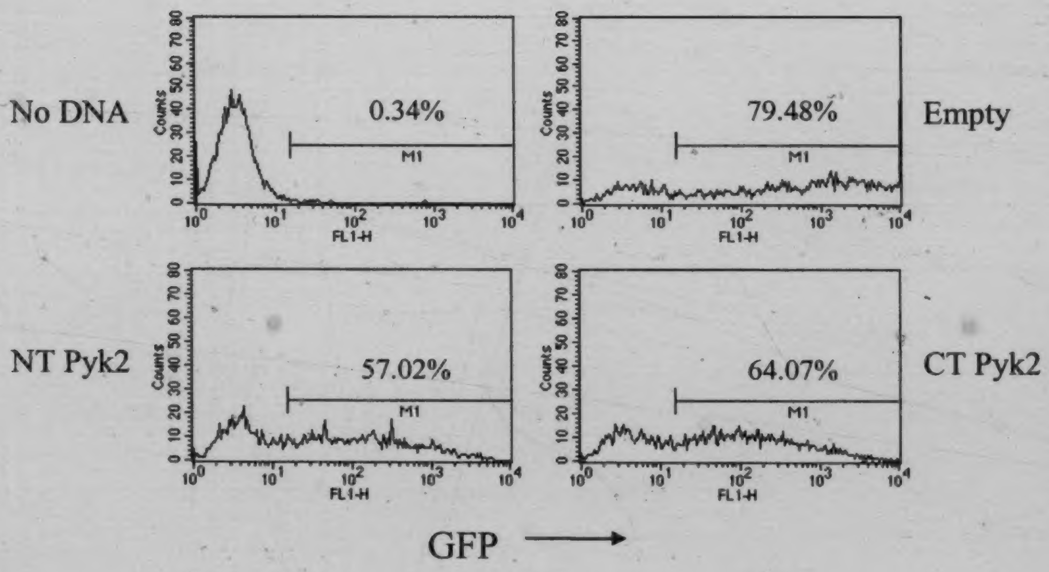

FIGURE 6-3. Transfection efficiency achieved using Amaxa nucleofection on CTL clones. CTL clone 11 were nucleofected with 4 μg of the pEGFP-C1 plasmid (empty vector or vector containing NT Pyk2 or CT Pyk2 sequences). Unfixed cells were assayed for EGFP expression by flow cytometry approximately 24 hours post-nucleofection. The percentages of EGFP-expressing cells are shown.

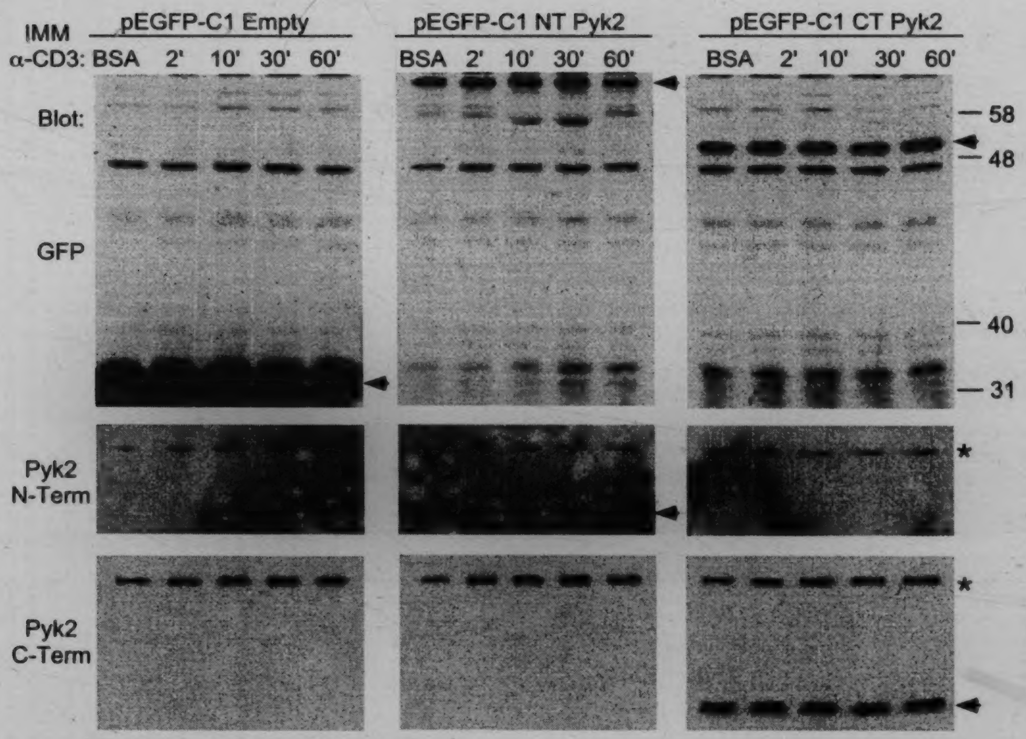

Average fold increase in expression
of construct over endogenous Pyk2: 4.3 2.4

FIGURE 6-4. The extent of overexpression of the NT Pyk2 and CT Pyk2 constructs. Clone 11 nucleofected with either pEGFP-C1, pEGFP-C1 NT Pyk2 or pEGFP-C1 CT Pyk2. Approximately 24 hours post-nucleofection, cells were added to wells of a 96 well plate coated with either BSA or anti-CD3. The plates were incubated at 37°C for 2, 10, 30 or 60 minutes. After the appropriate time, cells were lysed in the wells with reducing sample buffer (whole cell lysates). Samples were run on SDS-PAGE gels and transferred to membranes. The membrane was immunoblotted with anti-GFP. The arrowheads point to the EGFP fusion proteins. Note that the pre-stained molecular weight markers used are not very accurate. The membrane was also probed with antibodies generated against the N-terminus (N-19) and C-terminus (Pyk2 mAb) of Pyk2. The asterisks show endogenous Pyk2. The level of overexpression of the EGFP fusion proteins over endogenous Pyk2 was assessed by determining the pixel intensity for each band and dividing the value for the EGFP fusion protein by the value for endogenous Pyk2. The ratios of each of the five bands (BSA, 2', 10', 30' and 60') for both constructs were averaged to give an estimate of a 4.3 fold and 2.4 fold increase in expression of NT Pyk2 and CT Pyk2 respectively over endogenous Pyk2.

with these constructs. In this experiment, an approximate 4.3 fold and 2.4 fold increase in expression of EGFP-NT Pyk2 and -CT Pyk2, respectively, over endogenous Pyk2 was attained. The predicted molecular weights for NT Pyk2 (46.7 kDa) and CT Pyk2 (32.1 kDa) fused to EGFP (30 kDa) are 76.7 and 62.1 kDa respectively. Immunoblotting with anti-GFP shows the relative migration of the fusion proteins and that they are of the predicted molecular weights (Figure 6-4).

Localization of the N-terminal and C-terminal Pyk2 fusion proteins

I first determined the localization of EGFP and the NT Pyk2 and CT Pyk2 EGFP fusion proteins (Figure 6-5). I immunostained cells with anti-GFP to visualize the fusion proteins by confocal microscopy as opposed to examining EGFP fluorescence because EGFP fluorescence was not very intense and was reduced by exposure to formaldehyde (used to fix the cells). As expected, EGFP was found diffused throughout the cell and occasionally appeared to be present in the nucleus in clones nucleofected with the empty vector (Figure 6-5a). Anti-GFP staining of clone 11 nucleofected with NT Pyk2 demonstrated that when the fusion protein was highly expressed, some of the protein appeared to localize to the nucleus (Figure 6-5b, 6-6a, 6-6b). NT Pyk2 was also found in the cytoplasm. Co-immunostaining with anti-GFP and F298 antiserum (recognizes the N-terminus of Pyk2) showed that while some endogenous Pyk2 was found at the contact point between the CTL and its target, there was no significant enrichment of NT Pyk2 at the interface (Figure 6-6a). As expected, NT Pyk2 did not co-localize with the MTOC (Figure 6-6b).

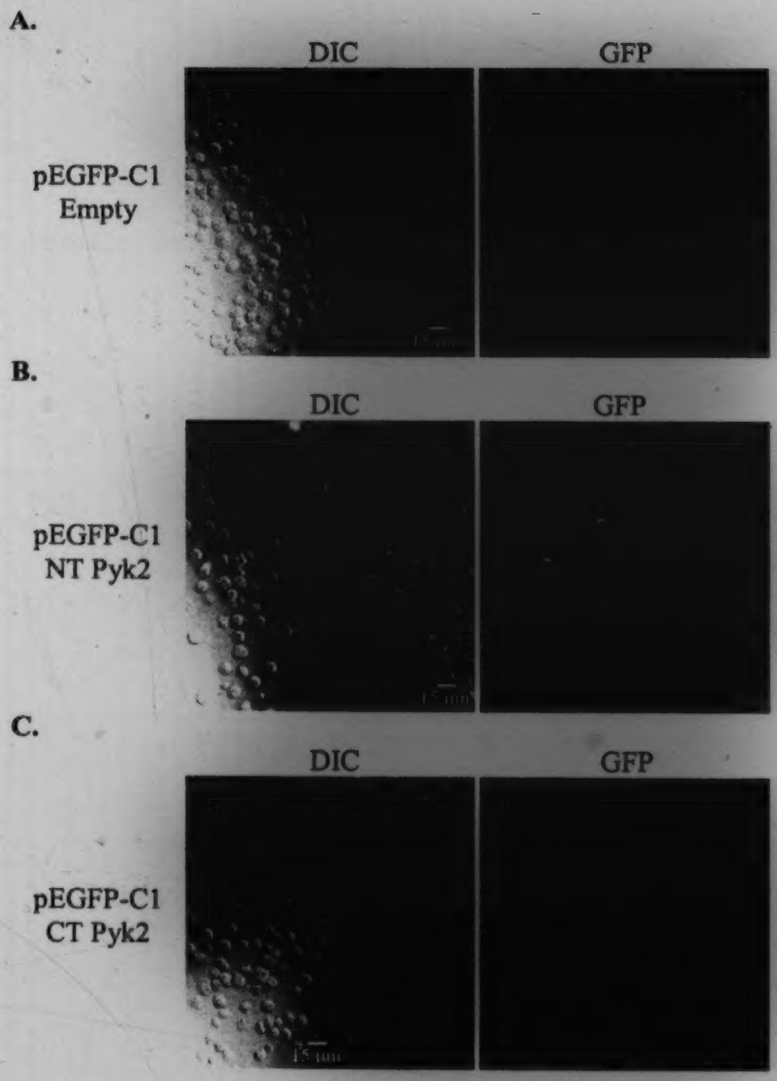
A.
DIC
GFP
pEGFP-C1
Empty
15 µm
B.
DIC
GFP
pEGFP-C1
NT Pyk2
15 µm
C.
DIC
GFP
pEGFP-C1
CT Pyk2
15 µm

FIGURE 6-5. The localization of EGFP and the EGFP-NT Pyk2 and -CT Pyk2 fusion proteins in CTL clones. CTL clone 11 were nucleofected with pEGFP-C1, pEGFP-C1 NT Pyk2 or pEGFP-C1 CT Pyk2. Approximately 24 hours post-nucleofection, the cells were harvested and stimulated with allogeneic target cells (L1210$^{Kb/Dd}$) for 2 or 3 minutes at 37°C. The conjugates were then fixed, permeabilized, immunostained and visualized by confocal microscopy. a, b, c) Clones nucleofected with pEGFP-C1 (empty vector) (a), pEGFP-C1 NT Pyk2 (b) or pEGFP-C1 CT Pyk2 (c) were immunostained with anti-GFP (Alexa 488). The arrows in (b) highlight cells with nuclear localization of EGFP-NT Pyk2.

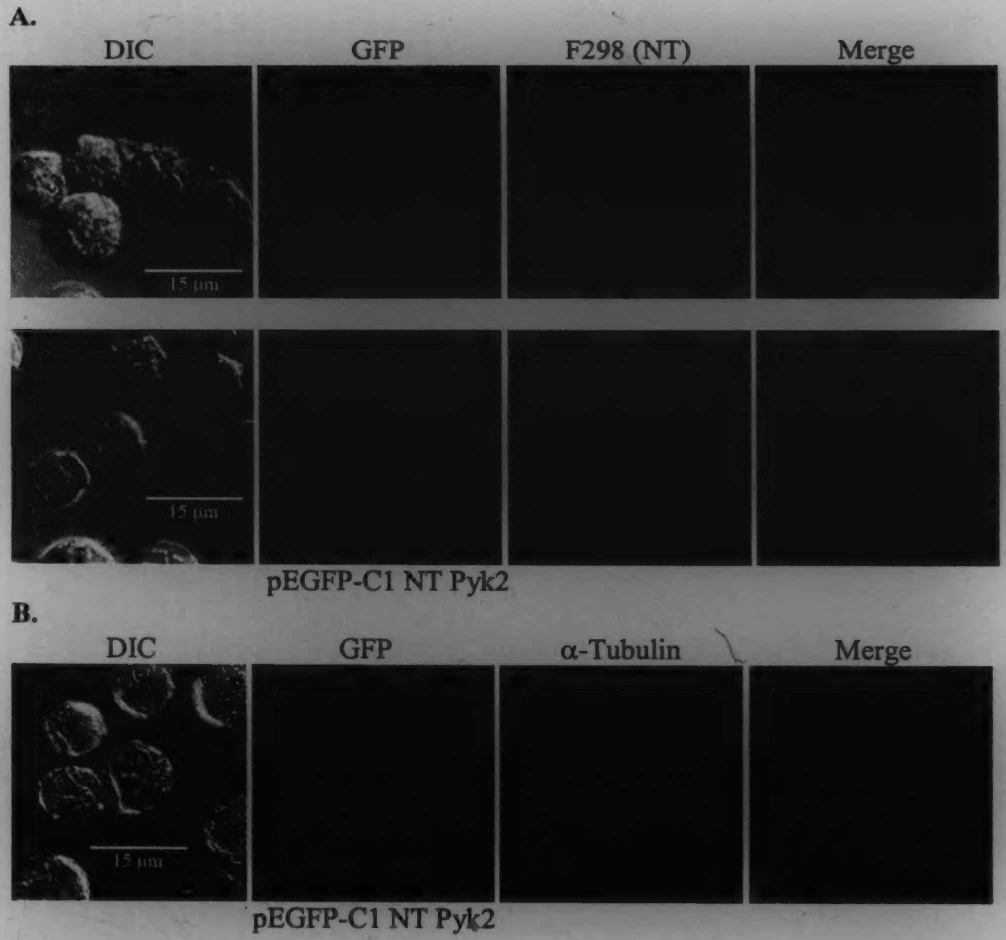
A.
DIC
GFP
F298 (NT)
Merge
15 µm
15 µm
pEGFP-C1 NT Pyk2
B.
DIC
GFP
α-Tubulin
Merge
15 µm
pEGFP-C1 NT Pyk2

FIGURE 6-6. A closer examination of the localization of the EGFP-NT Pyk2 fusion protein. Clone 11 nucleofected with pEGFP-C1 NT Pyk2 were stimulated with $L1210^{Kb/Dd}$ target cells as in Figure 6-5. The conjugates were then fixed, permeabilized, immunostained and visualized by confocal microscopy. All GFP staining was visualized with the Alexa 488 fluorochrome. a) Conjugates were immunostained with anti-GFP and F298 antisera (Alexa 594) which recognizes the N-terminus of Pyk2. Two examples are shown. (b) Conjugates were immunostained with anti-GFP and anti-α-tubulin (Alexa 594).

When clone 11 were nucleofected with CT Pyk2, it was found that the fusion protein was predominantly localized to the cytoplasm of the cell (Figure 6-5c, 6-7a). Co-immunostaining with anti-GFP and paxillin showed that there was co-localization of this fusion protein with paxillin at the MTOC as well as throughout the cytoplasm (Figure 6-7a). Cells immunostained with anti-GFP and anti-α-tubulin also demonstrated co-localization of CT Pyk2 with the MTOC (Figure 6-7b). When cells were immunostained for anti-GFP and with F245 antiserum (recognizes the C-terminus of Pyk2), I found that some endogenous Pyk2 accumulated at the MTOC and the CTL/target cell interface while CT Pyk2 was always seen at the MTOC and could sometimes be seen at the interface (Figure 6-7c). These results agree with those found in chapter 5, in which I showed that Pyk2 that associated with paxillin, co-localized with paxillin at the MTOC (Figure 5-6c). These results also suggest that since there is no co-localization of NT Pyk2 with the MTOC (Figure 6-6b), domains within the C-terminus of Pyk2 are responsible for this localization.

The effect of overexpression of NT Pyk2 and CT Pyk2 on MTOC reorientation

As mentioned above, overexpression of a kinase-inactive mutant of Pyk2 in NK cells led to defects in MTOC reorientation and killing (Gismondi et al. 2000; Sancho et al. 2000). As Pyk2 co-localizes with the MTOC, it is possible that it is performing some function there such as promoting the translocation of the MTOC to the T cell/target cell interface. I sought to determine whether the NT Pyk2 and CT Pyk2 constructs would have the same effect in CTL as the kinase-inactive Pyk2 had in NK cells. To examine MTOC reorientation in nucleofected clone 11, I immunostained fixed conjugates (with

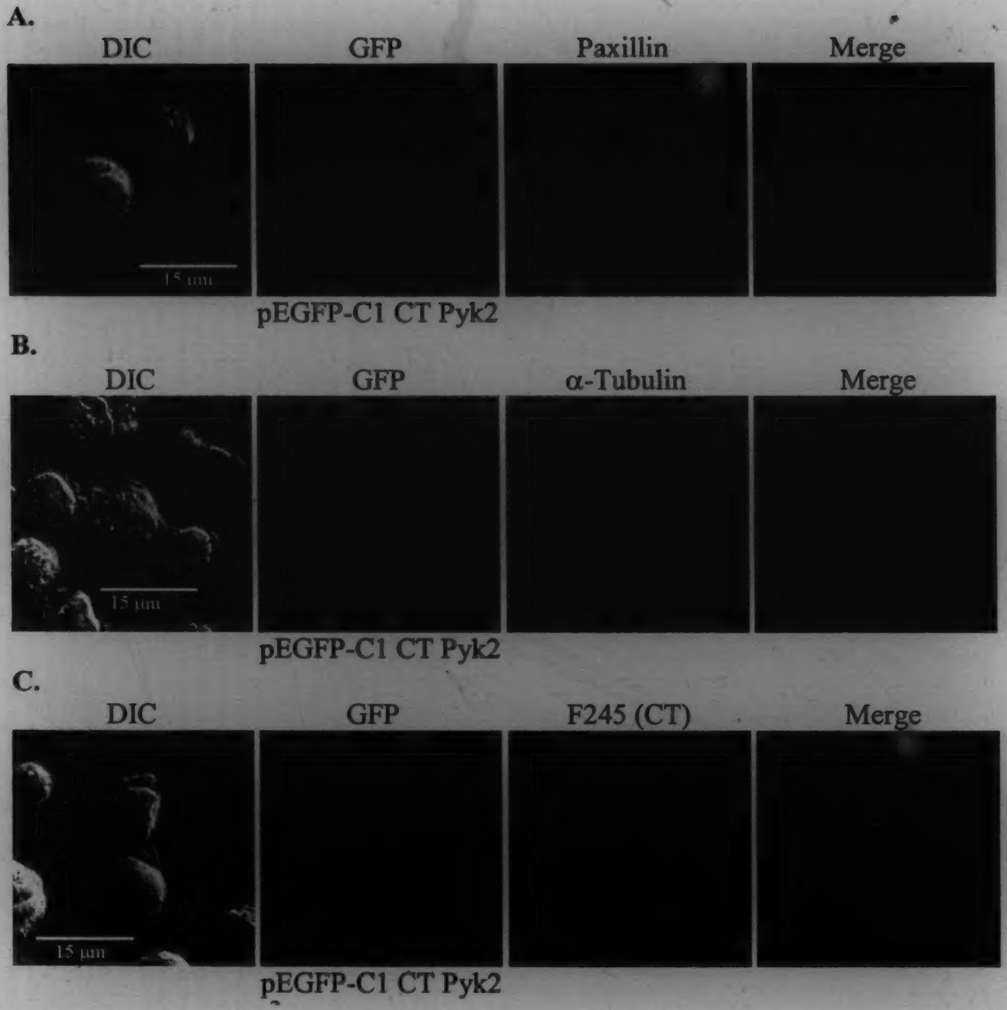
A.
DIC
GFP
Paxillin
Merge
15 μm
pEGFP-C1 CT Pyk2
B.
DIC
GFP
α-Tubulin
Merge
15 μm
pEGFP-C1 CT Pyk2
C.
DIC
GFP
F245 (CT)
Merge
15 μm
pEGFP-C1 CT Pyk2

FIGURE 6-7. A closer examination of the localization of the EGFP-CT Pyk2 fusion protein. Clone 11 nucleofected with pEGFP-C1 CT Pyk2 were either stimulated (b, c) with L1210$^{Kb/Dd}$ target cells as in Figure 6-5 or left unstimulated (a). The cells were then fixed, permeabilized, immunostained and visualized by confocal microscopy. All GFP staining was visualized with the Alexa 488 fluorochrome. (a) Unstimulated, nucleofected clones were immunostained with anti-GFP and anti-paxillin (rhodamine). b, c) Conjugates were immunostained with anti-GFP and anti-α-tubulin (Alexa 594) (b) or F245 antisera (Alexa 594) which recognizes the C-terminus of Pyk2 (c).

MTOC reorientation in nucleofected clone 11, I immunostained fixed conjugates (with allogeneic target cells) with anti-GFP and anti-α-tubulin and visualized them by confocal microscopy. Overexpression of the fusion proteins did not appear to affect the ability of the CTL to form conjugates. Conjugates were scored based on the extent of MTOC reorientation in transfected (EGFP positive) CTL. Three categories of MTOC positioning were used: 1) reoriented – the MTOC is centered near the interface and the nucleus has retracted (for example, see Figure 6-7b), 2) transition – the MTOC is nearly centered but the nucleus is off to one side and has not yet retracted (for example, see Figure 6-6b), 3) not reoriented – the MTOC is not in the vicinity of the interface. The data accumulated from two independent experiments is presented in Table 6-1. No significant difference between MTOC reorientation in CTL nucleofected with empty vector, NT Pyk2 or CT Pyk2 was observed. Therefore, overexpression of these Pyk2 constructs does not appear to interfere with the ability of CTL clones to reorient their MTOCs upon interaction with target cells.

The effect of overexpression of NT Pyk2 and CT Pyk2 on cell surface translocation of CD107a (Lamp-1)

I next examined whether Pyk2 was involved in the secretion of lytic granules. I first attempted to examine the movement of granzyme B-containing granules to the target cell contact site by confocal microscopy. However, CTL undergo piecemeal degranulation, therefore not all of the granules are directed to the contact site making it difficult to assess whether polarization has occurred. Instead, a fluorescence-activated cell sorting (FACS)-based assay was employed, in which degranulation is measured by

Construct	# Reoriented	# In Transition	# Not reoriented	Total # counted
pEGFP-C1 Empty	59	16	11	86
pEGFP-C1 NTPyk2	57	10	9	76
pEGFP-C1 CTPyk2	45	12	4	61

Construct	% Reoriented	% In Transition	% Not reoriented
pEGFP-C1 Empty	68.6	18.6	12.8
pEGFP-C1 NTPyk2	75	13.2	11.8
pEGFP-C1 CTPyk2	73.8	19.7	6.6

TABLE 6-1. Overexpression of NT Pyk2 and CT Pyk2 has no significant effect on MTOC reorientation. CTL clone 11 were nucleofected with pEGFP-C1, pEGFP-C1 NT Pyk2 or pEGFP-C1 CT Pyk2 and 24 hours later were conjugated with L1210$^{Kb/Dd}$ target cells for 3 minutes. Conjugates were fixed, permeabilized, stained with anti-GFP and anti-α-tubulin and examined by confocal microscopy. GFP^{+} conjugates were scored based on the extent of MTOC reorientation. Three categories of MTOC positioning were used: 1) reoriented – the MTOC is centered near the interface and the nucleus has retracted, 2) transition – the MTOC is nearly centered but the nucleus is off to one side and has not yet retracted, 3) not reoriented – the MTOC is not in the vicinity of the interface.

surface expression of CD107a (Lamp-1 or lysosome- associated membrane protein 1) which is present in granules and becomes externalized after fusion of the granules with the plasma membrane. To stimulate the CTL clones to degranulate, I plated the cells on wells coated with 10 μg/ml anti-CD3. This concentration of anti-CD3 provides maximal stimulation. After 30 minutes, the cells were removed from the plate and immunostained with anti-CD107a. The cells were gated for EGFP expression and the percentages of $GFP^+CD107a^+$ cells were determined for unstimulated and anti-CD3-stimulated cells. No significant difference in the mean fluorescence intensity of the GFP^+ $CD107a^+$ cells in clones expressing EGFP, EGFP-NT Pyk2 or EGFP-CT Pyk2 was noticed. Table 6-2 shows the ratios from three independent experiments of the percentages of GFP^+ $CD107a^+$ cells for clones nucleofected with NT Pyk2 or CT Pyk2 relative to clones nucleofected with empty vector. The averages of these ratios are plotted in Figure 6-8a. No detrimental effect on the ability of CTL expressing NT Pyk2 or CT Pyk2 to degranulate was observed. Interestingly, the results seem to suggest that expression of the EGFP-truncated Pyk2 fusion proteins results in a trend towards an increased number of cells expressing cell surface CD107a after degranulation. The average ratios for NT Pyk2 and CT Pyk2 displayed a respective 1.16 and 1.12 fold increase over EGFP alone. However, due to considerable variation in CD107a expression between experiments, there is large standard deviation and I cannot conclude that NT Pyk2 or CT Pyk2 expression affects CTL degranulation.

It is possible that, since I was maximally stimulating the cells, an increase in surface expression of CD107a could not be detected. I therefore decided to stimulate the

		% GFP$^+$ CD107a$^+$ cells (CD3 – BSA)			Pyk2 construct / Empty vector	
Stimulus	**Trial #**	**Empty**	**NT Pyk2**	**CT Pyk2**	**NT Pyk2**	**CT Pyk2**
10 µg/ml CD3	1	37.39	50.77	47.43	1.36	1.27
	2	44.86	47.14	49.01	1.05	1.09
	3	54.64	59.02	54.75	1.08	1
	Average	**45.63**	**52.31**	**50.40**	**1.16**	**1.12**
0.5 µg/ml CD3	1	23.34	34.65	39.03	1.48	1.67
	2	17.15	24.03	16.39	1.4	0.96
	3	23.02	31.33	32.1	1.36	1.39
	Average	**21.17**	**30.00**	**29.17**	**1.41**	**1.34**

TABLE 6-2. Comparison of the percentages of GFP$^+$ CD107a$^+$ cells between clones expressing EGFP, EGFP-NT Pyk2 and EGFP-CT Pyk2. Shown in the left hand columns are the percentages of GFP$^+$ CD107a$^+$ cells in which the value for the unstimulated cells (BSA) has been subtracted from the stimulated cells (CD3). Data from three independent trials are shown for stimulation with both 10 µg/ml and 0.5 µg/ml anti-CD3. In the right hand columns, the ratio of the percentage of GFP$^+$ CD107a$^+$ cells of clones nucleofected with either NT Pyk2 or CT Pyk2 relative to clones nucleofected with empty vector are shown.

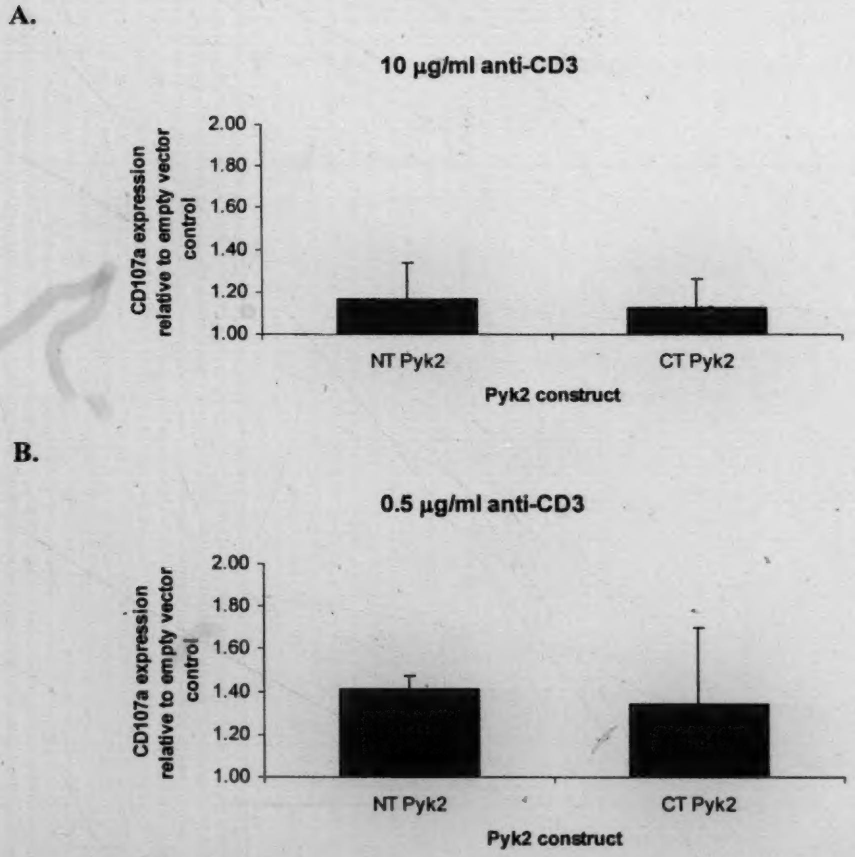

FIGURE 6-8. CD107a (Lamp-1) cell surface expression upon degranulation in response to immobilized anti-CD3 stimulation. Clone 11 were nucleofected with pEGFP-C1, pEGFP-C1 NT Pyk2 or pEGFP-C1 CT Pyk2. Approximately 24 hours post-nucleofection, the cells were harvested and stimulated on BSA-coated or 0.5 μg/ml anti-CD3-coated wells at 37°C for 30 minutes. After 30 minutes, the cells were removed from the wells and immunostained with anti-CD107a. The cells were assayed using flow cytometry. Cells were gated for EGFP expression. a, b) The percentages of gated GFP positive cells that express cell surface CD107a for clones expressing either pEGFP-C1 NT Pyk2 or pEGFP-C1 CT Pyk2 were used to calculate CD107a expression relative to clones expressing the empty vector. The calculation used was as follows: clones nucleofected with Pyk2 construct (stimulated with anti-CD3 – unstimulated) / clones nucleofected with empty vector (stimuated with anti-CD3 – unstimulated). A value of 1.00 means that there was no change when compared to the empty vector control. The values calculated for three independent trials (displayed in Table 6-2) were averaged and graphed for nucleofected clones stimulated on wells coated with either 10 μg/ml anti-CD3 (a) or 0.5 μg/ml anti-CD3 (b). c) Representative examples of CD107a cell surface expression on EGFP-expressing cells. The top panels show cells plated on BSA-coated wells and the bottom panels show cells stimulated on 0.5 μg/ml anti-CD3. MFI = mean fluorescence intensity of cells in M2. c) Next page.

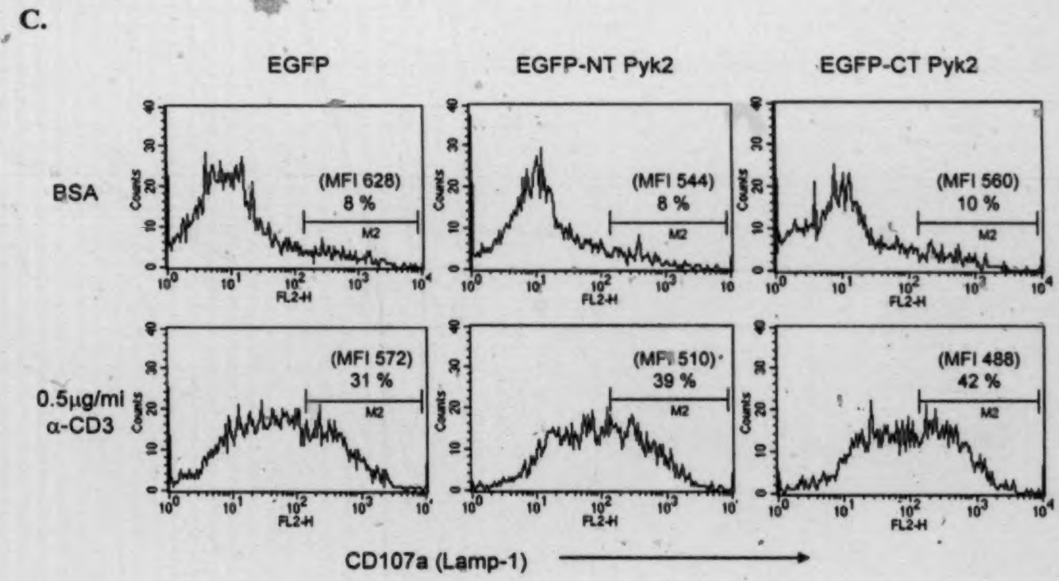C.
EGFP
EGFP-NT Pyk2
EGFP-CT Pyk2
BSA
0.5μg/ml
α-CD3
(MFI 628)
8 %
(MFI 544)
8 %
(MFI 560)
10 %
(MFI 572)
31 %
(MFI 510)
39 %
(MFI 488)
42 %
M2
Counts
FL2-H
CD107a (Lamp-1)

cells to degranulate using a lower concentration of anti-CD3 (0.5 μg/ml). The percentages of the GFP^+ $CD107a^+$ cells and ratios from three individual experiments are presented in Table 6-2 and the averages of the ratios from those three experiments are graphed in Figure 6-8b. A representative example of cell surface CD107a expression for cells nucleofected with each construct is shown in figure 6-8c. Stimulating CTL clones with this concentration of anti-CD3 resulted in a higher fold increase in expression of cell surface CD107a for clones expressing NT Pyk2 (1.41) and CT Pyk2 (1.34) over clones expressing EGFP than was seen using 10 μg/ml anti-CD3. When 0.5 μg/ml anti-CD3 was used as a stimulus, the fold increase in CD107a surface translocation in clones expressing NT Pyk2 over clones expressing EGFP was quite consistent (Table 6-2). However, in the case of cells nucleofected with CT Pyk2, there was large variability as was seen with a 10 μg/ml anti-CD3 stimulus (Table 6-2). Therefore I can only conclude that there appears to be a trend towards an increased number of cells expressing surface CD107a upon degranulation in CTL clones nucleofected with either NT Pyk2 or CT Pyk2.

One preliminary experiment was performed using target cells as a more physiological stimulus for degranulation to determine whether the results would differ from TCR stimulation. In this experiment, cell surface CD107a expression was determined in EGFP-expressing CTL upon interaction with target cells either expressing allogeneic MHC class I molecules ($L1210^{Kb/Dd}$) or not (L1210). The results from this experiment also suggest an increased CD107a expression in clones expressing both EGFP-truncated Pyk2 fusion proteins when compared to clones expressing EGFP. The values for the fold increase over empty vector were 1.34 and 1.18 for NT Pyk2 and CT

Pyk2 respectively. Of course more repeats of this experiment will need to be conducted to confirm this observation. I was thus unable to detect a defect in the ability of CTL clones to degranulate upon expression of the truncated Pyk2 fusion proteins. It is possible that the increased surface expression detected in these assays could be due to degranulation that is not restricted to the contact site as these assays cannot distinguish between polarized and unpolarized degranulation. However, as I did not detect a significant shift in mean fluorescence intensity in CD107a$^+$ cells (ie. each cell expresses a higher level of CD107a), I do not favor this hypothesis. There may also be differences in the rate of internalization of CD107a betewen the samples that may account for the observed increase in CD107a expression. Alternatively, as mentioned above, the results may indicate that the threshold for degranulation has been lowered upon expression of NT Pyk2 or CT Pyk2.

The effect of knockdown of Pyk2 expression on cell surface expression of CD107a on CTL clones

I also aimed to address the function of Pyk2 with the use of siRNA (short interfering ribonucleic acid). Double stranded RNA 21-mers were designed to target murine Pyk2. Pyk2 siRNA was nucleofected into CTL clones using Amaxa nucleofection technology. Knockdown of Pyk2 protein 48 hours post-nucleofection was assessed by western blot. A representative example of the extent of Pyk2 knockdown achieved with these oligomers is shown in Figure 6-9. In this example, approximately 55% knockdown of Pyk2 protein was attained. These Pyk2 oligos are believed to be

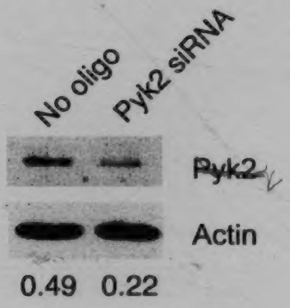

FIGURE 6-9. A representative example of the extent of knockdown of Pyk2 protein. CTL clone 11 were nucleofected with 3 μg of Pyk2 siRNA or an equivalent volume of vehicle. Clones were harvested approximately 48 hours post-nucleofection. Cell lysates were run on an SDS-PAGE gel and transferred to a membrane. The membrane was immunoblotted with anti-Pyk2 antiserum (F298) and anti-actin. The extent of knockdown was determined by assessing the ratio of pixel intensities for each Pyk2 band relative to each actin band and dividing the value for Pyk2 by the value for actin. The ratios are shown below the actin blot. In this example approximately 55% knockdown was achieved.

specific for Pyk2 as they did not affect ERK2 (extracellular regulated kinase 2) protein levels and likewise, ERK2 oligos did not affect Pyk2 protein levels (data not shown).

I performed flow cytometry on CTL clones nucleofected with Pyk2 siRNA to assess CD107a cell surface expression upon stimulation to degranulate with immobilized anti-CD3. One caveat to this experimental design is that there no marker for transfection. My previous experience, using fluorescein-labeled siRNA, demonstrated that these molecules could be quite "sticky". siRNA that had not entered the cells could bind to the outside of cells and was not effectively removed by washing. Thus, this kind of approach was not conducive to the identification of transfected cells. I performed the assay and ensured, by western blot, that at least 50% knockdown of Pyk2 had been achieved in nucleofected clone 11. Clones nucleofected with Pyk2 siRNA were stimulated on either 10 μg/ml or 0.5 μg/ml anti-CD3 to stimulate degranulation. Clones nucleofected with Pyk2 siRNA spread on the immobilized anti-CD3 to the same extent as cells nucleofected with vehicle. As was seen for clones nucleofected with the EGFP-Pyk2 constructs, there was great variation in CD107a surface expression between experiments. Two repeats were performed using both antibody concentrations. For both 10 μg/ml and 0.5 μg/ml anti-CD3, one experiment showed an increase in cell surface CD107a expression and the other indicated a decrease in CD107a expression on cells nucleofected with Pyk2 siRNA over control nucleofected cells (Table 6-3). Knockdown was assessed for each experiment and was typical of what was shown in Figure 6-9. Therefore, few conclusions can be drawn from these experiments, except to say that the cells are able to express CD107a on the cell surface after stimulation with immobilized anti-CD3. Many additional experiments will need to be performed to determine if knockdown of Pyk2

Stimulus	Trial #	CD107a surface expression relative to no siRNA control
10 µg/ml α-CD3	1	1.76
	2	0.93
0.5 µg/ml α-CD3	1	1.12
	2	0.63

TABLE 6-3. Comparison of the percentages of CD107a$^+$ cells between clones nucleofected with Pyk2 siRNA or vehicle. Shown are the ratios of the percentages of CD107a$^+$ cells of clones nucleofected with Pyk2 siRNA relative to those nucleofected with vehicle. The percentages of CD107a$^+$ cells were determined by subtracting the value for unstimulated cells from the value for stimulated cells. Data from two independent trials are shown.

impacts CTL degranulation. Perhaps the use of additional siRNAs targeted towards Pyk2 alone or in combination would further enhance the extent of knockdown of Pyk2 protein.

One interesting observation was made when examining conjugates formed between CTL clones nucleofected with Pyk2 siRNA and target cells. I have noticed that these clones appear to be more resistant to the disruption of conjugates with EDTA. Clones nucleofected with Pyk2 siRNA or vehicle were allowed to conjugate with CellTracker Orange-labeled EL4 target cells for 1 hour. The conjugates were then disrupted using washes with EDTA. Figure 6-10 shows forward versus side scatter plots of disrupted conjugates. Forward scatter is an indicator of cell size and side scatter is an indicator of internal complexity (ie. membrane roughness, the amount and type of cytoplasmic granules). Therefore, single cells will have low forward scatter while conjugates will increase the forward scatter due to an increase in size. Interestingly, the samples which contain clones nucleofected with Pyk2 siRNA display a higher percentage of cells (approximately 2 fold) that have increased forward scatter when compared to samples with cells nucleofected with vehicle (Figure 6-10). This is true even when the two cell types are mixed on ice (unstimulated). The histograms shown in Figure 6-10 demonstrate that the gated cells contain both unlabeled CTL and labeled EL4 cells, however it is not known at this time whether this represents mostly homoconjugates or heteroconjugates. The shift in forward scatter is greater in samples containing Pyk2 siRNA-nucleofected CTL than those that contain control CTL, which suggests that these samples may have an increased number of higher order conjugates (Figure 6-10). Together, the results suggest that there is no defect in the ability of CTL nucleofected with Pyk2 siRNA to form conjugates and that there may be increased adhesion between

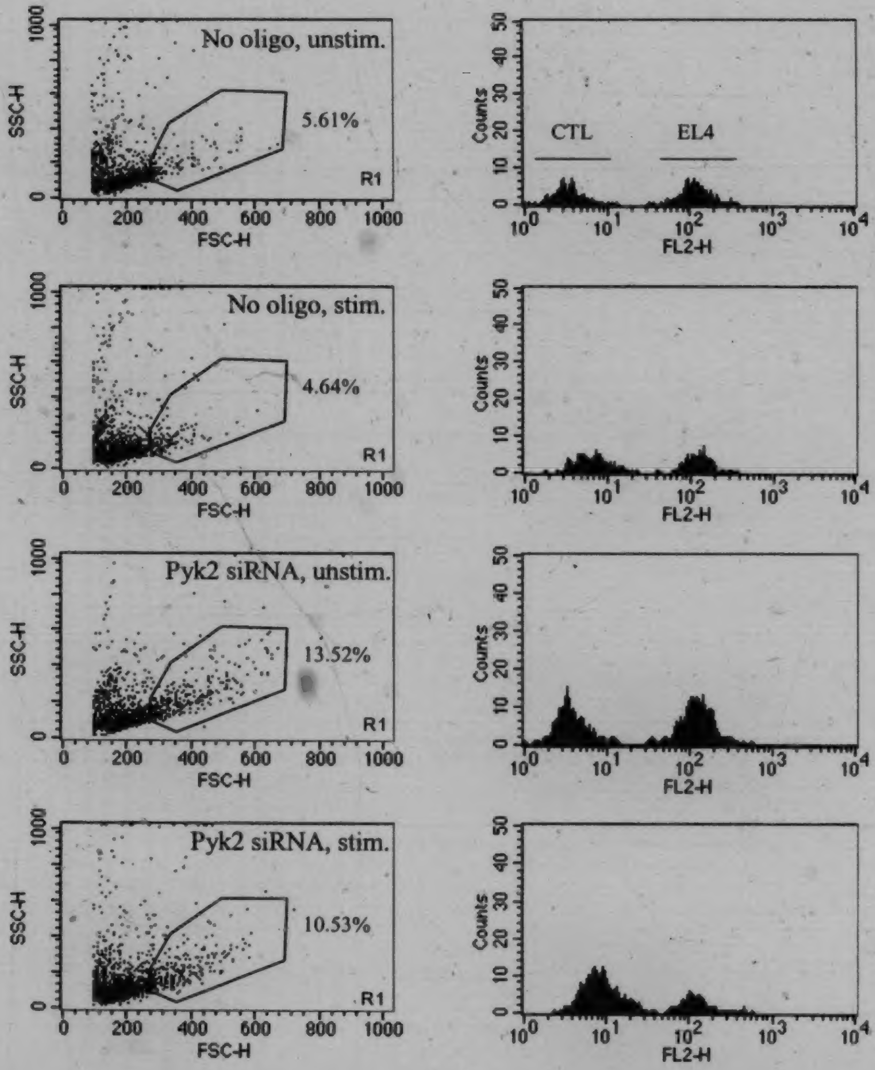

FIGURE 6-10. CTL clones nucleofected with Pyk2 siRNA may adhere to their targets better than clones nucleofected with vehicle. CTL clone 11 were nucleofected with 3 μg of Pyk2 siRNA or an equivalent volume of vehicle. Clones were harvested approximately 48 hours post-nucleofection. Clones nucleofected with Pyk2 siRNA or vehicle were mixed with CellTracker Orange-labeled EL4 target cells and allowed to conjugate for 1 hour at 37°C. For the unstimulated cells, clones and EL4 cells were mixed together on ice. The conjugates were then disrupted using washes with EDTA. The disrupted conjugates were then subjected to flow cytometry. FACS plots of forward scatter versus side scatter are shown. Forward scatter is an indicator of cell size and side scatter is an indicator of cell complexity. Also shown is a histogram demonstrating that the gated cells contain both CTL and targets.

these CTL and their targets. Additional studies are required to confirm this observation and the use of labeled CTL as well as labeled targets would aid in determining the nature of the conjugates.

The effect of overexpression of NT Pyk2 and CT Pyk2 on cell spreading on immobilized anti-CD3

Previous studies have demonstrated that overexpression of the C-terminus of Pyk2 inhibited cell spreading in monocytes (Watson et al. 2001) and neutrophils (Han et al. 2003). I sought to test whether expression of NT Pyk2 or CT Pyk2 had an effect on cell spreading on immobilized anti-CD3. Nucleofected CTL were allowed to adhere to anti-CD3-coated coverslips for 20 minutes at 37°C. The cells were then fixed, permeabilized and immunostained with anti-GFP. One preliminary experiment was performed. Figures 6-11a, 6-11b and 6-11c show examples of spreading cells nucleofected with empty vector, NT Pyk2 and CT Pyk2 respectively. Although no obvious differences in the shape of the spreading cells was noted, there were some differences in the percentages of EGFP$^+$ cells that were spreading. Table 6-4 shows the data for the absolute numbers and percentages of spreading EGFP$^+$ and EGFP$^-$ cells within a nucleofected sample. The table also shows the ratio of the percentages of spreading EGFP$^+$ cells to spreading EGFP$^-$ cells within the sample. Expression of EGFP or EGFP-NT Pyk2 did not significantly affect the percentage of cells that spread on anti-CD3 (fold changes of 0.9 and 1.1 respectively) (Table 6-4). However, when EGFP-CT Pyk2 was expressed, a 1.7 fold increase in the percentage of spread cells was observed (Table 6-4). This result suggests that CTL clones expressing the CT Pyk2 fusion protein

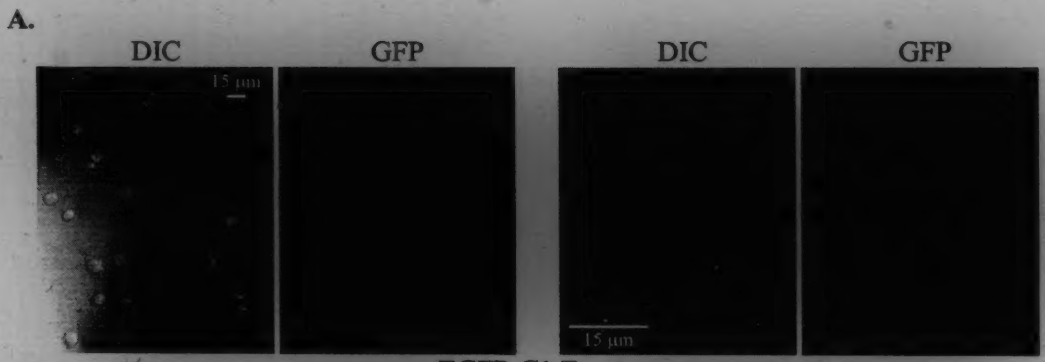
A.
DIC
GFP
DIC
GFP
15 µm
15 µm

pEGFP-C1 Empty

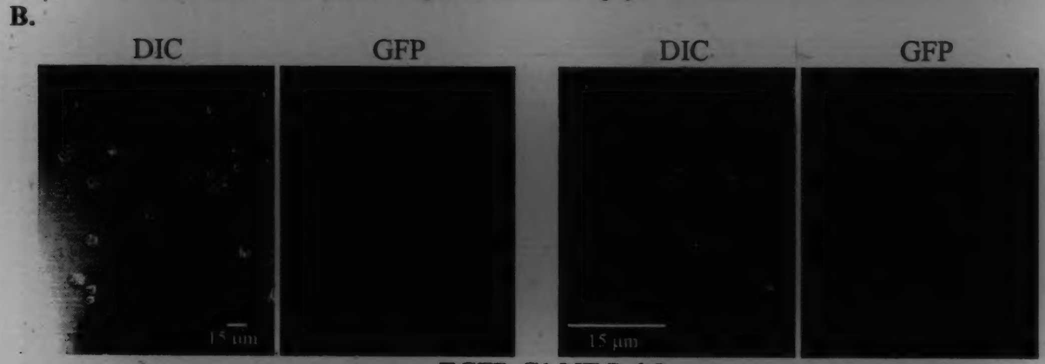
B.
DIC
GFP
DIC
GFP
15 µm
15 µm

pEGFP-C1 NT Pyk2

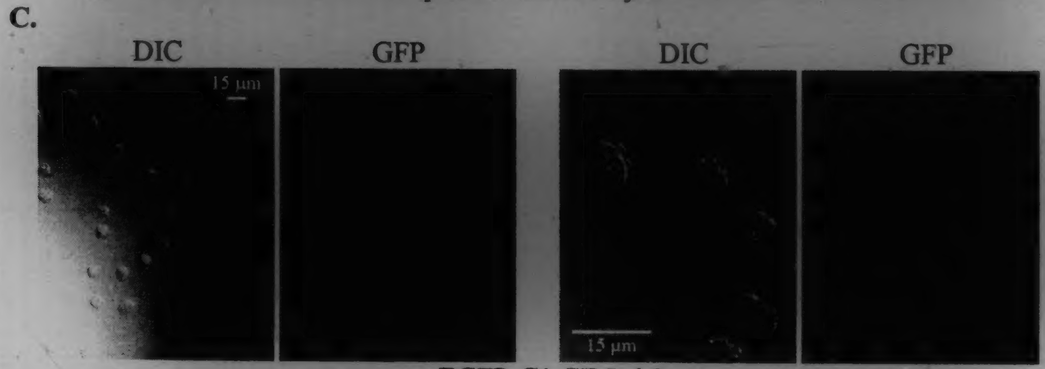
C.
DIC
GFP
DIC
GFP
15 µm
15 µm

pEGFP-C1 CT Pyk2

FIGURE 6-11. Examination of the morphology of nucleofected CTL clones spreading on immobilized anti-CD3. Clone 11 were nucleofected with pEGFP-C1, pEGFP-C1 NT Pyk2 or pEGFP-C1 CT Pyk2. Approximately 24 hours later, nucleofected CTL were allowed to adhere to anti-CD3-coated coverslips for 20 minutes at 37°C. The cells were then fixed, permeabilized, immunostained for anti-GFP and examined by confocal microscopy. GFP immunostaining was visualized with the Alexa 488 fluorochrome. Cells were imaged using a 40x objective. Left hand column = scan zoom 1.0. Right hand column = scan zoom 4.0 (Empty and CT Pyk2) and 5.0 (NT Pyk2).

Vector	Total # cells bound to anti-CD3	# GFP$^-$ cells spread	# GFP$^+$ cells spread	% GFP$^-$ cells spread	% GFP$^+$ cells spread	Fold change (%GFP$^+$ / %GFP$^-$)
pEGFP-C1 empty	284	80	74	28	26	0.9
pEGFP-C1 NTPyk2	365	97	108	27	30	1.1
pEGFP-C1 CTPyk2	142	32	54	23	38	1.7

TABLE 6-4. The absolute numbers and percentages of spreading nucleofected CTL clones. Clone 11 were nucleofected with pEGFP-C1, pEGFP-C1 NT Pyk2 or pEGFP-C1 CT Pyk2. Approximately 24 hours later, nucleofected CTL were allowed to adhere to anti-CD3-coated coverslips for 20 minutes at 37°C. The cells were then fixed, permeabilized, immunostained for anti-GFP and examined by confocal microscopy. Shown are the absolute numbers and percentages of spreading GFP$^-$ and GFP$^+$ cells within a nucleofected sample. Also shown is the fold change in the percentage of GFP$^+$ over the GFP$^-$ cells within the sample.

have an increased number of cells spreading on immobilized anti-CD3. A lowered threshold for activation upon stimulation with immobilized anti-CD3 in clones CT Pyk2 could also explain the observed increase in the number of cells spreading.

The effect of Pyk2 knockdown and overexpression of NT Pyk2 and CT Pyk2 on signalling after stimulation through the TCR

I also examined the role of Pyk2 in signalling after stimulation through the TCR. Pyk2 becomes phosphorylated and activated in response to numerous stimuli, therefore I determined whether Pyk2 plays a role in membrane proximal signalling. To this end, I analyzed the patterns of tyrosine phosphorylation in lysates from clones stimulated on immobilized anti-CD3. In this scenario, TCR stimulation, an increase in intracellular calcium and activation of the cytoskeleton upon spreading could all contribute to the induction of tyrosine phosphorylation of signalling proteins and of Pyk2. In a preliminary experiment, I compared untransfected clone 11, clone 11 nucleofected with Pyk2 siRNA or clone 11 nucleofected with vehicle. Cells were stimulated with immobilized anti-CD3 over the course of 60 minutes and general tyrosine phosphorylation in whole cell lysates was examined. In this experiment, approximately 50% knockdown of Pyk2 was achieved (Figure 6-12). Clones that have been subjected to nucleofection have a much less robust induction of tyrosine phosphorylation in response to immobilized anti-CD3 than do clones that have not been nucleofected (Figure 6-12). This is also demonstrated with phospho-ERK immunoblot, a more downstream signalling event, in which nucleofected clones have weaker induction of phosphorylation and a less sustained pattern of phosphorylation (Figure 6-12). Comparison of clones nucleofected

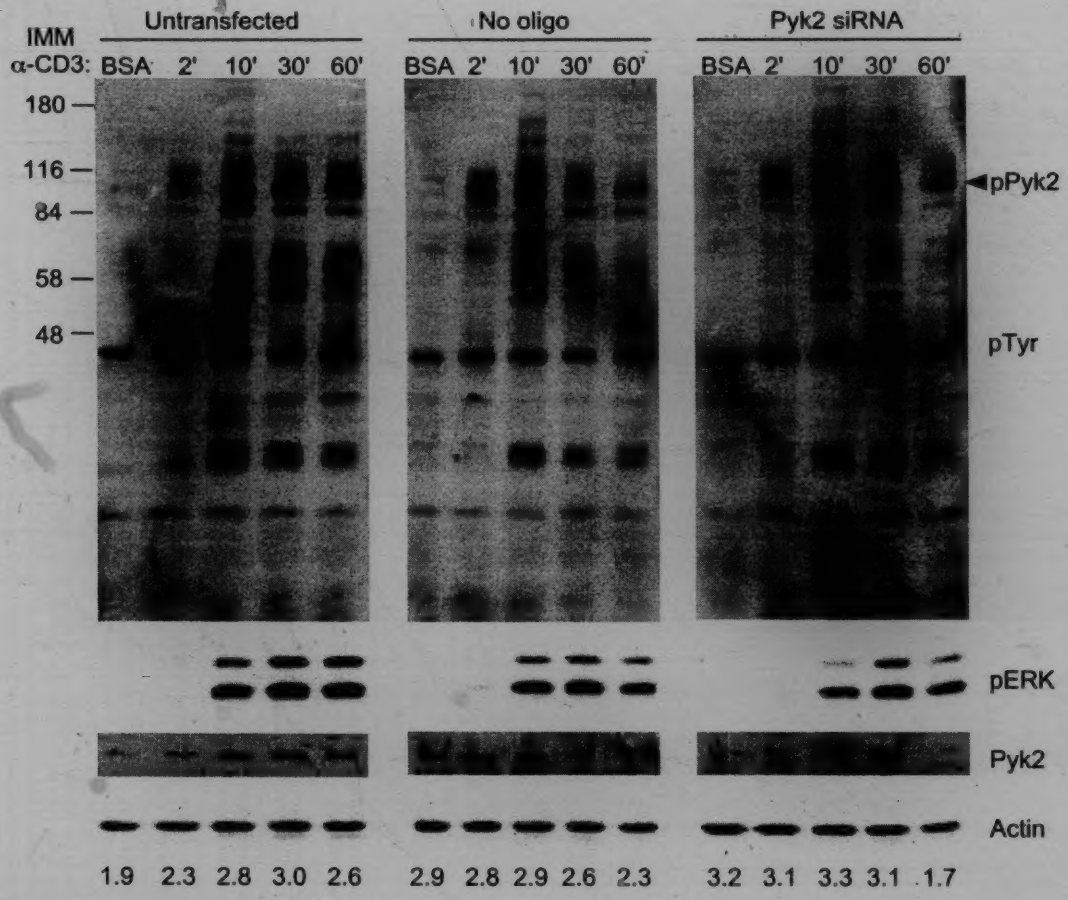
IMM
α-CD3:
Untransfected
BSA 2' 10' 30' 60'
No oligo
BSA 2' 10' 30' 60'
Pyk2 siRNA
BSA 2' 10' 30' 60'
180
116
84
58
48
pPyk2
pTyr
pERK
Pyk2
Actin
1.9 2.3 2.8 3.0 2.6
2.9 2.8 2.9 2.6 2.3
3.2 3.1 3.3 3.1 1.7

Avg pixel intensity: 0.35 0.33 0.17

FIGURE 6-12. The effect of knockdown of Pyk2 on the induction of general tyrosine phosphorylation in response to stimulation with immobilized anti-CD3. Clone 11 were either not transfected, or nucleofected with Pyk2 siRNA or vehicle. Cells were counted by trypan blue exclusion and 1 X 10^5 cells were added to wells of a 96 well plate coated with either BSA or anti-CD3. The plates were incubated at 37°C for 2, 10, 30 or 60 minutes. After the appropriate time, cells were lysed in the wells with reducing sample buffer (whole cell lysates). Samples were run on SDS-PAGE gels, transferred to membranes and the membranes were immunoblotted with anti-phosphotyrosine, anti-phospho-ERK, anti-actin and Pyk2 antiserum (F298). To assess the extent of Pyk2 knockdown in clones nucleofected with Pyk2 siRNA, the ratio of the pixel intensity for Pyk2 relative to pixel intensity for actin for each lane was determined. The ratios of the 5 samples (BSA, 2', 10', 30' and 60') were then averaged. The averages were 0.35 (untransfected clone 11), 0.33 (nucleofection with vehicle) and 0.17 (nucleofection with Pyk2 siRNA) which demonstrates that approximately 50% knockdown of Pyk2 was achieved. The pixel intensities for each actin band are shown below the actin immunoblot to allow for comparison of the amount of protein loaded in each lane.

with vehicle and clones nucleofected with Pyk2 siRNA reveals that knockdown of Pyk2 appears to have dampened tyrosine phosphorylation of numerous proteins in response to TCR stimulation (Figure 6-12). This was most obvious at the 10 minute time point which displayed the greatest induction of tyrosine phosphorylation of cell lysate proteins (Figure 6-12). The results from this experiment suggest that Pyk2 may play a role in signal amplification. However, there was no significant specific effect on the phosphorylation of ERK in clones nucleofected with Pyk2 siRNA. The observed dampening of tyrosine phosphorylation may thus not suffice to affect downstream signaling events. Alternatively, ERK phosphorylation may be maximal with low TCR engagement and may not be further enhanced by signal amplification. Additional repeats are necessary to confirm this result.

I next determined whether there was an effect on general tyrosine phosphorylation of whole cell lysates from clone 11 nucleofected with empty vector, NT Pyk2 or CT Pyk2. Two repeats of this experiment were performed in which cells were stimulated on immobilized anti-CD3 as above. For the first attempt, the extent of overexpression of the constructs compared to endogenous Pyk2 is shown in Figure 6-4 and the average fold increase for NT Pyk2 and CT Pyk2 was 4.3 and 2.4 respectively. In this experiment, no obvious difference in the amount of general tyrosine phosphorylation of the lysates between the samples was observed (Figure 6-13). Further, ERK phosphorylation patterns were similar to the control (Figure 6-13). Previous studies have demonstrated that overexpression of the C-terminal domain of Pyk2 inhibits endogenous Pyk2 phosphorylation (Watson et al. 2001; Han et al. 2003). Also, if the N-terminal FERM domain of Pyk2 mediates an autoinhibitory interaction within Pyk2, overexpression of

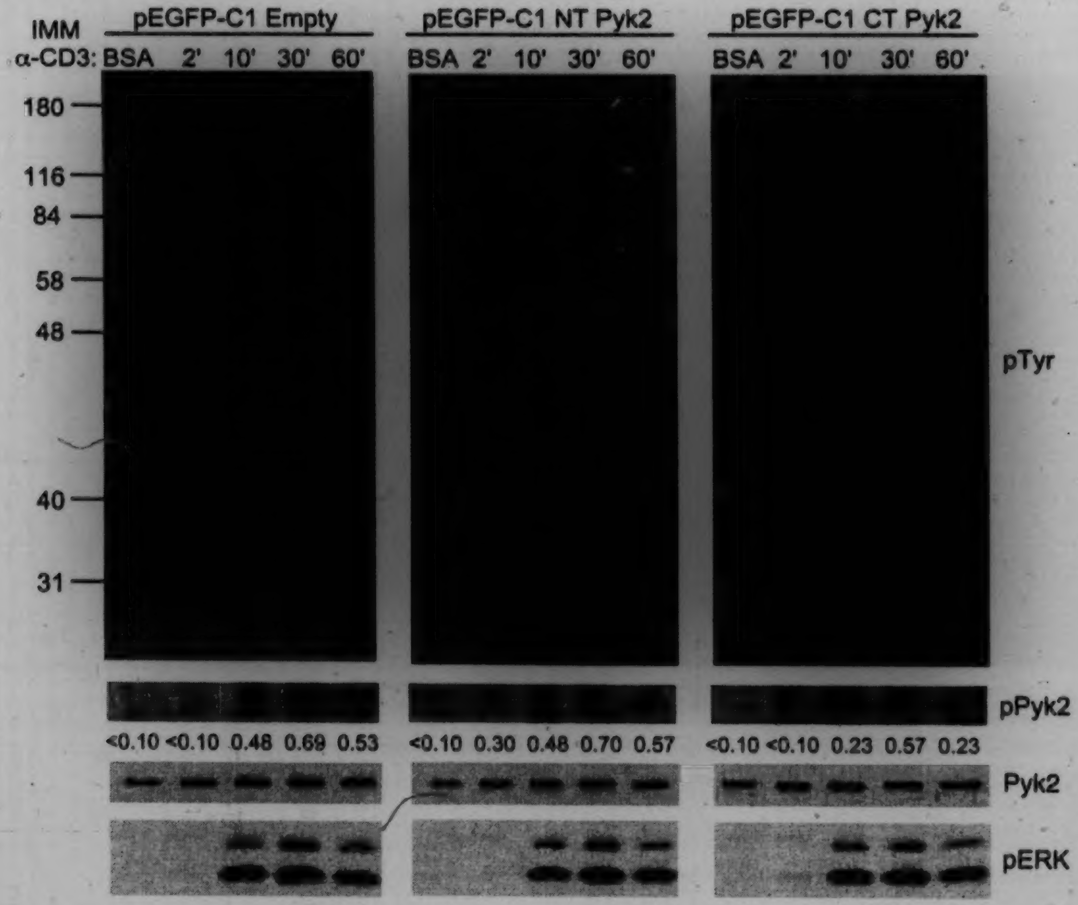
IMM
pEGFP-C1 Empty
pEGFP-C1 NT Pyk2
pEGFP-C1 CT Pyk2
α-CD3: BSA 2' 10' 30' 60'
BSA 2' 10' 30' 60'
BSA 2' 10' 30' 60'
180
116
84
58
48
40
31
pTyr
pPyk2
<0.10 <0.10 0.48 0.69 0.53
<0.10 0.30 0.48 0.70 0.57
<0.10 <0.10 0.23 0.57 0.23
Pyk2
pERK

FIGURE 6-13. The effect of overexpression of the NT Pyk2 and CT Pyk2 fusion proteins on the induction of general tyrosine phosphorylation in response to stimulation with immobilized anti-CD3. Clone 11 nucleofected with either pEGFP-C1, pEGFP-C1 NT Pyk2 or pEGFP-C1 CT Pyk2 were stimulated on immobilized anti-CD3 as in Figure 5-11. Note that the membrane used in this experiment is the same membrane used in Figure 6-4. The membrane was immunoblotted with anti-phosphotyrosine (PY72), anti-phospho-ERK and anti-Pyk2 (F298). The ratio of phosphorylated Pyk2 (PY72) to unphosphorylated Pyk2 (F298) was determined by dividing the pixel intensity of phosphorylated Pyk2 by the pixel intensity for unphosphorylated Pyk2. The ratios are displayed below the phospho-Pyk2 immunoblot.

the N-terminal domain might interfere with endogenous Pyk2 phosphorylation. Figure 6-13 demonstrates that overexpression of CT Pyk2, but not NT Pyk2, caused a decrease in Pyk2 phosphorylation as assessed by calculating the ratio of band intensities of phosphorylated endogenous Pyk2 to total endogenous Pyk2 protein. However, in a second attempt of the experiment no decrease in endogenous Pyk2 phosphorylation was observed. In this experiment NT Pyk2 and CT Pyk2 exhibited a much lower level of overexpression which could account for the difference. Therefore, further repeats with compatible levels of overexpression are necessary to conclusively determine the effects of NT Pyk2 and CT Pyk2 on the phosphorylation of endogenous Pyk2.

Assessing Pyk2 interacting proteins with GST-truncated Pyk2 fusion proteins

In an attempt to determine whether the NT Pyk2 and CT Pyk2 fusion proteins may act as dominant negatives and bind up normal interacting partners of Pyk2, I fused NT Pyk2 and CT Pyk2 C-terminally to GST. Expression of the GST fusion proteins was induced in *E.coli*, the bacteria were lysed, GST was bound to glutathione beads and the beads were used in a pull down assay with either unstimulated or stimulated (immobilized anti-CD3) AB.1 CTL clone post-nuclear lysates. GST is 26 kDa, therefore NT Pyk2 and CT Pyk2 have predicted molecular weights of 72.7 and 58.1 kDa respectively. The Coomassie Blue-stained gel in Figure 6-14a shows the relative migration of the fusion proteins (denoted by the asterisks) and that they are of the predicted molecular weight. It is likely that some of the faster migrating bands in the gel are degradation products of the fusion proteins. I have confirmed this for some of the bands by mass spectrometry. I was able to purify sufficient amounts of GST and GST-

A.

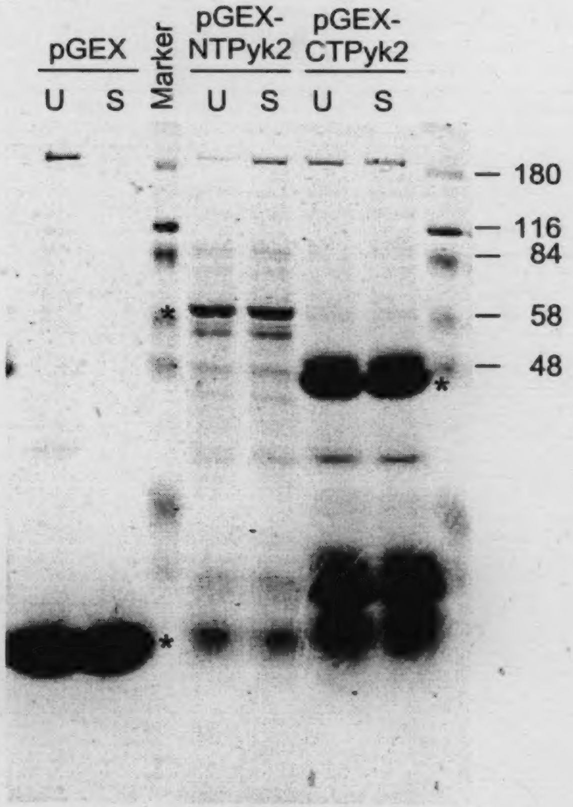

Coomassie Blue

FIGURE 6-14. Expression of the truncated Pyk2 GST fusion proteins. Expression of GST, GST-NT Pyk2 or GST-CT Pyk2 was induced in *E.coli*, the bacteria were lysed, GST was bound to glutathione beads and the beads were used in a pull down assay with either unstimulated (U) or anti-CD3-stimulated (S) AB.1 CTL clone post-nuclear lysates. a) The pulldowns were run on an SDS-PAGE gel and the gel was subsequently stained with Coomassie Blue. The asterisks denote the position of the fusion proteins in the gel. Note that the pre-stained molecular weight markers used are not very accurate. b) The pulldowns were run on an SDS-PAGE gel, the proteins were transferred to a membrane and the membrane was immunoblotted with anti-GST, anti-paxillin and anti-Pyk2. Note that the GST immunoblot for NT Pyk2 is a darker exposure than for GST and CT Pyk2. The arrowheads denote the position of the GST fusion proteins. The anti-Pyk2 antibody used is specific for the N-terminus of Pyk2 and will therefore recognize GST-NT Pyk2 (band present) and endogenous Pyk2 (which would run at approximately 116 kDa). b) Next page.

B.

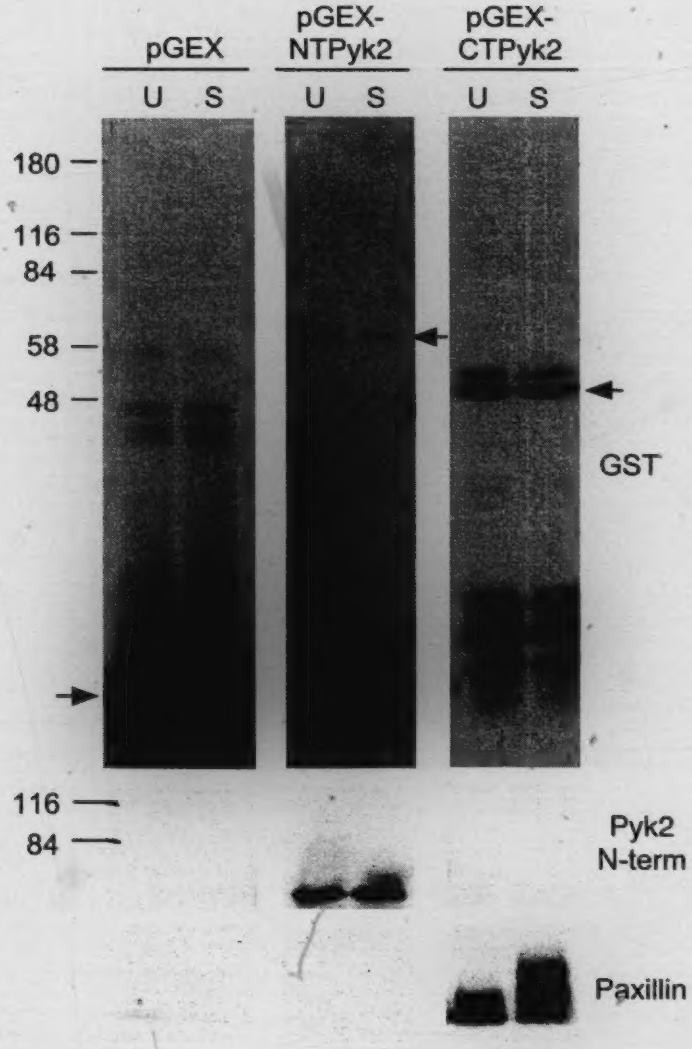
pGEX
pGEX-NTPyk2
pGEX-CTPyk2
U
S
U
S
U
S
180
116
84
58
48
GST
116
84
Pyk2 N-term
Paxillin

CT Pyk2. However, much of the GST-NT Pyk2 fusion protein is not released after bacterial lysis, suggesting that it may be trapped in inclusion bodies. Inclusion bodies are insoluble aggregates of misfolded protein that often form in situations where proteins are overexpressed. I repeated the same experiment, except this time transferred the samples to membranes in order to immunoblot for specific proteins. Unfortunately, this system is only amenable to determining binding partners that are not dependent on phosphotyrosine-SH2 domain interactions as the fusion proteins do not undergo phosphorylation in *E. coli*. I showed in chapter 5 that Pyk2 interacts with paxillin and co-localizes with paxillin at the MTOC in CTL clones. Therefore, I first examined whether CT Pyk2 binds to paxillin, which binds to the FAT domain of Pyk2 (Xiong et al. 1998). Figure 6-14b demonstrates that GST-CT Pyk2 is able to interact with both unphosphorylated and phosphorylated paxillin. Thus it is likely that EGFP-CT Pyk2 binds to paxillin upon transfection into CTL clones.

I was also interested in whether the N-terminus of Pyk2, which contains the FERM domain, could bind to the kinase domain of full length Pyk2 as has been described for FAK (Toutant et al. 2002; Cooper et al. 2003; Dunty et al. 2004). I immunoblotted the membrane in Figure 6-14b for Pyk2, but could not detect any association of full length Pyk2 with GST-NT Pyk2. It is also evident that there is no band running at approximately 116 kDa (full length Pyk2) in the GST-NT Pyk2 pull down lanes on the Coomassie-stained gel in Figure 6-14a. Therefore, my results do not suggest that an interaction occurs between the N-terminus of Pyk2 and full length Pyk2. I did not test for any additional potential interactions because very few proteins are known to interact with the N-terminus of Pyk2, other than those that bind to phosphorylated Y402.

C. Discussion

In this study, I have attempted to elucidate the function of Pyk2 in CTL by the use of Pyk2 siRNA and overexpression of truncated Pyk2 fusion proteins. These studies were only made possible towards the completion of my studies when I acquired the ability to transfect our CTL clones using Amaxa nucleofection technology. For this reason, many of the experiments performed in this chapter are only preliminary and need to be repeated, but may help guide the person who takes over the project. I hypothesized that Pyk2 might play a role in the polarization of CTL upon recognition of a target cell. I tested whether it was involved in MTOC reorientation, secretion of lytic granules towards the contact site and cell spreading on immobilized anti-CD3. I found that CTL clones overexpressing EGFP-NT Pyk2 and -CT Pyk2 fusion proteins had no defect in the ability to translocate the MTOC, when compared to clones expressing EGFP. To test for an effect on secretion of lytic granules, I measured cell surface expression of CD107a (Lamp-1) on transfected CTL clones upon stimulation on immobilized anti-CD3. I found that overexpression of the NT Pyk2 and CT Pyk2 fusion proteins had no adverse effect on degranulation. Instead, the fusion proteins appeared to cause an increase in the percentage of cells expressing surface CD107a. This effect was more consistent in cells expressing the NT Pyk2 fusion protein. When I examined cell spreading on immobilized anti-CD3, a higher percentage of cells expressing these constructs (NT Pyk2 to a lesser extent than CT Pyk2) were observed to spread than clones expressing EGFP. An greater number of cells spreading and degranulating suggests that expression of NT Pyk2 and CT Pyk2 may lower the threshold of activation upon stimulation on immobilized anti-CD3. CTL clones, in which the level of Pyk2 protein had been reduced by 50%, displayed increased adherence to target cells thus pointing to a possible role for Pyk2 in de-adhesion. A potential role for Pyk2 in signal amplification was also alluded to as knockdown of Pyk2 dampened tyrosine phosphorylation of numerous proteins upon stimulation with immobilized anti-CD3.

These results do not correlate well with the findings from the Santoni and Sánchez-Madrid groups that Pyk2 functions to regulate cytotoxicity in NK cells (Gismondi et al. 2000; Sancho et al. 2000). However, there are a number of reasons why there could be such a great discrepancy. First, overexpression of proteins can induce non-specific or non-physiological cell responses and results from such experiments should always be interpreted carefully. The extent of overexpression of the Pyk2 constructs achieved through vaccinia virus infection by the Sánchez-Madrid group (Sancho et al. 2000) was much greater than the level of overexpression that I achieved with nucleofection (Figure 6-4). Thus it is possible that a higher extent of overexpression is necessary to see some effects. Second, vaccinia virus infection causes dramatic alteration of cell morphology as a result of permutations of the actin and microtubule cytoskeletons (Ploubidou et al. 2000; Gouin et al. 2005; Schepis et al. 2006). Effects on the actin cytoskeleton have been recognized for some time now. However, since the publication of the results of the Santoni and Sánchez-Madrid groups, vaccinia virus infection has been shown to cause perturbations of the microtubule cytoskeleton (Ploubidou et al. 2000; Schepis et al. 2006). Schepis and colleagues have recently studied the effects of infection on the microtubule cytoskeleton of adherent cells (Schepis et al. 2006). They found that infection caused the cells to round up concomitantly with a retraction of the microtubules to an area surrounding the nucleus (Schepis et al. 2006).

Microtubule bundling and general disorganization of the microtubules were also observed (Schepis et al. 2006). These effects started to occur as early as 1 hour post-infection and involved viral early gene protein synthesis (Schepis et al. 2006). Vaccinia virus infection also greatly reduces the efficiency of target cell lysis by IL-2-activated human NK cells (Kirwan et al. 2006). The negative effect of vaccinia virus infection on NK cytotoxicity is likely due to the alterations of the actin and microtubule cytoskeletons. These alterations could affect processes such as target cell binding, MTOC reorientation and movement of lytic granules to the contact site. Thus, the use of vaccinia virus infection to overexpress proteins in NK cells may not be an ideal system for studying MTOC reorientation and lysis of target cells. The process of nucleofection also appeared to negatively affect CTL clone activation to a certain extent as the cells were observed to have a less robust induction of tyrosine phosphorylation upon stimulation through the TCR. It is also possible that the nuclear NT Pyk2 fusion protein could exert non-specific effects on transcription. Third, the Pyk2 constructs used by the Santoni and Sánchez-Madrid groups (WT Pyk2 and KD Pyk2) were different from the constructs that I utilized (NT Pyk2 and CT Pyk2). Perhaps full length Pyk2 is needed to have the proper sequestering effect or to properly localize Pyk2 to an area where it could have an effect. It is also possible that the differences observed were due to the fact the NK cell studies were performed in human cells and my CTL studies were performed in mouse cells. Mouse and human Pyk2 display 95% amino acid identity and the major sites of phosphorylation and proline-rich regions are conserved. Therefore, it is likely that this is not a major factor contributing to the observed inconsistency. Fourth, the discrepancy could reflect potential differences in the signalling pathways leading to MTOC reorientation between NK cells and CTL. FAK redundancy may also play a role as it was reported by Santoni's group that human peripheral blood NK cells do not express FAK (Gismondi et al. 1997) and our CTL clones do express FAK (although at lower levels than Pyk2). In order to examine which of these factors may contribute to the inconsistency observed between NK cells and CTL, one could infect human and mouse NK cells and CTL with recombinant vaccinia virus encoding full length Pyk2, kinase-inactive Pyk2, NT Pyk2 and CT Pyk2 and compare MTOC reorientation with human and mouse NK cells and CTL nucleofected with similar Pyk2 constructs.

Another problem in interpreting these results stems from the fact that it is unknown whether the EGFP-truncated Pyk2 fusion proteins act as dominant negatives towards endogenous Pyk2. Many of the studies examining overexpression of the C-terminus of Pyk2 have observed a decrease in the phosphorylation of endogenous Pyk2 (Watson et al. 2001; Han et al. 2003). In one experiment I did observe a reduction in endogenous Pyk2 phosphorylation upon expression of CT Pyk2 (Figure 6-13). However, this was not observed in a second attempt of the experiment. The discrepancy may be due to differences in the level of overexpression of CT Pyk2 compared to endogenous Pyk2 in each experiment. High levels of expression of NT Pyk2 appeared to have no effect on endogenous Pyk2 phosphorylation (Figure 6-13) which suggests that Pyk2 may not engage in an autoinhibitory interaction as has been described for FAK. An autoinhibitory interaction cannot be totally discounted, as much of the NT Pyk2 fusion protein localized to the nucleus (Figure 6-5b, 6-6a, 6-6b) where it would not interact with endogenous cytosolic Pyk2.

One way to determine whether the fusion proteins may act as dominant negatives is to assess whether they interact with known binding partners. This has been difficult to assess as we yield approximately 5 X 10^5 cells per transfection and 5 X 10^6 – 1 X 10^7 cells are generally required to perform immunoprecipitations on the CTL lysates. Furthermore, very few proteins have even been shown to associate with the N-terminus of Pyk2. I attempted to use the GST fusion proteins to identify binding partners. Unfortunately, interactions dependent on SH2 domain binding to phosphorylated tyrosine residues cannot be detected using this technique. I was able to demonstrate that GST-CT Pyk2 binds to paxillin (Figure 6-14b) and that EGFP-CT Pyk2 co-localizes with paxillin (Figure 6-7a). Only when a function for Pyk2 is firmly demonstrated, can the truncated Pyk2 fusion proteins be tested for their ability to disrupt this function.

Just as there are caveats to the overexpression studies, there are difficulties with interpreting results from the siRNA knockdown experiments. First, on average, only 50% knockdown of Pyk2 was achieved. This questions whether an effect would likely be seen with only half as much protein present in the cells. Second, these CTL clones express FAK, although not nearly as much as adherent cells typically express. As FAK and Pyk2 are closely related and bind to many of the same proteins, there is an issue of whether FAK can compensate for the loss of Pyk2. Third, Pyk2 knockdown was assessed on a population basis. Therefore, it is unknown whether 50% of Pyk2 protein was knocked down in all cells or if 50 % of the cells displayed total knock down of protein. This caveat relates to the lack of a marker for transfection and may further complicate the interpretation of results. In the future, these experiments could be improved by using different Pyk2 siRNA oligomers that result in greater than 50%

knockdown. The use of labelled siRNA would aid in identifying cells that have been successfully transfected. There are currently new and improved fluorescent labels that are more photostable, brighter, longer lasting than fluorescein. Also, concurrent knockdown of FAK and Pyk2 could eliminate the possibility of redundancy. A "scrambled" siRNA control should be included in future assays to ensure that any observed effects are not due to siRNA delivery. A better system to evalute the function of Pyk2 in CTL would be to generate Pyk2$^{-/-}$ CTL clones from Pyk2$^{-/-}$ mice. Our lab has attempted to obtain these mice on numerous occasions, but to no avail.

I chose to use the NT Pyk2 construct because a function for the N-terminal domain of Pyk2 has not yet been elucidated. As mentioned above, the N-terminus contains a divergent FERM domain. FERM domains have been implicated in both protein-protein interactions and protein-membrane interactions. For instance, the divergent FERM domains of FAK and JAK are involved in intramolecular interactions (Zhou et al. 2001; Toutant et al. 2002; Cooper et al. 2003; Dunty et al. 2004). Proteins containing FERM domains are also involved in linking membrane proteins with the actin cytoskeleton where the FERM domain is involved in binding directly to the cytoplasmic tail of membrane proteins. It is possible that the FERM domain of Pyk2 may be involved in recruiting Pyk2 to the membrane after T cell activation. If so, one might expect it to be enriched at the membrane. I did not see any evidence for accumulation of Pyk2 at the interface between a CTL and its target. Instead, a diffuse cytosolic localization and accumulation in the nucleus, similar to endogenous Pyk2, was observed (Figure 6-5b, 6-6a, 6-6b). Although it is possible that only a few binding sites exist at the membrane and NT Pyk2 may not be expressed to high enough levels to displace endogenous Pyk2, these results show no evidence that the FERM domain is involved in binding to transmembrane proteins. They do support, as suggested by other studies (Dunty and Schaller 2002), that the N-terminus may be responsible for the cytosolic localization of Pyk2.

The N-terminal divergent FERM domain of FAK has been implicated in binding to the FAK kinase domain and thereby conferring an autoinhibitory conformation (Toutant et al. 2002; Cooper et al. 2003; Dunty et al. 2004). I therefore sought to test whether the equivalent domain in Pyk2 may also be involved in such an intramolecular interaction. If so, overexpression of the NTPyk2 fusion protein would be predicted to decrease endogenous Pyk2 phosphorylation upon TCR stimulation by binding in trans to the kinase domain of endogenous Pyk2. To test this theory, I nucleofected clone 11 with NTPyk2 and then stimulated the cells on immobilized anti-CD3. I saw no detrimental effect on the ability of endogenous Pyk2 to become phosphorylated upon expression of EGFP-NT Pyk2 (Figure 6-13). However, as mentioned above, it is possible that I may not have seen an effect because much of the fusion protein was in the nucleus. I was also unable to detect an interaction between full length Pyk2 and GST-NT Pyk2 in the GST pull down assays. This result is in agreement with Dunty and colleagues who found that the N-terminus of Pyk2, fused to GST, does not bind to full length Pyk2 (Dunty et al. 2004). However, it is possible that I could not detect an interaction between NT Pyk2 and full length Pyk2 because the NT Pyk2 GST fusion protein was limiting. Alternatively, the NT Pyk2 fusion protein may not be properly folded. Therefore, although the results generated from this study show no evidence of an inhibitory intramolecular interaction for Pyk2, due to the aforementioned caveats, I cannot conclusively state that this interaction does not occur in CTL clones.

The CT Pyk2 construct (aa 678-1009) was chosen for the overexpression studies because it is closely related to the PRNK isoform (aa 780-1009) described at least at the mRNA level (Xiong et al. 1998). Other groups have transfected cells with plasmids containing the entire C-terminus of Pyk2 (Li et al. 1999) or transduced cells with fusion proteins comprised of the entire C-terminus (Watson et al. 2001; Han et al. 2003). These constructs could act as a dominant negative towards endogenous Pyk2 by inhibiting endogenous Pyk2 phosphorylation. Transduction of the C-terminus Pyk2 fusion proteins could also inhibit macrophage spreading in response to 5% serum (Watson et al. 2001) and neutrophils spreading in response to TNF-α (Han et al. 2003). I observed no defect in the ability of CT Pyk2-transfected CTL clones to spread in response to TCR stimulation. A lack of an effect could reflect the fact that I used the C-terminus of Pyk2-H, which is missing half of the first proline-rich region, whereas a full length Pyk2 C-terminus was likely used in the other studies. In this regard, it is possible that lack of recruitment of a protein that interacts with the first proline-rich region is responsible for the difference. Another factor may be that the stimulus for cell spreading is different (integrin and cytokine versus TCR stimulation).

I also examined the effect of overexpression of CT Pyk2 on MTOC reorientation. It was previously shown in NK cells that Pyk2 and paxillin co-localize at the MTOC (Sancho et al. 2000). It was also shown that overexpression of WT Pyk2 and KD Pyk2 inhibited MTOC reorientation in this system, however the mechanisms were not elucidated (Sancho et al. 2000). I demonstrated in chapter 5 that Pyk2 and paxillin also co-localize at the MTOC in CTL clones (Figure 5-6c). Pyk2 interacts with paxillin through the FAT domain located in its C-terminus. Therefore, expression of CT Pyk2 might have an effect on MTOC translocation in CTL, either by displacing endogenous Pyk2 at the MTOC or by interfering with the signalling pathways leading to MTOC reorientation. EGFP-CT Pyk2 co-localized with paxillin at the MTOC as predicted. Interestingly, CT Pyk2 also co-localized with paxillin throughout much of the cytoplasm (Figure 6-7a). However, expression of CT Pyk2 did not appear to have an adverse effect on MTOC reorientation (Table 6-1). It is unknown whether Pyk2 located at the MTOC is involved in movement of the MTOC, or whether Pyk2 plays a role in the upstream signalling events that result in MTOC repositioning. If the pool of Pyk2 at the MTOC is important, it is possible that since I detected a large amount of co-localization of CT Pyk2 and paxillin in the cytoplasm, there is not enough CT Pyk2 at the MTOC to have a sequestering effect. I was also unable to determine whether expression of CT Pyk2 interfered with localization of endogenous Pyk2 at the MTOC as the antibody used to detect Pyk2 at the MTOC also recognizes the CT Pyk2 construct. Transfection with full length Pyk2 and CT Pyk2 attached to different epitope tags could address this question. If Pyk2 is involved in the signalling events that lead to MTOC translocation, it is possible that there are redundant pathways that could compensate and allow for MTOC movement. It is also possible that only the scaffolding abilities of endogenous Pyk2, and not the kinase activity, may be inhibited by CT Pyk2. Pyk2 kinase activity may be the most important factor for MTOC reorientation.

As no adverse effect on MTOC reorientation was observed upon overexpression of either NT Pyk2 or CT Pyk2, I decided to test whether the fusion proteins would have an effect on degranulation (as measured by surface expression of CD107a). Unexpectedly, I observed a trend towards an increased percentage of cells expressing surface CD107a upon degranulation in response to immobilized anti-CD3 stimulation in clones expressing either NT Pyk2 or CT Pyk2 (Figure 6-8, Table 6-2). An increase in the percentage of cells spreading on immobilized anti-CD3 was also detected for clones expressing NT Pyk2 and CT Pyk2 (Table 6-4). The greater number of cells spreading and degranulating could indicate that the signalling threshold has been lowered.

How could expression of the NT Pyk2 or CT Pyk2 fusion proteins lead to a decreased threshold of activation upon stimulation with immobilized anti-CD3? The NT Pyk2 fusion protein retains the autophosphorylation site (Y402, the docking site for SFK) and the proposed SFK SH3 binding site (based on sequence similarity to FAK), located adjacent to and just upstream of Y402. Thus it is possible that NT Pyk2 could form high affinity interactions with SFK SH2 and SH3 domains and consequently disrupt the repressive intramolecular interaction of SFK. These interactions would activate SFK, thus lowering the threshold of activation.

The CT Pyk2 construct retains the Y881 phosphorylation site, however, it lacks the autophosphorylation/SFK docking site. Therefore, Y881 would likely not become phosphorylated upon stimulation as SFK are known to phosphorylate this site (Park et al. 2004). As I demonstrated in chapter 5 that Pyk2 less phosphorylated at Y881 binds preferentially to paxillin (Figure 5-4), it is likely that this construct remains in a conformation that favors binding of paxillin, or other LD domain-containing proteins, and not Grb2. Indeed I demonstrated that this truncated Pyk2 construct fused to GST could bind to paxillin (Figure 6-14b) and that EGFP-CT Pyk2 co-localized with paxillin to a greater extent than endogenous Pyk2 (ie. in the cytosol and at the MTOC as opposed to only at the MTOC) (Figure 6-7a). Therefore, CT Pyk2 may accumulate in sites where paxillin becomes enriched after stimulation with immobilized anti-CD3. Paxillin has been shown to interact with α- and γ-tubulin and actin-binding proteins (Turner 2000). Therefore, paxillin may facilitate cross-talk between the microtubule and actin cytoskeletons. The actin and microtubule cytoskeletons have both been implicated in T cell spreading on immobilized anti-CD3. The actin cytoskeleton is responsible for initiating cell spreading whereas the microtubule cytoskeleton stabilizes the contact with the antibody and may even play a role in the intitial expansion of contacts (via MTOC reorientation) (Bunnell et al. 2001). Expression of CT Pyk2 may displace and inhibit endogenous Pyk2 activation and therefore block SFK/Pyk2-mediated tyrosine phosphorylation of paxillin. Phosphorylation of paxillin may be involved in recruiting molecules that facilitate turnover of complexes formed during spreading such as the phosphatase PTP-PEST and the tyrosine kinase Csk, which phosphorylates the negative regulatory site on SFK (as reviewed in (Turner 2000). Spreading may occur rapidly in cells transfected with CT Pyk2 if negative regulators are not recruited, which may act to decrease the threshold of activation. CT Pyk2 may also inefficiently recruit Rho family GAP proteins which could lead to increased actin polymerization. The disruption of the association of Pyk2 and paxillin could also be involved in the turnover of complexes. Thus, if CT Pyk2 (which likely does not become phosphorylated on Y881) displaces endogenous Pyk2 association with paxillin, then this could also lead to a reduced activation threshold. This model would predict that the contact formed between the CT Pyk2-transfected cells and immobilized antibody would remain stable for a longer period of time than in control cells, a theory which could be tested in the future. Also, analyzing cell spreading on a less than maximal concentration of anti-CD3 might reveal more evidence for a reduced threshold for activation.

Increased adherence to target cells was implied from the results obtained with CTL clones treated with Pyk2 siRNA. Based on the flow cytometry profiles of side scatter versus forward scatter, conjugates that formed between CTL nucleofected with Pyk2 siRNA and target cells appeared to be more resistant to disruption by EDTA (Figure 6-10). This result could be indicative of tighter adhesion between the two cell types or even between CTL clones and suggests that Pyk2 may be involved in de-adhesion of CTL from their targets. In this scenario, reduced Pyk2 expression may cause inefficient recruitment of proteins such as phosphatases that may be involved in the release of CTL from their targets. Little is known about the mechanisms involved in this process. It is also possible that siRNA that had not entered the cells could mediate binding between cells. Positively-charged siRNA oligos may bind to negatively-charged cells. Therefore, a "scrambled" siRNA control should be included repeat experiments.

A potential role for Pyk2 in signal amplification was also suggested from the results with Pyk2 siRNA. Immobilized anti-CD3 stimulation of CTL clones nucleofected with Pyk2 siRNA displayed reduced tyrosine phosphorylation of a number of proteins in the whole cell lysate at the 10 minute time point (Figure 6-12). No effect on general tyrosine phosphorylation of lysate proteins was observed in clones transfected with NT Pyk2 and CT Pyk2 (Figure 6-13). The 10 minute time point appeared to display the greatest induction of tyrosine phosphorylation in nucleofected samples. Perhaps these experiments should be repeated using more time points in the 1-20 minute range to more accurately determine the effects on general tyrosine phosphorylation. Optimization of the transfection procedure to ensure a high level of overexpression is also necessary. Further, monitoring the effect on phosphorylation of known Pyk2 substrates (such as paxillin) would complement these results.

In this study, I did not gather any concrete evidence to corroborate a role for Pyk2 in properly polarizing CTL towards immobilized anti-CD3 or target cells. I did not detect any defects in MTOC reorientation or in the ability to degranulate. However, these results do not preclude a role for Pyk2 in other cell polarization events that were not tested, such as cell migration. I did detect an increase in the number of cells spreading on immobilized anti-CD3 upon expression of CT Pyk2 (and to a lesser extent with NT Pyk2). I also observed increased adherence in the target cell binding assays upon knockdown of Pyk2. These results are suggestive of a role for Pyk2 in de-adhesion or turnover of adhesive complexes. Pyk2-deficient macrophages exhibited a failure to properly polarize towards a chemokine gradient (Okigaki et al. 2003). Enhanced adherence was implied as there was an increase in the number of cells spreading and a failure to detach the lagging edge from the substratum (Okigaki et al. 2003). It was also observed that FAK-deficient fibroblasts have a greater number of focal adhesions (Ilic et al. 1995) which points to a role for FAK in focal adhesion disassembly or turnover. Thus, it would be interesting to test whether Pyk2 was involved in de-adhesion of CTL from their targets or from immobilized antibody. The results from this study also suggest that Pyk2 may play a role in signal amplification. Therefore, it is possible that Pyk2 may be involved in multiple processes in the cell and which function it is performing may depend upon the localization of the protein and which stimuli the cell receives.

CHAPTER 7: General Discussion

A. Summary of results

Pyk2 is a tyrosine kinase that becomes activated in T cells in response to numerous extracellular stimuli. The goal of the present study was to examine the role and regulation of Pyk2 in CTL in the context of CTL activation and function. It was previously demonstrated in T cells (Sancho et al. 2002) and NK cells (Sancho et al. 2000) that Pyk2 translocated to the contact site between a T cell or NK cell and a target cell. I sought to extend these findings and determine whether Pyk2 was recruited to the interface via an association with the TCR/CD3 complex. A common technique used to test for an association between proteins is immunoprecipitation. However, the use of standard immunoprecipitation to assess recruitment of proteins to the TCR/CD3 complex is technically limiting. This method isolates complexes that have been engaged as well as those that have not and consequently a positive signal could be diluted out. To circumvent this problem, I developed a biochemical assay which enriches for engaged TCR/CD3 complexes. In this assay, immobilized anti-CD3 stimulates the cells and is then used to capture protein complexes associated with the immobilized antibody after lysis of the cells. Using this assay, I found that Pyk2 was recruited to the TCR/CD3 complex upon immobilized anti-CD3 stimulation and that recruitment was not dependent upon SFK activity.

I also found that CD3ζ could become inducibly phosphorylated in the presence of the SFK inhibitor PP2. Further examination revealed that CD3ζ was not maximally phosphorylated, but was still capable of recruiting ZAP-70. Inhibition of SFK activity did not allow for inducible phosphorylation of the CD3ε ITAM or for phosphorylation of

ZAP-70. These results imply that there are differential requirements for phosphorylation of CD3ζ and CD3ε/ZAP-70 which were previously unrecognized. It is possible that another PP2-resistant SFK or tyrosine kinase is capable of phosphorylating CD3ζ. Alternatively, the type of SFK and/or level of SFK activity required for CD3ζ phosphorylation may differ from that of CD3ε.

Pyk2 was originally identified as a kinase whose activation was dependent upon Ca^{2+} (Lev et al. 1995; Yu et al. 1996). It has since been demonstrated in many different cell types that Pyk2 is activated by an increase in $[Ca^{2+}]_i$. However, the responsiveness of Pyk2 to a rise in $[Ca^{2+}]_i$ in T cells is somewhat controversial. I performed a thorough investigation of the role of Ca^{2+} in the regulation of Pyk2 phosphorylation in CTL. I found that Pyk2 was inducibly phosphorylated in response to the Ca^{2+} mobilizers ionomycin and thapsigargin. Chelation of extracellular Ca^{2+} with EGTA during treatment with Ca^{2+} mobilizers did not totally abrogate inducible Pyk2 phosphorylation, suggesting that release of Ca^{2+} from intracellular stores was sufficient to induce low levels of Pyk2 phosphorylation. Chelating intracellular Ca^{2+} with BAPTA during cross-linked anti-CD3 stimulation, but not immobilized anti-CD3 stimulation, decreased the level of Pyk2 phosphorylation. Although I was unable to determine the mechanism by which Pyk2 becomes phosphorylated in response to an increase in $[Ca^{2+}]_i$, I found that SFK may be important (Figure 7-1). I conclude that Pyk2 can be regulated by an increase in $[Ca^{2+}]_i$ in CTL. My results shed light upon why discrepancies exist in the literature with respect to whether Pyk2 is regulated by Ca^{2+} in T cells. Factors including the concentration of Ca^{2+} mobilizer, the method of TCR stimulation used with Ca^{2+} chelators and the cell type used in the assay may all affect the outcome of the experiment.

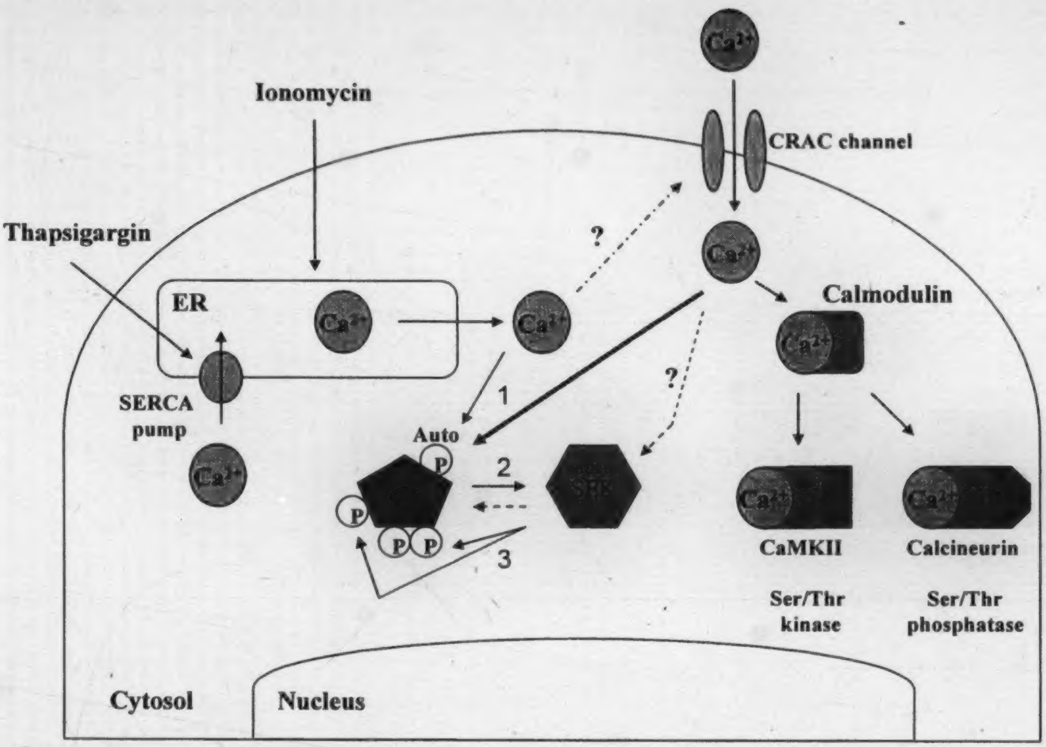
Ionomycin
Ca2+
CRAC channel
Thapsigargin
?
Ca2+
ER
Ca2+
Ca2+
Calmodulin
Ca2+
SERCA
pump
1
?
Auto
Ca2+
P
2
SFK
Ca2+
Ca2+
P
P
P
3
CaMKII
Calcineurin
Ser/Thr
kinase
Ser/Thr
phosphatase
Cytosol
Nucleus

FIGURE 7-1. Model for the induction of Pyk2 phosphorylation upon stimulation of CTL clones with ionomycin or thapsigargin. Ionomycin (a Ca^{2+} ionophore) transports Ca^{2+} across the ER membrane and into the cytosol, which in turn activates store-operated CRAC channels and causes an influx of Ca^{2+} from the extracellular space. Thapsigargin causes emptying of Ca^{2+} from the ER by inhibiting SERCA pumps (responsible for pumping Ca^{2+} back into the ER) and thereby creating an increase in the concentration of free Ca^{2+} in the cytosol and subsequent influx of Ca^{2+} from the extracellular space. An increase in $[Ca^{2+}]_i$ due to release from the intracellular stores is sufficient to induce low levels of Pyk2 phosphorylation. However, there is heightened Pyk2 phosphorylation upon an influx of Ca^{2+}. Calcinuerin and CaMKII appear to not be involved in the induction of Pyk2 phosphorylation upon stimulation with ionomycin. A role for Src family kinases (SFK) in the induction of Pyk2 phosphorylation upon treatment of cells with ionomycin is implicated. This may occur through the following sequence of events: 1) induction of phosphorylation of the Pyk2 autophosphorylation site (Y402) by an increase in $[Ca^{2+}]_i$, 2) activation of SFK by an interaction of the SFK SH2 and SH3 domains with pY402 and the adjacent proline-rich region of Pyk2, 3) phosphorylation of other tyrosine residues within Pyk2 by SFK. Alternatively, Ca^{2+} may activate SFK which, in turn, phosphorylate and activate Pyk2. Ca^{2+} also contributes to the induction of Pyk2 phosphorylation during cross-linked TCR stimulation (not depicted in the diagram).

To date, no structural information exists with respect to Pyk2. Therefore it is not known whether Pyk2 phosphorylation and activation are regulated by protein folding. In contrast, much has been learned of the structure of FAK. We may thus draw parallels between the two related kinases. Both proteins bind to paxillin through the C-terminal FAT domain (Hildebrand et al. 1995; Xiong et al. 1998). Conformational changes occur within the FAK FAT domain which dictate whether the protein can interact with paxillin and also dictate the efficiency of Y925 phosphorylation (Arold et al. 2002; Liu et al. 2002; Dixon et al. 2004; Prutzman et al. 2004). In the present study, I provide biochemical evidence suggesting a similar conformational change within Pyk2. I identified two populations of Pyk2 within CTL based on their differential ability to associate with paxillin. Pyk2 associated with paxillin, has little phosphorylation at Y881 and within the proline-rich region. Interestingly, a portion of this population co-localizes with paxillin at the MTOC. Pyk2 not associated with paxillin is more heavily phosphorylated at Y881 and within the proline-rich region and does not co-localize with paxillin or the MTOC. These results suggest that Pyk2, like FAK, displays a compact FAT domain when bound to paxillin and an unfolded FAT domain when not bound to paxillin. The unfolded conformation favours phosphorylation of Y881 and potentially phosphorylation within the proline-rich region (Figure 7-2).

Little is known about the function of Pyk2 in T cells. However, studies conducted using other hematopoietic cells may give an indication as to its function in T cells. Experiments performed in Pyk2-deficient macrophages and overexpression studies carried out in NK cells suggest a possible role for Pyk2 in cell polarization events such as cell spreading, migration and recognition of a target cell. I sought to test for a role for

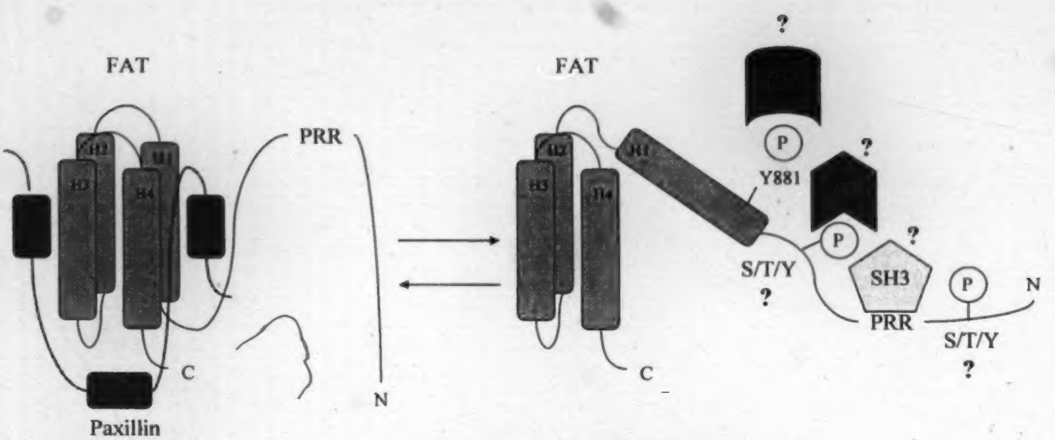

Closed conformation;
bound to paxillin

Open conformation;
disruption of paxillin binding,
favours phosphorylation of Y881
and proline-rich region (PRR)

FIGURE 7-2. Model for a conformational change within the FAT domain of Pyk2. Note that the structure of the FAT domain of Pyk2 has not been elucidated and the structure and conformational change depicted in this figure are based on the structure of the FAK FAT domain. The structures of the proline-rich regions (PRR) of FAK and Pyk2 are unknown. In this model, the closed conformation of the FAT domain of Pyk2 (tight helical bundle) binds to two LD motifs of paxillin (as has been shown for FAK). In the open conformation, helix 1 separates from the bundle and paxillin binding is disrupted at the interaction site between helix 1 and 4. This may allow for phosphorylation of Y881 (by SFK) and recruitment of SH2 domain-containing proteins. Potential causes for the conformational change are denoted by the question marks. These may include: 1) phosphorylation of serine/threonine/tyrosine residues (not yet identified) within the proline-rich region and subsequent binding of proteins to these phosphorylated sites, 2) binding of SH3 domain-containing proteins to the proline-rich regions or 3) phosphorylation of the Y881 site. H1-4 = alpha helicies 1-4 of the FAT domain, LD = Leucine-rich motif of paxillin, S/T/Y = Serine/threonine/tyrosine residues, P = phosphorylation, SH2 = SH2 domain-containing protein, SH3 = SH3 domain-containing protein.

Pyk2 in polarizing the lytic machinery of a CTL towards a target cell. I examined the effects of overexpression of the N- or C-terminal domain of Pyk2 and knockdown of Pyk2 protein on MTOC reorientation, degranulation, cell spreading and signal amplification. Expression of the N- or C-terminal domain of Pyk2 in CTL did not affect MTOC reorientation towards target cells or the ability of CTL to degranulate in response to immobilized anti-CD3 stimulation. Interestingly, I observed a trend towards increased sensitivity to stimulation with immobilized anti-CD3. An increase in the percentage of cells degranulating in response to and spreading on immobilized antibody was observed in CTL expressing the N- or C-terminus of Pyk2. Knockdown of Pyk2 protein by approximately 50% in CTL further revealed potential roles for Pyk2 in de-adhesion from target cells and in signal amplification upon stimulation on immobilized anti-CD3. Therefore, I hypothesize that Pyk2 may play multiple roles during CTL activation, depending on the localization of the protein within the cell and which stimuli the cell receives.

B. Points of special interest

Common themes in the induction of Pyk2 phosphorylation

Pyk2 becomes activated in response to numerous extracellular stimuli in T cells such as antigen receptor ligation (Berg and Ostergaard 1997; Ganju et al. 1997; Qian et al. 1997), integrin stimulation (Ma et al. 1997; van Seventer et al. 1998; Rodriguez-Fernandez et al. 1999) and chemokine binding (Davis et al. 1997; Dikic and Schlessinger 1998; Ganju et al. 2000). Thus it is possible that there are common factors involved in the induction of Pyk2 phosphorylation upon stimulation through these receptors. TCR ligation induces an increase in the concentration of intracellular free Ca^{2+} (as reviewed in (Lewis 2001). Chemokine binding to G protein-coupled chemokine receptors also causes a transient rise in $[Ca^{2+}]_i$ via activation of phospholipase C (Thelen 2001). Ligation of β1 (Weismann et al. 1997) and β2 integrins (Kanner et al. 1993) by ECM components induces an increase in $[Ca^{2+}]_i$ in T cells that is mediated by phosphorylation and activation of phospholipase C (Kanner et al. 1993; Schottelndreier et al. 2001). I have demonstrated, in CTL and ConA blasts, that Pyk2 can become phosphorylated in response to stimulation with Ca^{2+} mobilizers alone. Thus, it is possible that an increase in $[Ca^{2+}]_i$ is a common regulator of Pyk2 phosphorylation upon stimulation of the TCR, integrins and chemokine receptors. However, as mentioned before, the mechanism by which Pyk2 phosphorylation is induced by Ca^{2+} is unknown. My results suggest that Pyk2 phosphorylation induced by Ca^{2+} mobilizers is partially dependent on the activation of SFK. Interestingly, SFK have been implicated downstream of stimulation through the TCR (Palacios and Weiss 2004), integrins (Lowell 2004) and G protein-coupled receptors (Ma et al. 2000). The regulation of Pyk2 phosphorylation and activation by SFK is well documented (Park et al. 2004). Therefore, SFK activation may be another common factor in the induction of Pyk2 phosphorylation.

Pyk2 as a signal amplifier?

Pyk2 becomes phosphorylated in response to stimulation of numerous cell surface receptors, in addition to TCR ligation. This suggests that Pyk2 could play a role in signal amplification upon T cell activation. Stimulation through chemokine receptors (Davis et al. 1997; Dikic and Schlessinger 1998; Ganju et al. 2000), cytokine receptors such as the IL-2R (Miyazaki et al. 1998), integrins (Ma et al. 1997; van Seventer et al. 1998; Rodriguez-Fernandez et al. 1999) and other adhesion molecules such as CD2 (Fukai et al. 2000) and CD44 (Li et al. 2001) all induce Pyk2 phosphorylation and could all act to lower the threshold for TCR stimulation. Pyk2 could be involved in signal amplification by enhancing SFK-mediated responses. In this scenario, Pyk2 would interact with a SFK and together, the two kinases would phosphorylate proteins that are recruited to this complex.

The preliminary results that I generated with Pyk2 siRNA suggest that general tyrosine phosphorylation was dampened upon stimulation with immobilized anti-CD3. As SFK are thought to initiate the TCR ligation-induced phosphorylation cascade, this result supports a role for Pyk2 in amplifying SFK-mediated responses. Such a role for Pyk2 may also be supported by the studies involving the NT Pyk2 fusion protein. In these experiments, expression of NT Pyk2 increased the percentage of CTL degranulating in response to immobilized anti-CD3. This result suggests that the threshold for activation had been reduced. This fusion protein retains the SFK SH2 and SH3 binding domains. Therefore, overexpression of NT Pyk2 could result in increased SFK activation. In this scenario, Pyk2 plays a role in the activation of SFK but not in phosphorylation of SFK substrates.

The theory that Pyk2 is involved in signal amplification could also explain why there was no observed T cell defect in Pyk2$^{-/-}$ mice (Okigaki et al. 2003). Pyk2 may not be necessary for any specific signalling pathway involved in the development or homing of T cells to lymphoid organs (Okigaki et al. 2003). However, it does not support the result obtained by Katagiri and colleagues, who found that IL-2 production was significantly inhibited in maximally stimulated Jurkat T cells expressing a Y402F autophosphorylation mutant (Katagiri et al. 2000). In this case, the Pyk2 mutant would not be able to bind to SFK and would not become catalytically active, but SFK would still be active. Therefore, this mutant would not be expected to inhibit IL-2 signalling under optimal stimulation conditions if Pyk2 was functioning to amplify SFK signalling. It is possible that Pyk2 may amplify signals, but this may not be its sole function during TCR stimulation.

Recruitment of Pyk2 to the TCR/CD3 complex

I have found that Pyk2 is recruited to the TCR/CD3 complex upon stimulation with immobilized anti-CD3 (chapter 3). However, the mechanism by which Pyk2 is recruited is still unknown. My results suggest that SFK activity is not necessary for recruitment to the TCR/CD3 complex. SFK activity is not required for phosphorylation of the autophosphorylation site within Pyk2, which is also the binding site for SFK. Therefore, SFK could still participate in the initial recruitment of autophosphorylated protein. Alternatively, interactions via the proline-rich regions or the FAT domain could be involved. For instance, I have found that Nck is present in Pyk2 immunoprecipitations (Appendix Figure 5). It has been shown that Nck binds a proline-rich region within the CD3ε cytoplasmic tail which is exposed when a conformational change is induced in the TCR/CD3 complex by stimulation of the TCR (Gil et al. 2002). Pyk2 may be recruited to this complex through an interaction of its proline-rich region with an SH3 domain in Nck. Other proteins that have been reported to interact with Pyk2 that may be relevant to its recruitment to the TCR/CD3 complex are Fyn (Qian et al. 1997) and ZAP-70 (Katagiri et al. 2000).

Sancho and colleagues have examined the requirements for Pyk2 translocation to the T cell/APC interface. They demonstrated that a functional ITAM and Lck activity (presumably to phosphorylate the ITAMs) were necessary for Pyk2 translocation (Sancho et al. 2002). In this study, Pyk2 formed a cluster in the cytoplasm that translocated to the interface. This observation resembles what I observed for MTOC-associated Pyk2 movement. Whether the cluster of Pyk2 immunostaining co-localized with the MTOC was not addressed in the Sancho study. If the cluster represents MTOC-associated Pyk2 and Pyk2 moves with the MTOC, then it is possible that the authors may have examined coincidentally the requirements for MTOC reorientation.

A role for Pyk2 in MTOC polarization?

In NK cells, Pyk2 has been suggested to play a role in the relocation of the MTOC towards a target cell (Sancho et al. 2000). Sancho and colleagues found that MTOC reorientation and cytolytic activity was inhibited in NK cells infected with recombinant vaccinia virus encoding either wild type Pyk2 or kinase-inactive Pyk2 (Sancho et al. 2000). These results suggest that Pyk2 plays a role as a scaffolding protein and that its kinase activity may not be involved in this process. However, a second group found that only a kinase-inactive Pyk2 could reduce NK cell killing (Gismondi et al. 2000). In this study, MTOC reorientation was not examined. Therefore, it is not clear from these studies how Pyk2 acts during MTOC repositioning. I did not find any defects with respect to MTOC reorientation with the truncated Pyk2 fusion proteins in CTL. However, such findings do not necessarily discount a role for Pyk2 in MTOC translocation. The choice of construct, levels of overexpression or FAK redundancy could all account for the lack of observed defects. It is also possible that, if Pyk2 is indeed involved in MTOC reorientation in CTL, redundant pathways may compensate for the loss of Pyk2 function.

What is a possible mechanism by which Pyk2 could affect MTOC translocation? Numerous TCR-proximal signalling molecules are required for MTOC polarization. The Weiss group has demonstrated the importance of these proteins by the use of Jurkat T cell mutants deficient in different signalling molecules (Lowin-Kropf et al. 1998; Kuhne et al. 2003). This group has found that functional ITAMs, Lck, ZAP-70, LAT and SLP-76 are all involved in MTOC reorientation (Lowin-Kropf et al. 1998; Kuhne et al. 2003). The importance of the SFK Fyn in MTOC translocation has recently been demonstrated (Martin-Cofreces et al. 2006). Interestingly, Pyk2 has been reported to be a preferred substrate of Fyn (Qian et al. 1997). Therefore, these two kinases may act in concert to facilitate MTOC repositioning (Figure 7-3). The small GTPase CDC42 is another protein that has been shown to be involved in MTOC relocation and other cell polarization events

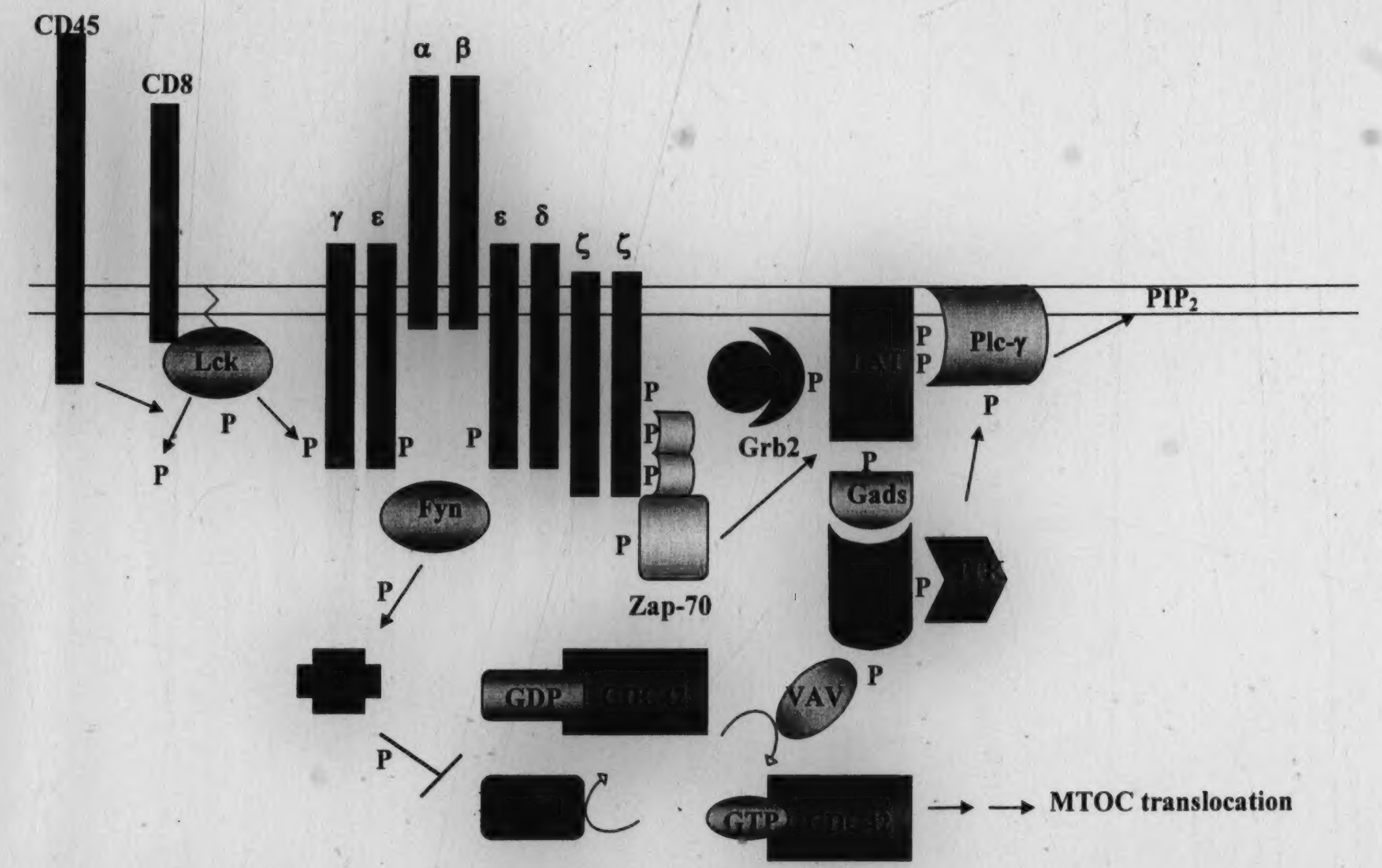
CD45
CD8
Lck
P
P
P
γ
ε
α
β
ε
δ
ζ
ζ
P
P
P
P
P
P
Fyn
P
Zap-70
Grb2
P
LAT
P
P
Gads
P
Plc-γ
P
PIP$_2$
P
VAV
P
GDP
GTP
P
MTOC translocation

FIGURE 7-3. Model for the potential involvement of Pyk2 in MTOC reorientation upon TCR stimulation. Note that redundant pathways involved in MTOC translocation may exist.

(Stowers et al. 1995). Pyk2 has been shown to interact with and phosphorylate the CDC42 GAP protein PSGAP thereby inhibiting its ability to stimulate the intrinsic GTPase activity of CDC42 (Ren et al. 2001). Inhibition of PSGAP would favor accumulation of the GTP-bound form of CDC42, a reaction that is catalyzed by VAV. A role for VAV in MTOC relocation has also been shown as VAV-deficient mice have defects in MTOC reorientation (Ardouin et al. 2003).

Not only has Pyk2 been implicated in the movement of the MTOC, but it has also been found to co-localize with the MTOC in T cells and NK cells (Rodriguez-Fernandez et al. 1999; Sancho et al. 2000; Rodriguez-Fernandez et al. 2002). Paxillin also co-localizes with this structure and was found to bind directly to α and γ tubulin (Herreros et al. 2000). It is possible that the Pyk2/paxillin interaction is important for targeting Pyk2 to the MTOC. I have found that the EGFP-CT Pyk2 fusion protein localized to this site in CTL, whereas the EGFP-NT Pyk2 protein did not. Based on its ability to target to the MTOC, Pyk2 may perform some function at this structure. MTOC and Golgi translocation is thought to be involved in polarizing the secretory machinery towards the T cell/target cell interface to restrict the delivery of cytokines or lytic granules to the contact site. Pyk2 has been shown to interact with and phosphorylate the ARF-GAP PAP (Andreev et al. 1999). ARF GTPases are typically involved in vesicular trafficking. It was therefore suggested in this study that Pyk2 may regulate some aspect of vesicular transport by interacting with PAP (Andreev et al. 1999). Thus it is possible that in CTL, Pyk2 could be involved in the secretion of lytic granules that track along the microtubules.

The potential involvement of Pyk2 in de-adhesion of CTL from target cells

FAK has been implicated in both focal adhesion assembly and disassembly (as reviewed in (Mitra et al. 2005). Which process it is involved with may be determined by the constant recruitment and dissociation of proteins within an evolving focal adhesion. Similarly, the role of Pyk2 may depend on its localization and the proteins with which it interacts at one point in time. Pyk2 is typically not found in focal adhesions or in adherent cells. However, it is predominantly found in hematopoietic cells in which it localizes to actin-rich structures. Pyk2 co-localized with F-actin at the leading edge and within membrane ruffles, but not in podosomes, in adhered, polarized monocytes (Williams and Ridley 2000; Watson et al. 2001). A small fraction of Pyk2 was observed at the leading edge of some NK cells migrating on fibronectin (Sancho et al. 2000). Pyk2 also co-localized with podosomes and actin in specialized adhesive zones, called sealing zones, in osteoclasts (Duong et al. 1998; Lakkakorpi et al. 1999). Osteoclasts are differentiated bone resorbing cells which become activated by binding to bone matrix. Once activated, these cells undergo significant cytoskeletal reorganization including the formation of a sealing zone and polarized ruffled membranes which allow for polarized secretion of acids and lysosomal enzymes onto the resorbing surface (Wang et al. 2003). Like monocytes and macrophages, osteoclasts form podosomes. The core of these structures is composed of actin aggregates surrounded by typical focal adhesion-associated proteins (Wang et al. 2003). Podosomes become clustered in a ring around the periphery of the osteoclast in the sealing zone during bone resorbtion (Wang et al. 2003). They are also involved in cell adhesion and migration (Wang et al. 2003).

The peripheral SMAC is a specialized actin-rich, adhesive structure formed between T cells and their targets. This structure may be related in some respects to a focal complex, focal adhesion or osteoclast sealing zone. First, the pSMAC contains a ring of clustered LFA-1 molecules. Second, the cytoskeletal adaptor protein talin, a focal adhesion-associated protein, is concentrated in the pSMAC. Talin is a FERM domain-containing protein that binds to the cytoplasmic face of integrins such as LFA-1 and to actin, thus linking integrins to the actin cytoskeleton. SMACs can be short lived (similar to a focal complex or podosome) or long-lived, stable structures (similar to a focal adhesion) depending on the type of T cell and target cell involved. For instance, a stable synapse is formed between a naïve T cell and an APC whereas a secretory IS forms between a CTL and its target. The latter lasts for a much shorter time as these cells deliver their 'lethal hit' in a matter of minutes. These structures must eventually dissolve, the cells must detach from one another and migration must once again be initiated in the CTL. It is not known whether dissolution of the SMAC is a prerequisite or a consequence of cell detachment. The factors involved in these steps have not yet been elucidated. The results generated in chapter 6 of this thesis suggest a possible role for Pyk2 in this process as CTL transfected with Pyk2 siRNA were more resistant to the disruption of conjugates by EDTA.

A potential mechanism that could be involved in the disruption of conjugates is the recruitment of molecules that act to disassemble protein-protein interactions around clustered adhesive molecules within the pSMAC and to initiate actin reorganization to promote cell migration. Little is known about the protein composition of the pSMAC, other than it includes LFA-1, talin and ADAP (adaptor adhesion and degranulation promoting adaptor protein) (Wang et al. 2004). Our lab has found that paxillin is concentrated at the interface of a CTL and its target and at the MTOC. A pSMAC-like localization of paxillin at the interface is observed in some conjugates (Ostergaard lab unpublished observation). Interestingly, paxillin interacts directly with the cytoplasmic domains of some integrins (α4 and α9) (Liu et al. 1999; Liu and Ginsberg 2000; Young et al. 2001). However, as of yet there is no evidence to suggest that paxillin interacts directly with LFA-1. I have found that some Pyk2 localizes to the CTL/target cell interface, as does paxillin (chapter 5). These two proteins may interact within the pSMAC. Whether Pyk2 is present in the pSMAC remains to be determined. If these proteins interact within the pSMAC, then the disruption of Pyk2/paxillin binding could be a mechanism by which contact with a target cell could be induced to de-stabilize.

This idea may be consistent with my findings desribed in chapter 5 in which I found that there were two populations of Pyk2 within CTL based on their differential ability to bind to paxillin. My results show that when Pyk2 is not associated with paxillin, the proline-rich region and Y881 are highly phosphorylated. These results are in agreement with a model proposed for the binding of FAK to paxillin. In this model, paxillin binds to the FAT domain when it is in a tight helical bundle (closed conformation) and is released when there is a change in the conformation of the FAT domain that favors phosphorylation of Y925 (open conformation) (Arold et al. 2002; Liu et al. 2002; Dixon et al. 2004; Prutzman et al. 2004). Such a conformational change within Pyk2 could likewise disrupt the Pyk2/paxillin interaction at the interface. Subsequent phosphorylation of Pyk2 at Y881 and within the proline-rich region may allow for the recruitment of proteins such as phosphatases and proteases to Pyk2, and also to the newly freed paxillin, that could favor dissolution of the contact. It is also possible that such a process could allow for binding of the FAT domain of Pyk2 to different LD motif-containing proteins. For instance, Pyk2 has been shown to directly associate with the actin-binding protein gelsolin through a FAT domain/LD motif interaction (Wang et al. 2003). Gelsolin exhibits actin capping and severing activity that is dependent on the presence of Ca^{2+} (Silacci et al. 2004). When gelsolin severs actin filaments, it caps the plus ends thus preventing the addition of actin monomers and consequently actin polymerization (Silacci et al. 2004). Gelsolin is released from the filament end upon binding to PIP_2 (Wang et al. 2003). Actin polymerization then proceeds from the uncapped sites (Wang et al. 2003). This sequence of events allows for rapid changes in the actin cytoskeleton which are necessary for motility. The important role of gelsolin in migration is evident in fibroblasts isolated from gelsolin-deficient mice. These cells exhibit an increased number of stress fibers, impaired actin polymerization and slower migration than their wild type counterparts (Witke et al. 1995). When Pyk2 and gelsolin were co-expressed in HEK 293 cells, gelsolin bound to less actin monomers and associated with PIP_2 to a greater extent than when Pyk2 was not co-expressed in these cells (Wang et al. 2003). These results suggest that the interaction of Pyk2 with gelsolin may lead to an increase in actin polymerization. Alternatively, Pyk2 may reduce the binding of gelsolin to actin in the presence of Ca^{2+}, thus increasing free gelsolin to sever existing actin filaments. Thus it is possible that an interaction between Pyk2 and gelsolin may act to induce actin depolymerization at the contact site or induce actin polymerization necessary for the re-onset of migration of a CTL upon deliver of its 'lethal hit'.

C. Future directions

The function of Pyk2 in CTL has remained elusive. Only very recently was I able to start to address this question after we acquired the ability to transfect our CTL clones. As of yet, I have only scratched the surface and many questions remain.

It is clear that there is a population of Pyk2 associated with paxillin at the MTOC in both NK cells and T cells. It would be of great interest to determine the function of Pyk2 at the MTOC. Pyk2 is also present at the T cell/target cell interface. A closer examination of the interface will be necessary to determine whether Pyk2 localizes to the pSMAC along with paxillin and LFA-1. The interaction between Pyk2 and paxillin is likely important either for the localization of Pyk2 or its function. Therefore, the significance of this association should be further investigated. In this respect, creation of a Pyk2 mutant that cannot be phosphorylated on Y881 (which should favour paxillin binding) could be used to address the importance of this interaction during CTL function. Introducing this mutation into Pyk2 with or without a functional kinase domain (K475A point mutation; disrupts kinase activity) would also address whether phosphorylation of paxillin or other proteins recruited to the Pyk2/paxillin complex by Pyk2 is important.

The findings from chapter 5 suggest that Pyk2 may be phosphorylated within the proline-rich region. To date, no phosphorylation sites have been identified within this region of Pyk2. Nineteen new phosphorylation sites were recently identified within FAK by mass spectrometry (Grigera et al. 2005). This methodology could be useful to determine whether there are phosphorylation sites within the proline-rich region of Pyk2. If such sites were identified, mutagenesis could be utilized to assess F245 antiserum binding to Pyk2. This approach could also be used to examine the binding of Pyk2 to known SH3 domain-containing interacting partners. Grigera and colleagues suggested that clustering of phosphorylation sites around the proline-rich regions of FAK may influence binding to SH3 domain-containing proteins (Grigera et al. 2005).

The results from this study suggest a possible role for Pyk2 in de-adhesion from target cells or in turnover of adhesive complexes. Future studies aimed at examining the involvement of Pyk2 in de-adhesion of CTL from targets should be performed. Resistance to conjugate disruption could be tested using assays in which conjugates are disrupted by either pipetting or vortexing. It would also be worth examining the spreading kinetics of CTL expressing CT Pyk2 on immobilized anti-CD3. Such experiments could determine whether there are deficiencies in the turnover of the contacts made with the immobilized antibody.

I did not detect a defect in the ability of CTL nucleofected with NT Pyk2 or CT Pyk2 to translocate the MTOC or to degranulate upon stimulation. However, these results do not preclude a role for Pyk2 in other cell polarization events such as cell migration. Pyk2-deficient B cells and macrophages exhibited defects in chemokine-induced cell migration (Guinamard et al. 2000; Okigaki et al. 2003). Thus, it would be of interest to examine a role for Pyk2 in chemokine-induced migration of CTL.

Pyk2 has been reported to directly bind to a number of proteins including PAP (Andreev et al. 1999), PSGAP (Ren et al. 2001) and gelsolin (Wang et al. 2003). However, most of the studies describing Pyk2 interacting partners have been performed in cell types other than T cells. Therefore, it will be imperative to first determine whether these interacting proteins are expressed in CTL and then whether they interact with Pyk2. Only then can we extrapolate findings from these studies to CTL. A more in-depth look at Pyk2 interacting partners may also aid in answering the question of how Pyk2 is recruited to the TCR/CD3 complex.

One interesting observation was made during the cloning of Pyk2 from our AB.1 cells. Using primers designed to amplify full length Pyk2, a PCR product of 850-1000 bp was observed (Figure 6-2). Two pieces of evidence suggest that this product is not the PRNK isoform. First, PRNK is 238 amino acids and is therefore 714 bp (smaller than the observed band). Second, initial sequencing using both primers used for amplification revealed only sequence corresponding to the N-terminus of Pyk2 (within the first 300 base pairs of the protein). Interestingly, when Pyk2 immunoprecipitations are performed from our AB.1 cells using antiserum generated against the N-terminus of Pyk2 (F298), a band of approximately 31 kDa is observed upon immunoblotting with the F298 antibody. Based on these observations, it is possible that this PCR product could represent another Pyk2 isoform. Sequencing the entire PCR product and identification of the protein product by mass spectrometry are necessary to determine whether this may be a splice variant of Pyk2.

The ability to transfect our CTL clones will greatly accelerate the progress in elucidating the role of Pyk2 in CTL. However, before future experiments are performed, it is advisable that attempts be made to increase transfection efficiency and efficiency of Pyk2 knockdown. It will also be advantageous to determine whether the CT Pyk2 truncation mutant is capable of inhibiting endogenous Pyk2 phosphorylation. By determining a role for this protein in CTL we can learn more about how these cells become activated to perform their cytolytic function to eliminate cells infected with pathogens and tumour cells.

CHAPTER 8: Bibliography

Andreev, J., J. P. Simon, D. D. Sabatini, J. Kam, G. Plowman, P. A. Randazzo and J. Schlessinger (1999). "Identification of a new Pyk2 target protein with Arf-GAP activity." Mol Cell Biol **19**(3): 2338-50.

Aoto, H., H. Sasaki, M. Ishino and T. Sasaki (2002). "Nuclear translocation of cell adhesion kinase beta/proline-rich tyrosine kinase 2." Cell Struct Funct **27**(1): 47-61.

Ardouin, L., M. Bracke, A. Mathiot, S. N. Pagakis, T. Norton, N. Hogg and V. L. Tybulewicz (2003). "Vav1 transduces TCR signals required for LFA-1 function and cell polarization at the immunological synapse." Eur J Immunol **33**(3): 790-7.

Arendt, C. W., G. Hsi and H. L. Ostergaard (1995). "Immobilized antibodies to CD45 induce rapid morphologic changes and increased tyrosine phosphorylation of p56lck-associated proteins in T cells." J Immunol **155**(11): 5095-103.

Arold, S. T., M. K. Hoellerer and M. E. Noble (2002). "The structural basis of localization and signaling by the focal adhesion targeting domain." Structure **10**(3): 319-27.

Astier, A., H. Avraham, S. N. Manie, J. Groopman, T. Canty, S. Avraham and A. S. Freedman (1997). "The related adhesion focal tyrosine kinase is tyrosine-phosphorylated after beta1-integrin stimulation in B cells and binds to p130cas." J Biol Chem **272**(1): 228-32.

August, A. and B. Dupont (1996). "Association between mitogen-activated protein kinase and the zeta chain of the T cell receptor (TcR) with the SH2,3 domain of p56lck. Differential regulation by TcR cross-linking." J Biol Chem **271**(17): 10054-9.

Avraham, H., S. Y. Park, K. Schinkmann and S. Avraham (2000). "RAFTK/Pyk2-mediated cellular signalling." Cell Signal **12**(3): 123-33.

Avraham, S., R. London, Y. Fu, S. Ota, D. Hiregowdara, J. Li, S. Jiang, L. M. Pasztor, R. A. White, J. E. Groopman and et al. (1995). "Identification and characterization of a novel related adhesion focal tyrosine kinase (RAFTK) from megakaryocytes and brain." J Biol Chem **270**(46): 27742-51.

Baniyash, M., P. Garcia-Morales, E. Luong, L. E. Samelson and R. D. Klausner (1988). "The T cell antigen receptor zeta chain is tyrosine phosphorylated upon activation." J Biol Chem **263**(34): 18225-30.

Barda-Saad, M., A. Braiman, R. Titerence, S. C. Bunnell, V. A. Barr and L. E. Samelson (2005). "Dynamic molecular interactions linking the T cell antigen receptor to the actin cytoskeleton." Nat Immunol **6**(1): 80-9.

Barry, M. and R. C. Bleackley (2002). "Cytotoxic T lymphocytes: all roads lead to death." Nat Rev Immunol **2**(6): 401-9.

Berg, N. N. and H. L. Ostergaard (1995). "Characterization of intercellular adhesion molecule-1 (ICAM-1)-augmented degranulation by cytotoxic T cells. ICAM-1 and anti-CD3 must be co-localized for optimal adhesion and stimulation." J Immunol **155**(4): 1694-702.

Berg, N. N. and H. L. Ostergaard (1997). "T cell receptor engagement induces tyrosine phosphorylation of FAK and Pyk2 and their association with Lck." J Immunol **159**(4): 1753-7.

Berg, N. N., L. G. Puente, W. Dawicki and H. L. Ostergaard (1998). "Sustained TCR signaling is required for mitogen-activated protein kinase activation and degranulation by cytotoxic T lymphocytes." J Immunol **161**(6): 2919-24.

Blakely, A., K. Gorman, H. Ostergaard, K. Svoboda, C. C. Liu, J. D. Young and W. R. Clark (1987). "Resistance of cloned cytotoxic T lymphocytes to cell-mediated cytotoxicity." J Exp Med **166**(4): 1070-83.

Blaukat, A., I. Ivankovic-Dikic, E. Gronroos, F. Dolfi, G. Tokiwa, K. Vuori and I. Dikic (1999). "Adaptor proteins Grb2 and Crk couple Pyk2 with activation of specific mitogen-activated protein kinase cascades." J Biol Chem **274**(21): 14893-901.

Bretscher, A., K. Edwards and R. G. Fehon (2002). "ERM proteins and merlin: integrators at the cell cortex." Nat Rev Mol Cell Biol **3**(8): 586-99.

Brinson, A. E., T. Harding, P. A. Diliberto, Y. He, X. Li, D. Hunter, B. Herman, H. S. Earp and L. M. Graves (1998). "Regulation of a calcium-dependent tyrosine kinase in vascular smooth muscle cells by angiotensin II and platelet-derived growth factor. Dependence on calcium and the actin cytoskeleton." J Biol Chem **273**(3): 1711-8.

Brown, M. C., J. A. Perrotta and C. E. Turner (1996). "Identification of LIM3 as the principal determinant of paxillin focal adhesion localization and characterization of a novel motif on paxillin directing vinculin and focal adhesion kinase binding." J Cell Biol **135**(4): 1109-23.

Brown, M. C. and C. E. Turner (2002). "Roles for the tubulin- and PTP-PEST-binding paxillin LIM domains in cell adhesion and motility." Int J Biochem Cell Biol **34**(7): 855-63.

Bunnell, S. C., V. Kapoor, R. P. Trible, W. Zhang and L. E. Samelson (2001). "Dynamic actin polymerization drives T cell receptor-induced spreading: a role for the signal transduction adaptor LAT." Immunity **14**(3): 315-29.

Burgaya, F. and J. A. Girault (1996). "Cloning of focal adhesion kinase, pp125FAK, from rat brain reveals multiple transcripts with different patterns of expression." Brain Res Mol Brain Res **37**(1-2): 63-73.

Burgaya, F., M. Toutant, J. M. Studler, A. Costa, M. Le Bert, M. Gelman and J. A. Girault (1997). "Alternatively spliced focal adhesion kinase in rat brain with increased autophosphorylation activity." J Biol Chem **272**(45): 28720-5.

Calalb, M. B., T. R. Polte and S. K. Hanks (1995). "Tyrosine phosphorylation of focal adhesion kinase at sites in the catalytic domain regulates kinase activity: a role for Src family kinases." Mol Cell Biol **15**(2): 954-63.

Campi, G., R. Varma and M. L. Dustin (2005). "Actin and agonist MHC-peptide complex-dependent T cell receptor microclusters as scaffolds for signaling." J Exp Med **202**(8): 1031-6.

Caplan, S., O. Almogi-Hazan, A. Ezernitchi, E. Manaster, A. Gazit and M. Baniyash (2001). "The cytoskeleton-associated TCR zeta chain is constitutively phosphorylated in the absence of an active p56(lck) form." Eur J Immunol **31**(2): 580-9.

Caplan, S. and M. Baniyash (1996). "Normal T cells express two T cell antigen receptor populations, one of which is linked to the cytoskeleton via zeta chain and displays a unique activation-dependent phosphorylation pattern." J Biol Chem **271**(34): 20705-12.

Caplan, S., S. Zeliger, L. Wang and M. Baniyash (1995). "Cell-surface-expressed T-cell antigen-receptor zeta chain is associated with the cytoskeleton." Proc Natl Acad Sci U S A **92**(11): 4768-72.

Ceccarelli, D. F., H. K. Song, F. Poy, M. D. Schaller and M. J. Eck (2006). "Crystal structure of the FERM domain of focal adhesion kinase." J Biol Chem **281**(1): 252-9.

Chan, A. C., M. Dalton, R. Johnson, G. H. Kong, T. Wang, R. Thoma and T. Kurosaki (1995). "Activation of ZAP-70 kinase activity by phosphorylation of tyrosine 493 is required for lymphocyte antigen receptor function." Embo J **14**(11): 2499-508.

Chan, A. C., M. Iwashima, C. W. Turck and A. Weiss (1992). "ZAP-70: a 70 kd protein-tyrosine kinase that associates with the TCR zeta chain." Cell **71**(4): 649-62.

Chen, H. C., P. A. Appeddu, J. T. Parsons, J. D. Hildebrand, M. D. Schaller and J. L. Guan (1995). "Interaction of focal adhesion kinase with cytoskeletal protein talin." J Biol Chem **270**(28): 16995-9.

Chen, R., O. Kim, M. Li, X. Xiong, J. L. Guan, H. J. Kung, H. Chen, Y. Shimizu and Y. Qiu (2001). "Regulation of the PH-domain-containing tyrosine kinase Etk by focal adhesion kinase through the FERM domain." Nat Cell Biol **3**(5): 439-44.

Cobb, B. S., M. D. Schaller, T. H. Leu and J. T. Parsons (1994). "Stable association of pp60src and pp59fyn with the focal adhesion-associated protein tyrosine kinase, pp125FAK." Mol Cell Biol **14**(1): 147-55.

Cooper, L. A., T. L. Shen and J. L. Guan (2003). "Regulation of focal adhesion kinase by its amino-terminal domain through an autoinhibitory interaction." Mol Cell Biol **23**(22): 8030-41.

Davis, C. B., I. Dikic, D. Unutmaz, C. M. Hill, J. Arthos, M. A. Siani, D. A. Thompson, J. Schlessinger and D. R. Littman (1997). "Signal transduction due to HIV-1 envelope interactions with chemokine receptors CXCR4 or CCR5." J Exp Med **186**(10): 1793-8.

Denny, M. F., B. Patai and D. B. Straus (2000). "Differential T-cell antigen receptor signaling mediated by the Src family kinases Lck and Fyn." Mol Cell Biol **20**(4): 1426-35.

Dikic, I. and J. Schlessinger (1998). "Identification of a new Pyk2 isoform implicated in chemokine and antigen receptor signaling." J Biol Chem **273**(23): 14301-8.

Dixon, R. D., Y. Chen, F. Ding, S. D. Khare, K. C. Prutzman, M. D. Schaller, S. L. Campbell and N. V. Dokholyan (2004). "New insights into FAK signaling and localization based on detection of a FAT domain folding intermediate." Structure **12**(12): 2161-71.

Donnadieu, E., G. Bismuth and A. Trautmann (1994). "Antigen recognition by helper T cells elicits a sequence of distinct changes of their shape and intracellular calcium." Curr Biol **4**(7): 584-95.

Doucey, M. A., D. F. Legler, M. Faroudi, N. Boucheron, P. Baumgaertner, D. Naeher, M. Cebecauer, D. Hudrisier, C. Ruegg, E. Palmer, S. Valitutti, C. Bron and I. F. Luescher (2003). "The beta1 and beta3 integrins promote T cell receptor-mediated cytotoxic T lymphocyte activation." J Biol Chem **278**(29): 26983-91.

Dransfield, I. and N. Hogg (1989). "Regulated expression of Mg2+ binding epitope on leukocyte integrin alpha subunits." Embo J **8**(12): 3759-65.

Dunty, J. M., V. Gabarra-Niecko, M. L. King, D. F. Ceccarelli, M. J. Eck and M. D. Schaller (2004). "FERM domain interaction promotes FAK signaling." Mol Cell Biol **24**(12): 5353-68.

Dunty, J. M. and M. D. Schaller (2002). "The N termini of focal adhesion kinase family members regulate substrate phosphorylation, localization, and cell morphology." J Biol Chem **277**(47): 45644-54.

Duong, L. T., P. T. Lakkakorpi, I. Nakamura, M. Machwate, R. M. Nagy and G. A. Rodan (1998). "PYK2 in osteoclasts is an adhesion kinase, localized in the sealing zone, activated by ligation of alpha(v)beta3 integrin, and phosphorylated by src kinase." J Clin Invest **102**(5): 881-92.

Duong, L. T. and G. A. Rodan (2000). "PYK2 is an adhesion kinase in macrophages, localized in podosomes and activated by beta(2)-integrin ligation." Cell Motil Cytoskeleton **47**(3): 174-88.

Durand, C. A., J. Westendorf, K. W. Tse and M. R. Gold (2006). "The Rap GTPases mediate CXCL13- and sphingosine1-phosphate-induced chemotaxis, adhesion, and Pyk2 tyrosine phosphorylation in B lymphocytes." Eur J Immunol **36**(8): 2235-49.

Dustin, M. L. and J. A. Cooper (2000). "The immunological synapse and the actin cytoskeleton: molecular hardware for T cell signaling." Nat Immunol **1**(1): 23-9.

Dustin, M. L. and T. A. Springer (1989). "T-cell receptor cross-linking transiently stimulates adhesiveness through LFA-1." Nature **341**(6243): 619-24.

Esser, M. T., B. Krishnamurthy and V. L. Braciale (1996). "Distinct T cell receptor signaling requirements for perforin- or FasL-mediated cytotoxicity." J Exp Med **183**(4): 1697-706.

Fox, G. L., I. Rebay and R. O. Hynes (1999). "Expression of DFak56, a Drosophila homolog of vertebrate focal adhesion kinase, supports a role in cell migration in vivo." Proc Natl Acad Sci U S A **96**(26): 14978-83.

Freiberg, B. A., H. Kupfer, W. Maslanik, J. Delli, J. Kappler, D. M. Zaller and A. Kupfer (2002). "Staging and resetting T cell activation in SMACs." Nat Immunol **3**(10): 911-7.

Fujimoto, J., K. Sawamoto, M. Okabe, Y. Takagi, T. Tezuka, S. Yoshikawa, H. Ryo, H. Okano and T. Yamamoto (1999). "Cloning and characterization of Dfak56, a homolog of focal adhesion kinase, in Drosophila melanogaster." J Biol Chem **274**(41): 29196-201.

Fujita, H., K. Kamiguchi, D. Cho, M. Shibanuma, C. Morimoto and K. Tachibana (1998). "Interaction of Hic-5, A senescence-related protein, with focal adhesion kinase." J Biol Chem **273**(41): 26516-21.

Fukai, I., R. E. Hussey, R. Sunder-Plassmann and E. L. Reinherz (2000). "A critical role for p59(fyn) in CD2-based signal transduction." Eur J Immunol **30**(12): 3507-15.

Gallo, E. M., K. Cante-Barrett and G. R. Crabtree (2006). "Lymphocyte calcium signaling from membrane to nucleus." Nat Immunol **7**(1): 25-32.

Ganju, R. K., S. A. Brubaker, R. D. Chernock, S. Avraham and J. E. Groopman (2000). "Beta-chemokine receptor CCR5 signals through SHP1, SHP2, and Syk." J Biol Chem **275**(23): 17263-8.

Ganju, R. K., W. C. Hatch, H. Avraham, M. A. Ona, B. Druker, S. Avraham and J. E. Groopman (1997). "RAFTK, a novel member of the focal adhesion kinase family, is phosphorylated and associates with signaling molecules upon activation of mature T lymphocytes." J Exp Med **185**(6): 1055-63.

Gao, G., K. C. Prutzman, M. L. King, D. M. Scheswohl, E. F. DeRose, R. E. London, M. D. Schaller and S. L. Campbell (2004). "NMR solution structure of the focal adhesion targeting domain of focal adhesion kinase in complex with a paxillin LD peptide: evidence for a two-site binding model." J Biol Chem **279**(9): 8441-51.

Gil, D., W. W. Schamel, M. Montoya, F. Sanchez-Madrid and B. Alarcon (2002). "Recruitment of Nck by CD3 epsilon reveals a ligand-induced conformational change essential for T cell receptor signaling and synapse formation." Cell **109**(7): 901-12.

Gilmore, A. P. and L. H. Romer (1996). "Inhibition of focal adhesion kinase (FAK) signaling in focal adhesions decreases cell motility and proliferation." Mol Biol Cell **7**(8): 1209-24.

Ginnan, R. and H. A. Singer (2002). "CaM kinase II-dependent activation of tyrosine kinases and ERK1/2 in vascular smooth muscle." Am J Physiol Cell Physiol **282**(4): C754-61.

Girault, J. A., G. Labesse, J. P. Mornon and I. Callebaut (1999). "The N-termini of FAK and JAKs contain divergent band 4.1 domains." Trends Biochem Sci **24**(2): 54-7.

Gismondi, A., L. Bisogno, F. Mainiero, G. Palmieri, M. Piccoli, L. Frati and A. Santoni (1997). "Proline-rich tyrosine kinase-2 activation by beta 1 integrin fibronectin receptor cross-linking and association with paxillin in human natural killer cells." J Immunol **159**(10): 4729-36.

Gismondi, A., J. Jacobelli, F. Mainiero, R. Paolini, M. Piccoli, L. Frati and A. Santoni (2000). "Cutting edge: functional role for proline-rich tyrosine kinase 2 in NK cell-mediated natural cytotoxicity." J Immunol **164**(5): 2272-6.

Gismondi, A., J. Jacobelli, R. Strippoli, F. Mainiero, A. Soriani, L. Cifaldi, M. Piccoli, L. Frati and A. Santoni (2003). "Proline-rich tyrosine kinase 2 and Rac activation by chemokine and integrin receptors controls NK cell transendothelial migration." J Immunol **170**(6): 3065-73.

Gouin, E., M. D. Welch and P. Cossart (2005). "Actin-based motility of intracellular pathogens." Curr Opin Microbiol **8**(1): 35-45.

Grakoui, A., S. K. Bromley, C. Sumen, M. M. Davis, A. S. Shaw, P. M. Allen and M. L. Dustin (1999). "The immunological synapse: a molecular machine controlling T cell activation." Science **285**(5425): 221-7.

Grigera, P. R., E. D. Jeffery, K. H. Martin, J. Shabanowitz, D. F. Hunt and J. T. Parsons (2005). "FAK phosphorylation sites mapped by mass spectrometry." J Cell Sci **118**(Pt 21): 4931-5.

Groscurth, P. and L. Filgueira (1998). "Killing Mechanisms of Cytotoxic T Lymphocytes." News Physiol Sci **13**: 17-21.

Guinamard, R., M. Okigaki, J. Schlessinger and J. V. Ravetch (2000). "Absence of marginal zone B cells in Pyk-2-deficient mice defines their role in the humoral response." Nat Immunol **1**(1): 31-6.

Guo, J., F. Meng, X. Fu, B. Song, X. Yan and G. Zhang (2004). "N-methyl-D-aspartate receptor and L-type voltage-gated Ca2+ channel activation mediate proline-rich tyrosine kinase 2 phosphorylation during cerebral ischemia in rats." Neurosci Lett **355**(3): 177-80.

Hall, A. (2005). "Rho GTPases and the control of cell behaviour." Biochem Soc Trans **33**(Pt 5): 891-5.

Han, H., M. Fuortes and C. Nathan (2003). "Critical role of the carboxyl terminus of proline-rich tyrosine kinase (Pyk2) in the activation of human neutrophils by tumor necrosis factor: separation of signals for the respiratory burst and degranulation." J Exp Med **197**(1): 63-75.

Hanke, J. H., J. P. Gardner, R. L. Dow, P. S. Changelian, W. H. Brissette, E. J. Weringer, B. A. Pollok and P. A. Connelly (1996). "Discovery of a novel, potent, and Src family-selective tyrosine kinase inhibitor. Study of Lck- and FynT-dependent T cell activation." J Biol Chem **271**(2): 695-701.

Hanks, S. K., M. B. Calalb, M. C. Harper and S. K. Patel (1992). "Focal adhesion protein-tyrosine kinase phosphorylated in response to cell attachment to fibronectin." Proc Natl Acad Sci U S A **89**(18): 8487-91.

Harder, T. and M. Kuhn (2000). "Selective accumulation of raft-associated membrane protein LAT in T cell receptor signaling assemblies." J Cell Biol **151**(2): 199-208.

Harte, M. T., J. D. Hildebrand, M. R. Burnham, A. H. Bouton and J. T. Parsons (1996). "p130Cas, a substrate associated with v-Src and v-Crk, localizes to focal adhesions and binds to focal adhesion kinase." J Biol Chem **271**(23): 13649-55.

Hatada, M. H., X. Lu, E. R. Laird, J. Green, J. P. Morgenstern, M. Lou, C. S. Marr, T. B. Phillips, M. K. Ram, K. Theriault and et al. (1995). "Molecular basis for interaction of the protein tyrosine kinase ZAP-70 with the T-cell receptor." Nature **377**(6544): 32-8.

Hayashi, I., K. Vuori and R. C. Liddington (2002). "The focal adhesion targeting (FAT) region of focal adhesion kinase is a four-helix bundle that binds paxillin." Nat Struct Biol **9**(2): 101-6.

Henry, C. A., B. D. Crawford, Y. L. Yan, J. Postlethwait, M. S. Cooper and M. B. Hille (2001). "Roles for zebrafish focal adhesion kinase in notochord and somite morphogenesis." Dev Biol **240**(2): 474-87.

Herreros, L., J. L. Rodriguez-Fernandez, M. C. Brown, J. L. Alonso-Lebrero, C. Cabanas, F. Sanchez-Madrid, N. Longo, C. E. Turner and P. Sanchez-Mateos (2000). "Paxillin localizes to the lymphocyte microtubule organizing center and associates with the microtubule cytoskeleton." J Biol Chem **275**(34): 26436-40.

Herzog, H., J. Nicholl, Y. J. Hort, G. R. Sutherland and J. Shine (1996). "Molecular cloning and assignment of FAK2, a novel human focal adhesion kinase, to 8p11.2-p22 by nonisotopic in situ hybridization." Genomics **32**(3): 484-6.

Hildebrand, J. D., M. D. Schaller and J. T. Parsons (1993). "Identification of sequences required for the efficient localization of the focal adhesion kinase, pp125FAK, to cellular focal adhesions." J Cell Biol **123**(4): 993-1005.

Hildebrand, J. D., M. D. Schaller and J. T. Parsons (1995). "Paxillin, a tyrosine phosphorylated focal adhesion-associated protein binds to the carboxyl terminal domain of focal adhesion kinase." Mol Biol Cell **6**(6): 637-47.

Hildebrand, J. D., J. M. Taylor and J. T. Parsons (1996). "An SH3 domain-containing GTPase-activating protein for Rho and Cdc42 associates with focal adhesion kinase." Mol Cell Biol **16**(6): 3169-78.

Hiregowdara, D., H. Avraham, Y. Fu, R. London and S. Avraham (1997). "Tyrosine phosphorylation of the related adhesion focal tyrosine kinase in megakaryocytes upon stem cell factor and phorbol myristate acetate stimulation and its association with paxillin." J Biol Chem **272**(16): 10804-10.

Hirotani, S., Y. Higuchi, K. Nishida, H. Nakayama, O. Yamaguchi, S. Hikoso, T. Takeda, K. Kashiwase, T. Watanabe, M. Asahi, M. Taniike, I. Tsujimoto, Y. Matsumura, T. Sasaki, M. Hori and K. Otsu (2004). "Ca(2+)-sensitive tyrosine kinase Pyk2/CAK beta-dependent signaling is essential for G-protein-coupled receptor agonist-induced hypertrophy." J Mol Cell Cardiol **36**(6): 799-807.

Hoellerer, M. K., M. E. Noble, G. Labesse, I. D. Campbell, J. M. Werner and S. T. Arold (2003). "Molecular recognition of paxillin LD motifs by the focal adhesion targeting domain." Structure **11**(10): 1207-17.

Hook, S. S. and A. R. Means (2001). "Ca(2+)/CaM-dependent kinases: from activation to function." Annu Rev Pharmacol Toxicol **41**: 471-505.

Hoth, M. and R. Penner (1992). "Depletion of intracellular calcium stores activates a calcium current in mast cells." Nature **355**(6358): 353-6.

Hurley, T. R., R. Hyman and B. M. Sefton (1993). "Differential effects of expression of the CD45 tyrosine protein phosphatase on the tyrosine phosphorylation of the lck, fyn, and c-src tyrosine protein kinases." Mol Cell Biol **13**(3): 1651-6.

Ilic, D., Y. Furuta, S. Kanazawa, N. Takeda, K. Sobue, N. Nakatsuji, S. Nomura, J. Fujimoto, M. Okada and T. Yamamoto (1995). "Reduced cell motility and enhanced focal adhesion contact formation in cells from FAK-deficient mice." Nature **377**(6549): 539-44.

Imboden, J. B. and J. D. Stobo (1985). "Transmembrane signalling by the T cell antigen receptor. Perturbation of the T3-antigen receptor complex generates inositol phosphates and releases calcium ions from intracellular stores." J Exp Med **161**(3): 446-56.

Isakov, N., R. L. Wange, W. H. Burgess, J. D. Watts, R. Aebersold and L. E. Samelson (1995). "ZAP-70 binding specificity to T cell receptor tyrosine-based activation motifs: the tandem SH2 domains of ZAP-70 bind distinct tyrosine-based activation motifs with varying affinity." J Exp Med **181**(1): 375-80.

Ivankovic-Dikic, I., E. Gronroos, A. Blaukat, B. U. Barth and I. Dikic (2000). "Pyk2 and FAK regulate neurite outgrowth induced by growth factors and integrins." Nat Cell Biol **2**(9): 574-81.

Iwashima, M., B. A. Irving, N. S. van Oers, A. C. Chan and A. Weiss (1994). "Sequential interactions of the TCR with two distinct cytoplasmic tyrosine kinases." Science **263**(5150): 1136-9.

Jones, G. and G. Stewart (2004). "Nuclear import of N-terminal FAK by activation of the FcepsilonRI receptor in RBL-2H3 cells." Biochem Biophys Res Commun **314**(1): 39-45.

Kadare, G., M. Toutant, E. Formstecher, J. C. Corvol, M. Carnaud, M. C. Boutterin and J. A. Girault (2003). "PIAS1-mediated sumoylation of focal adhesion kinase activates its autophosphorylation." J Biol Chem **278**(48): 47434-40.

Kane, K. P., L. A. Sherman and M. F. Mescher (1989). "Molecular interactions required for triggering alloantigen-specific cytolytic T lymphocytes." J Immunol **142**(12): 4153-60.

Kanner, S. B., L. S. Grosmaire, J. A. Ledbetter and N. K. Damle (1993). "Beta 2-integrin LFA-1 signaling through phospholipase C-gamma 1 activation." Proc Natl Acad Sci U S A **90**(15): 7099-103.

Katagiri, T., T. Takahashi, T. Sasaki, S. Nakamura and S. Hattori (2000). "Protein-tyrosine kinase Pyk2 is involved in interleukin-2 production by Jurkat T cells via its tyrosine 402." J Biol Chem **275**(26): 19645-52.

Kinashi, T. (2005). "Intracellular signalling controlling integrin activation in lymphocytes." Nat Rev Immunol **5**(7): 546-59.

Kinashi, T. and K. Katagiri (2004). "Regulation of lymphocyte adhesion and migration by the small GTPase Rap1 and its effector molecule, RAPL." Immunol Lett **93**(1): 1-5.

Kirwan, S., D. Merriam, N. Barsby, A. McKinnon and D. N. Burshtyn (2006). "Vaccinia virus modulation of natural killer cell function by direct infection." Virology **347**(1): 75-87.

Kruljac-Letunic, A. and A. Blaukat (2005). "Assay and functional properties of the tyrosine kinase Pyk2 in regulation of Arf1 through ASAP1 phosphorylation." Methods Enzymol **404**: 411-22.

Kruljac-Letunic, A., J. Moelleken, A. Kallin, F. Wieland and A. Blaukat (2003). "The tyrosine kinase Pyk2 regulates Arf1 activity by phosphorylation and inhibition of the Arf-GTPase-activating protein ASAP1." J Biol Chem **278**(32): 29560-70.

Kuhn, J. R. and M. Poenie (2002). "Dynamic polarization of the microtubule cytoskeleton during CTL-mediated killing." Immunity **16**(1): 111-21.

Kuhne, M. R., J. Lin, D. Yablonski, M. N. Mollenauer, L. I. Ehrlich, J. Huppa, M. M. Davis and A. Weiss (2003). "Linker for activation of T cells, zeta-associated protein-70, and Src homology 2 domain-containing leukocyte protein-76 are required for TCR-induced microtubule-organizing center polarization." J Immunol **171**(2): 860-6.

Kuhns, M. S., M. M. Davis and K. C. Garcia (2006). "Deconstructing the form and function of the TCR/CD3 complex." Immunity **24**(2): 133-9.

Kupfer, A. and G. Dennert (1984). "Reorientation of the microtubule-organizing center and the Golgi apparatus in cloned cytotoxic lymphocytes triggered by binding to lysable target cells." J Immunol **133**(5): 2762-6.

Kupfer, A., G. Dennert and S. J. Singer (1985). "The reorientation of the Golgi apparatus and the microtubule-organizing center in the cytotoxic effector cell is a prerequisite in the lysis of bound target cells." J Mol Cell Immunol **2**(1): 37-49.

Lakkakorpi, P. T., I. Nakamura, R. M. Nagy, J. T. Parsons, G. A. Rodan and L. T. Duong (1999). "Stable association of PYK2 and p130(Cas) in osteoclasts and their co-localization in the sealing zone." J Biol Chem **274**(8): 4900-7.

Lee, K. H., A. D. Holdorf, M. L. Dustin, A. C. Chan, P. M. Allen and A. S. Shaw (2002). "T cell receptor signaling precedes immunological synapse formation." Science **295**(5559): 1539-42.

Lev, S. (2004). "The role of the Nir/rdgB protein family in membrane trafficking and cytoskeleton remodeling." Exp Cell Res **297**(1): 1-10.

Lev, S., J. Hernandez, R. Martinez, A. Chen, G. Plowman and J. Schlessinger (1999). "Identification of a novel family of targets of PYK2 related to Drosophila retinal degeneration B (rdgB) protein." Mol Cell Biol **19**(3): 2278-88.

Lev, S., H. Moreno, R. Martinez, P. Canoll, E. Peles, J. M. Musacchio, G. D. Plowman, B. Rudy and J. Schlessinger (1995). "Protein tyrosine kinase PYK2 involved in Ca(2+)-induced regulation of ion channel and MAP kinase functions." Nature **376**(6543): 737-45.

Lewis, R. S. (2001). "Calcium signaling mechanisms in T lymphocytes." Annu Rev Immunol **19**: 497-521.

Li, R., N. Wong, M. D. Jabali and P. Johnson (2001). "CD44-initiated cell spreading induces Pyk2 phosphorylation, is mediated by Src family kinases, and is negatively regulated by CD45." J Biol Chem **276**(31): 28767-73.

Li, X., R. C. Dy, W. G. Cance, L. M. Graves and H. S. Earp (1999). "Interactions between two cytoskeleton-associated tyrosine kinases: calcium-dependent tyrosine kinase and focal adhesion tyrosine kinase." J Biol Chem **274**(13): 8917-24.

Li, X. and H. S. Earp (1997). "Paxillin is tyrosine-phosphorylated by and preferentially associates with the calcium-dependent tyrosine kinase in rat liver epithelial cells." J Biol Chem **272**(22): 14341-8.

Li, X., D. Hunter, J. Morris, J. S. Haskill and H. S. Earp (1998). "A calcium-dependent tyrosine kinase splice variant in human monocytes. Activation by a two-stage process involving adherence and a subsequent intracellular signal." J Biol Chem **273**(16): 9361-4.

Liu, G., C. D. Guibao and J. Zheng (2002). "Structural insight into the mechanisms of targeting and signaling of focal adhesion kinase." Mol Cell Biol **22**(8): 2751-60.

Liu, S. and M. H. Ginsberg (2000). "Paxillin binding to a conserved sequence motif in the alpha 4 integrin cytoplasmic domain." J Biol Chem **275**(30): 22736-42.

Liu, S., S. M. Thomas, D. G. Woodside, D. M. Rose, W. B. Kiosses, M. Pfaff and M. H. Ginsberg (1999). "Binding of paxillin to alpha4 integrins modifies integrin-dependent biological responses." Nature **402**(6762): 676-81.

Liu, S. K., N. Fang, G. A. Koretzky and C. J. McGlade (1999). "The hematopoietic-specific adaptor protein gads functions in T-cell signaling via interactions with the SLP-76 and LAT adaptors." Curr Biol **9**(2): 67-75.

Liu, Y., J. C. Loijens, K. H. Martin, A. V. Karginov and J. T. Parsons (2002). "The association of ASAP1, an ADP ribosylation factor-GTPase activating protein, with focal adhesion kinase contributes to the process of focal adhesion assembly." Mol Biol Cell **13**(6): 2147-56.

Lowell, C. A. (2004). "Src-family kinases: rheostats of immune cell signaling." Mol Immunol **41**(6-7): 631-43.

Lowin-Kropf, B., V. S. Shapiro and A. Weiss (1998). "Cytoskeletal polarization of T cells is regulated by an immunoreceptor tyrosine-based activation motif-dependent mechanism." J Cell Biol **140**(4): 861-71.

Luo, C., K. T. Shaw, A. Raghavan, J. Aramburu, F. Garcia-Cozar, B. A. Perrino, P. G. Hogan and A. Rao (1996). "Interaction of calcineurin with a domain of the transcription factor NFAT1 that controls nuclear import." Proc Natl Acad Sci U S A **93**(17): 8907-12.

Ma, E. A., O. Lou, N. N. Berg and H. L. Ostergaard (1997). "Cytotoxic T lymphocytes express a beta3 integrin which can induce the phosphorylation of focal adhesion kinase and the related PYK-2." Eur J Immunol **27**(1): 329-35.

Ma, Y. C., J. Huang, S. Ali, W. Lowry and X. Y. Huang (2000). "Src tyrosine kinase is a novel direct effector of G proteins." Cell **102**(5): 635-46.

Maguire, J. E., K. M. Danahey, L. C. Burkly and G. A. van Seventer (1995). "T cell receptor- and beta 1 integrin-mediated signals synergize to induce tyrosine phosphorylation of focal adhesion kinase (pp125FAK) in human T cells." J Exp Med **182**(6): 2079-90.

Marchand, J. B., D. A. Kaiser, T. D. Pollard and H. N. Higgs (2001). "Interaction of WASP/Scar proteins with actin and vertebrate Arp2/3 complex." Nat Cell Biol **3**(1): 76-82.

Martin-Cofreces, N. B., D. Sancho, E. Fernandez, M. Vicente-Manzanares, M. Gordon-Alonso, M. C. Montoya, F. Michel, O. Acuto, B. Alarcon and F. Sanchez-Madrid

(2006). "Role of Fyn in the rearrangement of tubulin cytoskeleton induced through TCR." J Immunol **176**(7): 4201-7.

Marwali, M. R., M. A. MacLeod, D. N. Muzia and F. Takei (2004). "Lipid rafts mediate association of LFA-1 and CD3 and formation of the immunological synapse of CTL." J Immunol **173**(5): 2960-7.

Marzia, M., R. Chiusaroli, L. Neff, N. Y. Kim, A. H. Chishti, R. Baron and W. C. Horne (2006). "Calpain is required for normal osteoclast function and is down-regulated by calcitonin." J Biol Chem **281**(14): 9745-54.

Mason, M. J., C. Garcia-Rodriguez and S. Grinstein (1991). "Coupling between intracellular Ca2+ stores and the Ca2+ permeability of the plasma membrane. Comparison of the effects of thapsigargin, 2,5-di-(tert-butyl)-1,4-hydroquinone, and cyclopiazonic acid in rat thymic lymphocytes." J Biol Chem **266**(31): 20856-62.

Mason, M. J. and S. Grinstein (1993). "Ionomycin activates electrogenic Ca2+ influx in rat thymic lymphocytes." Biochem J **296 (Pt 1)**: 33-9.

Matsuya, M., H. Sasaki, H. Aoto, T. Mitaka, K. Nagura, T. Ohba, M. Ishino, S. Takahashi, R. Suzuki and T. Sasaki (1998). "Cell adhesion kinase beta forms a complex with a new member, Hic-5, of proteins localized at focal adhesions." J Biol Chem **273**(2): 1003-14.

McLeod, S. J., A. J. Shum, R. L. Lee, F. Takei and M. R. Gold (2004). "The Rap GTPases regulate integrin-mediated adhesion, cell spreading, actin polymerization, and Pyk2 tyrosine phosphorylation in B lymphocytes." J Biol Chem **279**(13): 12009-19.

Mitra, S. K., D. A. Hanson and D. D. Schlaepfer (2005). "Focal adhesion kinase: in command and control of cell motility." Nat Rev Mol Cell Biol **6**(1): 56-68.

Miyazaki, T., A. Takaoka, L. Nogueira, I. Dikic, H. Fujii, S. Tsujino, Y. Mitani, M. Maeda, J. Schlessinger and T. Taniguchi (1998). "Pyk2 is a downstream mediator of the IL-2 receptor-coupled Jak signaling pathway." Genes Dev **12**(6): 770-5.

Monks, C. R., B. A. Freiberg, H. Kupfer, N. Sciaky and A. Kupfer (1998). "Three-dimensional segregation of supramolecular activation clusters in T cells." Nature **395**(6697): 82-6.

Moran, M. and M. C. Miceli (1998). "Engagement of GPI-linked CD48 contributes to TCR signals and cytoskeletal reorganization: a role for lipid rafts in T cell activation." Immunity **9**(6): 787-96.

Negulescu, P. A., T. B. Krasieva, A. Khan, H. H. Kerschbaum and M. D. Cahalan (1996). "Polarity of T cell shape, motility, and sensitivity to antigen." Immunity **4**(5): 421-30.

Nolan, K., J. Lacoste and J. T. Parsons (1999). "Regulated expression of focal adhesion kinase-related nonkinase, the autonomously expressed C-terminal domain of focal adhesion kinase." Mol Cell Biol **19**(9): 6120-9.

Norman, J. C., D. Jones, S. T. Barry, M. R. Holt, S. Cockcroft and D. R. Critchley (1998). "ARF1 mediates paxillin recruitment to focal adhesions and potentiates Rho-stimulated stress fiber formation in intact and permeabilized Swiss 3T3 fibroblasts." J Cell Biol **143**(7): 1981-95.

Nowakowski, J., C. N. Cronin, D. E. McRee, M. W. Knuth, C. G. Nelson, N. P. Pavletich, J. Rogers, B. C. Sang, D. N. Scheibe, R. V. Swanson and D. A. Thompson (2002). "Structures of the cancer-related Aurora-A, FAK, and EphA2 protein kinases from nanovolume crystallography." Structure **10**(12): 1659-67.

Ohba, T., M. Ishino, H. Aoto and T. Sasaki (1998). "Interaction of two proline-rich sequences of cell adhesion kinase beta with SH3 domains of p130Cas-related proteins and a GTPase-activating protein, Graf." Biochem J **330 (Pt 3)**: 1249-54.

Okigaki, M., C. Davis, M. Falasca, S. Harroch, D. P. Felsenfeld, M. P. Sheetz and J. Schlessinger (2003). "Pyk2 regulates multiple signaling events crucial for macrophage morphology and migration." Proc Natl Acad Sci U S A **100**(19): 10740-5.

Ostergaard, H. and W. R. Clark (1987). "The role of Ca2+ in activation of mature cytotoxic T lymphocytes for lysis." J Immunol **139**(11): 3573-9.

Ostergaard, H. L., K. P. Kane, M. F. Mescher and W. R. Clark (1987). "Cytotoxic T lymphocyte mediated lysis without release of serine esterase." Nature **330**(6143): 71-2.

Ostergaard, H. L., O. Lou, C. W. Arendt and N. N. Berg (1998). "Paxillin phosphorylation and association with Lck and Pyk2 in anti-CD3- or anti-CD45-stimulated T cells." J Biol Chem **273**(10): 5692-6.

Ostergaard, H. L. and T. L. Lysechko (2005). "Focal adhesion kinase-related protein tyrosine kinase Pyk2 in T-cell activation and function." Immunol Res **31**(3): 267-82.

Ostergaard, H. L., D. A. Shackelford, T. R. Hurley, P. Johnson, R. Hyman, B. M. Sefton and I. S. Trowbridge (1989). "Expression of CD45 alters phosphorylation of the lck-encoded tyrosine protein kinase in murine lymphoma T-cell lines." Proc Natl Acad Sci U S A **86**(22): 8959-63.

Palacios, E. H. and A. Weiss (2004). "Function of the Src-family kinases, Lck and Fyn, in T-cell development and activation." Oncogene **23**(48): 7990-8000.

Palmer, R. H., L. I. Fessler, P. T. Edeen, S. J. Madigan, M. McKeown and T. Hunter (1999). "DFak56 is a novel Drosophila melanogaster focal adhesion kinase." J Biol Chem **274**(50): 35621-9.

Park, S. Y., H. K. Avraham and S. Avraham (2004). "RAFTK/Pyk2 activation is mediated by trans-acting autophosphorylation in a Src-independent manner." J Biol Chem **279**(32): 33315-22.

Pitcher, L. A. and N. S. van Oers (2003). "T-cell receptor signal transmission: who gives an ITAM?" Trends Immunol **24**(10): 554-60.

Pitcher, L. A., J. A. Young, M. A. Mathis, P. C. Wrage, B. Bartok and N. S. van Oers (2003). "The formation and functions of the 21- and 23-kDa tyrosine-phosphorylated TCR zeta subunits." Immunol Rev **191**: 47-61.

Ploubidou, A., V. Moreau, K. Ashman, I. Reckmann, C. Gonzalez and M. Way (2000). "Vaccinia virus infection disrupts microtubule organization and centrosome function." Embo J **19**(15): 3932-44.

Pollard, T. D. and G. G. Borisy (2003). "Cellular motility driven by assembly and disassembly of actin filaments." Cell **112**(4): 453-65.

Polte, T. R. and S. K. Hanks (1995). "Interaction between focal adhesion kinase and Crk-associated tyrosine kinase substrate p130Cas." Proc Natl Acad Sci U S A **92**(23): 10678-82.

Poullet, P., A. Gautreau, G. Kadare, J. A. Girault, D. Louvard and M. Arpin (2001). "Ezrin interacts with focal adhesion kinase and induces its activation independently of cell-matrix adhesion." J Biol Chem **276**(40): 37686-91.

Prutzman, K. C., G. Gao, M. L. King, V. V. Iyer, G. A. Mueller, M. D. Schaller and S. L. Campbell (2004). "The focal adhesion targeting domain of focal adhesion kinase contains a hinge region that modulates tyrosine 926 phosphorylation." Structure **12**(5): 881-91.

Putney, J. W., Jr. (1990). "Capacitative calcium entry revisited." Cell Calcium **11**(10): 611-24.

Qian, D., S. Lev, N. S. van Oers, I. Dikic, J. Schlessinger and A. Weiss (1997). "Tyrosine phosphorylation of Pyk2 is selectively regulated by Fyn during TCR signaling." J Exp Med **185**(7): 1253-9.

Raja, S., S. Avraham and H. Avraham (1997). "Tyrosine phosphorylation of the novel protein-tyrosine kinase RAFTK during an early phase of platelet activation by an integrin glycoprotein IIb-IIIa-independent mechanism." J Biol Chem **272**(16): 10941-7.

Randriamampita, C. and A. Trautmann (2004). "Ca2+ signals and T lymphocytes; "New mechanisms and functions in Ca2+ signalling"." Biol Cell **96**(1): 69-78.

Ren, X. R., Q. S. Du, Y. Z. Huang, S. Z. Ao, L. Mei and W. C. Xiong (2001). "Regulation of CDC42 GTPase by proline-rich tyrosine kinase 2 interacting with PSGAP, a novel pleckstrin homology and Src homology 3 domain containing rhoGAP protein." J Cell Biol **152**(5): 971-84.

Richardson, A., R. K. Malik, J. D. Hildebrand and J. T. Parsons (1997). "Inhibition of cell spreading by expression of the C-terminal domain of focal adhesion kinase (FAK) is rescued by coexpression of Src or catalytically inactive FAK: a role for paxillin tyrosine phosphorylation." Mol Cell Biol **17**(12): 6906-14.

Richardson, A. and T. Parsons (1996). "A mechanism for regulation of the adhesion-associated proteintyrosine kinase pp125FAK." Nature **380**(6574): 538-40.

Rodriguez-Fernandez, J. L., M. Gomez, A. Luque, N. Hogg, F. Sanchez-Madrid and C. Cabanas (1999). "The interaction of activated integrin lymphocyte function-associated antigen 1 with ligand intercellular adhesion molecule 1 induces activation and redistribution of focal adhesion kinase and proline-rich tyrosine kinase 2 in T lymphocytes." Mol Biol Cell **10**(6): 1891-907.

Rodriguez-Fernandez, J. L., L. Sanchez-Martin, C. A. de Frutos, D. Sancho, M. Robinson, F. Sanchez-Madrid and C. Cabanas (2002). "LFA-1 integrin and the microtubular cytoskeleton are involved in the Ca(2)(+)-mediated regulation of the activity of the tyrosine kinase PYK2 in T cells." J Leukoc Biol **71**(3): 520-30.

Rodriguez-Fernandez, J. L., L. Sanchez-Martin, M. Rey, M. Vicente-Manzanares, S. Narumiya, J. Teixido, F. Sanchez-Madrid and C. Cabanas (2001). "Rho and Rho-associated kinase modulate the tyrosine kinase PYK2 in T-cells through regulation of the activity of the integrin LFA-1." J Biol Chem **276**(44): 40518-27.

Rose, D. M., S. Liu, D. G. Woodside, J. Han, D. D. Schlaepfer and M. H. Ginsberg (2003). "Paxillin binding to the alpha 4 integrin subunit stimulates LFA-1 (integrin alpha L beta 2)-dependent T cell migration by augmenting the activation of focal adhesion kinase/proline-rich tyrosine kinase-2." J Immunol **170**(12): 5912-8.

Rozdzial, M. M., R. T. Kubo, S. L. Turner and T. H. Finkel (1994). "Developmental regulation of the TCR zeta-chain. Differential expression and tyrosine phosphorylation of the TCR zeta-chain in resting immature and mature T lymphocytes." J Immunol **153**(4): 1563-80.

Rozdzial, M. M., B. Malissen and T. H. Finkel (1995). "Tyrosine-phosphorylated T cell receptor zeta chain associates with the actin cytoskeleton upon activation of mature T lymphocytes." Immunity **3**(5): 623-33.

Salgia, R., S. Avraham, E. Pisick, J. L. Li, S. Raja, E. A. Greenfield, M. Sattler, H. Avraham and J. D. Griffin (1996). "The related adhesion focal tyrosine kinase forms a complex with paxillin in hematopoietic cells." J Biol Chem **271**(49): 31222-6.

Samelson, L. E., A. F. Phillips, E. T. Luong and R. D. Klausner (1990). "Association of the fyn protein-tyrosine kinase with the T-cell antigen receptor." Proc Natl Acad Sci U S A **87**(11): 4358-62.

Samstag, Y., S. M. Eibert, M. Klemke and G. H. Wabnitz (2003). "Actin cytoskeletal dynamics in T lymphocyte activation and migration." J Leukoc Biol **73**(1): 30-48.

Sancho, D., M. C. Montoya, A. Monjas, M. Gordon-Alonso, T. Katagiri, D. Gil, R. Tejedor, B. Alarcon and F. Sanchez-Madrid (2002). "TCR engagement induces proline-rich tyrosine kinase-2 (Pyk2) translocation to the T cell-APC interface independently of Pyk2 activity and in an immunoreceptor tyrosine-based activation motif-mediated fashion." J Immunol **169**(1): 292-300.

Sancho, D., M. Nieto, M. Llano, J. L. Rodriguez-Fernandez, R. Tejedor, S. Avraham, C. Cabanas, M. Lopez-Botet and F. Sanchez-Madrid (2000). "The tyrosine kinase PYK-2/RAFTK regulates natural killer (NK) cell cytotoxic response, and is translocated and activated upon specific target cell recognition and killing." J Cell Biol **149**(6): 1249-62.

Santoni, G., R. Lucciarini, C. Amantini, J. Jacobelli, E. Spreghini, P. Ballarini, M. Piccoli and A. Gismondi (2002). "Candida albicans expresses a focal adhesion kinase-like protein that undergoes increased tyrosine phosphorylation upon yeast cell adhesion to vitronectin and the EA.hy 926 human endothelial cell line." Infect Immun **70**(7): 3804-15.

Sarosi, G. A., P. M. Thomas, M. Egerton, A. F. Phillips, K. W. Kim, E. Bonvini and L. E. Samelson (1992). "Characterization of the T cell antigen receptor--p60fyn protein tyrosine kinase association by chemical cross-linking." Int Immunol **4**(11): 1211-7.

Sasaki, H., K. Nagura, M. Ishino, H. Tobioka, K. Kotani and T. Sasaki (1995). "Cloning and characterization of cell adhesion kinase beta, a novel protein-tyrosine kinase of the focal adhesion kinase subfamily." J Biol Chem **270**(36): 21206-19.

Schaeffer, E. M., J. Debnath, G. Yap, D. McVicar, X. C. Liao, D. R. Littman, A. Sher, H. E. Varmus, M. J. Lenardo and P. L. Schwartzberg (1999). "Requirement for Tec kinases Rlk and Itk in T cell receptor signaling and immunity." Science **284**(5414): 638-41.

Schaller, M. D., C. A. Borgman, B. S. Cobb, R. R. Vines, A. B. Reynolds and J. T. Parsons (1992). "pp125FAK a structurally distinctive protein-tyrosine kinase associated with focal adhesions." Proc Natl Acad Sci U S A **89**(11): 5192-6.

Schaller, M. D., C. A. Borgman and J. T. Parsons (1993). "Autonomous expression of a noncatalytic domain of the focal adhesion-associated protein tyrosine kinase pp125FAK." Mol Cell Biol **13**(2): 785-91.

Schaller, M. D., J. D. Hildebrand, J. D. Shannon, J. W. Fox, R. R. Vines and J. T. Parsons (1994). "Autophosphorylation of the focal adhesion kinase, pp125FAK, directs SH2-dependent binding of pp60src." Mol Cell Biol **14**(3): 1680-8.

Schaller, M. D. and T. Sasaki (1997). "Differential signaling by the focal adhesion kinase and cell adhesion kinase beta." J Biol Chem **272**(40): 25319-25.

Schepis, A., B. Schramm, C. A. de Haan and J. K. Locker (2006). "Vaccinia virus-induced microtubule-dependent cellular rearrangements." Traffic **7**(3): 308-23.

Schlaepfer, D. D., S. K. Hanks, T. Hunter and P. van der Geer (1994). "Integrin-mediated signal transduction linked to Ras pathway by GRB2 binding to focal adhesion kinase." Nature **372**(6508): 786-91.

Schottelndreier, H., B. V. Potter, G. W. Mayr and A. H. Guse (2001). "Mechanisms involved in alpha6beta1-integrin-mediated Ca(2+) signalling." Cell Signal **13**(12): 895-9.

Shaw, K. T., A. M. Ho, A. Raghavan, J. Kim, J. Jain, J. Park, S. Sharma, A. Rao and P. G. Hogan (1995). "Immunosuppressive drugs prevent a rapid dephosphorylation of transcription factor NFAT1 in stimulated immune cells." Proc Natl Acad Sci U S A **92**(24): 11205-9.

Shimonaka, M., K. Katagiri, T. Nakayama, N. Fujita, T. Tsuruo, O. Yoshie and T. Kinashi (2003). "Rap1 translates chemokine signals to integrin activation, cell polarization, and motility across vascular endothelium under flow." J Cell Biol **161**(2): 417-27.

Sieg, D. J., C. R. Hauck, D. Ilic, C. K. Klingbeil, E. Schaefer, C. H. Damsky and D. D. Schlaepfer (2000). "FAK integrates growth-factor and integrin signals to promote cell migration." Nat Cell Biol **2**(5): 249-56.

Sieg, D. J., D. Ilic, K. C. Jones, C. H. Damsky, T. Hunter and D. D. Schlaepfer (1998). "Pyk2 and Src-family protein-tyrosine kinases compensate for the loss of FAK in fibronectin-stimulated signaling events but Pyk2 does not fully function to enhance FAK- cell migration." Embo J **17**(20): 5933-47.

Silacci, P., L. Mazzolai, C. Gauci, N. Stergiopulos, H. L. Yin and D. Hayoz (2004). "Gelsolin superfamily proteins: key regulators of cellular functions." Cell Mol Life Sci **61**(19-20): 2614-23.

Stowers, L., D. Yelon, L. J. Berg and J. Chant (1995). "Regulation of the polarization of T cells toward antigen-presenting cells by Ras-related GTPase CDC42." Proc Natl Acad Sci U S A **92**(11): 5027-31.

Straus, D. B., A. C. Chan, B. Patai and A. Weiss (1996). "SH2 domain function is essential for the role of the Lck tyrosine kinase in T cell receptor signal transduction." J Biol Chem **271**(17): 9976-81.

Straus, D. B. and A. Weiss (1992). "Genetic evidence for the involvement of the lck tyrosine kinase in signal transduction through the T cell antigen receptor." Cell **70**(4): 585-93.

Su, Y. W., Y. Zhang, J. Schweikert, G. A. Koretzky, M. Reth and J. Wienands (1999). "Interaction of SLP adaptors with the SH2 domain of Tec family kinases." Eur J Immunol **29**(11): 3702-11.

Sunder-Plassmann, R. and E. L. Reinherz (1998). "A p56lck-independent pathway of CD2 signaling involves Jun kinase." J Biol Chem **273**(37): 24249-57.

Tachibana, K., T. Sato, N. D'Avirro and C. Morimoto (1995). "Direct association of pp125FAK with paxillin, the focal adhesion-targeting mechanism of pp125FAK." J Exp Med **182**(4): 1089-99.

Takayama, H. and M. V. Sitkovsky (1987). "Antigen receptor-regulated exocytosis in cytotoxic T lymphocytes." J Exp Med **166**(3): 725-43.

Tamura, G. S., M. O. Dailey, W. M. Gallatin, M. S. McGrath, I. L. Weissman and E. A. Pillemer (1984). "Isolation of molecules recognized by monoclonal antibodies and antisera: the solid phase immunoisolation technique." Anal Biochem **136**(2): 458-64.

Tang, H., Q. Hao, T. Fitzgerald, T. Sasaki, E. J. Landon and T. Inagami (2002). "Pyk2/CAKbeta tyrosine kinase activity-mediated angiogenesis of pulmonary vascular endothelial cells." J Biol Chem **277**(7): 5441-7.

Taylor, J. M., C. P. Mack, K. Nolan, C. P. Regan, G. K. Owens and J. T. Parsons (2001). "Selective expression of an endogenous inhibitor of FAK regulates proliferation and migration of vascular smooth muscle cells." Mol Cell Biol **21**(5): 1565-72.

Thelen, M. (2001). "Dancing to the tune of chemokines." Nat Immunol **2**(2): 129-34.

Thomas, J. W., B. Ellis, R. J. Boerner, W. B. Knight, G. C. White, 2nd and M. D. Schaller (1998). "SH2- and SH3-mediated interactions between focal adhesion kinase and Src." J Biol Chem **273**(1): 577-83.

Timmerman, L. A., N. A. Clipstone, S. N. Ho, J. P. Northrop and G. R. Crabtree (1996). "Rapid shuttling of NF-AT in discrimination of Ca2+ signals and immunosuppression." Nature **383**(6603): 837-40.

Toutant, M., A. Costa, J. M. Studler, G. Kadare, M. Carnaud and J. A. Girault (2002). "Alternative splicing controls the mechanisms of FAK autophosphorylation." Mol Cell Biol **22**(22): 7731-43.

Trambas, C. M. and G. M. Griffiths (2003). "Delivering the kiss of death." Nat Immunol **4**(5): 399-403.

Tsuchida, M., E. R. Manthei, S. J. Knechtle and M. M. Hamawy (1999). "CD28 ligation induces rapid tyrosine phosphorylation of the linker molecule LAT in the absence of Syk and ZAP-70 tyrosine phosphorylation." Eur J Immunol **29**(7): 2354-9.

Turner, C. E. (2000). "Paxillin and focal adhesion signalling." Nat Cell Biol **2**(12): E231-6.

Turner, C. E., M. C. Brown, J. A. Perrotta, M. C. Riedy, S. N. Nikolopoulos, A. R. McDonald, S. Bagrodia, S. Thomas and P. S. Leventhal (1999). "Paxillin LD4 motif binds PAK and PIX through a novel 95-kD ankyrin repeat, ARF-GAP protein: A role in cytoskeletal remodeling." J Cell Biol **145**(4): 851-63.

Turner, C. E. and J. T. Miller (1994). "Primary sequence of paxillin contains putative SH2 and SH3 domain binding motifs and multiple LIM domains: identification of a vinculin and pp125Fak-binding region." J Cell Sci **107 (Pt 6)**: 1583-91.

Turner, J. M., M. H. Brodsky, B. A. Irving, S. D. Levin, R. M. Perlmutter and D. R. Littman (1990). "Interaction of the unique N-terminal region of tyrosine kinase p56lck with cytoplasmic domains of CD4 and CD8 is mediated by cysteine motifs." Cell **60**(5): 755-65.

Tybulewicz, V. L. (2005). "Vav-family proteins in T-cell signalling." Curr Opin Immunol **17**(3): 267-74.

van Oers, N. S., N. Killeen and A. Weiss (1994). "ZAP-70 is constitutively associated with tyrosine-phosphorylated TCR zeta in murine thymocytes and lymph node T cells." Immunity **1**(8): 675-85.

van Oers, N. S., N. Killeen and A. Weiss (1996). "Lck regulates the tyrosine phosphorylation of the T cell receptor subunits and ZAP-70 in murine thymocytes." J Exp Med **183**(3): 1053-62.

van Oers, N. S., W. Tao, J. D. Watts, P. Johnson, R. Aebersold and H. S. Teh (1993). "Constitutive tyrosine phosphorylation of the T-cell receptor (TCR) zeta subunit: regulation of TCR-associated protein tyrosine kinase activity by TCR zeta." Mol Cell Biol **13**(9): 5771-80.

van Oers, N. S., B. Tohlen, B. Malissen, C. R. Moomaw, S. Afendis and C. A. Slaughter (2000). "The 21- and 23-kD forms of TCR zeta are generated by specific ITAM phosphorylations." Nat Immunol **1**(4): 322-8.

van Seventer, G. A., M. M. Mullen and J. M. van Seventer (1998). "Pyk2 is differentially regulated by beta1 integrin- and CD28-mediated co-stimulation in human CD4+ T lymphocytes." Eur J Immunol **28**(11): 3867-77.

Wang, H., F. E. McCann, J. D. Gordan, X. Wu, M. Raab, T. H. Malik, D. M. Davis and C. E. Rudd (2004). "ADAP-SLP-76 binding differentially regulates supramolecular activation cluster (SMAC) formation relative to T cell-APC conjugation." J Exp Med **200**(8): 1063-74.

Wang, Q., Y. Xie, Q. S. Du, X. J. Wu, X. Feng, L. Mei, J. M. McDonald and W. C. Xiong (2003). "Regulation of the formation of osteoclastic actin rings by proline-rich tyrosine kinase 2 interacting with gelsolin." J Cell Biol **160**(4): 565-75.

Wange, R. L., R. Guitian, N. Isakov, J. D. Watts, R. Aebersold and L. E. Samelson (1995). "Activating and inhibitory mutations in adjacent tyrosines in the kinase domain of ZAP-70." J Biol Chem **270**(32): 18730-3.

Wange, R. L., S. N. Malek, S. Desiderio and L. E. Samelson (1993). "Tandem SH2 domains of ZAP-70 bind to T cell antigen receptor zeta and CD3 epsilon from activated Jurkat T cells." J Biol Chem **268**(26): 19797-801.

Watson, J. M., T. W. Harding, V. Golubovskaya, J. S. Morris, D. Hunter, X. Li, J. S. Haskill and H. S. Earp (2001). "Inhibition of the calcium-dependent tyrosine kinase (CADTK) blocks monocyte spreading and motility." J Biol Chem **276**(5): 3536-42.

Weismann, M., A. H. Guse, L. Sorokin, B. Broker, M. Frieser, R. Hallmann and G. W. Mayr (1997). "Integrin-mediated intracellular Ca2+ signaling in Jurkat T lymphocytes." J Immunol **158**(4): 1618-27.

Weiss, A. and D. R. Littman (1994). "Signal transduction by lymphocyte antigen receptors." Cell **76**(2): 263-74.

Williams, L. M. and A. J. Ridley (2000). "Lipopolysaccharide induces actin reorganization and tyrosine phosphorylation of Pyk2 and paxillin in monocytes and macrophages." J Immunol **164**(4): 2028-36.

Witke, W., A. H. Sharpe, J. H. Hartwig, T. Azuma, T. P. Stossel and D. J. Kwiatkowski (1995). "Hemostatic, inflammatory, and fibroblast responses are blunted in mice lacking gelsolin." Cell **81**(1): 41-51.

Wong, P. and E. G. Pamer (2003). "CD8 T cell responses to infectious pathogens." Annu Rev Immunol **21**: 29-70.

Wozniak, M. A., K. Modzelewska, L. Kwong and P. J. Keely (2004). "Focal adhesion regulation of cell behavior." Biochim Biophys Acta **1692**(2-3): 103-19.

Wu, J., D. G. Motto, G. A. Koretzky and A. Weiss (1996). "Vav and SLP-76 interact and functionally cooperate in IL-2 gene activation." Immunity **4**(6): 593-602.

Xiong, W. C., M. Macklem and J. T. Parsons (1998). "Expression and characterization of splice variants of PYK2, a focal adhesion kinase-related protein." J Cell Sci **111 (Pt 14)**: 1981-91.

Yokosuka, T., K. Sakata-Sogawa, W. Kobayashi, M. Hiroshima, A. Hashimoto-Tane, M. Tokunaga, M. L. Dustin and T. Saito (2005). "Newly generated T cell receptor microclusters initiate and sustain T cell activation by recruitment of Zap70 and SLP-76." Nat Immunol **6**(12): 1253-62.

Young, B. A., Y. Taooka, S. Liu, K. J. Askins, Y. Yokosaki, S. M. Thomas and D. Sheppard (2001). "The cytoplasmic domain of the integrin alpha9 subunit requires the adaptor protein paxillin to inhibit cell spreading but promotes cell migration in a paxillin-independent manner." Mol Biol Cell **12**(10): 3214-25.

Yu, H., X. Li, G. S. Marchetto, R. Dy, D. Hunter, B. Calvo, T. L. Dawson, M. Wilm, R. J. Anderegg, L. M. Graves and H. S. Earp (1996). "Activation of a novel calcium-dependent protein-tyrosine kinase. Correlation with c-Jun N-terminal kinase but not mitogen-activated protein kinase activation." J Biol Chem **271**(47): 29993-8.

Zaidel-Bar, R., C. Ballestrem, Z. Kam and B. Geiger (2003). "Early molecular events in the assembly of matrix adhesions at the leading edge of migrating cells." J Cell Sci **116**(Pt 22): 4605-13.

Zamir, E. and B. Geiger (2001). "Molecular complexity and dynamics of cell-matrix adhesions." J Cell Sci **114**(Pt 20): 3583-90.

Zhang, W., J. Sloan-Lancaster, J. Kitchen, R. P. Trible and L. E. Samelson (1998). "LAT: the ZAP-70 tyrosine kinase substrate that links T cell receptor to cellular activation." Cell **92**(1): 83-92.

Zheng, C., Z. Xing, Z. C. Bian, C. Guo, A. Akbay, L. Warner and J. L. Guan (1998). "Differential regulation of Pyk2 and focal adhesion kinase (FAK). The C-terminal domain of FAK confers response to cell adhesion." J Biol Chem **273**(4): 2384-9.

Zhou, Y. J., M. Chen, N. A. Cusack, L. H. Kimmel, K. S. Magnuson, J. G. Boyd, W. Lin, J. L. Roberts, A. Lengi, R. H. Buckley, R. L. Geahlen, F. Candotti, M. Gadina, P. S. Changelian and J. J. O'Shea (2001). "Unexpected effects of FERM domain mutations on catalytic activity of Jak3: structural implication for Janus kinases." Mol Cell **8**(5): 959-69.

Zhu, X., J. L. Kim, J. R. Newcomb, P. E. Rose, D. R. Stover, L. M. Toledo, H. Zhao and K. A. Morgenstern (1999). "Structural analysis of the lymphocyte-specific kinase Lck in complex with non-selective and Src family selective kinase inhibitors." Structure **7**(6): 651-61.

APPENDIX

A.1 *CTL clones AB.1 and Clone 11 express low levels of Fyn*

I established a biochemical approach to detect proteins recruited to the TCR/CD3 complex by capturing engaged TCR/CD3 complexes and associated proteins after cell stimulation with immobilized anti-CD3ε. I demonstrated that proteins known to associate with this complex (Lck and Zap-70) are present in the antibody-captured complexes (Figure 3-1a). The SFK Fyn is thought to directly associate with the TCR/CD3 chains (Samelson 1990, Sarosi 1992), therefore I would have expected to capture it in this assay. However, I was unable to detect Fyn in the TCR/CD3 complexes, likely because our CTL clones express very little Fyn when compared to Jurkat T cells. This experiment shows that Jurkat T cells express approximately 8 fold and 3.5 fold more Fyn than AB.1 or Clone 11 respectively (Appendix Figure 1).

A.2 *The protein complexes that form around the TCR/CD3 chains are not pre-formed*

I sought to determine whether recruitment of proteins to the TCR/CD3 complex was inducible or whether the complex of proteins was pre-formed. I analyzed the pattern of tyrosine phosphorylated proteins captured by immobilized anti-CD3ε when either unstimulated lysate, pre-stimulated lysate or intact cells were plated onto dishes coated with immobilized anti-CD3ε (Appendix Figure 2). Very few tyrosine phosphorylated proteins bound to the immobilized antibody in the unstimulated and pre-stimulated lysate. This result suggests that intact cells must be stimulated to induce complex formation around the TCR/CD3 complex and that the complexes are not pre-formed.

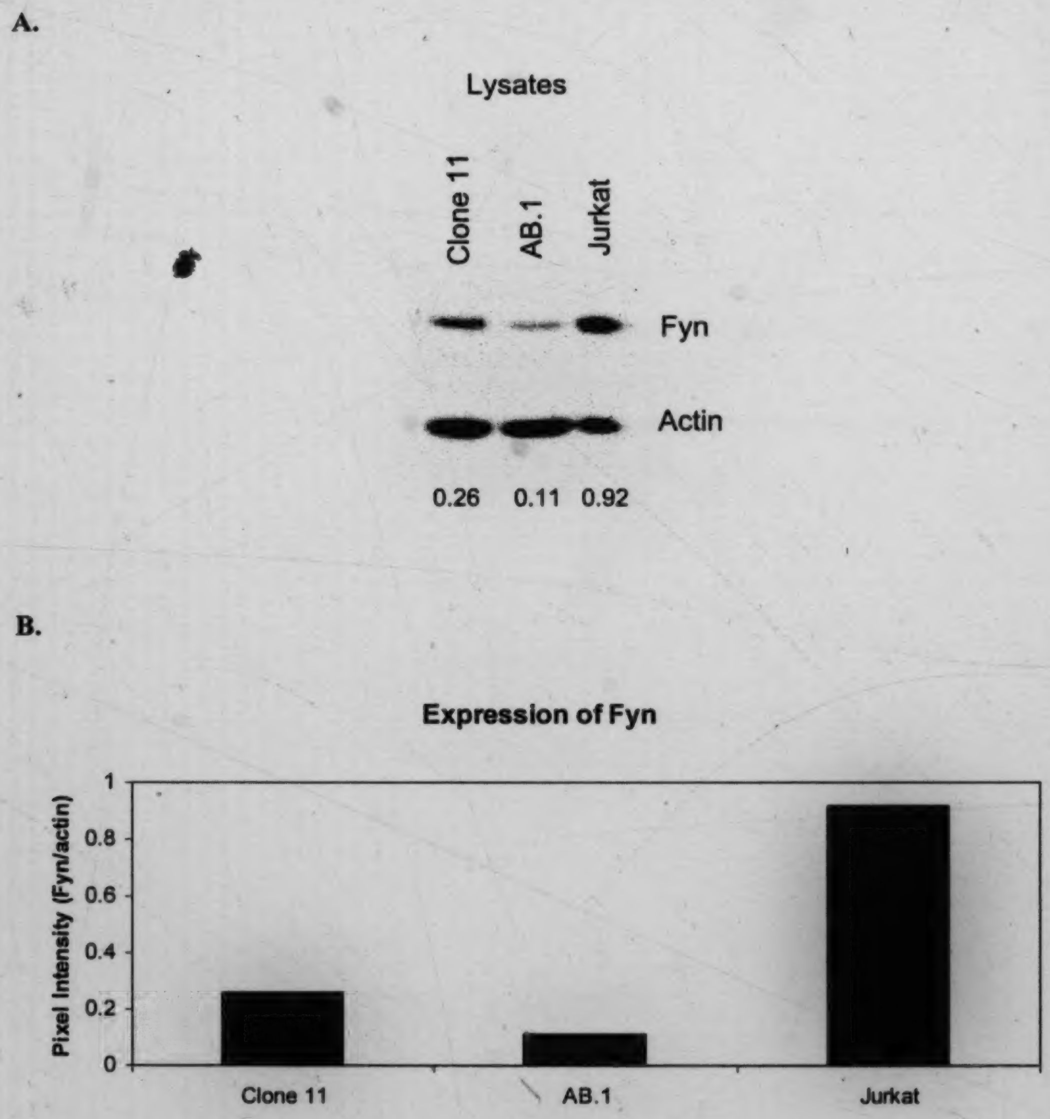

APPENDIX FIGURE 1. CTL clones express very little Fyn compared to Jurkat T cells. a) Lysates from 2 X 10^5 cell equivalents of unstimulated clone 11, AB.1 CTL clones or Jurkat T cells were run on a 7.5% SDS-PAGE gel and transferred to a membrane. The membrane was blotted with anti-Fyn and anti-actin. b) Ratios of pixel volumes for each Fyn band to actin band were calculated as follows: integrated intensity – background (Fyn) / integrated intensity – background (actin) and are presented in a chart. The number values of the ratios are shown in (a).

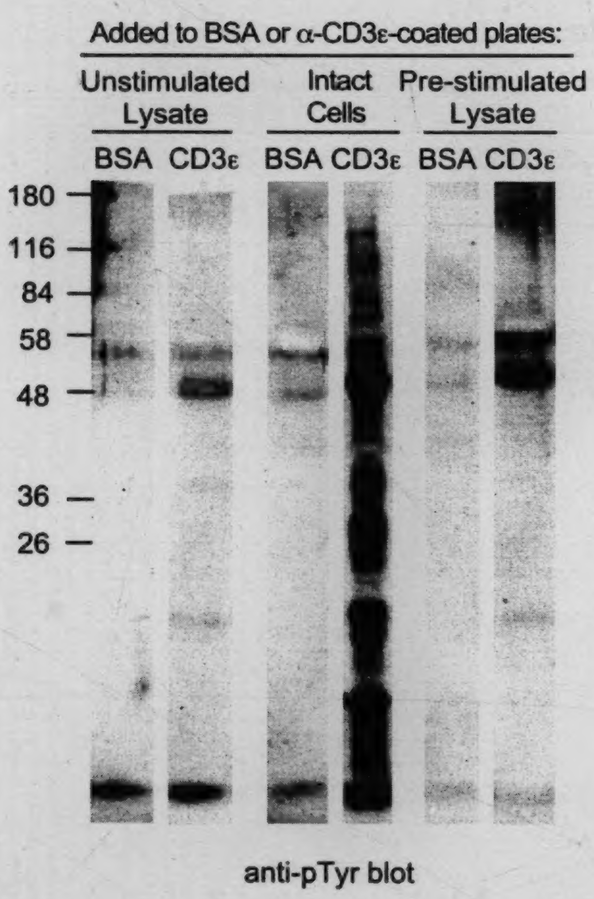
Added to BSA or α-CD3ε-coated plates:
Unstimulated Lysate
Intact Cells
Pre-stimulated Lysate
BSA
CD3ε
BSA
CD3ε
BSA
CD3ε
180
116
84
58
48
36
26
anti-pTyr blot

APPENDIX FIGURE 2. Recruited complexes are not pre-formed. Either intact cells (1 x 10^7 AB.1 CTL clones), an unstimulated cell lysate (1 x 10^7 cell equivalents) or a cell lysate (1 x 10^7 cell equivalents) from cells stimulated on 10 μg/ml immobilized anti-CD3 for 20 minutes was added to plates coated with BSA or 10 μg/ml anti-CD3. Plates were then incubated at 37°C for 20 min. Complexes were recovered from the plates as described in the *Materials and Methods*. Samples were run on SDS-PAGE gels, transferred to membranes, and probed with anti-phosphotyrosine.

A.3 *Two populations of Pyk2 exist in NIH-3T3 fibroblasts based on their differential ability to associate with paxillin*

Based on the observation that an association between Pyk2 and paxillin could only be detected using the F245 antiserum to immunoprecipitated Pyk2, I examined whether there were two populations of Pyk2 in CTL clones by performing sequential Pyk2 immunoprecipitations on unstimulated cell lysates with the F298 (does not recover Pyk2 associated with paxillin) and F245 antisera. Immunoprecipitation was performed first with one antibody, then non-antibody-bound lysate was recovered and transferred to a new tube and immunoprecipitation was performed with the second anti-Pyk2 antibody. The results for AB.1 cells are presented in Figure 5-2b. To demonstrate that this occurs in cells other than the CTL clones, I performed the same experiment in NIH-3T3 fibroblasts. Results similar to those found for AB.1 cells were obtained with the NIH-3T3 cells (Appendix Figure 3). The control sample in which the first and second antibody used was F298 showed that most Pyk2 that is immunoreactive with this antibody was removed after the first immunoprecipitation. A similar situation occurred in the instance where F245 was used as the first and second antibody. When F245 was used to pre-clear the lysate, F298 recovered more Pyk2 which was not associated with paxillin. Performing an F245 immunoprecipitation on an F298-pre-cleared lysate recovered Pyk2 that was clearly associated with paxillin. These results suggest that there are two different populations of Pyk2 in NIH-3T3 fibroblasts based on their differential ability to associate with paxillin.

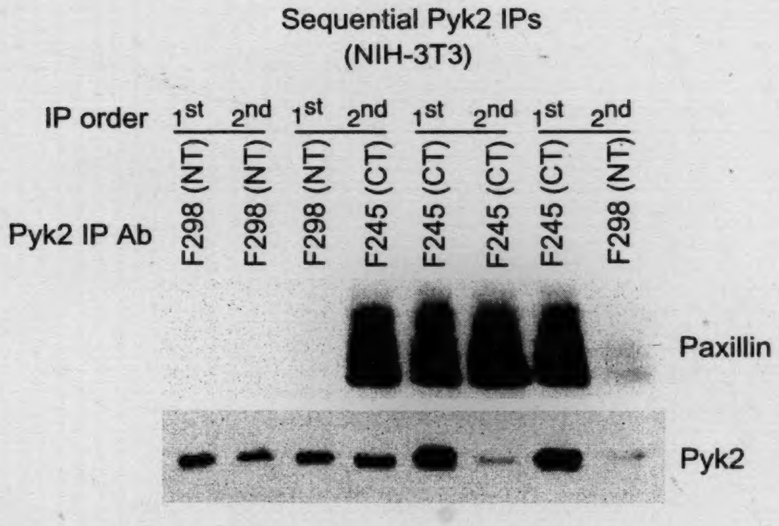
Sequential Pyk2 IPs
(NIH-3T3)
IP order
1st
2nd
1st
2nd
1st
2nd
1st
2nd
Pyk2 IP Ab
F298 (NT)
F298 (NT)
F298 (NT)
F245 (CT)
F245 (CT)
F245 (CT)
F245 (CT)
F298 (NT)
Paxillin
Pyk2

APPENDIX FIGURE 3. Two populations of Pyk2 exist in NIH-3T3 fibroblasts based on their differential ability to associate with paxillin. Sequential Pyk2 immunoprecipitations were performed on unstimulated cell lysates from NIH-3T3 fibroblasts. After immunoprecipitation using the first anti-Pyk2 antibody, beads were pelleted and supernatants were transferred to new tubes. Immunoprecipitation with the second anti-Pyk2 antibody was then performed. Samples collected from the first and second immunoprecipitations were run on gels. Immunoblots for Pyk2 (Pyk2 monoclonal) and paxillin are shown.

A. 4 *Phosphorylated Pyk2 is recruited to the CTL/target cell interface*

Upon stimulation through the TCR, Pyk2 becomes phosphorylated on four tyrosine residues (Y402, Y579, Y580 and Y881). To determine the localization of phosphorylated (and presumably activated) Pyk2, I immunostained CTL/target cell conjugates with Pyk2 phospho-specific antibodies generated against the Y402, Y580 and Y881 phosphorylation sites. Appendix figures 4a, b and c show that Pyk2 phosphorylated at Y402, Y580 and Y881 respectively was enriched at the contact site. Although these antisera recognize Pyk2, it is possible that there is cross-reactivity with other phosphorylated proteins concentrated at the interface that bear similar sequences surrounding the tyrosine in question as much cross-reactivity is observed in a western blot of cell lysates. Therefore, the staining at the interface may not be due solely to Pyk2 phosporylation.

Interestingly, co-staining with anti-paxillin and anti-pY881 showed no co-localization at the MTOC in either stimulated or unstimulated CTL (Appendix Figures 4d, e) which corroborates my biochemical data that suggests that phosphorylation at this site interferes with paxillin binding. The apparent co-localization of Pyk2 phosphorylated on Y881 and paxillin at the interface may not represent a direct association between the two proteins but only that they are in close proximity as many proteins become concentrated in this area. Alternatively, Pyk2 that is phosphorylated on Y881 may still be able to bind to one LD motif of paxillin (as there are two potential sites of interaction) and co-localization could be detected by confocal microscopy, but the interaction could be too weak to withstand immunoprecipitation. The anti-Y881 antibody may also cross-react with other tyrosine phosphorylated proteins at the interface.

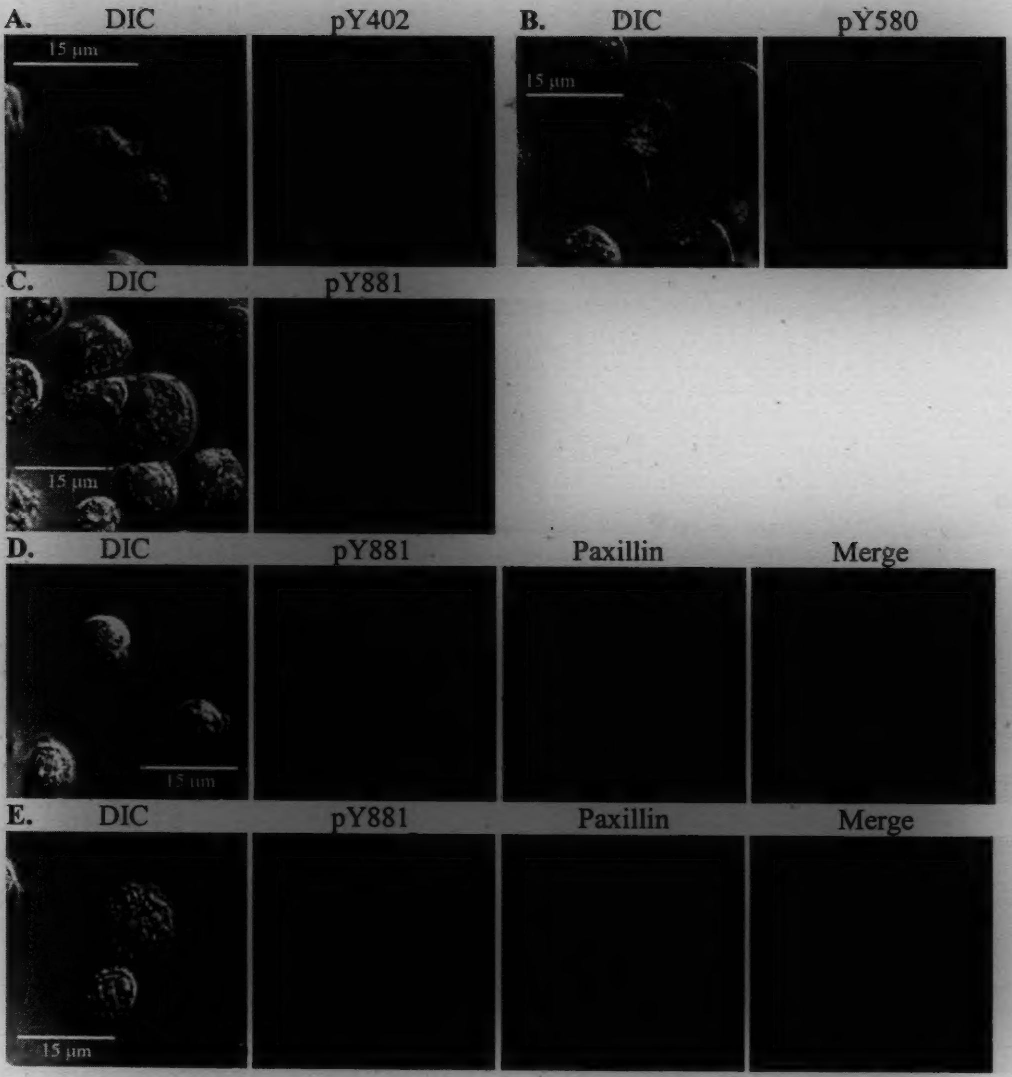
A.
DIC
pY402
15 µm
B.
DIC
pY580
15 µm
C.
DIC
pY881
15 µm
D.
DIC
pY881
Paxillin
Merge
15 µm
E.
DIC
pY881
Paxillin
Merge
15 µm

APPENDIX FIGURE 4. Phosphorylated Pyk2 is concentrated at the CTL/target cell interface. a, b, c) AB.1 CTL clones were mixed with $L1210^{Kb/Dd}$ for 6 min to allow for conjugates to form. Conjugates were adhered to poly-L-lysine-coated coverslips, fixed and permeabilized. Immunostaining with Pyk2 phospho-specific antibodies was performed: anti-pY402 (a), anti-pY580 (b) and anti-pY881 (c). d, e) AB.1 cells alone (d) or stimulated with $L1210^{Kb/Dd}$ (e) were co-immunostained with anti-pY881 and anti-paxillin. The cells were visualized by confocal microscopy. The green flurorochrome used was Alexa 488 and the red flurorochrome used was rhodamine.

A.5 *Nck and ZAP-70 are present in a Pyk2 immunoprecipitation*

I have found that Pyk2 is recruited to the TCR/CD3 complex upon stimulation with immobilized anti-CD3 (Figure 3-7). However, the mechanism by which Pyk2 is recruited is unknown. I performed Pyk2 immunoprecipitations on stimulated AB.1 clone lysates and immunoblotted the membrane with antibodies generated against proteins that are recruited to the TCR/CD3 complex. I found that the SH2/SH3 adaptor protein Nck and the Syk family kinase ZAP-70 associate with Pyk2 (Appendix Figure 5).

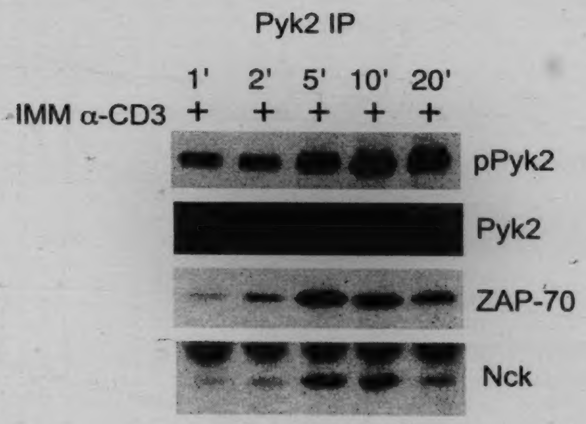

APPENDIX FIGURE 5. Nck and ZAP-70 are present in a Pyk2 immunoprecipitation. AB.1 cells were stimulated on immobilized anti-CD3 for the indicated time. Pyk2 immunoprecipitations were performed on the stimulated cell lysates. The immunoprecipitates were run on an SDS-PAGE gel, transferred to a membrane and the membrane was immunoblotted with anti-phosphotyrosine, anti-Pyk2 (F298), anti-ZAP-70 and anti-Nck.